UCSF
UC San Francisco Electronic Theses and Dissertations

Title

Mechanism and Evolution of Mammalian Hedgehog Signaling

Permalink

https://escholarship.org/uc/item/3xb7606n

Author

Wilson, Christopher William

Publication Date

2009

Peer reviewed|Thesis/dissertation

Mechanism and Evolution of Mammalian Hedgehog Signaling

by

Christopher William Wilson

DISSERTATION

Submitted in partial satisfaction of the requirements for the degree of

DOCTOR OF PHILOSOPHY

in

Developmental Biology

in the

GRADUATE DIVISION

of the

UNIVERSITY OF CALIFORNIA, SAN FRANCISCO

ii

Dedication

This dissertation is dedicated both to my parents and to the memory of Bernice Nesbitt,

who encouraged my curiosity as a child.

Acknowledgements

First and foremost, I would like to thank Pao-Tien Chuang, my principal investigator and dissertation advisor. Pao-Tien has been extremely involved in every aspect of my work since I first joined his lab, and I have learned about nearly every aspect of conducting research, writing manuscripts and grants, and forging ahead with new directions of investigation under his supervision. I thank him for his diligence, rigor, patience, and for always having an open door.

Miao-Hsueh (Ashley) Chen joined the lab as a postdoctoral fellow shortly after I started, and over the years we have developed a close, productive, and collaborative working relationship. I sincerely thank her for her patience, and for the significant amount of time she spent teaching and discussing science. None of the work presented in this dissertation would have been possible without her effort.

I would also like to thank other members of the lab, past and present, for their support and encouragement: Chi-Sheng (Jason) Lu, Jehn-Hsien (Jason) Yang, Takatoshi Kawakami, Nan Gao, Yajun Li, Tony Gerber, Rachel Sutherland, Erica Yao, Yoko Nozawa, Rhodora Gacayan, Chuwen Lin, Sarah Kaufman, Phillip Dumesic, Richard Tabor, and Leonor Patel. A special thanks also to Dave Casso of the Kornberg lab for many stimulating discussions over the years.

Didier Stainier, Tom Kornberg, Gail Martin and Wendell Lim were members of my qualifying and dissertation committees, and provided superb and succinct guidance in my studies. Thank you for your time and encouragement.

From: Lo, Christina
Sent: Monday, July 13, 2009 3:16 PM
To: Garite, Bibi
Subject: FW: CSHL Press Reprint Permission Request Form

-----Original Message-----
From: reprint@cshl.edu [mailto:reprint@cshl.edu]
Sent: Monday, July 13, 2009 3:06 PM
To: Reprint
Subject: CSHL Press Reprint Permission Request Form

Default Intro
Default Intro - line2

Name: Christopher Wilson
CompanyInstitution: University of California - San Francisco Library Address: 600 16th
St Library Address (line 2): Genentech Hall, Room S476
City: San Francisco
State (US and Canada): CA
Country: USA
Zip: 94114
Title: Graduate Student
Lab/Department: Chuang Lab/CVRI
Phone: 415-514-1202
Fax: 415-476-8173
Email: christopher.wilson@ucsf.edu
Title of Publication: Ciliumindependent regulation of Gli protein function by Sufu in
Hedgehog signaling is evolutionarily conserved
Authors/Editors: Miao-Hsueh Chen
Christopher W Wilson
Ya-Jun Li
Kelvin King Lo Law
Chi-Sheng Lu
Rhodora Gacayan
Xiaoyun Zhang
Chi-chung Hui
Pao-Tien Chuang

Date of Publication: Not published - accepted/in press
Publisher: Genes and Development
Title of CSHLP Journal/Book:
Title of Article/Chapter:
CSHL Authors/Editors:
Page Numbers:
Figure Numbers:
Figure Page Numbers:
Copyright Date:
Language: English
Territory: USA
Format: print - use for dissertation
Additional comments: The manuscript has been accepted and copyright was transferred to
G+D on or around 7/11/09. I intend to use this material as a chapter for my dissertation
which must be completed by 7/31/09, so I would like to obtain permission ASAP. Thanks.

Default Footer
Default Footer - line2

1

Statement from Research Advisor: Author Contributions

The following summarizes the contributions of the author, Christopher W. Wilson (CWW), to the work described in this dissertation. The work performed is comparable to a standard thesis.

Chapter I: CWW wrote Chapter I.

Chapter II: The work presented in this chapter was published in 2009 by Nature and is reprinted with permission. CWW performed all experiments and analysis in the mouse or *in vitro*, with the exception of isotopic *in situ* hybridization, which was conducted by Miao-Hsueh Chen (MHC) and Jehn-Hsien Yang. Zebrafish experiments were conducted by Catherine T.Nguyen (CN) and Jau-Nian Chen (JNC), with experimental design and input by CWW, JNC, and Pao-Tien Chuang (PTC). Rhodora Gacayan (RG) and Jie Huang provided technical support and animal husbandry. CWW and CTN contributed equally to the manuscript. CWW and PTC wrote the manuscript.

Chapter III: The work was a collaboration between CWW and MHC, with equal contribution from both authors, and is currently in press at Genes and Development. The work is reprinted with permission. Ya-Jun Li executed purification of Gli3 antigen for antibody production. Chi-Sheng Lu executed experiments regarding Spop and Gli protein level reductions, and ubiquitination assays. RG provided technical support and animal husbandry. Kelvin King Lo Law, Xiaoyun Zhang and Chi-chung Hui provided the conditional allele of *Sufu*. CWW and PTC wrote the manuscript.

Chapter IV: The work presented in this chapter was published in 2009 by PLoS ONE and is reprinted under the Creative Commons Attribution License (CCAL). CWW performed

all experiments. MHC derived cell lines used in all experiments. CWW and PTC wrote

the manuscript

Chapter V: CWW wrote Chapter V.

Mechanism and Evolution of Mammalian Hedgehog Signaling

Christopher W. Wilson

Abstract

The Hedgehog (Hh) signaling pathway is an evolutionarily conserved cascade important for embryonic development and postnatal regeneration. Mutations in components of the Hh pathway in humans result in a number of congenital birth defects, such as holoprosencephaly, as well as numerous cancers. In the fruit fly *Drosophila melanogaster*, transduction of the Hh signal from the positive membrane effector Smoothened (Smo) to the Ci/Gli transcription factors is mediated by a large cytoplasmic complex. This complex is scaffolded by the kinesin Costal-2, and contains the key regulator Fused (Fu), a putative serine-threonine kinase, and Suppressor of Fused (Sufu), a regulator of Ci/Gli proteins. The role of Fu and Sufu in mammalian Hh signaling and development are less well-characterized. In this dissertation, we show that mouse Fu is dispensable for mammalian Hh signaling, but instead participates in construction of the central pair apparatus of motile cilia. Strikingly, zebrafish Fu participates in both motile ciliogenesis and Hh signaling. We link Fu and a Costal-2 ortholog, Kif27 in mouse and Kif7 in zebrafish, to motile ciliogenesis, and advance hypotheses as to how these proteins evolved functions in diverse processes. We also show that mouse Sufu plays an evolutionarily conserved role in promoting the stabilization of Gli2 and Gli3. In part, Sufu opposes the activity of Spop, an adaptor protein for E3 ubiquitin ligases. The

x

increased Hh pathway activity observed in *Sufu* mutant mice and embryonic fibroblasts can be attributed in part to elevated *Gli1* activity. Finally, we investigate the trafficking of mouse Smo to the primary cilium, an organelle required for its activity in Hh transduction. We demonstrate that translocation of Smo to the cilium is necessary but not sufficient for pathway activation, as some classes of Smo antagonists can stimulate movement to the cilium. This result suggests a multi-step model for Smo activation in mammalian Hh transduction. Taken together, the data presented in this dissertation shed light on the evolution of the Hh pathway from invertebrates to mammals, and provide a deeper mechanistic understanding of mammalian Hh transduction that will be useful in the future design of rational therapies.

Table of Contents

List of Tables

List of Figures

CHAPTER II

CHAPTER III

CHAPTER IV

CHAPTER I

Introduction

A central question in developmental biology is how a staggering assortment of cell and tissue types is ultimately produced from a single progenitor cell – the fertilized egg. Remarkably, a limited number of signal transduction pathways are repeatedly used throughout embryonic and postnatal development both to provide instruction to naïve fields of cells and to control differentiation and regeneration. The Hedgehog (Hh) signal transduction pathway is an evolutionarily conserved signaling cascade essential for proper patterning and development of tissues in metazoan organisms (McMahon et al. 2003; Huangfu and Anderson 2006). Misregulation or mutation in essential core components of the Hh pathway often results in congenital birth defects, such as polydactyly and holoprosencephaly; in adults, inappropriate activation of Hh signaling results in a number of cancers, the most common being basal cell carcinoma (McMahon et al. 2003). Understanding the molecular mechansisms of Hh signaling is therefore critical in developing rational therapies and drugs, in order to treat embryonic pathologies and neoplasia. Unlike other major signaling pathways (such as Notch, FGF and Wnt), the core genes in the Hh pathway have not experienced a significant amount of gene duplication or expansion in mammalian lineages (Pires-daSilva and Sommer 2003). Despite this, there appear to be significant differences in the detailed molecular mechanism of Hh transduction in responding cells between *Drosophila melanogaster* and mammals (Huangfu and Anderson 2006). This review/introduction summarizes our current understanding of the molecular mechanisms of Hh signaling, with a particular emphasis on cytoplasmic events in fly and mouse.

2

Hedgehog production, secretion and reception

The basic scheme of Hh morphogen production, movement, and transduction in receiving cells is generally conserved in widely used model organisms. Hh proteins are synthesized as ~45 kilodalton (kDa) precursors, which are targeted to the secretory pathway via a classical signal peptide (Lee et al. 1994). Hh then undergoes an autoproteolytic cleavage catalyzed by its C-terminal intein domain (Bumcrot et al. 1995; Porter et al. 1995). A cholesterol moiety is concomitantly attached to the C-terminus of the released N-terminal signaling fragment (Porter et al. 1996); cholesterol functions in oligomerization or packaging of Hh into signaling complexes/particles, and also restricts Hh movement in the morphogenetic field (Zeng et al. 2001; Chen et al. 2004a; Panakova et al. 2005). A second lipid, palmitic acid, is attached to the N-terminus of the signaling peptide by the acyltransferase *Skinny hedgehog* (*Ski/Skn)* (Amanai and Jiang 2001; Chamoun et al. 2001; Chen et al. 2004a). Palmitic acid is critical for high-level signaling of Hh, although the precise mechanism of action is currently unclear. At some undefined point during trafficking and release, Hh is packaged into a lipophorin-containing (in fly) (Panakova et al. 2005) or phospholipid-containing (in mammalian cell culture) particle (Zeng et al. 2001; Chen et al. 2004a), which may be necessary both for concentration of Hh molecules proximal to sites of secretion, and movement of Hh through the morphogenetic field. Release of Hh from producing cells is facilitated by the sterol-sensing domain (SSD) protein Dispatched (Disp) (Burke et al. 1999; Caspary et al. 2002; Kawakami et al. 2002; Ma et al. 2002), although the site(s) and mechanism of Disp action are currently unknown.

3

After release from producing cells, Hh containing particles are distributed through the extracellular matrix (ECM), where interactions with heparan sulfate proteoglycan (HSPG) side chains and core proteins are critical for shaping the Hh gradient (Yan and Lin 2008). In responding cells, the key function of Hh is binding to its core receptor Patched (Ptc/Ptch), a twelve-pass SSD transmembrane protein that binds Hh ligands with low nanomolar affinity (Stone et al. 1996). In the absence of Hh ligand, Ptch represses the activity of the seven-pass transmembrane protein Smoothened (Smo), a member of the G-protein coupled receptor (GPCR) superfamily. The mechanism of Ptch-mediated Smo repression is currently unknown. Early reports of direct inhibition of Smo through Ptch binding were subsequently shown to be overexpression artifacts, and Smo inhibition is achieved by sub-stoichiometric amounts of Ptch (Stone et al. 1996; Taipale et al. 2002). Sequence analysis places Ptch in the resistance-nodulation-cell division (RND) superfamily of permeases and transporters; consistent with this, both truncated and full-length forms of fly Ptc are capable of trimerization (Lu et al. 2006). The prevailing hypothesis in the field is that Ptch inhibits Smo through transport of a small molecule, either by increasing local concentrations of an inhibitor or decreasing levels of an activator (Taipale et al. 2002). Binding of Hh to Ptch would therefore disrupt small molecule transport, perhaps by dispersing the Ptch oligomer.

Relief of Ptch inhibition on Smo leads to its activation, again through poorly characterized biochemical mechanisms. In *Drosophila*, conformational changes in Smo upon activation are thought to be communicated to the cytosol through a Hh signaling

4

complex (HSC). The end result of Smo activation is modulation of the forms of the Ci/Gli zinc-finger transcription factors. Generally, in the "off" state of the pathway, Ci/Gli2/Gli3 undergo phosphorylation by protein kinase A (PKA), casein kinase I (CKI) and glycogen synthase kinase 3 (GSK3), targeting the proteins for SCF$^{\text{Slimb/β-TrCP}}$ proteasome-dependent limited proteolysis (Price and Kalderon 2002; Pan et al. 2006; Wang and Li 2006). This cleavage event eliminates C-terminal transactivation domains from full-length Ci/Gli2/Gli3, forming a transcriptional repressor comprised of the DNA-binding zinc finger domains and a poorly characterized N-terminal repression domain (Aza-Blanc et al. 1997). Smo activation inhibits Ci/Gli2/Gli3 proteolysis and promotes the formation of Ci/Gli activator forms. These activator forms are biochemically undefined, but are posited to exist on the basis of data demonstrating that elimination of Ci/Gli phosphorylation is insufficient for maximal induction of Hh target genes (Methot and Basler 1999). Additional posttranslational modifications, such as acetylation or SUMOylation, as well as control of the lability of full-length Ci/Gli proteins, may be critical for modulation of the activator forms (Ohlmeyer and Kalderon 1998). Recent data have suggested that the uncleavable form of Ci used in these experiments is still subject to complete degradation in the absence of Hh signaling, casting doubt on the existence of a biochemically distinct Ci activator form (Smelkinson et al. 2007). Ultimately, the relative ratio of Ci/Gli activator and repressor forms is considered to be the critical factor in interpreting the extracellular Hh gradient and determining concentration-dependent cell fates.

Communication from Smo to Ci/Gli is an obviously critical step in Hh signal

transduction, and would be predicted to be tightly regulated. In both fruit fly and

mammals, two general principles have emerged regarding Ptch and Smo at the

membrane. First, opposite localization of Ptch and Smo is associated with the off and on

states of the pathway. Second, conformational changes in Smo are required for activation

of the pathway and coupling to downstream factors via scaffolds for communication to

Ci/Gli. Surprisingly, the subcellular localization of these events, as well as the nature of

the factors required for linking Smo to Ci/Gli, do not appear to be evolutionarily

conserved between invertebrates and mammals. Below, the known species-specific

differences between *Drosophila* and mammalian Hh signaling, both at the cell membrane

and intracellularly, are discussed.

Smo trafficking and conformational changes in *Drosophila*

Biochemical and cell biological studies of Ptc and Smo localization in the fly

wing imaginal disc and salivary gland revealed a complex interplay between their

trafficking and stability. In the absence of Hh, Ptc is found both on plasma membrane,

and in intracellular compartments distributed both in perinuclear and cytoplasmic regions

(Denef et al. 2000; Zhu et al. 2003). Ptc inhibits Smo by promoting both its turnover and

preventing it from accumulating on the cell surface. Oncogenic mutations in Smo or

forced targeting to the cell surface via fusion to GAP43 or a glycophosphatidylinositol

(GPI) anchor are capable of inducing stronger Hh phenotypes than wild type Smo (Zhu et

al. 2003). Conversely, retention of Smo in the endoplasmic reticulum (ER) through

6

addition of a canonical ER retention signal prevents ectopic activation of the pathway. Binding of endogenous or ectopic Hh to Ptc promotes Hh-Ptc complex movement from the cell surface, into intracellular vesicles where no significant co-localization with Smo is observed. Thus, a critical role of Ptc is control of Smo trafficking, and a forced bypass of this inhibition is sufficient to allow activation of Smo. Consistent with other data, the mechanism by which Ptc regulates Smo trafficking is unlikely to involve direct binding.

Exposure of cells to exogenous Hh or a genetic reduction in Ptc levels promotes Smo stabilization and hyperphosphorylation of its intracellular C-terminal tail of Smo (Zhang et al. 2004). This region of Smo contains several consensus PKA sites, as well as CKI sites that require prior "priming" PKA phosphorylation. Mass spectroscopy indicated a total of 26 phosphorylated serine/threonine (Ser/Thr) residues in this region. Mutagenesis studies mimicking gain-and loss-of phosphorylation have demonstrated that graded activity of Smo correlates with the extent of C-terminal phosphorylation. Further, phosphorylated Smo accumulates on the cell surface, consistent with its ability to activate the Hh pathway. Phosphorylation of Smo has thus been proposed to inhibit its endocytosis or promote rapid recycling between endosomal vesicles and the cell surface.

How does Smo phosphorylation mechanistically lead to its activation? Insight into this process came with the discovery that deletion of the Smo C-tail resulted in accumulation of the protein at the cell surface without activation of downstream events. Mutational analysis revealed the importance of several clusters of positively charged arginine (Arg) and lysine (Lys) residues, located adjacent to PKA/CKI clusters.

7

Phosphorylation by PKA and CKI creates a negative electrostatic charge capable of neutralizing the inherent postive charge of the Arg clusters. Since the negative charge is the essential element for neutralization of the Arg clusters, the same effect can be achieved by replacement of the PKA/CKI clusters with negatively charged amino acids such as glutamic acid (Glu) or aspartic acid (Asp). Thus, it would theoretically not be essential for the role of PKA and CKI in this process to be evolutionarily conserved.

Studies of Smo conformation by fluorescence resonance energy transfer (FRET) with various Smo-fluorescent protein (FP) fusions has provided further understanding of the role of the Arg and PKA/CKI clusters in Smo activation. Smo, like other members of the Fz subfamily of GPCRs, is a constitutive dimer, and homodimerization is mediated by the extracellular N-terminus. Within the homodimer, the Arg clusters keep individual Smo molecules in a "closed" conformation, where the Arg clusters interact with endogenous acidic residues in the Smo C-tail. Phosphorylation of the PKA/CKI clusters disrupts the intramolecular Smo interaction, and instead promotes formation of an "open" conformation. In the open conformation, intermolecular interactions between the Smo C-termini in the constitutive dimer are formed, and are required for pathway activation, potentially through coupling to downstream components of the fly Hh signaling complex (HSC). The graded nature of Smo C-tail phosphorylation may provide a sensitive method to interpret varying amounts of extracellular Hh ligand and promote a proportionate Ci response.

Smo trafficking, conformational changes, and the primary cilium in mammals

Understanding the details of Hh signal transduction in mammals is complicated by the fact that the primary cilium, an evolutionarily conserved organelle, is apparently utilized for proper Hh signaling (Huangfu et al. 2003). The primary cilium is a microtubule-based organelle analogous to the flagella found in numerous single-celled eukaryotes such as *Chlamydomonas reinhardtii* (Marshall and Nonaka 2006). Assembly and disassembly of the cilium is mediated by intraflagellar transport (IFT) proteins, and their associated kinesin-II (Kif3 family) and dynein motors (Rosenbaum and Witman 2002). Mice deficient in genes essential for these processes display a lack of response to Hh ligand, implicating the primary cilium in proper reception and interpretation of the Hh signal (Huangfu et al. 2003; Huangfu and Anderson 2005; Liu et al. 2005; May et al. 2005). Analysis of endogenous and overexpressed Smo, Ptch1, Gli1, Gli2, Gli3, and Suppressor of fused (Sufu), all core components of mammalian Hh signaling, indicates that these proteins localize to the primary cilium (Corbit et al. 2005; Haycraft et al. 2005; Rohatgi et al. 2007) (Chen *et al*, manuscript in press). Dynamic trafficking of endogenous Ptch1, Smo, Gli2 and Gli3 has been observed through assessment of cells at various time points after Hh stimulation (Rohatgi et al. 2007; Rohatgi et al. 2009) (Corbit et al. 2005; Wang et al. 2009; Wilson et al. 2009a)(Chen *et al*, manuscript in press). Cultured cells that lack cilia are refractory to stimulation by exogenous Hh ligand, and overexpression of constitutively active forms of Smo or treatment with Smo agonists fails to activate the pathway in the absence of the cilium. By contrast, primary cilia do not seem to be involved in *Drosophila* Hh signaling. In the fly, only a few cell types are ciliated (sensory

neurons and spermatozoa), and IFT mutants do not exhibit any sign of altered Hh signaling (Han et al. 2003). Further analysis of the mechanism of Hh signal transduction in additional metazoan model organisms is needed to definitively address whether the primary cilium was originally involved in Hh signaling, or if it is a relatively late evolutionary acquisition in vertebrate or mammalian lineages.

Despite the apparent divergence in the subcellular location of Hh transduction between *Drosophila* and mammals, the general principle of opposing Smo and Ptch translocation appears to hold true. In the absence of Hh ligand, mammalian Ptch1 is found on the primary cilium, and may serve as a concentrated local sensor for extracellular ligand concentration (Rohatgi et al. 2007). Binding of Hh to Ptch1 causes the removal of Ptch1 from the primary cilium (Rohatgi et al. 2007). Concomitant with this, Smo, which is either distributed intracellularly or on other regions of the plasma membrane, translocates to the primary cilium in a Kif3a- and β-arrestin-dependent manner (Corbit et al. 2005; Kovacs et al. 2008). Interestingly, the opposing translocation of Ptch1 and Smo can be decoupled, primarily through the modulation of Smo conformation via agonists and antagonists. Treatment of cells with the Smo antagonist cyclopamine, the Smo agonist SAG, or the pathway agonist 20-α-hydroxysterol results in Smo trafficking to the cilium, without corresponding removal of Ptch1 (Rohatgi et al. 2007; Rohatgi et al. 2009; Wang et al. 2009; Wilson et al. 2009a). Two principles may be inferred from this data. First, movement of Smo to the primary cilium appears to be necessary, but not sufficient for signal transduction. Second, the absence or presence of

Ptch1 on cilia is less critical than the status of Smo, as active conformations of Smo override the localized presence of Ptch1.

Ultimately, disruption of primary cilium formation affects the formation of the Gli3 repressor, and genetic data implies that Gli activator function is compromised (Liu et al. 2005). Taken together, the data suggest that the cilium is important for limited proteolysis of Gli3 in the absence of ligand, and that the organelle is also critical for relaying the state of Smo activation to full-length Gli proteins. There are many outstanding questions concerning the precise role of the primary cilium in Hh signaling. First, it is unclear if the cilium is required for transduction in all vertebrates, and there are conflicting published data as to the requirement of cilia/IFT in zebrafish Hh signaling (Aanstad et al. 2009; Lunt et al. 2009). Second, the biochemical nature of events that occur on the cilium which affect Gli repressor and Gli activator function are not clear. Finally, a full understanding of the requirement of the cilium for Smo function and Gli regulation is impaired by a lack of knowledge concerning the factors that mediate communication from Smo to Gli in mammals, although potential clues to this have once again arisen from studies in *Drosophila*.

The *Drosophila* Hh signaling complex (HSC)

The molecular details of signaling from Smo to Ci remained unclear for many years, in spite of many meticulous genetic epistatic analyses. It is now known that a cytosolic hedgehog signaling complex (HSC), comprised of the transcription factor

Cubitus interruptus (Ci), the atypical kinesin Costal-2 (Cos2), the putative

serine/threonine kinase Fused (Fu), and a sub-stoichiometric amount of the PEST domain

protein Suppressor of Fused (Su(fu), also Sufu) is critical for transducing the signal from

Smo to the nucleus. The HSC accomplishes this through control of the equilibrium

between limited proteolysis and activation of full-length Ci. In the absence of Hh ligand,

the HSC associates with microtubules through Cos2, which assembles PKA, CKI, and

GSK3 to convert Ci into its truncated repressor form through Slimb-dependent limited

proteolysis. Binding of Hh to Ptc alleviates repression on Smo, resulting in

conformational changes in the Smo molecule. This is accompanied by binding of the

HSC to the cytoplasmic tail of Smo, mediated by Cos2. The resulting physical

association may be sufficient to disrupt binding of the three kinases to Cos2, thus

attenuated limited proteolysis of Ci and providing a key mechanistic step in pathway

activation. The interplay of the components of the HSC and Smo is complex, and may

involve multiple levels of feedback. Genetic studies, as well as the currently known

mechanistic functions of each component of the HSC are described in detail below.

Cos2

The *Costal-2* locus was originally identified in an ethylmethanesulfonate (EMS)

mutagenesis screen in *Drosophila* (Whittle 1976). *Cos2* mutants lacking both maternal

and zygotic contributions of transcript display a classical segment polarity phenotype

similar, but not identical to *ptc* mutants. In embryonic segments, expression of the Hh

target gene *wingless* (*wg*) is expanded, and the segments exhibit mirror-image

duplications. Phenotypes of *cos2* adults are similar to those seen with removal of *ptc*, or

12

overexpression of *hh*. From the phenotypic data, *cos2* was inferred to be a negative

regulator of the pathway (Wang and Holmgren 1999). Closer examination of patterning

in fly wing imaginal discs revealed a more complicated role for *cos2* in Hh transduction

(Wang et al. 2000b). In Hh-responding cells at the anterior-posterior (A-P) boundary of

the wing disc, Ci protein is stabilized in *cos2* mutant clones. Surprisingly, expression of

the Hh target gene *engrailed* (*en*) does not show a corresponding increase, indicating that

Cos2 is necessary for the highest levels of Hh signaling (Wang et al. 2000b; Wang and

Holmgren 2000). This observation was further substantiated both by analysis of

additional reporters (Wang and Holmgren 2000) and RNA interference (RNAi) in

cultured fly clone-8 (cl-8) cells (Lum et al. 2003b). Knockdown of *ptc* results in ligand-

independent pathway activation, which can be partially blocked by simultaneous *cos2*

knockdown. Thus, Cos2 plays a critical role in interpreting and transducing positive and

negative aspects of the Hh pathway, instead of simply being a constitutive negative

regulator.

How does Cos2 participate in both aspects of Ci regulation? Insight into these

processes has come primarily from biochemical and cell biological studies of Cos2

protein. Cos2 was identified to be a kinesin-like molecule, which upon further

phylogenetic analysis can be grouped in the kinesin-IV (also known as chromokinesin)

subfamily of anterograde, microtubule-binding molecular motors (Miki et al. 2005).

Initial sequence analysis of Cos2 revealed that critical amino acid residues in nucleotide-

binding regions of the motor domain were not well-conserved with *bona fide* kinesins,

suggesting that despite binding microtubules, Cos2 might not be a processive motor

(Robbins et al. 1997; Sisson et al. 1997). Later analysis indicated that Cos2 colocalizes with microtubules in live cells, and appears to move along microtubules in a motor-domain and ATP-dependent fashion, albeit at a slower rate than other kinesin molecules (Farzan et al. 2008). This dynamic movement of Cos2 within the cell may be important for localizing it to its relevant binding partners in the "off" and "on" states of the Hh cascade.

The molecular consequences of *cos2* removal are accumulation of the full-length form of Ci (Ci-155) and thus loss of the proteolytically processed form of Ci (Ci-75) (Zhang et al. 2005). Cos2 directly participates in this process through direct binding to Ci-155. Interestingly, Cos2 was shown to bind to PKA, GSK3, and both CKIα and CKIε, leading to the hypothesis that Cos2 acts as a scaffold for these kinases to allow efficient phosphorylation of Ci-155, thus promoting Ci-75 production. In *cos2* wing discs, concurrent overexpression of PKA, GSK3, and *Xenopus* CKIε rescues the Ci processing defect, supporting this notion (Zhang et al. 2005). Binding of Cos2 to the C-terminal CORD domain of Ci also tethers the transcription factor in the cytoplasm, preventing nuclear accumulation. These inhibitory Cos2-Ci complexes are enriched in vesicular membranes, primarily endosomes, through Cos2 binding (Stegman et al. 2004).

Large-scale immunoprecipitation of Smo revealed an interaction with the HSC, specifically with Cos2 (Jia et al. 2003; Lum et al. 2003b; Ogden et al. 2003; Ruel et al. 2003). The amount of the Smo-Cos2 complex increases after Hh stimulation, and Cos2 is redistributed to the plasma membrane after association with Smo. There are conflicting

views on whether formation of the Smo-Cos2 complex causes release of Ci, but Smo

binding to Cos2 appears to compete with PKA, GSK3, and CKIa/e binding. Thus, Smo-

Cos2 complexes, at minimum, would inhibit efficient processing of Ci-155. Cos2 also

binds phosphorylated Smo with greater affinity, although the phosphoresidues are not

predicted to be part of the interacting surface. It is possible that phosphorylation of Smo,

which leads to neutralization of the autoinhibitory Arg clusters and a conformational

shift, also exposes Cos2 interacting surfaces. A net shift in the ratio of active:inactive

Smo would thus shift the balance of active: repressive HSCs, leading to release of Ci-155

and generation of Ci-Act through uncharacterized cellular and biochemical mechanisms.

Fu

The *fused* locus was originally discovered in the early 1900s, but was also "re-

discovered" in screens for genes affecting the polarity and number of *Drosophila*

embryonic segments (Nusslein-Volhard and Wieschaus 1980). The locus was named

'fused' as *fu* adults produced from *fu*/+ females develop an apparent fusion of the third

and fourth longitudinal wing veins. *Fu* embryos display phenotypes similar to *hh* and *ciD*

embryos, indicating an essential role for *fu* in transducing high levels of Hh signaling

(Préat et al. 1993). Cloning and sequence analysis of the *fu* gene revealed that it encodes

a putative serine-threonine kinase with a large C-terminal extracatalytic domain (Préat et

al. 1990). Fu kinase activity has not been observed by any groups *in vitro*, yet key

nucleotide binding residues are conserved, suggesting that, similar to other defined

kinases, Fu may require a specific stimulus or microenvironment for activation. Two

classes of *fu* alleles have been defined, with different epistatic relationships to other Hh

pathway loci. Class I alleles contain mutations in the putative catalytic domain, whereas Class II alleles are defective in the large C-terminal extracatalytic domain. Both classes of *fu* alleles produce the same phenotype, although class II alleles show *cos2*-like phenotypes when *Su(fu)* is removed (Préat et al. 1993).

Fused protein is found in the HSC through direct association with Cos2 (Robbins et al. 1997; Sisson et al. 1997). In the absence of Hh ligand, Fu plays a minor role in promoting Ci-75 phosphorylation and proteolysis. Rapid phosphorylation of Fu is seen roughly 10 to 15 minutes after exposure of cultured cells to Hh ligand, making this one of the earliest known biochemical responses to Hh (Thérond et al. 1996). Fu is required for phosphorylation of Cos2 on Ser572 (Ruel et al. 2007). This phosphorylation event requires an intact Fu kinase domain, suggesting that Fu directly phosphorylates Cos2.

Recent data suggests that Fu is also capable of directly binding the cytoplasmic tail of Smo, specifically to the last 59 amino acids (Malpel et al. 2007). Surprisingly, deletion of this region, which is distinct from the PKA/CKI, Arg clusters and Cos2 binding domain, results in constitutive activation of the pathway. This region of Smo is also required to recruit Fu to the plasma membrane in response to Hh (Claret et al. 2007). Intriguingly, direct targeting of Fu to the plasma membrane via fusion to the palmitoylated domain of GAP43 is also sufficient to activate the pathway in cultured cells (Claret et al. 2007). Smo-mediated recruitment of Fu to the plasma membrane also does not require Cos2 (Claret et al. 2007). This has led to the proposal that Fu may function as a switch in Hh transduction, as opposed to simply being a downstream

16

effector of Smo. One possible sequence of events is a rearrangement of the HSC in relation to Smo after activation of Fu. Phosphorylation of Cos2 Ser572 by Fu could lead to partial dissociation of the HSC, followed by direct binding of Fu to the Smo C-tail, and weakened affinity of Cos2 for its cognate binding site on Smo (Claret et al. 2007; Ruel et al. 2007). Further biochemical studies, combined with a detailed understanding of the temporal series of events with respect to reception of Hh ligand at the cell surface, are necessary to resolve the issue of the mechanism of Fu function in the HSC.

Sufu

As indicated by the name, the *suppressor of fused* locus was identified as an extragenic suppressor of *fu* mutants (Préat 1992). Sufu contains no significant homology to unrelated proteins, other than a weakly conserved PEST domain, typically found in proteins that undergo rapid degradation and turnover (Pham et al. 1995). Sufu is weakly associated with the Fu-Cos2-Ci complex, and is also found in a trimeric complex with Ci and Fu, as well as bound solely to the N-terminus of Ci (Monnier et al. 1998; Stegman et al. 2000) Interestingly, *sufu* mutants display no overt phenotype, although the protein levels of both Ci-155 and Ci-75 are reduced in roughly equivalent proportions (Préat 1992; Ohlmeyer and Kalderon 1998; Lefers et al. 2001). Further, overexpression of Su(fu) inhibits nuclear accumulation of both full-length Ci and Ci-75, in a Cos2-dependent manner (Méthot and Basler 2000; Lefers et al. 2001), a fact confirmed by examination of transgenic Ci in *Su(fu)* mutant imaginal wing discs (Wang et al. 2000b). As Su(fu) undergoes Fu-dependent phosphorylation (Lum et al. 2003b), the genetic and

17

biochemical studies have led to a model where phosphorylation of Su(fu) by Fu alleviates cytoplasmic retention of Ci.

The observation that Ci protein levels are reduced in *Su(fu)* mutants, yet result in no obvious phenotype, are perplexing. Initially, it was proposed that Su(fu) opposes the formation of a labile, hyperactive form of Ci (Ohlmeyer and Kalderon 1998). There are numerous examples of transcription factors whose activities are controlled by the ubiquitin-proteasome system (Kodadek et al. 2006), and it has been shown in some instances that ubiquitination is required for full activation of proteins such as Myc (Muratani and Tansey 2003). Distinguishing a potential requirement of the proteasome in activating Ci will be challenging, given its essential function in limited proteolysis of full-length Ci to Ci-75. Further, since uncleavable forms of Ci are capable of activating Hh target genes yet do not show a reduction in protein levels (Price and Kalderon 1999; Méthot and Basler 2000; Price and Kalderon 2002), an absolute correlation between reduction in Ci levels and pathway activation remains to be demonstrated. An alternative explanation for the reduction of Ci protein levels in a *Su(fu)* background is increased degradation by factors such as HIB/roadkill (Kent et al. 2006; Zhang et al. 2006a). HIB is a member of a protein family with a conserved arrangement of MATH and BTB domains that serve as adapters for Cullin3-based ubiquitin ligases. Overexpression of HIB results in degradation of full-length Ci protein, which can be inhibited by Sufu in a dose-dependent manner. HIB and Sufu compete for Ci binding, thus removal of Sufu would be predicted to result in greater turnover of full-length Ci (Zhang et al. 2006a). Interestingly, *HIB* is upregulated in response to Hh signaling, so it may participate in a feedback loop

designed to limit the effects of Ci-Act after pathway activation. Low levels of *HIB* may

be sufficient for an increased rate of Ci turnover in the absence of Sufu. However, the

action of Ci-Act and Ci-75 is unlikely to be significantly perturbed without Sufu, thus

explaining the lack of phenotype observed in the relevant mutants (Préat 1992).

Evolutionary changes to the HSC in vertebrates

One of the most challenging aspects in understanding the mechanism of Hh

transduction in vertebrates is the fact that the functions of the components of the HSC do

not appear to be completely evolutionarily conserved. Further, it is unclear at this point in

time whether incorporation of the primary cilium into the Hh signal cascade has replaced

the *Drosophila* HSC, or if the primary cilium is a site of action for a kinesin-scaffolded

HSC.

Cos2 orthologs and vertebrate Hh signaling

Sequence analysis of kinesin-like proteins in vertebrate genomes revealed the

presence of several putative orthologs – Kif7 in zebrafish, and both Kif7 and Kif27 in

mice (Katoh and Katoh 2004a; Katoh and Katoh 2004b; Tay et al. 2005). In zebrafish,

cloning and analysis of Kif7 has shown that it behaves similarly to *Drosophila* Cos2, as a

predominantly negative regulator of Hh target genes. Further, zKif7 physically interacts

with Gli1, a Ci ortholog, suggesting it may indeed function as a cytosolic scaffold in this

system (Tay et al. 2005). Kif7 also plays a Hh-independent role in the establishment of

left-right asymmetry (Wilson et al. 2009b), a process that does not rely on Smo function in zebrafish (Chen et al. 2001).

A role for Kif7 or Kif27 in mammalian Hh transduction has been elusive. Single or combined knockdown of *Kif7* and *Kif27* in NIH 3T3 cells, a mouse fibroblast cell line that is responsive to Hh ligands, resulted in no significant perturbation of Gli reporter activity (Varjosalo et al. 2006). Further, the cargo domains of Kif7 and Kif27 displayed no potential to interact with Smo, and neither Kif7 nor Kif27 could restrict Gli2 or Gli3 nuclear translocation (Varjosalo et al. 2006). One possibility is that the primary cilium has replaced a Cos2-like scaffold to provide switch-like behavior downstream of Smo. This is consistent with the genetic and biochemical data in IFT mutant mice, which have compromised formation of Gli repressors and activators (Huangfu et al. 2003; Huangfu and Anderson 2005; Liu et al. 2005). In addition, Smo has been physically linked to the anterograde kinesin subunit Kif3a through a physical interaction with β-arrestin on the cilium (Kovacs et al. 2008). Nevertheless, given the caveats associated with reliance on RNAi to conclusively infer gene function, definitive proof of the involvement, or lack thereof, of *Kif7* and *Kif27* in mammalian Hh transduction can only be achieved by targeted deletion in mice. A major step towards this was recently reported, with disruption of *Kif7* in mice resulting in an increase in Hh signaling (Cheung et al. 2009) (Endoh-Yamagami et al. 2009). Further, Kif7 was reported to bind to the three mouse Gli proteins, although a direct association between full-length Kif7 and Smo has not yet been reported (Cheung et al. 2009; Endoh-Yamagami et al. 2009). Thus, initial evidence demonstrates that Kif7 plays an integral role in vertebrate Hh transduction, although the

extent of the mechanistic similarities between mouse Kif7 and *Drosophila* Cos2 remain

to be fully characterized.

Fused has divergent roles in vertebrate Hh signaling and motile ciliogenesis

The role of the Fu kinase has been another enigma in vertebrate Hh signal

transduction. Early studies indicated a weak role of Fu in potentiating Gli activator

function *in vitro* and in opposing the actions of Sufu (Murone et al. 2000). In zebrafish,

morpholino knockdown of *fu* results in weak Hh phenotypes in the developing somite

(Wolff et al. 2003); stronger Hh phenotypes, including cyclopia, can be seen when the *fu*

morpholino is co-injected with a *p53* morpholino (Eisen and Smith 2008; Wilson et al.

2009b). *Fu* also displays epistatic relationships with other Hh pathway genes in a similar

fashion to their *Drosophila* counterparts (Wolff et al. 2003). Surprisingly, targeted

disruption of the single mouse *Fu* ortholog had no discernible effect on embryonic

patterning (Chen et al. 2005; Merchant et al. 2005). *Fu* mutant animals die by 21 days

after birth, and display a Hh-independent defect in the central pair of microtubules of

motile cilia (Wilson et al. 2009a). Re-examination of *fu* morphant phenotypes in

zebrafish revealed a Hh-independent role for *fu* in proper biogenesis of motile cilia

(Wilson et al. 2009a). In addition to Hh patterning defects, *fu* morphants exhibit defects

in left-right asymmetry, which are not observed in *smo* morphants (Chen et al. 2001;

Wilson et al. 2009a). Thus, the design of Hh signal transduction in zebrafish can be

viewed as an "intermediate" state, in which components of the HSC are also utilized in

another unrelated cellular process. Intriguingly, mouse Kif27, but not Kif7, physically

interacts with mouse Fu, and localizes to the basal body of motile cilia (Wilson et al. 2009b), suggesting that Kif27 and Fu may partner in some fashion to control central pair microtubule assembly in motile cilia.

Sufu plays a prominent role in regulation of vertebrate Hh transduction

Mammalian Sufu was originally shown to bind all three Gli proteins, and is able to prevent Gli1, Gli2, or Gli3 from entering the nucleus when overexpressed (Ding et al. 1999; Kogerman et al. 1999). In sharp contrast to fly *su(fu)* mutants, targeted disruption of mouse *Sufu* results in a drastic upregulation of the Hh pathway, and lethality by embryonic day 9.5 (Cooper et al. 2005; Svärd et al. 2006). Consistent with this, knockdown or genetic ablation of *Sufu* in NIH 3T3 cells or mouse embryonic fibroblasts (MEFs) results in ligand-independent activation of Gli reporters (Svärd et al. 2006) (Varjosalo et al. 2006). In addition, morpholino knockdown of *sufu* results in a weak gain-of function Hh phenotype in the zebrafish myotome (Wolff et al. 2003). The essential role of Sufu in vertebrate Hh transduction could be explained if the function of Sufu, or its relationship with other cytoplasmic effectors of Hh signaling was altered during evolution. Alternatively, the basic mechanistic function of Sufu could be evolutionarily conserved, but its ability to interact with and regulate the three Gli proteins (as opposed to only Ci in *Drosophila*) may be affected. The altered role of Fu in vertebrate Hh transduction (Chen et al. 2005; Merchant et al. 2005; Wilson et al. 2009b) suggests that the cytoplasmic regulatory circuitry has been altered; this observation is supported by the fact that mouse *Sufu*; *Fu* double mutants phenocopy *Sufu* mutants (Chen

22

et al, manuscript in press). Mouse *Sufu* loss-of function models also indicate that, in contrast to *Drosophila* Sufu, mouse Sufu is not essential for cytosolic retention of overexpressed Gli1-eGFP, or endogenous Gli2 or Gli3 (Svärd et al. 2006)(Chen et al, manuscript in press). Yeast two-hybrid screens identified the mSin3a-SAP18 core-repressor complex as a potential binding partner of Sufu (Cheng and Bishop 2002; Paces-Fessy et al. 2004), indicating a potential nuclear role for Sufu in assembly of transcriptional repression complexes. Studies on a synthetic multimerized Gli-luciferase transcriptional reporter indicated that Sufu and SAP18 synergistically repressed transcription in HEK 293T cells (Cheng and Bishop 2002), but this result has thus far not been replicated, either in other cell lines or *in vivo* (Chen et al, manuscript in press).

Loss of *Sufu* in mammals leads to a drastic reduction in the levels of Gli2 and Gli3 protein (Chen et al, manuscript in press). Further, despite the ciliary localization observed with commercial Sufu antibodies, Sufu's effect on Gli2 and Gli3 stability is independent of the primary cilium (Chen et al, manuscript in press)(Jia et al. 2009). The role of Sufu in controlling Ci/Gli stability appears to be evolutionarily conserved, as the antagonism between Sufu and Spop, a mouse ortholog of *Drosophila* HIB, is maintained *in vitro* in mammalian cell culture (Chen et al, manuscript in press)(Zhang et al. 2006a). Gli may be a major contributor to the *Sufu* phenotype, as its expression is upregulated in a *Sufu*–/– background, it is refractory to Spop-promoted degradation, and RNAi of *Gli1* in *Sufu*–/– MEFs significantly reduces pathway activity (Svärd et al. 2006)(Chen et al, manuscript in press). Thus, duplication of the ancestral *Ci* gene, coupled with subfunctionalization and the formation of novel transcriptional feedback loops (*vide*

infra), may explain why the evolutionarily conserved action of Sufu has different net effects in various model organisms.

Contrasts between the Drosophila HSC and vertebrate cytosolic transduction

Relay of the Hh signal from the cell membrane requires kinesins and microtubule scaffolds both in *Drosophila* and vertebrates (Lum et al. 2003b; Tay et al. 2005; Cheung et al. 2009). Costal-2 and its orthologs, which are all members of the kinesin-IV subfamily, appear to be critical for control of generation of Ci/Gli activators and repressors. In mammals, the role of Fu in regulating the HSC has changed (Chen et al. 2005) (Merchant et al. 2005). If a Fu-like activity is required for control of mammalian Kif7, it is likely provided by an unrelated kinase. Coupling of Cos2 family members to Smo may be restricted to *Drosophila*, although this has not yet been exhaustively investigated in zebrafish or mice (Tay et al. 2005; Varjosalo et al. 2006; Cheung et al. 2009). Thus, it is currently unclear if binding of the HSC to Smo is an evolutionarily conserved step in connecting events at the membrane to Ci/Gli proteins. Despite this, Cos2 family members retain the ability to bind to Ci/Gli proteins (Tay et al. 2005; Cheung et al. 2009). Finally, the major effect of Sufu in mammals is independent of the primary cilium, but the relationship between Sufu function and Kif7 is unexplored.

Modifications in Ci/Gli regulation

In *Drosophila*, Ci is believed to provide all known Hh-dependent transcriptional activation and repression functions (Methot and Basler 2001). Regulation of limited proteolysis or activation of Ci is therefore of paramount importance. In invertebrates and some chordates, only one *Ci/Gli* gene has been identified (Takatori et al. 2002; Shimeld et al. 2007). Duplication of the ancestral *Ci/Gli* gene thus far appears to be specific to vertebrate lineages (Shimeld et al. 2007). Mice contain three *Gli* genes, *Gli1, Gli2*, and *Gli3* (Hui et al. 1994); further duplication in zebrafish has given rise to *Gli2a* and *Gli2b*, descendants of *Gli2* (Ke et al. 2005; Ke et al. 2008). The activator and repressor functions of Ci have been partitioned between the *Gli* genes (Sasaki et al. 1999). Gli3 functions predominantly as a transcriptional repressor, and has little activity in *in vitro* transcription assays, but in some limited contexts may contribute to transcriptional activation (Dai et al. 1999; Sasaki et al. 1999; Chen et al. 2004c; Tyurina et al. 2005). *Gli2* provides most of the essential *in vivo* Gli activator function in both zebrafish and all essential positive activity in mice (Park et al. 2000) (Matise et al. 1998; Karlstrom et al. 1999; Bai and Joyner 2001; Bai et al. 2002). *Gli1* makes a minor contribution to Hh-dependent responses in fish, but is dispensable in mice (Bai et al. 2002; Karlstrom et al. 2003).

There are several factors complicating the dissection of the precise role of individual Gli factors in the Hh response. First, redundancy in Gli activator and repressor function in a number of tissues and organs precludes attribution of specific phenotypic outcomes to a single *Gli* gene (Motoyama et al. 1998; Bai and Joyner 2001; Bai et al. 2002; Motoyama et al. 2003). Second, evolution of *Gli* transcriptional feedback loops in vertebrates has added robustness and additional layers of complexity to the Hh-dependent

transcriptional network. A major factor in this may be regulation of *Gli1* by both Gli3

repressor and Gli2 activator, as shown by *in situ* analysis and more recently, chromatin

immunoprecipitation (Marigo et al. 1996; Lee et al. 1997; Motoyama et al. 2003; Hu et

al. 2006; Vokes et al. 2008). Removal of Gli3 repressor, either genetically or through

modulation of factors controlling its stability, may result in derepression or even

activation at the *Gli1* locus. Third, post-transcriptional regulation of the Gli proteins is

more complex, as changes in ancestral Ci domain architecture in the individual Gli

proteins have led to alterations in regulation of specific Gli proteins by limited

proteolysis, complete destruction.

The PKA/GSK3/CKI cassette required for limited proteolysis of Ci into a

repressor is well-conserved in mammalian Gli2 and Gli3, but less so in Gli1 (Price and

Kalderon 2002). Despite this, Gli2 is much less efficiently cleaved into a repressor, and

this form can only be detected after an enriching precipitation with oligonucleotides

containing Gli consensus sites (Wang et al. 2000a; Pan et al. 2006; Pan et al. 2009). The

reduced capacity of Gli2 for limited proteolysis is attributed to two amino acid changes in

the recently identified processing determinant domain (PDD) (Pan and Wang 2007). The

PDD, which is similar in principle to a region of simple sequence in Ci, may provide a

region of unfolded or accessible protein backbone for degradation by the 26S proteasome

(Tian et al. 2005; Pan and Wang 2007). The stability of adjacent folded domains may

affect the processivity of the proteasome, thus determining whether proteolysis proceeds

and completely degrades the protein, or stops after the generation of a truncated

repressor. There are conflicting reports as to the role of PKA in regulation of Gli1, but

there is little substantial evidence supporting the notion that Gli1 is regulated by limited

proteolysis *in vivo* (Ruiz i Altaba 1999; Kaesler et al. 2000). Instead, PKA sites in Gli1

may regulate its activity through control of nuclear-cytoplasmic shuttling (Kaesler et al.

2000; Sheng et al. 2006).

The stability of Ci is regulated at multiple levels by different tissue-specific

adapters to E3 ubiquitin ligases (Dai et al. 2003; Zhang et al. 2006a). Similar to Ci, all

three Gli proteins have numerous signals for limited and complete proteolysis. Notably,

degradation sequences (termed degrons) are found in Gli1 and Gli2 binding to β-TrCP,

an adapter for E3 ubiquitin ligases (Bhatia et al. 2006; Huntzicker et al. 2006; Pan et al.

2006). These degrons are utilized differentially, as they are required for destruction of

Gli1, and either limited proteolysis or destruction of Gli2 (Bhatia et al. 2006; Huntzicker

et al. 2006; Pan et al. 2006). In addition, β-TrCP is required for limited proteolysis of

Gli3 (Wang and Li 2006). Additional degrons are present in Gli, which may utilize the

Numb-Itch ubiquitination pathway, or other, unidentified mechanisms of degradation (Di

Marcotullio et al. 2006; Huntzicker et al. 2006). Further studies are needed to resolve

how these multiple degradative pathways are utilized to control the availability of full-

length and repressor forms of the Gli proteins. It is also not known how a cell

discriminates or "decides" between specific degrons within a Gli. Finally, whether Sufu

is a general protective factor, or specifically antagonizes Spop-mediated degradation of

Gli2 and Gli3, remains to be investigated.

Future directions

Several major outstanding issues remain in the delineation of the mechanism of

Hh signal transduction, and many are common to invertebrates and vertebrates.

Cytosolic transduction of Hh in mammals

It is currently unclear how, once Smo is relieved from Ptch-mediated repression,

how activation of Smo is communicated to the Gli transcription factors. As described

earlier, a complex similar in principle to the *Drosophila* HSC has not yet been identified

in mammals, and it is not known if zebrafish Kif7 interacts directly with Smo to modulate

Gli activity (Tay et al. 2005). Further experimentation is needed to clarify whether the

Kif3a-β-arrestin-Smo complex is analogous to the HSC (Kovacs et al. 2008), or if either

Kif7 or Kif27 actually behaves in a manner similar to Cos2. In each case, the ability of

the full-length kinesin proteins to associate with Smo, Sufu, and the Gli proteins needs to

be assessed, as well as the subcellular localization of these components. Based on genetic

data, it has also been suggested that Smo signals to Sufu (Svärd et al. 2006; Jia et al.

2009). Biochemical evidence supporting this hypothesis is currently unavailable,

although it is noteworthy that mammalian Sufu is extensively phosphorylated, implying

that it is subject to some degree of post-transcriptional control (Paces-Fessy et al. 2004).

If true, this would represent another instance of re-wiring of cytosolic transduction, as fly

Smo is not known to communicate directly with Sufu. Identification of the cytosolic

28

intermediaries of vertebrate Hh signaling is critical to a thorough mechanistic understanding of the pathway.

Smo physically resembles a G-protein coupled receptor (GPCR), yet there are conflicting data as to whether coupling to a Gα subunit is essential for activation of Hh-dependent transcriptional responses (DeCamp et al. 2000; Lum et al. 2003a; Riobo et al. 2006; Low et al. 2008; Ogden et al. 2008). In cultured *Xenopus* melanophores, insect cells, and mammalian tissue culture, Smo appears to simulate Gαi-dependent responses, and GTP binding to Gαi proteins (DeCamp et al. 2000; Riobo et al. 2006). Despite this, no *in vivo* effect on Hh signaling has been observed upon activation or inhibition of Gαi in vertebrates. Recent data has shown that genetic manipulation of Gαi in *Drosophila* affects Hh signaling, primarily through classical effects of Gαi on PKA activity (Ogden et al. 2008). Surprisingly, Gαi interacted with Cos2 in a Hh-dependent fashion, but no physical associated with Smo has been reported (Ogden et al. 2008). A common role for G-protein receptor coupled kinase 2 (GRK2) has been demonstrated, suggesting that there may be some link between the classical GPCR machinery and Smo activation (Chen et al. 2004b; Meloni et al. 2006; Philipp et al. 2008; Philipp and Caron 2009). GRK2/GPRK2 and beta-arrestins may influence the membrane trafficking of Smo, thus affecting pathway activity through controlling the ability of Smo to reach the cell surface in fly, or the cilium in vertebrates (Chen et al. 2004b; Meloni et al. 2006).

Unique vertebrate modulators of Hh signaling?

A number of genes that may play unique, specific roles in vertebrate Hh transduction have been identified in the past several years. Many of these genes, such as *Iguana*/*DZip1* (encoding a zinc-finger / coiled-coil domain protein) and *Tectonic* (encoding a secreted / transmembrane protein of unknown function), appear to affect both Gli activator and repressor function, and impact the pathway downstream of Smo (Sekimizu et al. 2004; Wolff et al. 2004; Reiter and Skarnes 2006). This is similar to the chicken *talpid3* mutant, recently shown to encode a coiled-coil protein required for basal body docking to the membrane, and thus, ciliogenesis (Yin et al. 2009). It seems possible that *Iguana* and *Tectonic* might also impact cilium function, based on similar mutant phenotypes, but this requires further investigation. Genetic studies of the vesicle transport protein Rab23, a GTPase that is a cell-autonomous negative regulator of vertebrate Hh signaling, showed that Rab23 controls Gli2 and Gli3 activity (Eggenschwiler et al. 2006). Rab23 may regulate trafficking of Hh pathway components that inhibit Gli activator function. By contrast, the GTPase Arl13b appears to be required for generation of the Gli2 activator (Caspary et al. 2007). These, and other Rab proteins involved in biogenesis of the primary cilium (Oro 2007; Yoshimura et al. 2007), are likely to be useful targets for investigating the dynamics of Smo and Gli movement within the cell and on the primary cilium, and their relationships to states of pathway activation.

Mechanism of Ci/Gli action on target enhancers and promoters

30

A large gap in our understanding of the ultimate outcome of Hh signaling, namely Gli-dependent transcription, stems from a dearth of information regarding the mechanism of action of Gli proteins on endogenous enhancers and promoters. A number of putative co-activators (such as CBP, Mediator, and Hoxd12) and co-repressors (such as SAP18, mSin3a, and Ski) have been identified, although these effects and interactions have not been observed in a native context (Akimaru et al. 1997; Cheng and Bishop 2002; Dai et al. 2002; Chen et al. 2004c; Zhou et al. 2006). Recent work, using chromatin immunoprecipitation of an artificially tagged Gli1 activator and Gli3 repressor has allowed the identification of a number of *bona fide* endogenous Gli binding sites (Vokes et al. 2007; Vokes et al. 2008). Further studies of the detailed biochemical mechanism of Gli factors at these newly identified loci should continue to shed light on a number of unanswered questions. First, whether Gli activator and repressor forms act at the same Gli binding site is unknown, although the data suggest that this, in principle, could be the case for a subset of genes expressed both in neural tissue and the limb mesenchyme (Vokes et al. 2007; Vokes et al. 2008). This issue is of paramount importance, since many of the transcriptional mechanisms inferred from developmental studies of Hh pathway components rely on the assumption that Gli activator and repressor forms act on the same binding sites. Second, a comparison of the modes of transcriptional activation and the requisite cofactors for different classes of genes will be thoroughly informative. The expression of some Hh target genes is dependent on pathway activation (e.g. *Gli1*), whereas others must be expressed prior to induction of Gli activators but have their expression increased via positive feedback (e.g. *Ptch1*). Thus, it will be quite interesting

31

to discover possible similarities and differences in transcription of different types of

target genes.

Hh and Wnt signaling

Several studies and reviews have noted the similarities in Hh and Wnt signal

transduction (reviewed in (Kalderon 2002; Nusse 2003)). Both Hh and Wnt ligands are

palmitoylated, and this lipid modification is essential for high-level signaling activity

(Nusse 2003). Hh and canonical Wnt signaling modulate activity of the Ci/Gli and

Lef/Tcf transcription factors. In the case of Hh transduction, this is through direct control

of Ci/Gli proteolysis; in the Wnt cascade this is through control of the stability of β-

catenin, an activating cofactor of Lef/Tcf (Kalderon 2002; Nusse 2003). Both Ci/Gli and

β-catenin proteolysis are regulated through stepwise PKA/CKI/GSK3β phosphorylation,

followed by binding to SCF$^{\text{Slimb/β-TrCP}}$ and targeting to the proteasome. Scaffold protein

complexes (Cos2 for Hh; axin and APC for Wnt) play key roles in assembling the

relevant kinases and facilitating phosphorylation. Further, recruitment of these scaffold

proteins to positive membrane effectors (Smo, LRP) might serve as a common

mechanism for disruption of ordered phosphorylation and proteolysis (Mao et al. 2001;

Lum et al. 2003b; Tolwinski et al. 2003). Thus, despite the fact that Wnt and Hh

signaling likely do not derive from the same ancestral pathway, numerous aspects of Hh

and Wnt transduction share similar aspects of design.

32

With the discovery that primary cilia play a key role in transducing the Hh signal, it was logical to speculate that this organelle might also be involved in Wnt signaling. Disruption of genes such as *inversin* and the Bardet-Biedl Syndrome (BBS) family, which are integral for proper basal body structure and function, results in perturbation of planar cell polarity, a non-canonical branch of Wnt signal transduction (Ross et al. 2005; Simons et al. 2005; Gerdes et al. 2007). Supporting this, *Kif3a* mutant MEFs, which fail to grow cilia, show an increase in stabilized β-catenin (Corbit et al. 2008). This led to the hypothesis that cilia restrict the β-catenin/Lef/Tcf transcriptional response to extracellular Wnt ligand, and may control a balance between canonical and non-canonical arms of Wnt signaling (Corbit et al. 2008). It is thus surprising that mouse IFT mutants lack overt Wnt phenotypes, such as defects in gastrulation, and exhibit pronounced morphological defects apparently only from misregulated Hh transduction (Eggenschwiler and Anderson 2007). It is possible that specific IFT proteins that are not needed for proper cilium architecture are utilized for Wnt signaling, or that Wnt signaling through cilia is only required at later embryonic or post-natal stages. In addition, as the cytoplasmic 'switches' for Wnt and Hh signaling require the proteasome, it is worth noting that knockdown of BBS genes affects proteasomal function (Gerdes et al. 2007), and the proteasome was reported to accumulate at basal bodies/centrioles. Thus, any assessment of the role of cilia in Wnt signaling should take these cautions into account.

Ancestral roles of the primary cilium, Fu, and evolution of Hh signaling

The recent discoveries of the role of the primary cilium in vertebrate Hh transduction, as well as the evidence indicating that the Fu kinase is not essential in mice, raises several interesting questions concerning the origins and evolution of the Hh pathway. One central issue is whether the utilization of the primary cilium in Hh signaling reflects an ancient role for the organelle, or whether the cilium has been incorporated into the molecular circuitry of a pre-existing Hh architecture. Experiments focused on the role of primary cilia in Hh signaling in other vertebrates, such as *Ciona intestinalis* or *Branchiostoma floridae*, will provide key insights into this issue.

Strikingly, genes containing a Fu kinase domain are easily identifiable in all branches of the eukarya, with the exception of fungi. This includes plants, and single-celled eukaryotes such as *Chlamydomonas reinhardtii* and *Dictyostelium discoideum*. To date, every identified role of the Fu kinase family in eukarya involves microtubules and/or some aspect of cell polarity, even in organisms that lack cilia (Oh et al. 2005; Tang et al. 2008; Wilson et al. 2009b). Thus, it is possible that Fu may function in a basic, structural or polarizing pathway that has been co-opted by the Hh pathway in organisms such as *Drosophila* or zebrafish. The fact that mouse Fu can rescue the Hh-dependent and independent phenotypes in zebrafish *fu* morphants implies that the underlying mode of Fu action could be similar for two seemingly unrelated processes. An examination of the role of the Fu kinase in single-celled eukaryotes such as *Chlamydomonas*, which are biflagellated yet lack an intact Hh pathway, will shed light on this problem.

Assembly of the components of the Hh pathway into an ordered signaling pathway during evolution is a poorly-understood process, yet recent genome surveys and functional studies have shed light on possible events. The choanoflagellate *Monosiga brevicollis* contains orthologs of *Hh, Ptc, Disp* and *Fu*, yet lacks a *recognizable Smo* homolog (King et al. 2008). The basic principles of Disp-mediated release of Hh, and subsequent binding to Ptc, may have thus been established in the last common ancestor of choanoflagellates and metazoans. Acquisition of Smo, co-option of Fu, and recruitment of the cilium or the HSC in signaling may have subsequently occurred after the split of these two lineages. Both *Ciona intestinalis* and *Branchiostoma floridae* contain a single Ci/Gli and Smo ortholog; functional studies of *B. floridae* Gli indicate that activator and repressor functions are encoded by two different spliceoforms (Shimeld 1999; Hino et al. 2003; Yamada et al. 2003; Shimeld et al. 2007). Thus, other chordates and single-celled flagellated eukaryotes provide a unique and exciting opportunity to test mechanistic theories of Hh pathway evolution.

CHAPTER II

Fused has evolved divergent roles in vertebrate Hedgehog signaling and motile

ciliogenesis

Introduction

Modulation of Gli/Ci transcription factor form and activity is a key to generating graded Hedgehog (Hh) responses essential for correct tissue patterning (McMahon et al. 2003; Hooper and Scott 2005; Huangfu and Anderson 2006; Jia and Jiang 2006). In *Drosophila*, this cascade utilizes a microtubule-associated cytoplasmic signaling complex scaffolded by the atypical kinesin-4 family member Costal2 (Cos2), the putative serine-threonine kinase Fused (Fu), and the novel PEST protein Suppressor of Fused (Sufu) (Robbins et al. 1997; Sisson et al. 1997; Lum et al. 2003b; Hooper and Scott 2005; Miki et al. 2005; Jia and Jiang 2006). Understanding the molecular mechanism of Hh signal transduction is complicated by multiple observations indicating that cytoplasmic signaling events downstream of the positive membrane transducer Smoothened (Smo) do not appear to be conserved between different species (Huangfu and Anderson 2006). In mammals, Hh signaling is dependent on the presence of the primary cilium, an organelle present in most cell types during G0 (Eggenschwiler and Anderson 2007), and many components of the Hh cascade, including Smo, Patched1 (Ptch1), Gli1, Gli2, Gli3, and Sufu are found in this organelle (Corbit et al. 2005; Haycraft et al. 2005; Rohatgi et al. 2007). By contrast, Fu, which is essential for achieving maximal levels of Hh transduction in *Drosophila* (Préat et al. 1990; Préat et al. 1993), is dispensable for Hh signaling in mammals (Chen et al. 2005; Merchant et al. 2005). *Fu/Stk36*-deficient mice are viable and show no hallmarks of aberrant Hh signal transduction during embryogenesis (Chen et al. 2005; Merchant et al. 2005). Interestingly, *fu* morphants in zebrafish exhibit Hh-dependent phenotypes in the somites and are epistatic to *sufu*,

indicating that a subset of vertebrate species utilize Fu in the Hh cascade (Wolff et al. 2003). Investigating the role of Fu in mammals, and studying Fu in different species thus provides a unique opportunity to illuminate the design and evolution of the Hh signaling cascade. In the studies presented in this chapter, I demonstrate that mouse Fu is dispensable for Hh signaling at the cellular level, but is instead essential for the construction of the central pair (CP) apparatus of motile, 9+2 cilia. *Fu* mutant animals thus provide a novel mouse model of human primary ciliary dyskinesia. I show that multiple aspects of motile cilia ultrastructure and polarity are disrupted in *Fu* mutants. Mouse Fu interacts with Kif27, a mammalian Cos2 ortholog that participates in CP construction, as well as SPAG16L, an evolutionarily conserved component of the CP. Furthermore, we show that zebrafish Fu participates in both Hh signaling and generation of functional motile cilia, implying that a role of Fu in motile ciliogenesis is evolutionarily conserved. We hypothesize that gene duplication, particularly in the Cos2 kinesin subfamily, has led to partitioning of protein function between Hh transduction and motile ciliogenesis.

Results

Mouse *Fu* is essential for proper construction of the central pair (CP) apparatus of motile cilia

Fu/Stk36–deficient mice do not display defects in production of Hh ligands, or in *in vivo* activation of the target genes *Ptch1*, *Gli1*, or *Hip1* (Chen et al. 2005; Merchant et al. 2005).To further examine a potential, subtle role of Fu in mammalian Hh signaling,

we asked whether Hh-dependent Smo localization to the primary cilium was affected in the absence of Fu. Primary cilia, which have a "9+0" arrangement of 9 outer doublet microtubules (MTs) without two singlet central pair (CP) apparatus MTs, are required for Hh responses, and several Hh pathway components localize to the primary cilium (Davenport and Yoder 2005; Huangfu and Anderson 2006). We found that primary cilia formed normally in *Fu–/–* mouse embryonic fibroblasts (MEFs), trafficked Smo to the primary cilium in response to Hh signaling, and exhibited a typical Gli transcriptional response (Figure 2-1). This suggests that the single mammalian Fu ortholog is dispensable for Hh signaling. To investigate the function of *Fu* in mice, we examined its expression in postnatal tissues by *in situ* hybridization. *Fu* transcript was expressed strongly in the respiratory epithelium, the ependymal lining of the ventricles in the brain, and in oviduct and testis (Figure 2-2; data not shown). These expression patterns were reminiscent of genes that play a role in the biogenesis of motile cilia, which function in the respiratory tract, brain, oviduct, and testes to propel mucus, fluid, and cells. Disruption of motile cilia function in humans leads to primary ciliary dyskinesia (PCD), which is associated with recurrent respiratory infection, hydrocephalus, and infertility (Afzelius 2004; Zariwala et al. 2007; Marshall 2008). To determine whether motile cilia function is compromised in *Fu–/–* mice, we studied cilia axonemal ultrastructure by transmission electron microscopy (TEM). In wild-type animals, over 99% of motile cilia in the trachea and ependyma of the lateral ventricles of the brain displayed the classical "9+2" arrangement of 9 outer doublet MTs and two singlet CP apparatus MTs (Figure 2-3, Figure 2-4). By contrast, approximately 40% of *Fu–/–* cilia lacked the central pair apparatus (Figure 2-3); in a subset of these axonemes, outer doublet translocations, in

which an outer doublet MT pair moves to the position occupied by the CP, were also observed. The remaining 20% of ciliary axonemes displayed a wider variety of MT defects, including loss or gain of a single CP MT, and loss of outer doublet MTs. Notably, the total percentage of tracheal cilia with ultrastructural defects was similar at postnatal days 1 and 14, suggesting that loss of CP MTs might stem from a failure to initiate outgrowth of the structure, rather than progressive loss of the CP resulting from microtubule instability or external mechanical forces.

The CP apparatus plays a key role in regulating ciliary motility (Smith and Lefebvre 1997; Smith 2002), but the process of CP formation is poorly understood. Unlike the outer doublet MTs, which utilize the triplet cartwheel of the basal body as a template for MT outgrowth (Dawe et al. 2007), no definitive microtubule template for the CP apparatus has been identified. The CP MTs originate at a region of the basal body known as the basal plate, which is characterized by electron-dense material between the outer doublet and CP MTs (McKean et al. 2003). Studies of conditional γ-tubulin mutants in trypanosomes have led to the hypothesis that γ-tubulin may assist in CP nucleation in this region of the basal body (McKean et al. 2003). Although we did not observe gross mislocalization of gamma tubulin in tracheal epithelial cells, analysis of the basal plate region in *Fu*–/– animals showed that CP MTs do not form in this region (Figure 2-5), further supporting the hypothesis that Fu is required for efficient initiation of CP outgrowth. Taken together, our findings indicate that mammalian *Fu* is dispensable for Hh signaling and specifically participates in generation of the CP apparatus in motile cilia axonemes.

Mice lacking functional *Fu* are born with no immediately obvious phenotype, but fail to thrive in comparison with wild-type or heterozygous littermates and die between postnatal days 7 and 21 (Chen et al. 2005; Merchant et al. 2005). The precise cause of death is unknown, but *Fu*–/– animals display bilateral suppurative rhinitis and partially penetrant hydrocephalus, which in many cases may arise from failure of motile cilia to directionally propel fluid (Marshall 2008; Marshall and Kintner 2008). To reveal the functional consequences of loss of the CP apparatus in *Fu* –/– animals, we examined fluid flow in tracheal explants. Analysis of fluorescent bead movement revealed strong coordinated distal-proximal directional flow in wild-type explants, whereas beads overlaid on *Fu*–/– tracheae exhibited severely impaired velocity and little to no directional movement (Figure 2-6). Quantification of linear particle velocity showed a drastic reduction from a mean velocity of ~25 µm/sec in wild-type explants to 5 µm/sec in *Fu*–/– mutant explants. We next asked if elimination of the CP apparatus in *Fu*–/– animals was sufficient to completely disrupt motion of the cilia themselves. In wild-type tracheae, cilia beat in a linear path with a quick forward power stroke and a slower recovery stroke (Chilvers et al. 2003a; Chilvers et al. 2003b), which was verified by time-lapse differential interference contrast (DIC) microscopy on tracheal explants (Figure 2-7). *Fu*–/– cilia moved stiffly and had a significantly reduced stroke amplitude; a subset of these cilia were either virtually immotile or beat in a slow, circular motion (Figure 2-6). In contrast to wild-type cilia, which beat in a coordinated fashion with neighboring cilia to produce a metachronic wave (Yang et al. 2008), those cilia in *Fu*–/– animals which did beat appeared disoriented and frequently collided with neighboring cilia (Figure 2-7).

This prompted us to investigate if the polarity of cilia orientation was perturbed. Cilia polarity is specified by a basal body structure known as the basal foot, a triangular protrusion that points in the direction of the effective stroke (Frisch and Farbman 1968; Mitchell et al. 2007). We first measured the mean polar orientation of basal feet in TEM micrographs representing individual cells from wild-type and *Fu–/–* tracheae. Next, the circular standard deviation (CSD), which measures the variation of cilia orientation around the mean, was calculated (Mitchell et al. 2007). In wild-type tracheae, basal feet generally pointed along similar paths, and had a CSD of approximately 16-17˚. In *Fu–/–* mutants, basal feet were disoriented and were frequently found pointing at right angles or antiparallel to one another, and the CSD of cilia polar orientation within a given cell was significantly higher, ranging from 34-37˚. Notably, the mean CSD values in both wild-type and *Fu–/–* cells did not appreciably differ when measured at postnatal days 1 and 14, suggesting that cilia polarity does not change over time. Thus, loss of CP microtubules in *Fu–/–* mice eliminated directional fluid flow, resulting from failure to generate a coordinated ciliary beat and global disorganization of cilia polarity. It is currently unclear whether cilia polarity is directly linked to assembly of CP MTs, and whether Fu regulates both processes via shared or distinct mechanisms needs to be further investigated.

Zebrafish Fu functions in both the Hh signal transduction pathway and motile ciliogenesis

The striking observation that mouse *Fu* is dispensable for Hh signaling yet participates in construction of the motile cilium prompted us to investigate Fu function in

other vertebrates. We re-examined the role of Fu in zebrafish, since prior reports have indicated that *fu* morphants exhibit mild Hh-dependent somite phenotypes, and genetically interact with other Hh pathway genes in a manner identical to *Drosophila* (Wolff 2003). By delivering a higher concentration of *fu* morpholino and blocking non-specific cell death by co-injection of a *p53* morpholino (Eisen and Smith 2008), we observed stronger Hh phenotypes, including cyclopia (data not shown). Next, we looked at the floor plate, which contains two cell subpopulations. The medial floorplate (MFP), which is comprised of a single row of cells, is specified by the actions of the *cyclops*, *one-eyed pinhead*, and *schmalspur* genes, and expresses *sonic hedgehog* (*shh*) (Odenthal et al. 2000). The lateral floor plate (LFP), which occupies 2-3 additional rows of cells flanking the MFP, expresses *fork head 4* (*fkd4*), and requires *shh* expression from the MFP or notochord for *fkd4* induction (Odenthal and Nüsslein-Volhard 1998; Schauerte et al. 1998). Morpholino knockdown of *fu* resulted in a reduction of *shh* expression in the MFP (Figure 2-8), possibly a result of failure to maintain the MFP population (Varga et al. 2001). In addition, the number of *fkd4*+ LFP cells was reduced (Figure 2-8), consistent with a requirement of *fu* for promotion of *shh*-dependent cell fates in the zebrafish ventral neural tube.

Knockdown of zebrafish *fu* activity also greatly reduced *ptc1* staining in the somites, suggesting disruption of Hh responses in this tissue (Fig 2-9). The muscle pioneer population, which is specified by Hh signaling and marked by expression of *engrailed1* (*en1*), was also lost (Figure 2-9). In addition, *fu* morphants developed U-shaped somites in place of normal, chevron-shaped somites (Figure 2-9), which are

43

characteristic of Hh signaling defects and are observed in the zebrafish *you* class of mutants (van Eeden et al. 1996). Finally, we asked if knockdown of *fu* was sufficient to rescue constitutive, cell-autonomous pathway activation caused by loss of *patched*. Indeed, up-regulation of Hh target genes was abolished in *ptc1*; *fu* double morphants, arguing in favor of a cell-autonomous role of Fu in Hh transduction downstream of *ptc1* (Figure 2-9). Taken together, these results provide convincing evidence for an integral role of Fu in the zebrafish Hh pathway, comparable to the role of Fu in *Drosophila* Hh transduction. Notably, genetic analyses of core Hh pathway components in both *Drosophila* and fish demonstrate a common set of epistatic relationships (Wolff et al. 2003).

We next asked if mouse Fu was able to compensate for loss of zebrafish Fu. Surprisingly, co-injection of mouse *Fu* mRNA and the zebrafish *fu* morpholino was able to rescue all Hh phenotypes, including cyclopia, loss of lateral floor plate, and muscle pioneer differentiation (Figure 2-9). Thus, mouse Fu retains the information necessary to participate in the fish Hh pathway, implying that a common mechanism underlies critical aspects of Hh signaling and motile ciliogenesis.

The involvement of Fu in mammalian motile cilia function could represent an evolutionary innovation that occurred after divergence of mammalian and teleost lineages. Alternatively, Fu may play a role in motile cilia function in a number of species. Interestingly, the genomes of a diverse range of organisms, including plants and flagellated unicellular eukaryotes, contain genes encoding a highly conserved Fu kinase

domain (Figure 2-10). To test this idea, we first examined *Fu* expression by *in situ* hybridization in different vertebrate species and found strong expression in the chick tracheal epithelium and the oviduct and testis of *Xenopus tropicalis* (Figure 2-11; data not shown), in patterns similar to mouse *Fu*. Thus, *Fu* is expressed in a similar range of adult tissues in tetrapods, strongly suggesting that it plays a conserved role in 9+2 cilia function. We then focused on zebrafish, which utilize a population of motile, 9+2 cilia in Kupffer's vesicle to establish left-right asymmetry (Kramer-Zucker et al. 2005). In contrast to mice, Hh signaling does not appear to be essential for L-R asymmetry in zebrafish, as *smo* mutants do not display laterality defects (Chen et al. 2001). Therefore, we reasoned that L-R asymmetry would be disrupted in zebrafish if Fu also participated in 9+2 cilia biogenesis. We examined the positioning of the heart and visceral organs by *cardiac myosin light chain 2* (*cmlc2*) and *fork head domain protein FKD2* (*fkd2*) expression, respectively. 41% of *fu* morphants displayed reversed or straight hearts (Figure 2-11), while 30% of injected embryos had abnormal positioning of the gut, liver and pancreas (Figure 2-11). Thus, Fu is required for proper cardiac jogging/looping and orientation of endoderm-derived organs. In agreement with prior reports, *smo* mutants exhibited no significant L-R defects (Figure 2-11). To investigate if Fu is required for early establishment of symmetric gene expression in the left lateral plate mesoderm (LPM), we studied the expression of *southpaw* (*spaw*) and *paired-like homeodomain transcription factor 2* (*pitx2*) in *fu* morphants (Long et al. 2003). In 73% of *fu* morphants, *spaw* was found to be on the right side, bilaterally distributed, or absent in the LPM (Figure 2-11). Similarly, 71% of *fu* morphants had significantly reduced or absent *pitx2c* staining in the LPM (data not shown). Co-injection of mouse *Fu*, but not *Drosophila fu*

with *fu* morpholino was sufficient to restore left-right asymmetry (Figure 2-11; data not shown).

To confirm a direct role of Fu in regulating KV function, and thus explain the observed defects in L-R asymmetry establishment, we injected fluorescein-labeled *fu* morpholino into dorsal forerunner cells (DFCs), which migrate at the leading edge of the embryonic shield to produce KV (Shu et al. 2007). 44% of embryos with a strong fluorescent signal in the DFCs developed cardiac laterality defects (data not shown), indicating that knockdown of *fu* in KV accounts for the L-R asymmetry defects. Cells in both the ventral roof and dorsal floor of KV possess motile cilia, which point posteriorly and generate fluid flow. The direction of fluid flow is clockwise when viewed from the apical surface, and counterclockwise when viewed basolaterally (Okabe et al. 2008). This fluid flow is essential for proper establishment of L-R asymmetry. Examination of KV cilia in *fu* morphants by electron microscopy revealed disorganized axonemal structures, including loss and acquisition of CP MTs and outer doublet translocations, which were similar to the defects observed in mouse *fu* mutants (Figure 2-11). Therefore, vertebrate Fu has a conserved role in CP apparatus construction. Loss of *fu* also affected cilia motility, as revealed by injecting rhodamine-conjugated dextran beads into KV of *fu* morphants at the 8-somite stage (Figure 2-12). Of the 6 morphants evaluated, 5 were defective in establishing a counterclockwise flow, and no consisted, directional pattern of flow was observed. As with the other phenotypes examined in *fu* morphants, the defect in cilium-generated counterclockwise flow was rescued by co-injection of mouse *Fu*, but not *Drosophila* Fu (Figure 2-12; data not shown). Taken together, the data strongly

support a conserved, Hh-independent role of Fu in vertebrate 9+2 cilia biogenesis and/or function.

Fu interacts with a vertebrate ortholog of *Drosophila* Costal-2 that also participates in motile ciliogenesis

Studies of Hh signaling in *Drosophila* have established that Fu binds to the atypical kinesin Cos2, a member of the kinesin-4 subfamily, in order to transduce the signal downstream of Smo . In mammals, two Cos2 orthologs, Kif7 and Kif27, have been identified (Katoh and Katoh 2004a; Katoh and Katoh 2004b; Varjosalo et al. 2006). It is currently unclear if either participates in Hh transduction; RNAi studies have indicated that neither Kif7 nor Kif27 is essential for Hh signaling in cultured cells (Varjosalo 2006), although technical limitations in measuring the efficacy of knockdown in these experiments may have clouded interpretation of the reported results. In zebrafish, Kif7 is the only identified Cos2 ortholog, and morpholino knockdown of *kif7* results in Hh phenotypes (Tay 2005). In order to understand how Fu might function in motile ciliogenesis, we examined if mouse Fu retained the ability to bind to Cos2 orthologs. When expressed in HEK 293T cells and mouse tracheal epithelial cells (MTECs), Fu-FLAG was able to bind strongly to Kif27-myc, but not Kif7-myc (Figure 2-13). This suggested a possible role for Kif27 in generation or regulation of 9+2 cilia. To pursue this, we acquired *Kif27* knockout mice from Chi-Chung Hui at the University of Toronto. Similar to *Fu* mutant mice, *Kif2* –/– animals survived embryogenesis and displayed no overt defects characteristic of perturbed Hh signaling (data not shown). *Kif27*–/– mice

were hydrocephalic, displayed mild ataxia, and were smaller than wild-type or heterozygous littermates (data not shown). Analysis of tracheal cilia revealed a spectrum of CP MT defects, similar to *Fu–/–* animals (Figure 2-14). In addition, a qualitative assessment of basal foot orientation in *Kif27–/–* animals showed an increased degree of disorder (Figure 2-14). Taken together, the data indicate that Kif27, like Fu, participates in motile ciliogenesis in mice. RT-PCR analysis of *Fu* and *Kif27* transcript levels during differentiation of ciliated cells indicated upregulation of both messages after initiation of differentiation (Figure 2-15).

Analysis of available Cos2, Kif7, and Kif27 protein sequences indicates that the tetrapod Kif7/Kif27 genes may have arisen through a duplication event (Figure 2-16). The four fish species examined did not contain an obvious Kif27 ortholog, suggesting either a fish *Kif27* gene may have been lost after gene duplication, or that the duplication event occurred after divergence of the fish and amphibian lineages. To distinguish between these possibilities, we first tested whether zebrafish Fu and zebrafish Kif7 physically interacted. Transfected myc-tagged zKif7 weakly co-immunoprecipitated with zFu-FLAG in HEK 293T lysates, further demonstrating an evolutionarily conserved physical interaction between Fu and a Cos2 ortholog (Figure 2-13). This suggested that *kif7* could have an essential function in motile ciliogenesis in zebrafish. Morpholino knockdown of *kif7* in zebrafish resulted in both Hh-specific phenotypes (Tay et al. 2005)(data not shown) and disruption of L-R asymmetry (Figure 2-17). We also found that mouse Fu co-precipitated zebrafish Kif7 (Figure 2-13); this interaction provides a mechanistic explanation for the ability of mouse *Fu* to rescue zebrafish *fu* morphants.

To gain more insight into the cellular functions of mouse Fu and Kif27, we turned

to an *in vitro* model of mouse tracheal epithelial cell (MTEC) differentiation (You et al.

2002). Primary MTECs are seeded on a semi-permeable collagen-coated filter with

culture media supplied to the apical and basolateral surface. After the MTECs reach

confluence and tight junctions form, media is removed from the apical surface to create

an air-liquid interface (ALI), which serves as a cue to initiate further apical-basolateral

polarization and ciliogenesis. During this process, hundreds of centrioles form within the

cytosol, migrate to the apical surface of the cell, dock with the membrane to form basal

bodies, and serve as templates for the outgrowth of the outer MT doublets of the ciliary

axoneme (Dawe et al. 2007). We lentivirally transduced Kif27-GFP into wild-type

MTECs and assessed its localization throughout a time course of MTEC differentiation.

At ALI days 0 and 5, Kif27-GFP punctae were associated with centrioles as determined

by antibody staining against γ-tubulin (Figure 2-18). Three-dimensional rendering of

acquired confocal stacks indicated that the Kif27-GFP fusion protein localized to the side

of the centriole; it is presently unclear whether this corresponds to the location of

accessory structures such as the basal foot or ciliary rootlet (Yang et al. 2002). At ALI

day 7 and beyond, Kif27-GFP was associated with the base of the cilium after cilia

outgrowth was initiated, but was not detected on the axoneme in significant quantities

(Figure 2-19). Localization of Kif27-GFP to basal bodies was also observed in polarized

MDCK cells, indicating that this ability to cluster at the basal body is an inherent

property of Kif27 (Figure 2-18).

We assessed localization of a Fu-mCherry fusion protein in MTECs. By contrast with Kif27-GFP, Fu-mCherry was distributed throughout the cytoplasm of MTECs throughout differentiation, and was not observed to discretely localize to either the cilium base or axoneme (Figure 2-17; Figure 2-20). When overexpressed in *Fu–/–* MTECs, Kif27-GFP was still found at the centriole/basal body during differentiation, indicating that Fu is not essential for controlling subcellular localization of Kif27 (data not shown). Taken together, the data favor a model in which Kif27 may direct or coordinate the localization or activity of Fu. Further studies utilizing kinase dead versions of Fu and identifying potential substrates of Fu are necessary to further clarify its precise role in construction of motile cilia.

Fu physically interacts with an evolutionarily conserved component of the CP apparatus

The process of CP construction in 9+2 cilia is poorly characterized, and Fu and Kif27 are the first non-axonemal components known to control its assembly. To determine how Fu and Kif27 regulate this process, we explored potential relationships between Fu/Kif27 and known CP structural components. Two of the best-studied mammalian CP proteins are SPAG6 and SPAG16L, evolutionarily conserved orthologs of the *Chlamydomonas reinhardtii* flagellar proteins PF16 and PF20 (Sapiro et al. 2000; Pennarun et al. 2002; Zhang et al. 2002). PF20 was shown to decorate the C2 microtubule along the intermicrotubule bridges between CP MTs (Smith 1997), and PF6 was found to localize to the C1 MT (Smith and Lefebvre 1996). Loss of PF16 or PF20 leads to

paralyzation of flagella and loss of the CP MTs, indicating the importance of these proteins in construction and/or maintenance of the CP (Dutcher et al. 1984). Knockout studies of SPAG6/PF16 and SPAG16L/PF20 in mice revealed a conserved role of these genes in mammalian motile cilia/flagella function. Genetic elimination of *Spag6* in mice disrupts proper formation of the sperm flagellum, with loss of CP MTs, resulting in male infertility (Sapiro et al. 2002). *Spag6* null animals also develop hydrocephalus, implying that motile cilia are affected (Sapiro et al. 2002). Loss of *Spag16L* causes male infertility, although in contrast to *Chlamydomonas* Pf20 mutants, the CP MTs are intact (Zhang et al. 2006b). Interestingly, *Spag6*; *Spag16L* double mutants display more severe phenotypes, including more pronounced hydrocephalus and growth retardation, yet the CP MTs in both the brain and lung remain unaffected (Zhang et al. 2007). Given the paucity of other identified players in CP assembly, we investigated if either Fu or Kif27 physically interacted with SPAG6 or SPAG16L. When expressed in HEK 293T cells, Fu-FLAG efficiently co-immunoprecipitated SPAG16L-HA, but not SPAG6-HA (Figure 2-21). Immunoprecipitated Kif27-myc was unable to co-immunoprecipitate either SPAG16L-HA or SPAG6-HA, further confirming the specificity of the SPAG16L-Fu interaction (data not shown). Antibody staining against SPAG6 or SPAG16L in *Fu–/–* MTECs did not show any disruption of SPAG6 or SPAG16L localization along the motile cilium axoneme (Figure 2-22). Therefore, while SPAG16L links Fu to a potential site of action, the mechanism of Fu action remains elusive.

Discussion

A model for Fu and Kif27 function in motile cilium assembly

The data favor a model in which Kif27 and/or Spag16L direct the localization or activity of Fu for central pair construction (Figure 2-23), since the distribution patterns of overexpressed Kif27-GFP or endogenous Spag16L are not altered in *Fu*–/– MTECs. After targeting to an appropriate region of the cell, Fu may phosphorylate additional target proteins that participate in central pair assembly. We were unable to detect a specific interaction between Fu and either α-, β-, or γ-tubulin (data not shown), implying that the effect of Fu on microtubules is indirect. Kif27 resembles a classical, functional kinesin heavy chain molecule (Katoh and Katoh 2004b), and a Spag6/Spag16 complex has been shown to decorate cytoplasmic microtubules (Zhang et al. 2002), supporting a model where these proteins target Fu for subsequent action on microtubules and their associated proteins. Efforts to demonstrate Fu kinase activity *in vitro* have not been successful (data not shown) (Ascano and Robbins 2004), suggesting that Fu may require a specific stimulus or microenvironment for its activity, similar to other better-characterized kinases (Ramaswamy et al. 1998; Elzi et al. 2001). Use of a putative kinase-dead form of Fu to rescue defects in *Fu*–/– MTECs or animals will partially resolve the issue of whether Fu kinase activity is required for central pair assembly. Identification of *bona fide* Fu substrates and other interacting partners is also essential for a complete understanding of the mechanism of Fu function in central pair construction. Unbiased orthophosphate labeling experiments in wild-type and *Fu*–/– MTECs, coupled with chemical genetics approaches (Allen et al. 2007), are appropriate methodologies to use in addressing this issue.

A connection between Fu and the evolutionarily conserved planar cell polarity (PCP) pathway may exist. The PCP pathway has recently been implicated in multiple aspects of ciliogenesis, and Dishevelled and Rho GTPase have been shown to be critical for both formation and orientation of cilia in amphibians (Marshall and Kintner 2008; Park et al. 2008). The observed defects in basal foot polarity in *Fu*–/– mice could result from defects in PCP signaling, and it will be instructive to determine whether Fu or Kif27 physically or genetically interact with known components of the PCP network. Notably, a conserved member of the PCP pathway, Vangl2/Lpp1, localizes to apically docked basal bodies in MTECs (Figure 2-24). Another possibility is that loss of the central pair microtubules, with the resulting disruption of directional fluid flow, affects small-scale refinement of pre-existing polarity. Prior work using *Xenopus* skin explants, which possess motile cilia, has shown that imposition of an external fluid flow can bias cilia orientation (Mitchell et al. 2007). Establishment of directional fluid flow over cultured MTECs, which do not produce a directionally coordinated beat after differentiation (data not shown), would provide a first step to address this question in a wild-type and *Fu*–/– background.

The phenotype of *Fu*–/– animals, combined with the lack of discernible effects on Hh-dependent cellular assays, indicate that the single mouse *Fu* ortholog has no essential role in Hh signal transduction. To date, the Hh pathway has not been implicated in any aspect of ciliogenesis, either with primary or motile cilia. Our data also indicate that motile cilia outgrowth or gross motility is unaffected when cultured in the presence of

pharmacologic inhibitors of Smo activity (Fig). Thus, if a "Fu-like" activity is required in mammalian Hh signaling, it is likely provided by an unrelated kinase. Indeed, mouse Fu is more closely related by sequence to a putative *Chlamydomonas* Fu ortholog than to other mouse kinases (Table 1). Several kinases that affect vertebrate Hh transduction have recently been identified (Chen et al. 2004b; Evangelista et al. 2008), and their relationships to Smo and the Gli proteins bears further investigation.

There are conflicting reports on the role of Kif7 and Kif27, the closest vertebrate relatives of *Drosophila* Cos2, in Hh signaling (Tay et al. 2005; Varjosalo et al. 2006). Based on the data presented here, we predict that Kif27 does not play a significant role in mammalian Hh signal transduction, as mice lacking functional Kif27 exhibit phenotypes similar to Fu. As zebrafish Kif7 and Fu participate both in Hh signaling and central pair assembly, we speculate that Fu evolved or retained an ancestral function in vertebrate central pair construction. Duplication of ancestral Cos2 in the vertebrate lineage likely led to a partition of Hh-related and motile-cilium dependent functions for Kif7 and Kif27, with Kif27 retaining its partnership with Fu. This phenomenon has been termed 'subfunctionalization', and is one potential mechanism for the evolution of new protein interaction networks (Lynch and Conery 2000; Wagner et al. 2007). With the apparent loss of essential Fu and Kif27 function in Hh signaling, one major outstanding question is how are signals at the cell membrane transmitted from Smo to the Gli proteins? Despite the lack of *in vitro* evidence for Kif7 in this role (Varjosalo et al. 2006), genetic loss-of-function studies are required to definitively address if Kif7 participates in this process. Alternatively, the involvement of the primary cilium as a scaffold for Hh pwathway

components in vertebrates could circumvent the need for a Fu-kinesin complex in transducing the signal (Kovacs et al. 2008). Further analysis of Fu and Kif27 function in motile ciliogenesis and Hh signaling in diverse species will provide additional insight into the evolution of both processes.

Figure Legends

Figure 2-1: Primary cilium formation and Smo trafficking are unaffected in *Fu* null MEFs

Immunofluorescent images of wild-type (top) and *Fu* null (bottom) MEFs stained with antibodies against acetylated tubulin (red) and Smo (green). Primary cilia form in both cell lines, and Smo traffics to the cilium in response to exogenous ShhN ligand.

Figure 2-2: *Fu* transcript is expressed in respiratory epithelium, neural ependymal cells, and testis

Expression of *Fu* (pink signal) in the mouse tracheal epithelium (**A**), ependyma of the lateral ventricles (**B**), and testis (**C**) at postnatal (p) day 14 by section *in situ* hybridization to *Fu*. Arrows indicate sites of *Fu* expression.

Figure 2-3: *Fu* mutant tracheal motile cilia display abnormal central pair ultrastructure at post-embryonic days 1 and 14

Transmission electron micrographs (TEM) of motile cilia from wild-type (wt) (**A**) and

$Fu^{-/-}$ (**B**) tracheae. Arrows denote the CP microtubules. (**C**) Quantification of

ultrastructural defects from p1 (wt, n = 4 animals, mean 88 cilia/animal; $Fu^{-/-}$, n = 4

animals, mean 64 cilia/animal) and p14 (wt, n = 7, mean 113 cilia/animal; $Fu^{-/-}$, n = 6

animals, mean 93 cilia/animal) tracheae. Error bars indicate standard deviation (s.d.).

Figure 2-4: Motile cilia in neural ependymal cells of *Fu* mutant mice display ultrastructural defects in central pair microtubules

Transmission electron micrographs (TEM) of motile cilia from wild-type (wt) (**A**) and

$Fu^{-/-}$ (**B**) neural ependymal cells. Arrows denote the CP microtubules. (**C**)

Quantification of ultrastructural defects from p14 (wt, n = 2 animals, mean 147

cilia/animal; $Fu^{-/-}$, n = 2, mean 61 cilia/animal). Error bars indicate standard deviation

(s.d.). *Fu*-deficient mice do not display organ laterality defects (data not shown),

indicating normal function of the mouse node, which establishes left-right asymmetry

during embryogenesis. $Fu^{-/-}$ mice developed respiratory infections, highly penetrant

hydrocephalus, stunted growth and poor general health that likely led to lethality (data

not shown).

Figure 2-5: Central pair microtubules are absent from the basal plate of *Fu* mutant tracheal motile cilia

(**A-F**) Transmission electron micrographs of motile cilia axonemes from wild-type (wt) and $Fu^{-/-}$ tracheae. Arrows denote the CP microtubules. In $Fu^{-/-}$ animals, CP microtubules are missing in both the axonemes (**D**) and in the basal plate (**E**), which is characterized by electron dense material surrounding the outer microtubules and is the site of CP outgrowth (McKean et al. 2003). Outer microtubule doublets and associated structures are grossly normal in $Fu^{-/-}$ animals (**F**). (**G**) Schematic lateral view of a wt 9+2 cilium depicting the locations of the transition zone, basal plate, and ciliary axoneme.

Figure 2-6: Reduced tracheal flow, velocity, and cilium motion in motile cilia from *Fu* mutants

(**A, B**) Traces of fluorescent bead movement over tracheal explants. (**C**) Mean particle velocity in p14 wt (n = 5) and $Fu^{-/-}$ (n = 5) tracheae. Error bars indicate s.d. (**D, E**) Traces of cilia beat path overlaid on still DIC images of tracheal cilia (upper), and lateral traces of cilia waveform (lower). Mean ciliary beat frequency (CBF) was calculated from 30 cilia (n = 3 animals for wt and $Fu^{-/-}$). Arrows indicate directions of the forward effective strokes.

Figure 2-7: *Fu* mutants display disorganized motile cilium polarity in the trachea

(**A, B**) Representative TEM images of basal foot polarity (arrows) in p14 wt and $Fu^{-/-}$ tracheae. (**C**) Quantification of circular standard deviation (CSD) of basal feet from p1 (wt, n = 24 cells from 4 animals; $Fu^{-/-}$, n = 38 cells from 4 animals; $P < 3.4 \times 10^{-6}$;

unpaired Student's *t*-test) and p14 (wt, n = 31 cells from 4 animals; $Fu^{-/-}$, n = 36 cells

from 3 animals; P < 2.6 x 10^{-7}; unpaired Student's *t*-test). Error bars indicate s.d.

Figure 2-8: Reduction of *shh* and *fkd4* expression in zebrafish *fu* morphants

(**A-C**) Whole-mount *in situ* hybridization to *shh* (purple signal) in the medial floor plate

of wt, *fu* morphants, and *fu* morphants expressing mouse *Fu* at 24 hours post fertilization

(hpf). View is dorsal. Reduced *shh* expression in *fu* morphants (**B**) (arrows) is consistent

with an inability to maintain medial floor plate in the absence of *fu*; *shh* expression in *fu*

morphants is restored to wt levels when mouse *Fu* is expressed (**C**). mf, medial floor

plate. (**D-F**) Cross section of embryos shown in **A-C** at the trunk region. (**G**) Whole-

mount *in situ* hybridization to *fkd4* (purple signal) in both medial and lateral floor plates

of wt zebrafish embryos at 24 hpf. View is dorsal. (**H, I**) *fkd4* expression is lost in the

lateral floor plate of *fu* morphants (**H**) and is restored when mouse *Fu* is expressed (**I**).

mf, medial floor plate; lf, lateral floor plate. (**J-L**) Cross section of embryos shown in **G-

I** at the trunk region.

Figure 2-9: Mouse *Fu* rescues Hh-dependent defects in zebrafish *fu* morphants

(**A**) Whole-mount in situ hybridization to *fkd4* (also known as *foxa*; purple signal) in both

medial and lateral floor plate of wild-type (WT) zebrafish embryos at 24 h post

fertilization (h.p.f.). (**B, C**) *fkd4* expression is lost in the lateral floor plate of *fu*

morphants (MO) (**B**) and is restored when mouse *Fu* is expressed (**C**). (**D**) Whole-mount

in situ hybridization to *nkx2.2b* (purple signal) in the lateral floor plate of wild-type

zebrafish embryos at 24 h.p.f. (**E, F**) nkx2.2b expression is lost in the lateral floor plate of

fu morphants (**D**) and is restored when mouse *Fu* is expressed (**E**). View is dorsal. LF,

lateral floor plate; MF, medial floor plate. (**G**) Whole- mount in situ hybridization to ptc1

(purple signal) in somites of wild-type zebrafish embryos at the 10-somite stage. View is

dorsal. (**H, I**) *ptc1* expression is greatly reduced in somites of *fu* morphants (**H**) and is

restored when mouse Fu is expressed (**I**). (**J**) Immunohistochemistry against Eng1a and

Eng1b (En) (arrow), which labels the muscle pioneer population in wild-type zebrafish

somites at 24 h.p.f. View is lateral. (**K, L**) Rescue of En expression in fu morphant

somites (**K**) by co-injection with mouse Fu (**L**). (**M**) Lateral view of chevron-shaped

somites in wild-type zebrafish embryos at 24 h.p.f. (**N, O**) Rescue of U-shaped somites in

fu morphants (**N**) by co-injection with mouse Fu (**O**). Dotted lines delineate the

boundaries of somites. (**P**) Whole- mount in situ hybridization to *ptc1* (purple signal) in

somites of wild-type zebrafish embryos at the 10-somite stage. View is dorsal. (**Q, R**)

Upregulation of *ptc1* expression in *ptc1* morphants (**Q**) is abolished by knocking down *fu*

(**R**). Original magnification, 3200x (**A–I**, **P–R**), 3105.6x (**J–L**) and 364x (**M–O**).

Figure 2-10: Cladogram of aligned Fu kinase domains from eukaryotes

Cladogram of identified proteins containing a recognizable Fu kinase domain as assessed

by BLAST against the Genbank, Ensembl v49, and JGI databases. Protein sequences of

Fu kinase domains (compared against amino acids 1-289 of mouse Fu) were aligned

using ClustalX and a Neighbor-Joining tree was constructed using 1000 bootstrap trials.

The cladogram was constructed using FigTree v1.1.2 (Andrew Rambaut, http://tree.bio.ed.ac.uk/software/figtree). Fu kinase domains were found in metazoans, unicellular eukaryotes (many of which are flagellated, such as *Chlamydomonas reinhardtii*), and plant lineages.

Sequences used for alignments:

Genbank: Aedes aegypti: XP_001658684; Anopheles gambiae: XP_307416; Apis mellifera: XP_001122254; Arabidopsis thaliana: AAZ66047; Bos taurus: XP_585177; Canis familiaris: XP_536072; Danio rerio: AAI54436; Dictyostelium discoideum: XP_647449; Drosophila americana: AAK52244; Drosophila melanogaster: NP_477499; Drosophila montana: AAK52263; Drosophila pseudoobscura: XP_001354387; Drosophila virilis: AAF08703; Homo sapiens: AAF97028; Leishmania braziliensis: XP_001563169; Leishmania infantum: XP_001464058; Leishmania major: XP_001681788; Leishmania mexicana: CAC07966; Mus musculus Akt3: NP_035915; Mus musculus Fu: NP_778196; Mus musculus Nek1: NP_780298; Mus musculus Slk: NP_033315; Mus musculus Ulk2: NP_038909; Mus musculus Ulk3: XP_930106; Oryza sativa: NP_001066683; Paramecium tetraaurelia: XP_001423533; Rattus norvegicus: XP_217435; Strongylocentrus purpuratus: XP_001199175; Tetrahymena thermophila: XP_001029696; Tetraodon nigroviridis: CAG02878; Tribolium castaneum: XP_968708; Trichomonas vaginalis: XP_001579585, XP_001315744; Trypanosoma brucei: XP_828523; Trypanosoma cruzi: XP_806327; Vitis vinifera: CAN74245

Ensembl v49: Ciona intestinalis: translation of GENSCAN00000086241; Ciona savignyi: translation of FGENESH00000074666; Erinaceus europaeus: translation of GENSCAN_GS00000265665; Felis catus: ENSFCAG00000004156; Gallus gallus: ENSGALP00000018526; Gasterosteus aculeatus: ENSGACG00000020417; Macaca mulatta: ENSMMUP00000008885; Monodelphis domestica: ENSMODP00000019211; Oryzias latipes: translation of GENSCAN00000055611; Pan troglodytes: ENSPTRP00000022091; Pongo pygmaeus: ENSPPYP00000014729; Takifugu rubripes: Translation of GENSCAN00000027428

JGI: Branchiostoma floridae: estExt_gwp.C_740166, protein ID 280005; Chlamydomonas reinhardtii: e_gwH.30.66.1, protein ID 104702; Daphnia pulex: fgenesh1_pg.C_scaffold_99000069; protein ID: 112727; Monosiga brevicollis: fgenesh2_pg.scaffold_34000051, protein ID 29411; Naegleria gruberi: e_gw1.30.5.1, protein ID 34462; fgeneshNG_pm.scaffold_72000002, protein ID 60972; Nematostella vectensis: e_gw.384.53.1, protein ID 136852; Ostreococcus lucimarinus: e_gwEuk.15.194.1, protein ID 40725; Ostreococcus tauri: e_gw1.16.00.183.1, protein ID 21800; Physcomitrella patens: e_gw1.53.10.1, protein ID 125145; e_gw1.72.81.1, protein ID 128827; Phytophthora ramorum: fgenesh1_pg.C_scaffold_23000141, protein ID 77329; Populus trichocarpa: fgenesh4_pg.C_LG_XIX000544, protein ID 780405; Volvox carterii: e_gw1.64.130.1, protein ID 67317; Xenopus tropicalis: estExt_fgenesh1_pg.C_6450031, protein ID 459387

Figure 2-11: Zebrafish *fu* morphants exhibit Hh-independent L-R asymmetry defects resulting from abnormal Kupffer's vesicle cilia architecture

(**A, B**) Section *in situ* hybridization to *Fu* (pink signal) in chick trachea (**A**) and *X. tropicalis* testis (**B**). Arrow indicates sites of *Fu* expression. (**C**) Whole mount *in situ* hybridization to *cmlc2* (purple signal) in *smo*^{hi1640Tg} fish embryos at 24 hpf. View is dorsal. (**D, E**) Whole-mount *in situ* hybridization to *cmlc2* in wt (**D**) and *fu* morphants (**E**) at 24 hpf. View is dorsal. (**F**) Summary of cardiac laterality defects in wt, *fu* morphants, and *fu* morphants rescued with mouse *Fu*. L, left; R, right; M, medial. (**G, H**) Whole mount *in situ* hybridization to *spaw* at 15-somite stage. View is dorsal. (**I**) Summary of *spaw* expression in the lateral plate mesoderm (LPM). L, left; R, right; A, absent; B, bilateral. (**J, K**) Electron micrograph of Kupffer's vesicle (KV) cilia from wt (**J**) and *fu* morphant (**K**). (**L**) Quantification of ultrastructural defects in KV cilia from wt and *fu* morphants.

Figure 2-12: Mouse Fu rescues loss of counterclockwise fluid flow in Kupffer's vesicle of zebrafish *fu* morphants

Traces of bead movement used to measure fluid flow in Kupffer's vesicle (KV) in zebrafish embryos at the 8-10 somite stage. Magnification is 40x, and view is from the ventral side. In wild-type embryos (top panel), fluid flow is coordinated and proceeds in a counterclockwise direction. In *fu* morphants (MO) (middle panel), coordinated flow is

disrupted. Co-injection of mouse *Fu* mRNA with *fu* morpholino restores

counterclockwise flow.

Figure 2-13: Mouse Fu physically interacts with mouse Kif27 and zebrafish Kif7

(**A**) Western blot of immunoprecipitated Fu-FLAG to determine its physical association

with mouse Kif7-myc or Kif27-myc from HEK 293T lysates. WB, western blot; in, input;

IP, immunoprecipitation. (**B**) Western blot of immunoprecipitated zebrafish Fu (epitope-

tagged with four copies of FLAG) to detect physical interaction with zebrafish Kif7

(epitope-tagged with two copies of Myc) from HEK 293T lysates. Zebrafish Fu interacts

weakly with zebrafish Kif7, but not with an unrelated control protein (Myc-tagged mouse

Ext2). Transfections, cell lysis, and immunoprecipitation with FLAG-M2 agarose were

performed as described in **Materials and Methods**, except the concentration of NaCl

used in the wash buffer was raised to 300 mM. Similar results were obtained when cell

lysis and immunoprecipitation were performed in RIPA buffer (data not shown). (**C**)

Western blot of immunoprecipitated mouse Fu (epitope-tagged with once copy of FLAG)

to detect physical interaction with zebrafish Kif7 (epitope-tagged with two copies of

Myc) from HEK 293T lysates. Mouse Fu co-immunoprecipitates zebrafish Kif7 and

mouse Kif27, but not mouse Kif7. The interaction of mouse Fu with zebrafish Kif7

provides a mechanistic explanation for the ability of mouse *Fu* to rescue zebrafish *fu*

morphants.

**Figure 2-14: *Kif27* mutant mice exhibit loss of central pair microtubules in tracheal
motile cilia**

Transmission electron micrographs (TEM) of motile cilia from wild-type (wt) (left panel) and *Kif27*⁻ᐟ⁻ (right panel) tracheae. As with *Fu* mutants, *Kif27* mutants display a loss of the central pair microtubules.

Figure 2-15: *Fu* and *Kif27* transcripts are upregulated after initiation of MTEC differentiation *in vitro*

(**A**) Semi-quantitative RT-PCR showing that *Fu* transcript is upregulated during MTEC differentiation. *Fu* transcript is upregulated at air-liquid interface (ALI) day 3, and this increase in *Fu* expression continues throughout differentiation. (**B**) Semi-quantitative RT-PCR demonstrates that *Kif27* transcript is upregulated during MTEC differentiation, in a manner similar to *Fu*.

Figure 2-16: Cladogram of insect Costal-2 and vertebrate Kif7 and Kif27 amino acid sequences

Cladogram of Costal-2 (Cos2), Kif27, and Kif7 protein sequences. Full-length sequences were aligned, bootstrapped and displayed as in Figure 2-10. No obvious definitive homologs to mammalian Kif27 were found in the four fish lineages examined; the closest relative to mouse Kif27 in *Danio rerio*, *Oryzias latipes*, *Takifugu rubripes*, and *Gasterosteus aculeatus* is Kif7 (data not shown). Taken together, two orders of events seem possible. First, an ancient duplication of the Cos2 ancestor resulted in the Kif7 and Kif27 genes, and the Kif27 gene was lost in the fish lineage. Second, the ancestral Kif7

gene may have undergone duplication in the tetrapod lineage, favored by the presence of both Kif7 and Kif27 in *Xenopus tropicalis*. Comprehensive sequence analysis of the kinesin superfamily indicates that the kinesin-4 family, of which Kif7 and Kif27 are members, has a high number of gene duplication events, which may underlie potential subfunctionalization of Kif7/Kif27 in mammals (Lynch and Conery 2000; Miki et al. 2005).

Sequences used for alignments:

Genbank: Aedes aegypti Cos2: XP_001660954; Anopheles gambiae Cos2: XP_001688251; Apis mellifera Cos2: XP_624554; Danio rerio Kif7: NP_001014816; Drosophila melanogaster Cos2: NP_477092; Drosophila pseudoobscura Cos2: XP_001360209; Homo sapiens Kif7: Q2M1P5; Homo sapiens Kif27: NP_060046; Mus musculus Kif7: XP_001478724; Mus musculus Kif27: NP_780423; Rattus norvegicus Kif7: XP_218828; Rattus norvegicus Kif27: NP_932167; Tribolium castaneum Cos2: XP_973391

Ensembl v49: Canis familiaris Kif7: translation of GENSCAN00000060692; annotated peptide is ENSCAFP00000017637; Canis familiaris Kif27: ENSCAFP00000002032; Cavia porcellus Kif7: translation of GENSCAN00000188145, annotated peptide is ENSCPOP00000013857; Cavia porcellus Kif27: ENSCPOP00000002264; Gasterosteus aculeatus Kif7: ENSGACP00000021024; Loxodonta africana Kif7: translation of GENSCAN00000074353, annotated peptide is ENSLAFP00000005104; Loxodonta africana Kif27: ENSLAFP00000014808; Monodelphis domestica Kif7: translation of

GENSCAN00000048146, annotated peptide is ENSMODP00000024385; Monodelphis

domestica Kif27: ENSMODP00000035142; Oryzias latipes Kif7:

ENSORLP00000011669; Pan troglodytes Kif7: XR_024331.1; Pan troglodytes Kif27:

ENSPTRP00000035996; Sorex araneus Kif7: translation of GENSCAN00000271575,

annotated peptide is ENSSARP00000010204; Sorex araneus Kif27:

ENSSARP00000011952; Takifugu rubripes Kif7: ENSTRUP00000046370; Xenopus

tropicalis Kif7: translation of GENSCAN00000012159, annotated peptide is

ENSXETP00000038484; Xenopus tropicalis Kif27: ENSXETP00000005053

Figure 2-17: Morpholino knockdown of zebrafish *kif7* results in L-R asymmetry

defects

(**A, B**) Whole mount *in situ* hybridization to *cmlc2* in wt and *kif7* morphants at 24 hpf.

View is dorsal. (**C**) Summary of cardiac laterality defects in wt and *kif7* morphants. (**D**)

Summary of essential Fu and Cos2/Kif27 functions in metazoan model organisms.

Figure 2-18: Kif27-GFP associates with centrioles/basal bodies, and overlaps with

Fu-mCherry expression

(**A-F**) Confocal immunofluorescence of lentivirally transduced Kif27-GFP and mouse

anti-γ-tubulin (red) (Sigma, 1:1000) in mouse tracheal epithelial cells (MTECs) at air-

liquid interface (ALI) days 0 (**A-C**) and 5 (**D-F**). Kif27-GFP remains associated with

centrioles throughout ciliogenesis. The inset in (**F**) is a 3-dimensional reconstruction of

the confocal stack in (**F**) using the VolumeViewer plugin in NIH ImageJ. (**G-I**) Kif27-GFP localizes to apical basal bodies (assessed by epifluorescence) in polarized Madin-Darby canine kidney (MDCK) cells. MDCK cells were maintained in MEM Eagle's with Earle's balanced salt solution (Cellgro) supplemented with 5% fetal bovine serum (Gibco) and grown on gelatin-coated glass coverslips. Kif27 in pEGFP-N1 was transfected using Lipofectamine 2000 (Invitrogen) according to manufacturer's instructions. (**J-L**) Confocal immunofluorescence (*xz* projections) of lentivirally transduced Kif27-GFP and Fu-mCherry (red) in MTECs at ALI day 5. Fu-mCherry is broadly expressed in the cytoplasm and overlaps with Kif27-GFP expression. Similar expression patterns were observed in MDCKs and MEFs (data not shown). We have also examined localization of Kif27-GFP in *Fu* –/– MTECs and found that its localization to the base of the cilium is not drastically perturbed (data not shown).

Figure 2-19: Kif27-GFP localizes to basal bodies at the base of motile cilia in differentiated MTECs

(**A-F**) Confocal images of fully differentiated mouse tracheal epithelial cells (MTECs) to visualize localization of Kif27-GFP to the basal body (marked by anti-γ-tubulin, **D-F**) of motile cilia labeled with acetylated tubulin (ac-tubulin **A-C**).

Figure 2-20: Fu-mCherry is broadly distributed thoughout the cytoplasm of MTECs, but overlaps with Kif27 punctae

Fu-mCherry is broadly expressed in the cytoplasm and overlaps with Kif27-GFP

expression. Images are xy confocal projections, and the xz projections in Figure 2-18 (**F**)

are derived from these images.

Figure 2-21: Mouse Fu physically interacts with Spag16, but not Spag6

Western blot of immunoprecipitated mouse Fu-FLAG to detect its physical interaction

with mouse SPAG6-HA or SPAG16L-HA from HEK 293T lysates. WB, western blot;

in, input; IP, immunoprecipitation.

Figure 2-22: Spag6 and Spag16 localization are unaffected in *Fu* mutant MTECs

Confocal immunofluorescent projections of MTECs at ALI day 14, stained with

antibodies against actylated tubulin (red) and Spag6 or Spag16 (green). Detectable Spag6

and Spag16 signal is present in ciliary axonemes of both wild-type (top panels) or *Fu*

mutant (bottom panels) MTECs.

Figure 2-23: A speculative model of Fu and Kif27 function in motile ciliogenesis

Fu physically associates with Kif27 and Spag16. By virtue of this association, Fu may be

targeted to appropriate locations such as the basal body or the ciliary axoneme, where it

participates in construction of the central pair microtubules at or after the initiation of

cilium outgrowth. Fu may also indirectly interact with the microtubule cytoskeleton

through Kif27. Further, Fu and Kif27 may directly or indirectly affect the planar cell

polarity (PCP) pathway. This might occur through direct modulation of basal foot

orientation, or indirectly via a hypothesized relationship between cilia motility and

polarity.

Figure 2-24: Lpp1/Vangl2 is found at the apical surface of wild-type MTECs,

proximal to basal bodies

Antibodies directed against mouse Lpp1/Vangl2, a conserved gene involved in the planar

cell polarity (PCP) pathway, detect Lpp1/Vangl2 foci (green) at the apical surface of

MTECs. These foci overlap with basal bodies, as assessed by γ-tubulin staining (red)

Figure 2-1: Primary cilium formation and Smo trafficking are unaffected in *Fu* null MEFs
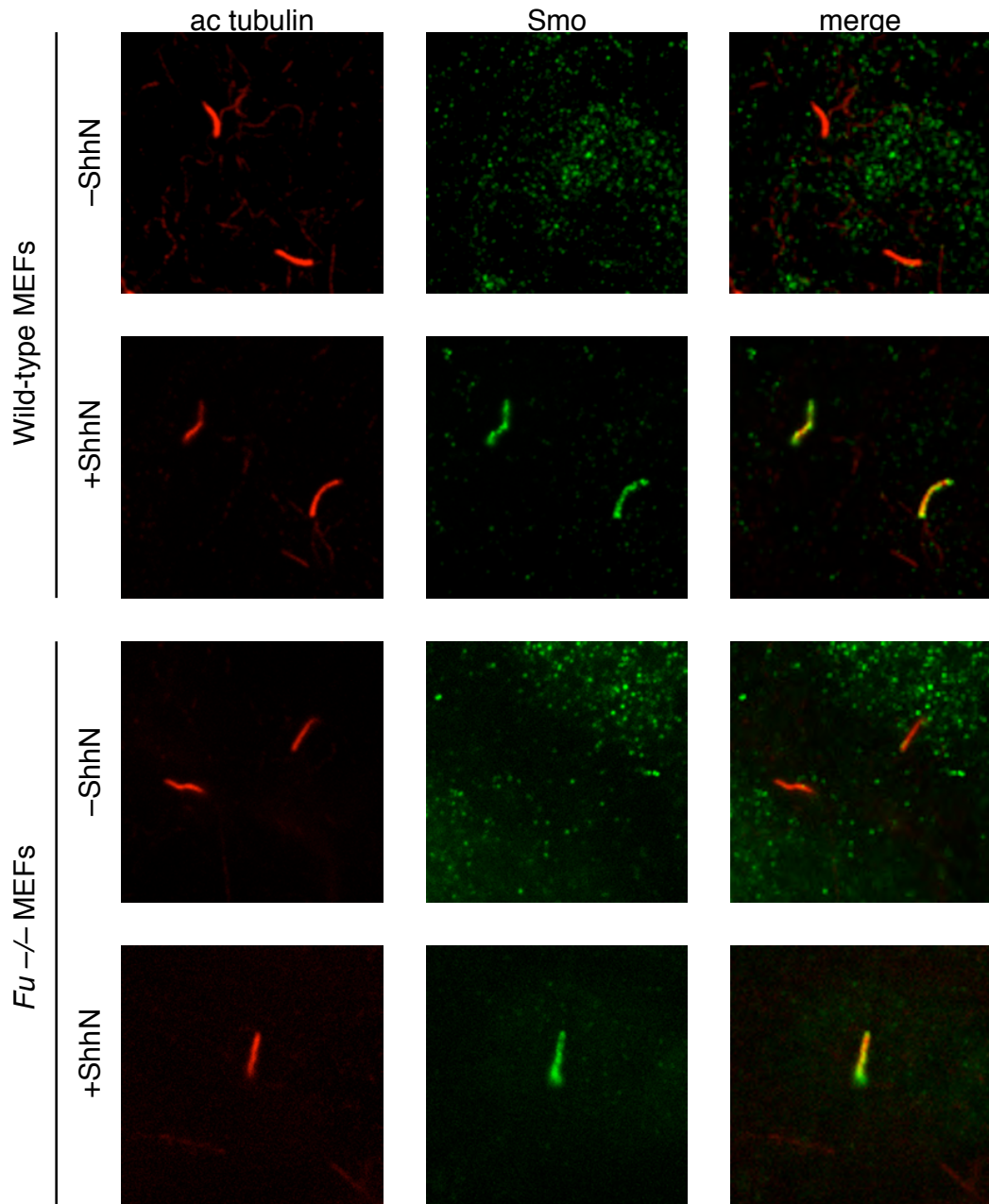
Figure 2-2: *Fu* transcript is expressed in respiratory epithelium, neural ependymal cells and testis

A

B

C
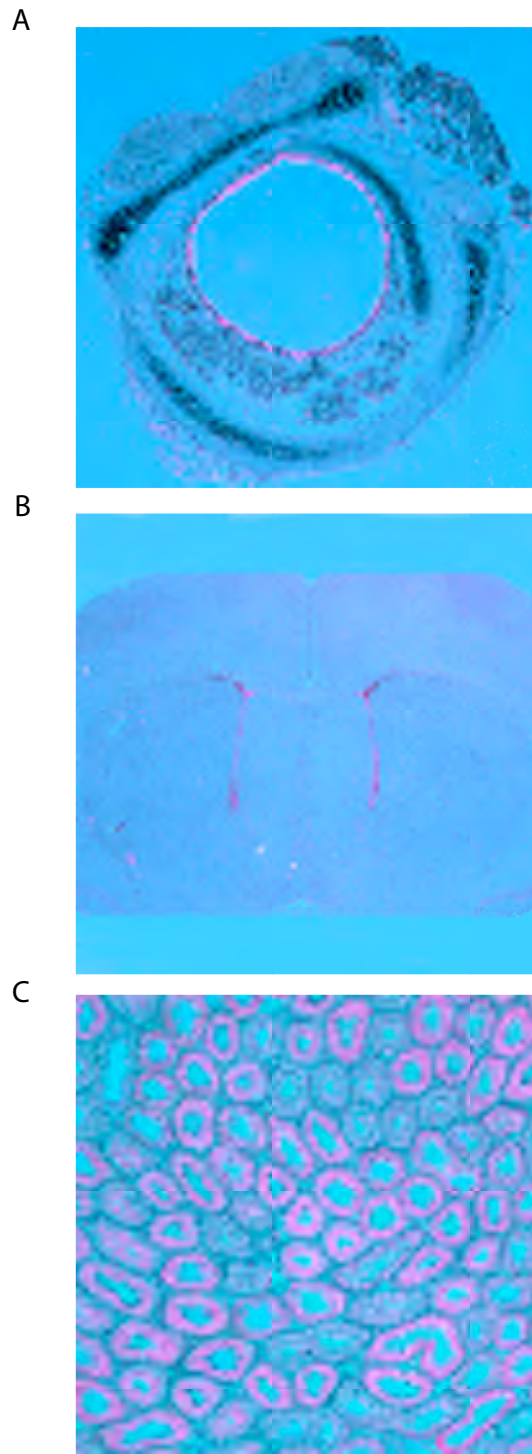
Data provided by Miao-Hsueh Chen
and Jehn-Hsiang Yang

Figure 2-3: *Fu* mutant tracheal motile cilia display abnormal central pair ultrastructure at post-embryonic days 1 and 14

Figure 2-4: Motile cilia in neural ependymal cells of *Fu* mutant mice display ultrastructural defects in central pair microtubules

A

B

C
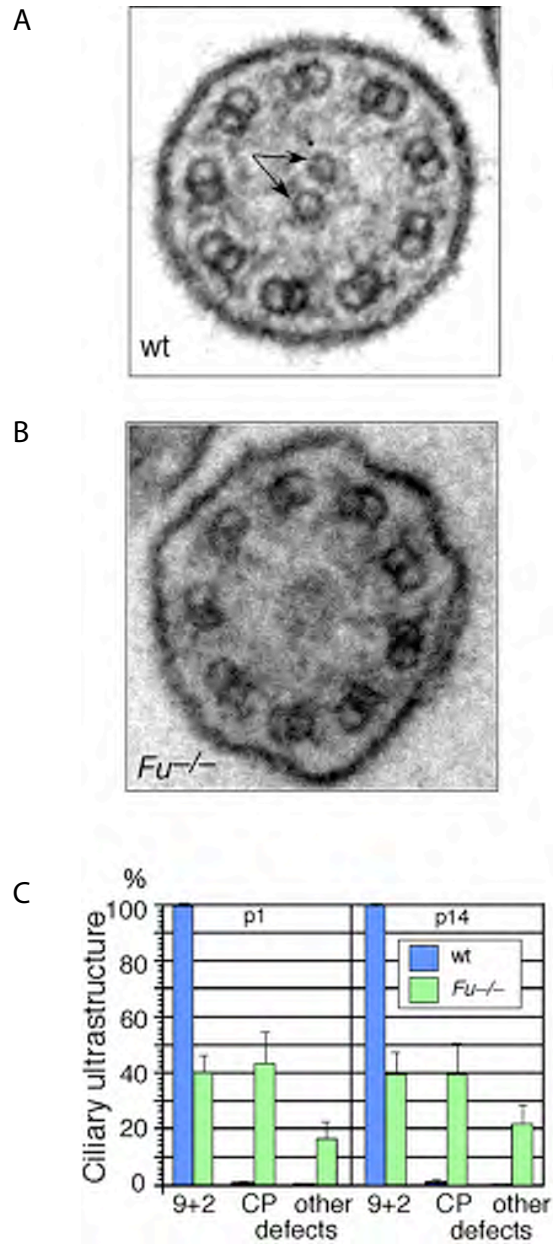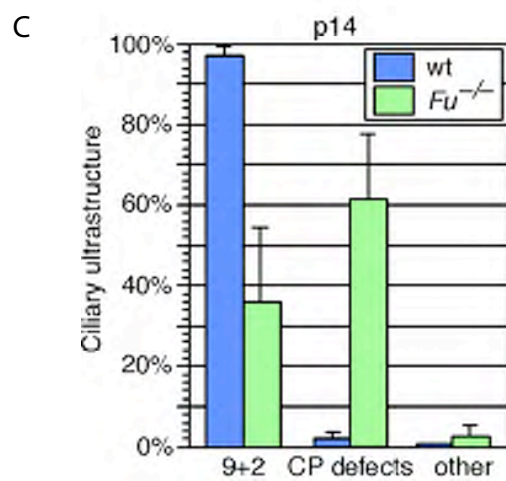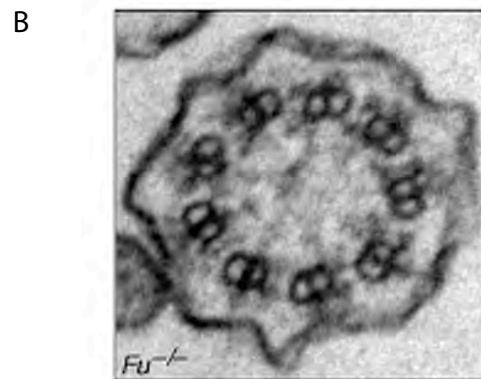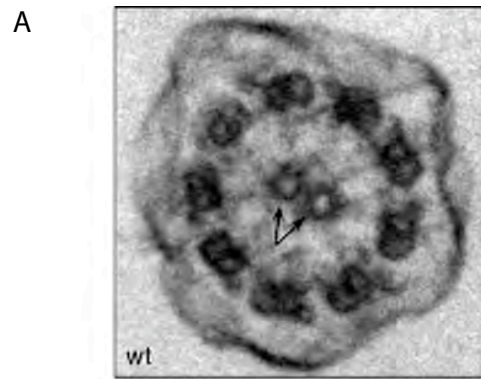
Figure 2-5: Central pair microtubules are absent from the basal plate of *Fu* mutant tracheal motile cilia
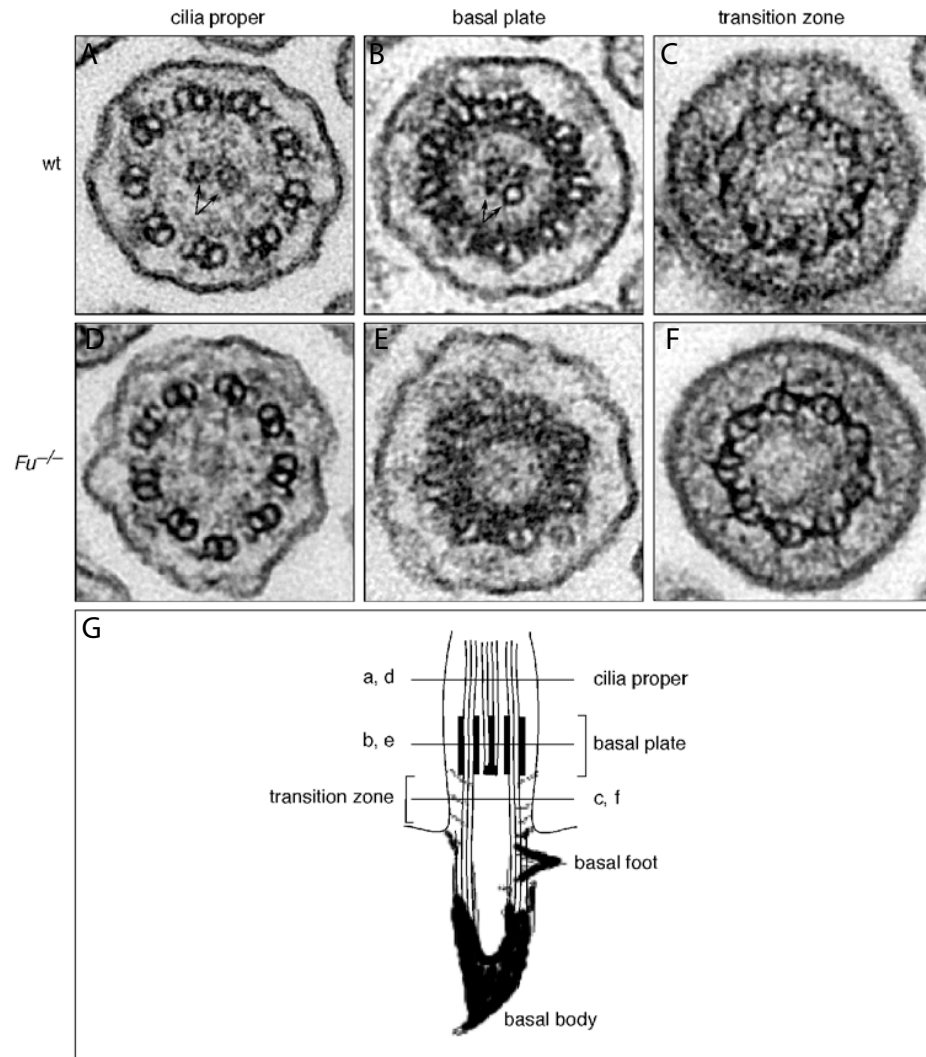
Figure 2-6: Reduced tracheal flow, velocity, and cilium motion in motile cilia from *Fu* mutants
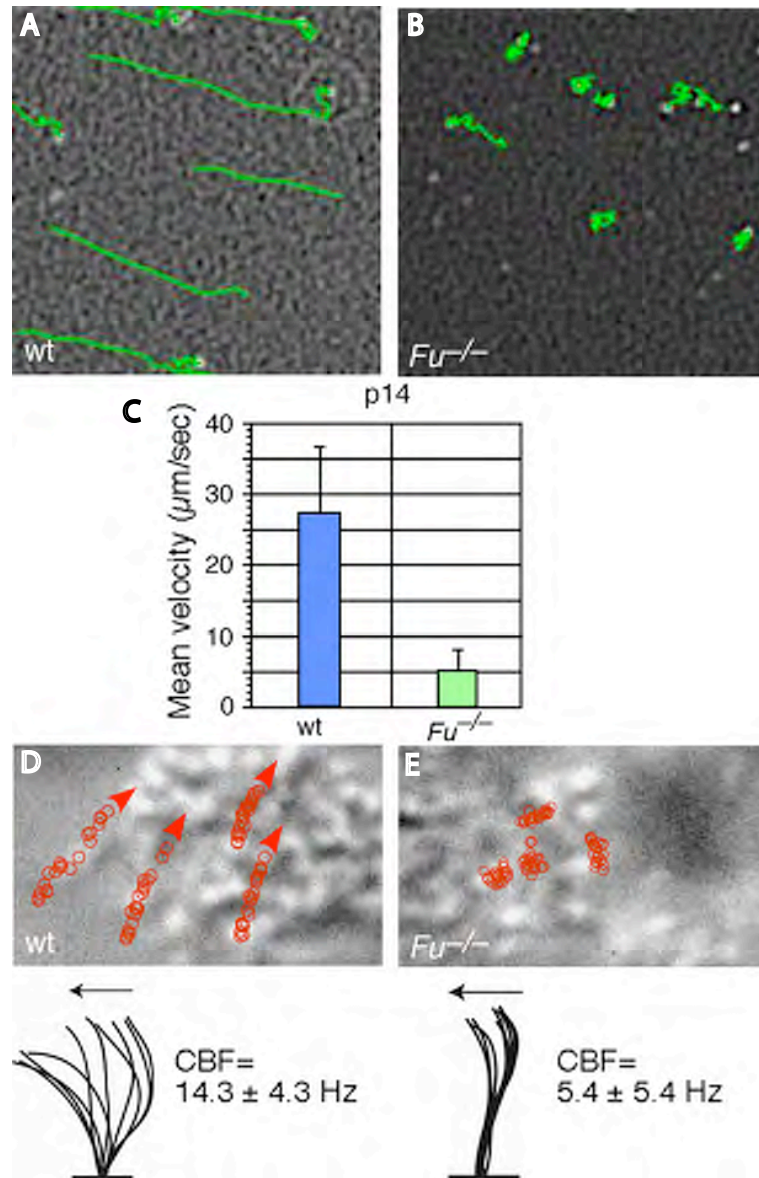
Figure 2-7: *Fu* mutants display disorganized motile cilium polarity in the trachea
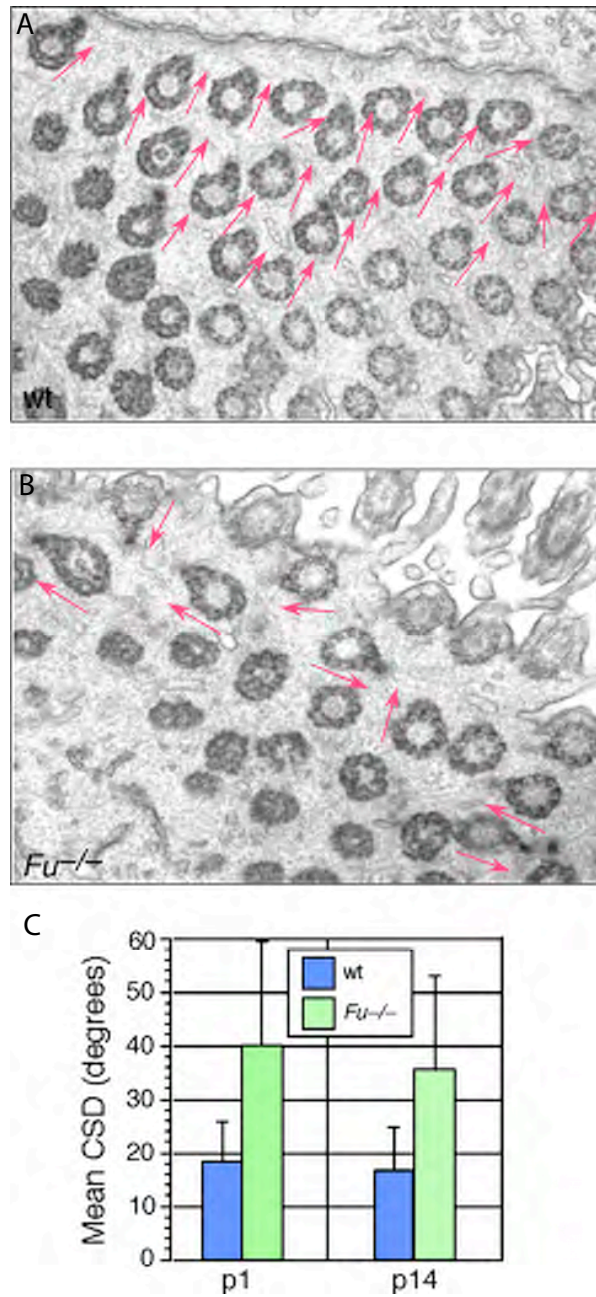
Figure 2-8: Reduction of *shh* and *fxd4* expression in zebrafish *fu* morphants
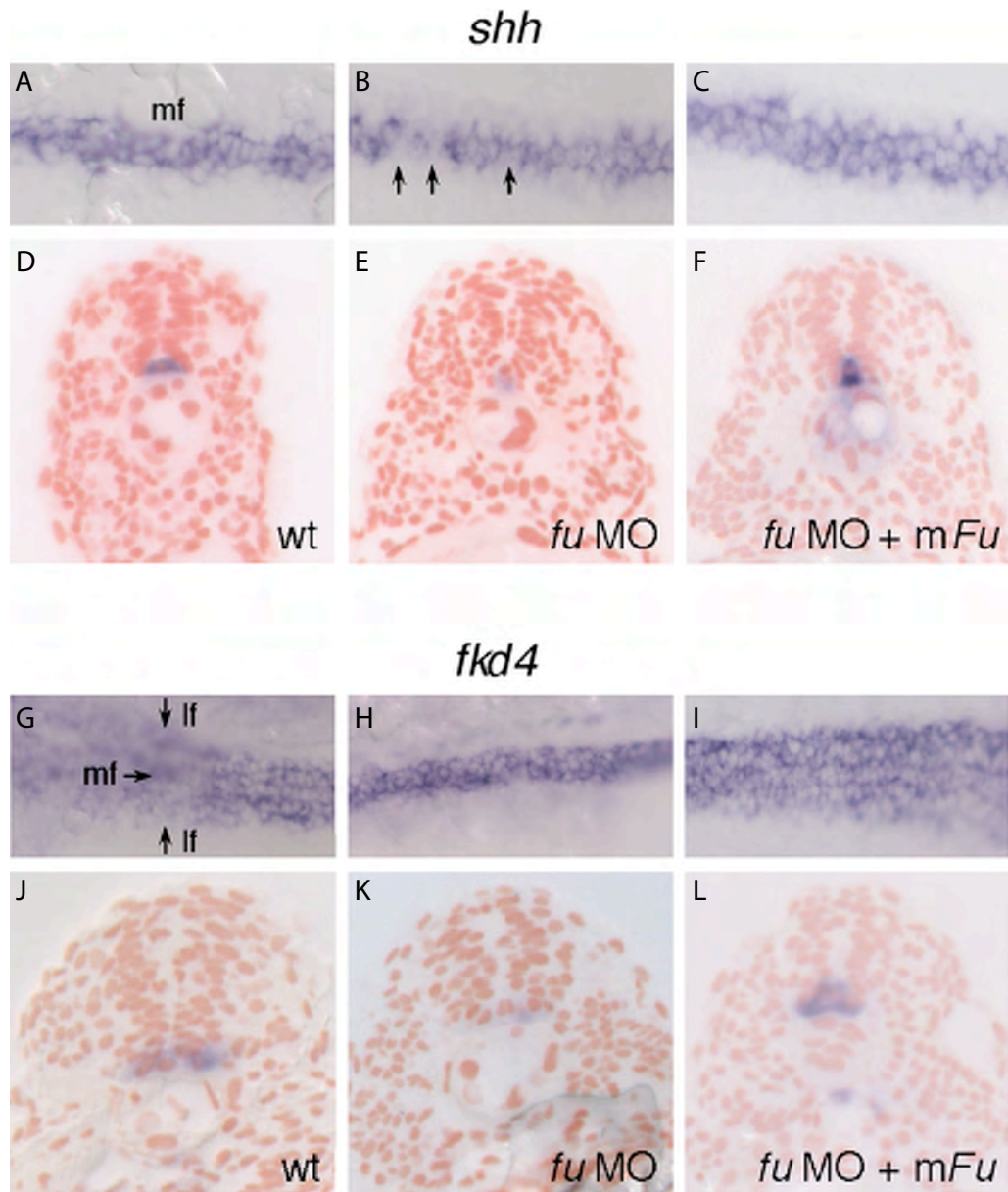
Data acquired in collaboration with Catherine Nguyen and Jau-Nian Chen

Figure 2-9: Mouse *Fu* rescues Hh-dependent defects in zebrafish *fu* morphants
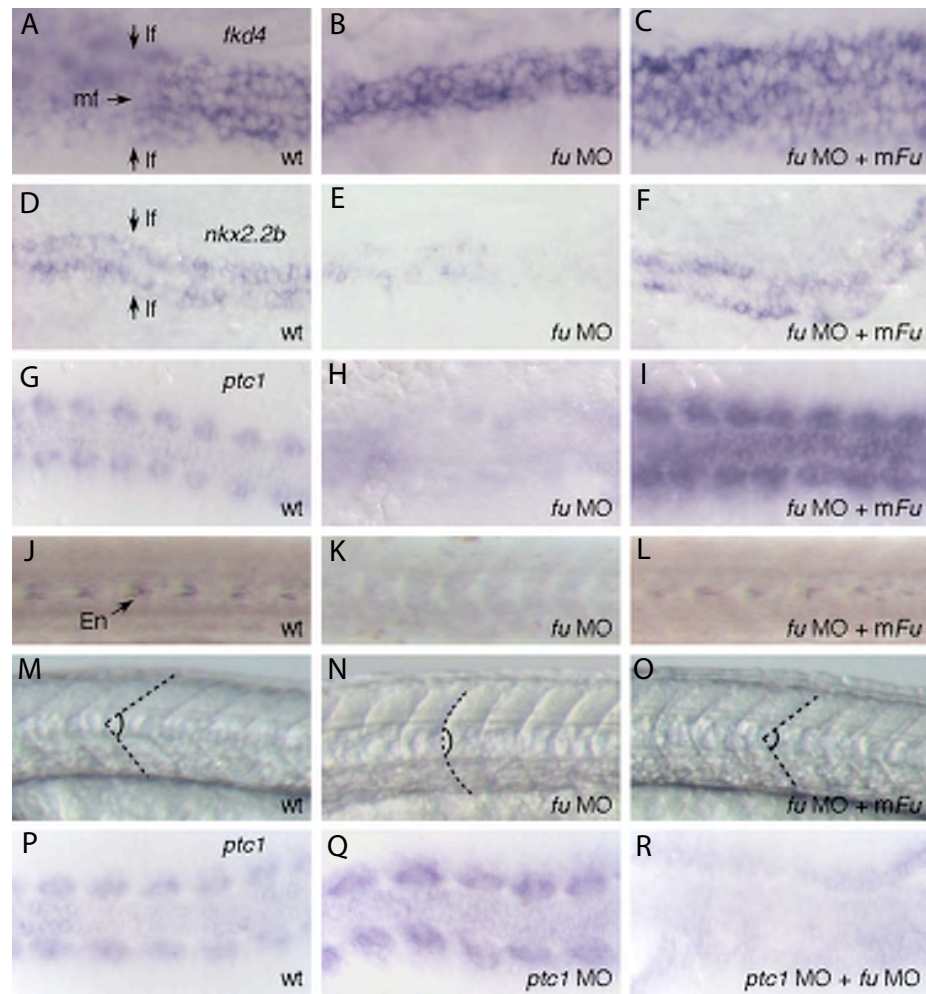
Data acquired in collaboration with Catherine Nguyen and Jau-Nian Chen

Figure 2-10: Cladogram of aligned Fu kinase domains from eukaryotes
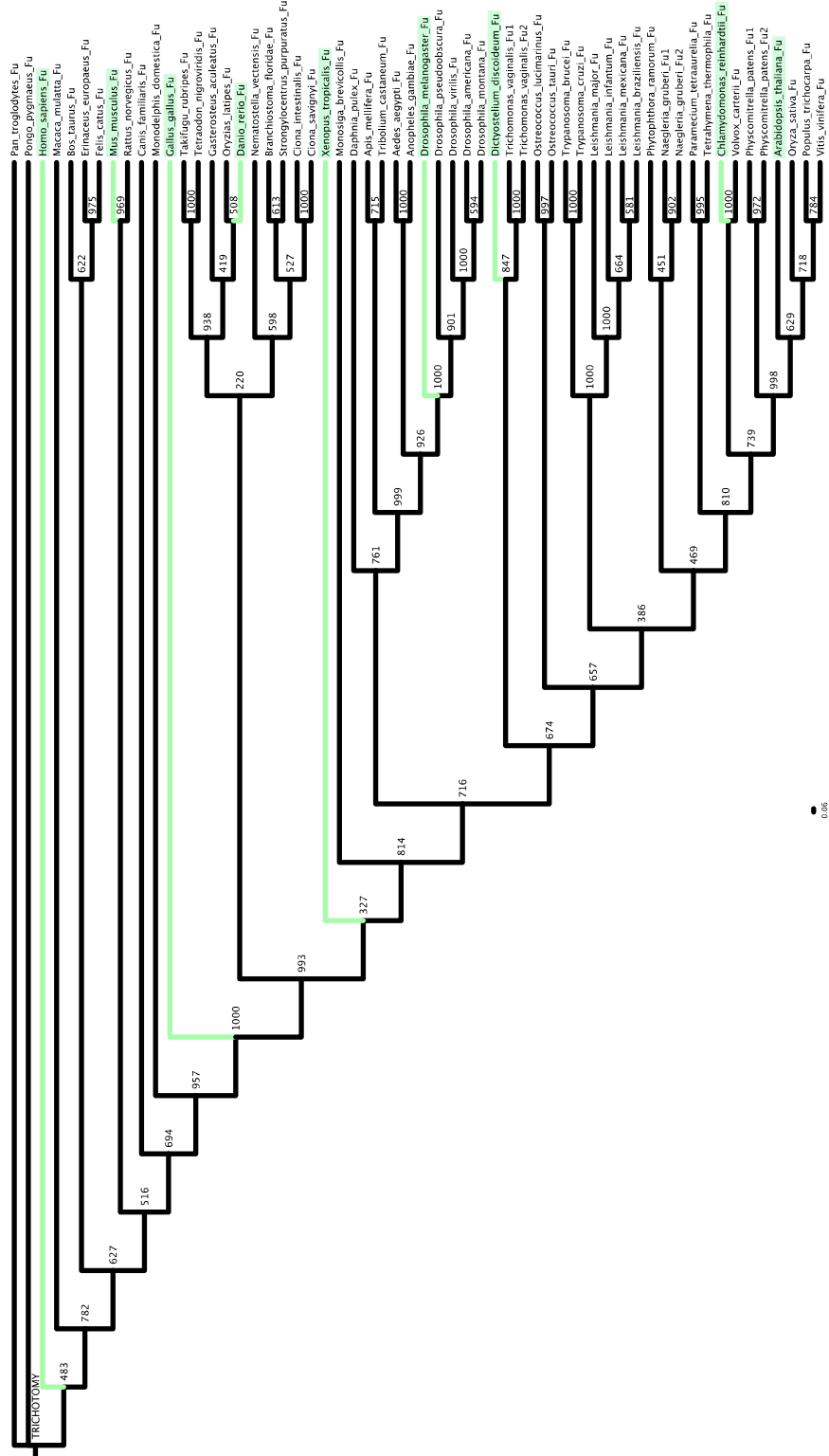
Figure 2-11: Zebrafish *fu* morphants exhibit Hh-independent L-R asymmetry defects resulting from abnormal Kupffer's vesicle cilia architecture
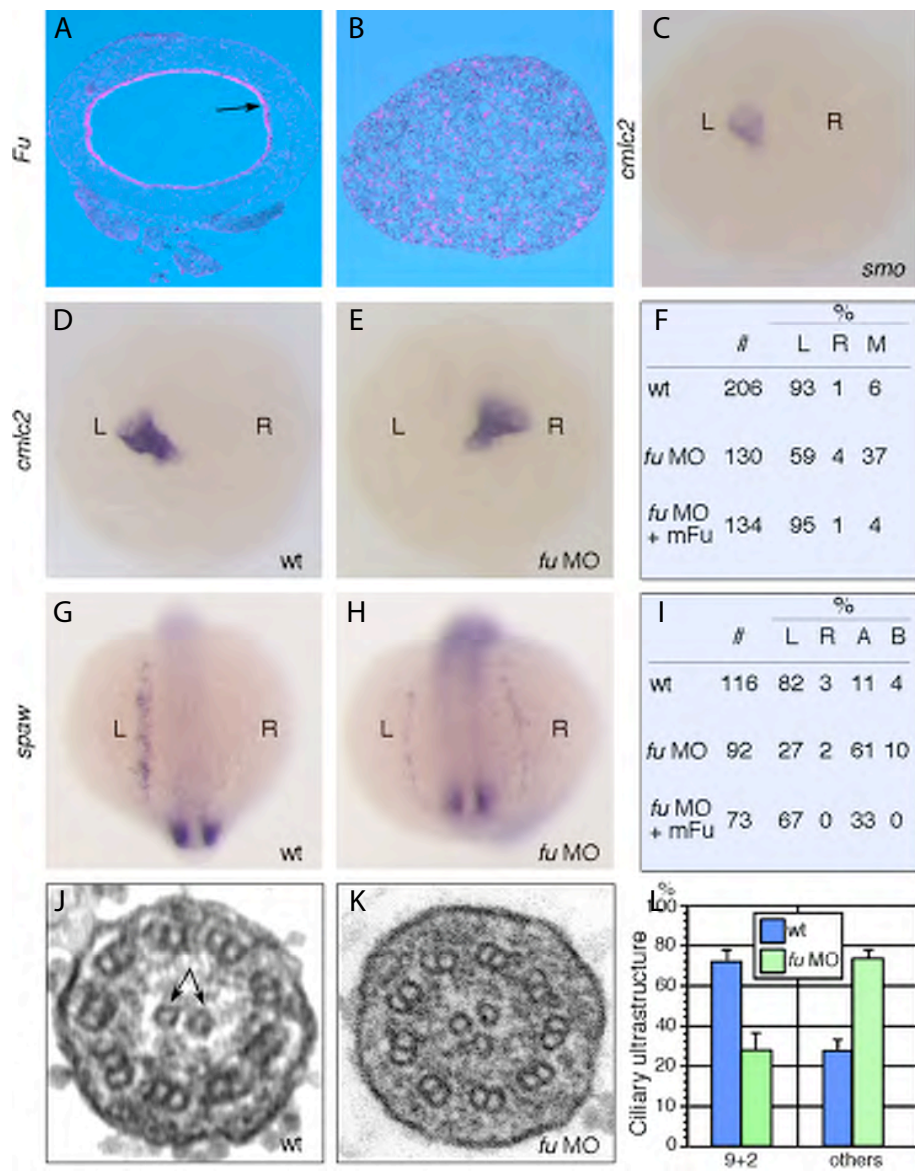
Data in panels A and B kindly provided by Miao-Hsueh Chen and Jehn-Hsien Yang
Data in panels C-L acquired in collaboration with Catherine Nguyen and Jau-Nian Chen

Figure 2-12: Mouse Fu rescues loss of counterclockwise fluid flow in Kupffer's vesicle of zebrafish *fu* morphants

wild-type
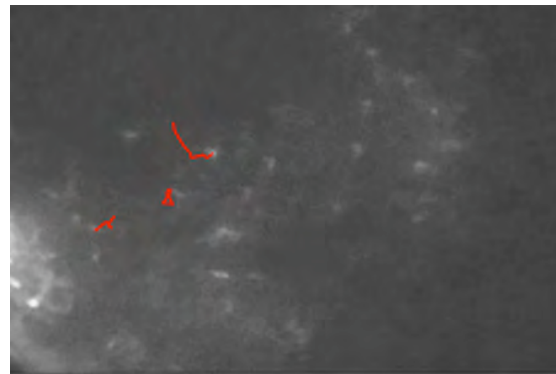
fu MO

fu MO + mouse *Fu* mRNA

Data acquired in collaboration with Catherine Nguyen and Jau-Nian Chen

Figure 2-13: Mouse Fu physically interacts with mouse Kif27 and zebrafish Kif7
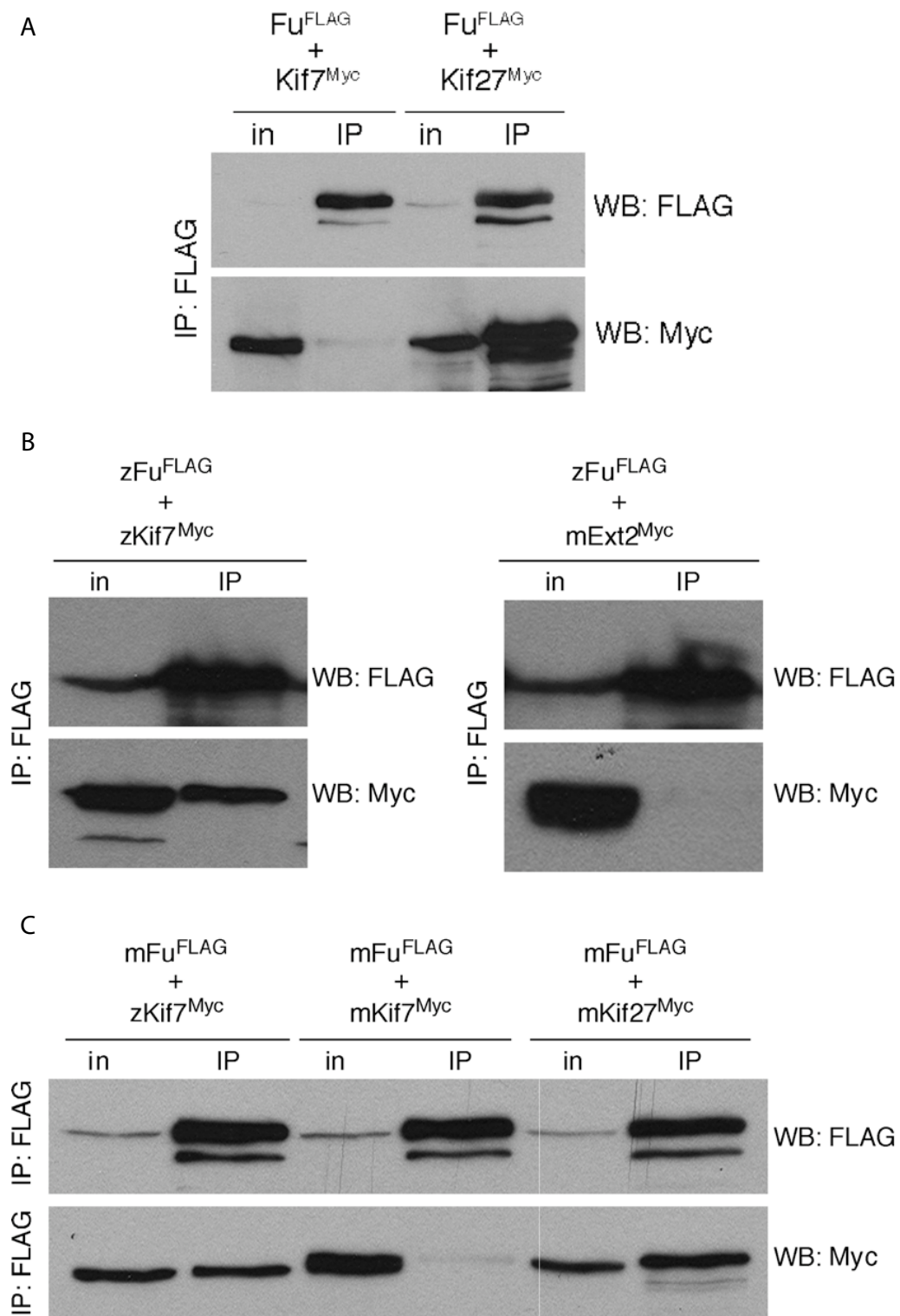
Figure 2-14: *Kif27* mutant mice exhibit loss of central pair microtubules in tracheal motile cilia
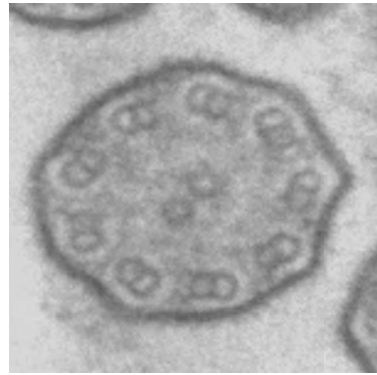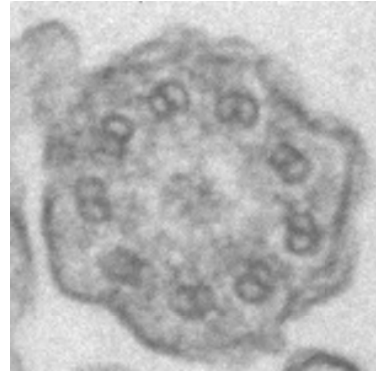
wild-type   *Kif27* null

Figure 2-15: *Fu* and *Kif27* transcripts are upregulated after initiation of MTEC differentiation *in vitro*
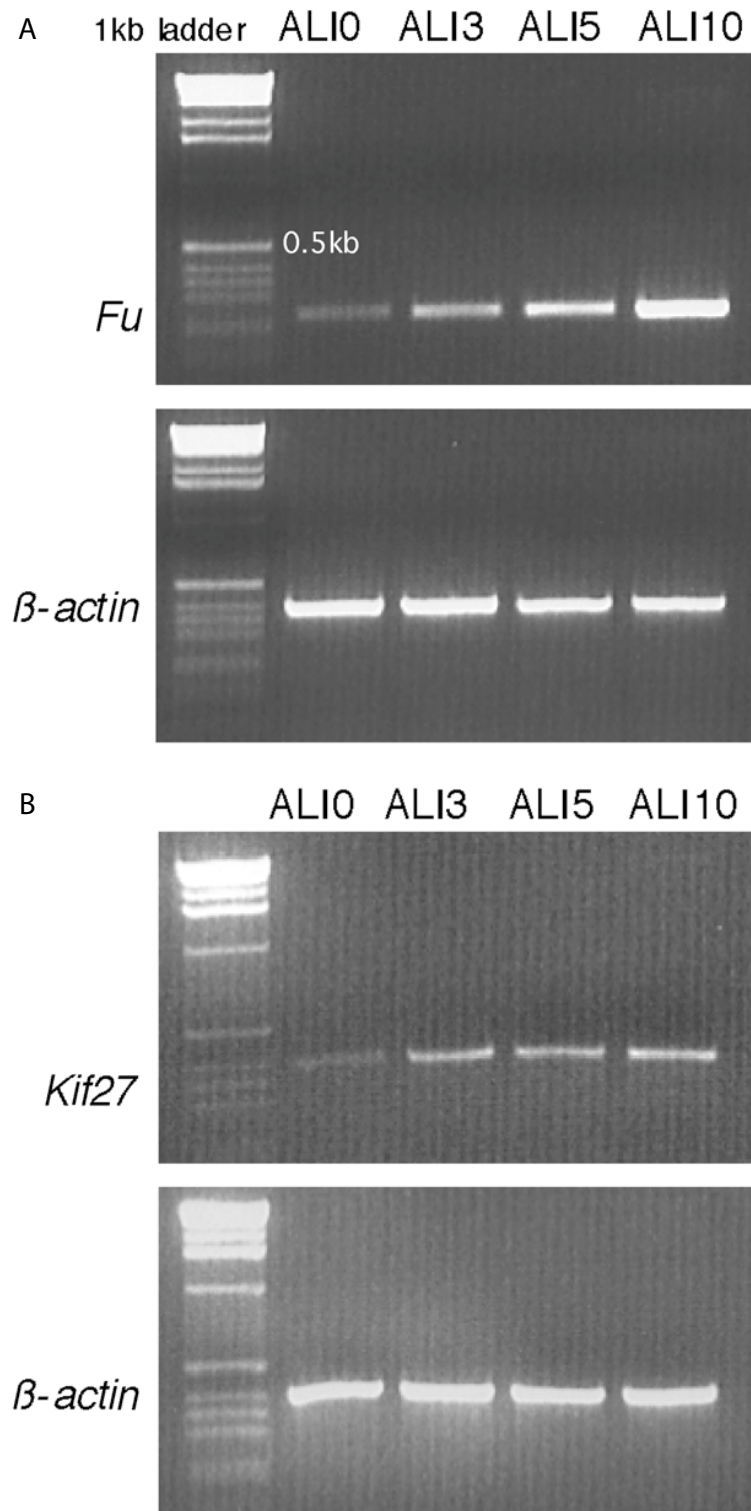
Figure 2-16: Cladogram of insect Costal-2 and vertebrate Kif7 and Kif27 amino acid sequences

Figure 2-17: Morpholino knockdown of zebrafish *kif7* results in L-R asymmetry defects

	%			
	#	L	R	M
wt	87	93	1	6
kif7 MO	109	68	18	14

	Hh signaling	Fu & Cos2/Kif27 motile cilia function
fly	+	− (?)
zebrafish	+	+
mouse	−	+
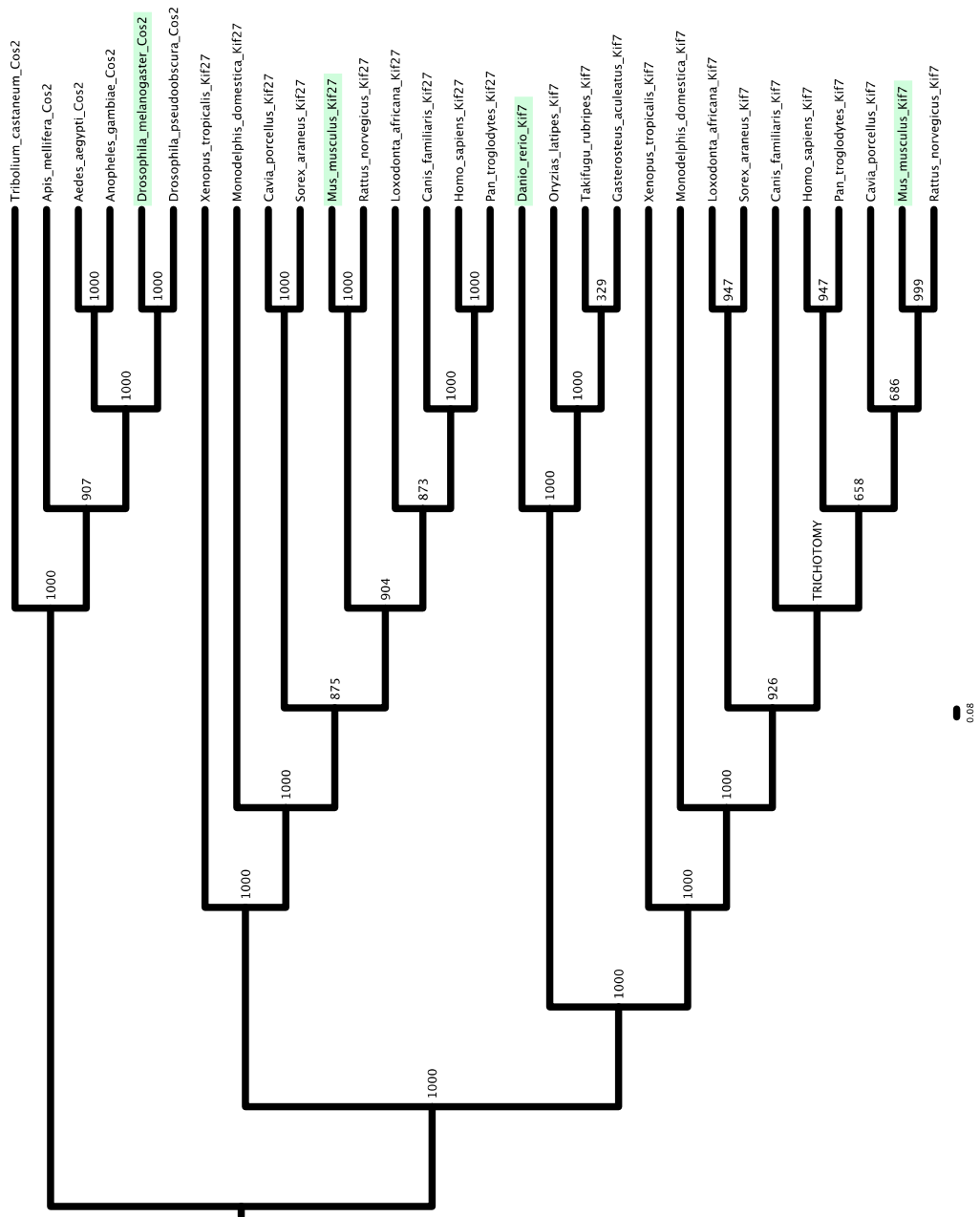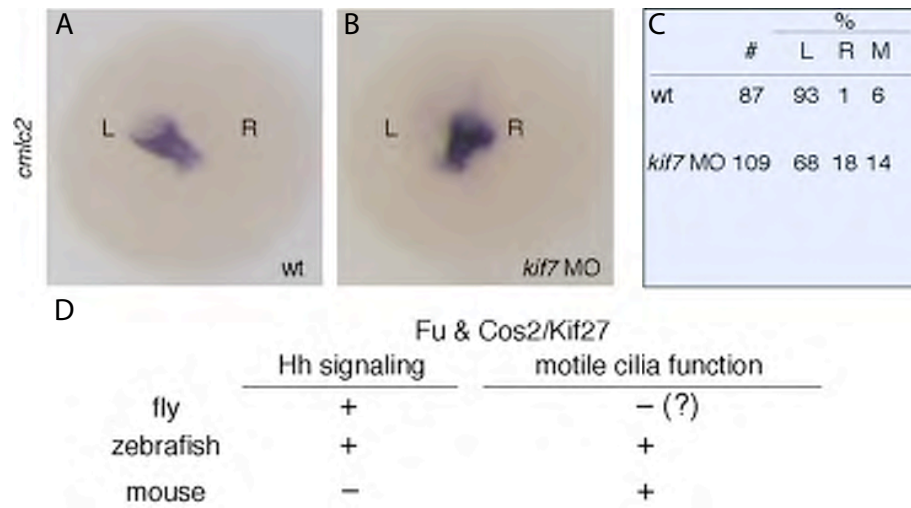
Data acquired in collaboration with Catherine Nguyen and Jau-Nian Chen

Figure 2-18: Kif27-GFP associates with centrioles/basal bodies, and overlaps with Fu-mCherry expression
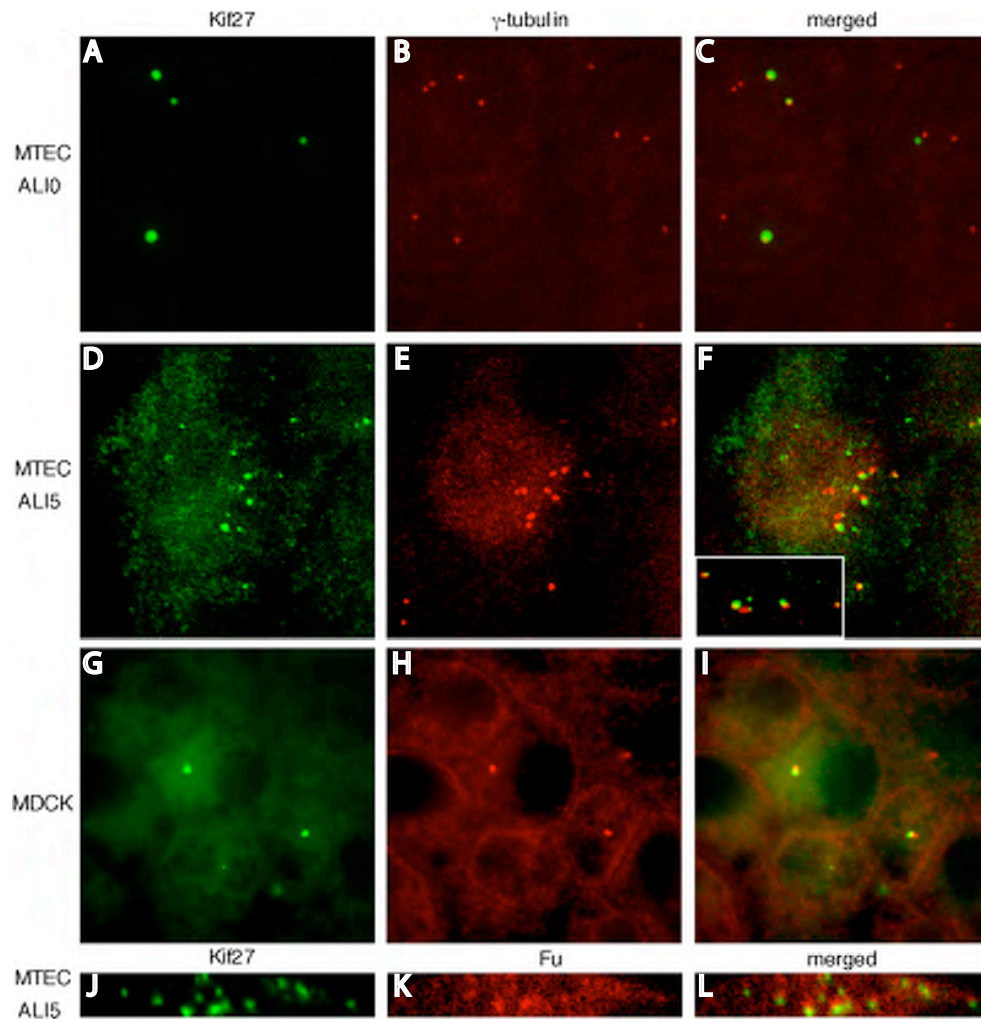
Figure 2-19: Kif27-GFP localizes to basal bodies at the base of motile cilia in differentiated MTECs
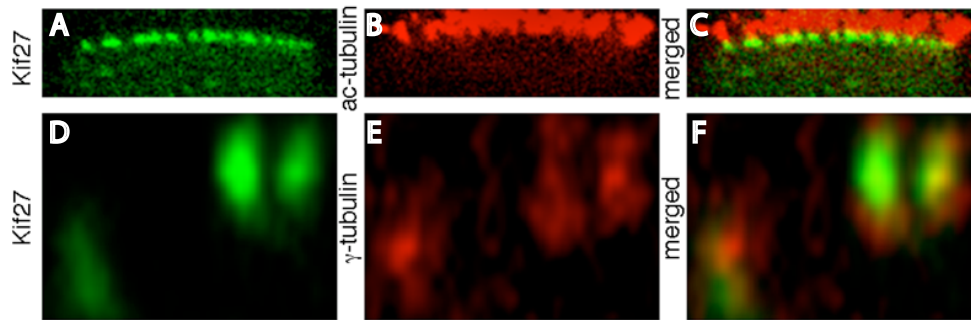
Figure 2-20: Fu-mCherry is broadly distributed throughout the cytoplasm of MTECs, but overlaps with Kif27-GFP punctae
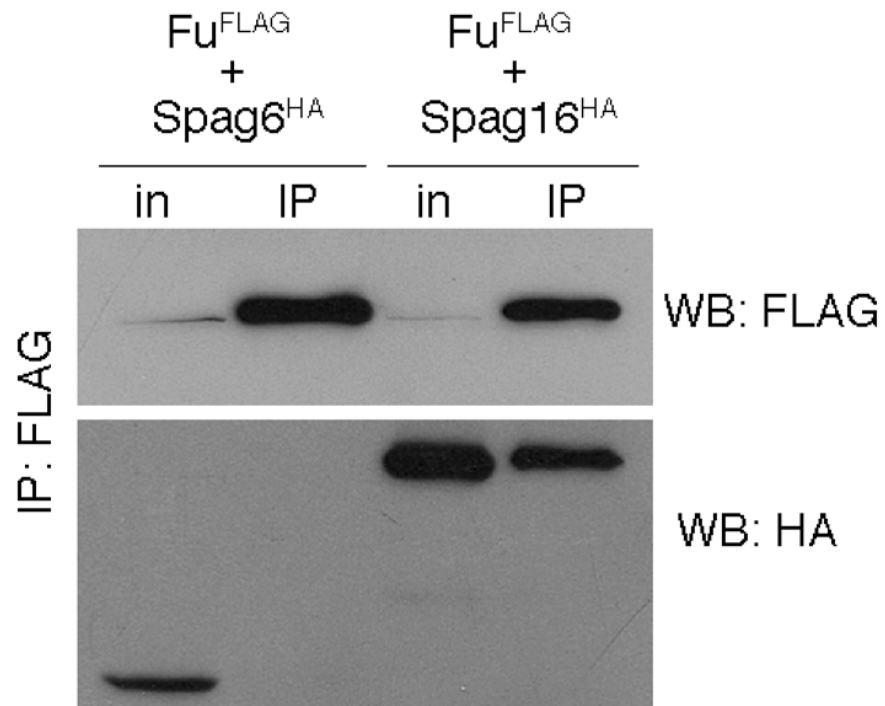
Kif27-GFP   Fu-mCherry   Merge

Figure 2-21: Mouse Fu physically interacts with Spag16, but not Spag6

Figure 2-22: Spag6 and Spag16 localization are unaffected in *Fu* mutant MTECs

Wild-type MTECs

Fu null MTECs
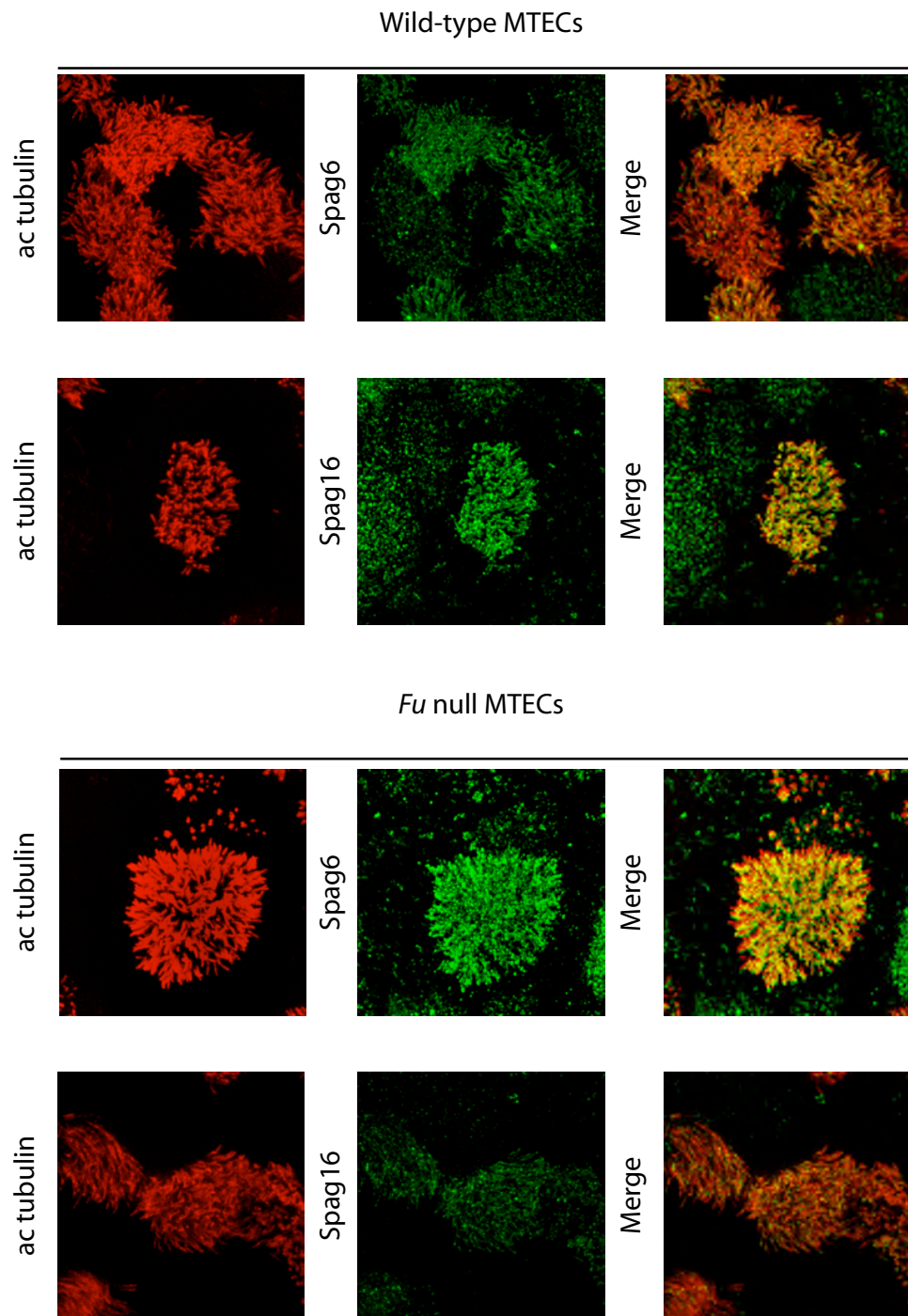
Figure 2-23: A speculative model of Fu and Kif27 function in motile ciliogenesis
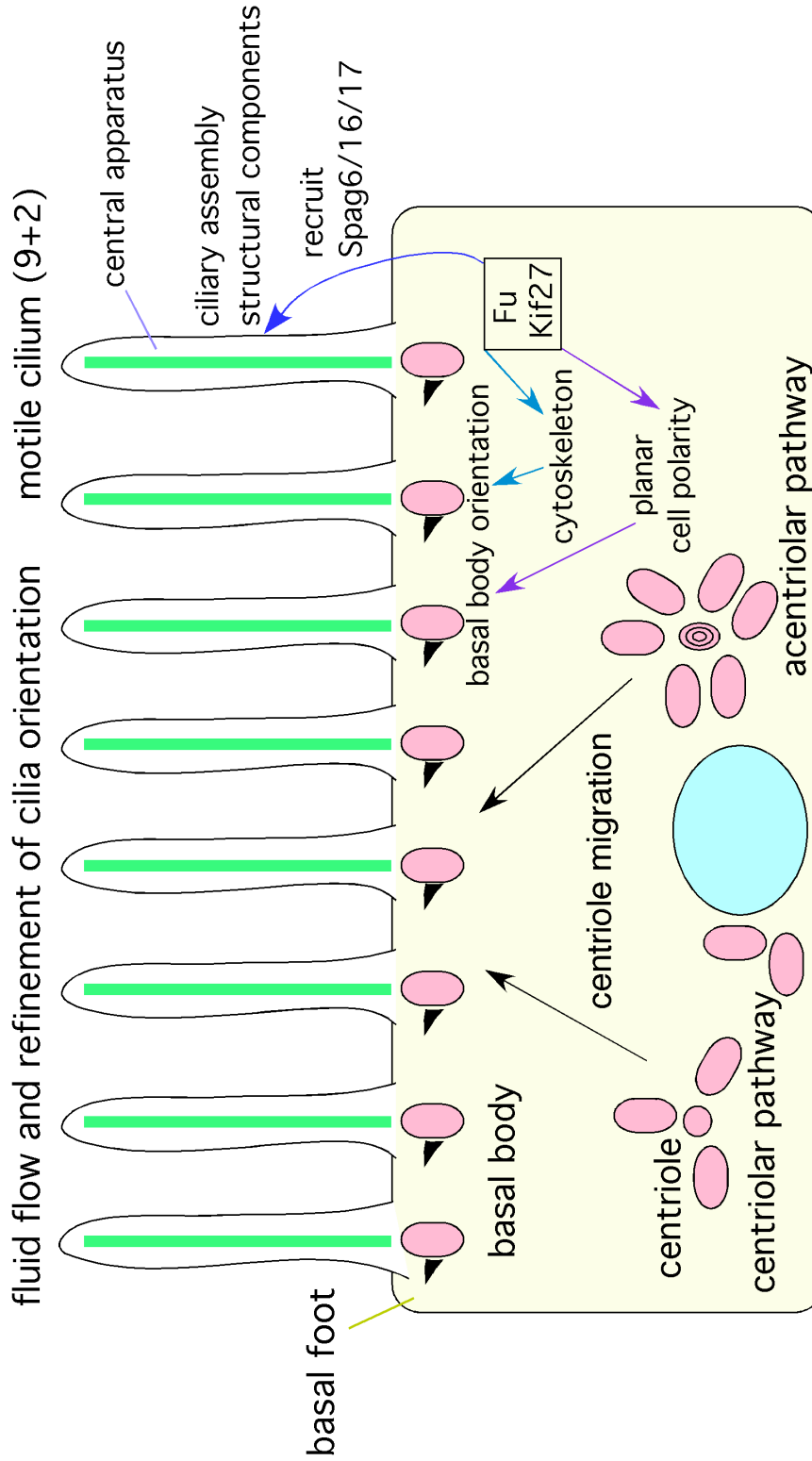
Figure 2-24: Lpp1/Vangl2 is found at the apical surface of wild-type MTECs, proximal to basal bodies
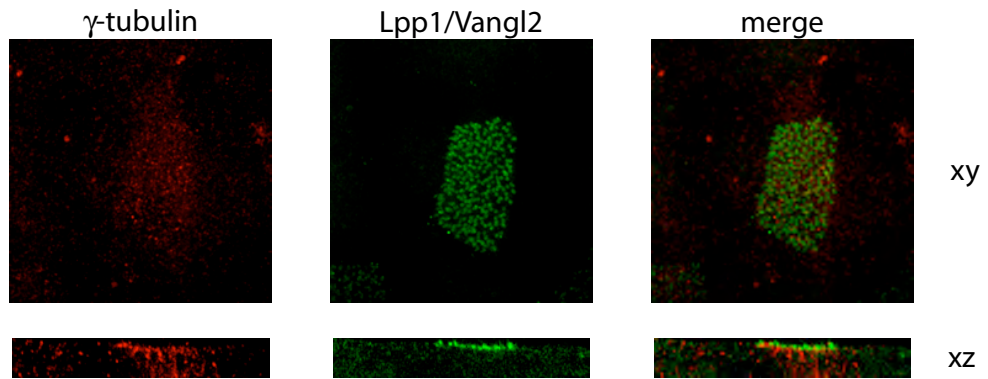
Table 2-1: Sequence identify and similarity of mouse Fu to other eukaryotic mouse kinases, and other mouse kinases

% ID (Sim)	H. sapiens	M. musculus	G. gallus	D. rerio	X. tropicalis	A. thaliana	D. melanogaster	C. reinhardtii	D. discoideum
H. sapiens		97 (98)	82 (90)	71 (85)	71 (84)	65 (83)	51 (69)	66 (83)	48 (74)
M. musculus	97 (98)		82 (90)	72 (86)	70 (83)	65 (83)	51 (70)	66 (83)	47 (73)
G. gallus	82 (90)	82 (90)		75 (87)	69 (84)	63 (81)	51 (70)	69 (86)	47 (74)
D. rerio	71 (85)	72 (86)	75 (87)		68 (83)	67 (83)	50 (70)	67 (85)	49 (74)
X. tropicalis	71 (84)	70 (83)	69 (84)	68 (83)		58 (77)	51 (71)	59 (81)	44 (74)
A. thaliana	65 (83)	65 (83)	63 (81)	67 (83)	58 (77)		49 (66)	78 (89)	52 (73)
D. melanogaster	51 (69)	51 (70)	51 (70)	50 (70)	51 (71)	49 (66)		51 (71)	42 (64)
C. reinhardtii	66 (83)	66 (83)	69 (86)	67 (85)	59 (81)	78 (89)	51 (71)		53 (74)
D. discoideum	48 (74)	47 (73)	47 (74)	49 (74)	44 (74)	52 (73)	42 (64)	53 (74)	

% ID (Sim)	Fu/Stk36
Akt3	34 (58)
Nek1	35 (54)
Slk	36 (56)
Ulk2	36 (55)
Ulk3	38 (58)

CHAPTER III

Suppressor of Fused promotes stability of Ci/Gli proteins, an evolutionarily

conserved cilium-independent function

I. Introduction

Elucidating the molecular mechanism of Hedgehog (Hh) signal transduction is critical for understanding both normal embryonic patterning and pathological conditions such as human congenital anomalies and cancers arising from misregulated Hh signaling. The main components of the Hh signaling pathway appear to be conserved between invertebrates and vertebrates; however, recent studies indicate that several aspects of Hh signaling have diverged (Svärd et al. 2006; Varjosalo et al. 2006). In particular, the primary cilium, an ancient and evolutionarily conserved organelle, is essential for mammalian Hh signal transduction, but is dispensable for Hh signaling in *Drosophila*. The extent of Hh pathway divergence in different model organisms is a major unresolved issue. Delineating cilium-depedendent and –independent processes of Hh signal transduction is crucial to understanding how the mammalian Hh pathway has evolved. Insight into this question will not only advance our mechanistic understanding of Hh signaling but also serve as a paradigm for investigating the evolution of signal transduction pathways.

Most vertebrate cells possess a non-motile primary cilium (Huangfu and Anderson 2005). Primary cilia contain a long microtubular axoneme that extends from the basal body and is surrounded by an external membrane that is continuous with the plasma membrane (Rosenbaum and Witman 2002). Assembly and maintenance of the primary cilium are mediated by a process called intraflagellar transport (IFT), which involves bidirectional movement of IFT particles powered by anterograde kinesin (Kif3a,

b and c) and retrograde dynein motors (Rosenbaum and Witman 2002). Mouse

ethylnitrosourea (ENU) mutants in genes encoding IFT proteins, or the respective motors,

have defective Hh signaling (Huangfu et al. 2003; Liu et al. 2005), providing strong

evidence that the primary cilium plays a key role in mammalian Hh signaling. Moreover,

most core mammalian Hh pathway components, including Smoothened (Smo), Patched1

(Ptch1), Suppressor of fused (Sufu), and Gli1, Gli2, and Gli3, localize to the primary

cilium (Corbit et al. 2005; Haycraft et al. 2005; Rohatgi et al. 2007). Further, production

of both Gli activators and repressors appears to be affected in *IFT* mutant mice (Huangfu

and Anderson 2005; Liu et al. 2005). These results establish a strong connection between

primary cilia and mammalian Hh signaling. Interestingly, *Drosophila* mutations in either

the anterograde kinesin motor or components of the IFT particles cause neuronal

phenotypes but do not seem to disrupt Hh signaling (Han et al. 2003), highlighting a

unique role of the cilium in mammalian Hh signaling.

Binding of Hh to its twelve-pass transmembrane receptor Ptch1 triggers ciliary

localization of Smo, a seven-pass transmembrane protein (Corbit et al. 2005) with

concomitant loss of Ptch1 on the cilium (Rohatgi et al. 2007), leading to Smo activation.

Otherwise, Ptch1 inhibits Smo activity via unknown mechanisms. In the absence of the

Hh ligand, Gli2 and Gli3 transcription factors (homologs of *Drosophila* Cubitus

interruptus (Ci)) undergo limited proteolysis in which the C-terminal activator domains

are cleaved, thus generating transcriptional repressors (Aza-Blanc et al. 1997; Wang et al.

2000a; Pan et al. 2006). The Hh signal transduction cascade represses Ci/Gli2/3

proteolysis, promoting the generation of transcriptional activators which presumably are

97

derived from full-length Ci/Gli proteins. By contrast, the Gli1 protein lacks an N-terminal repressor domain and functions solely as a transcriptional activator. The delicate balance between Gli activators and repressors is believed to be the major determinant of graded Hh responses. It is widely speculated that many key events of cytoplasmic Hh signal transduction downstream of Smo occur on the cilium, the absence of which is known to perturb the ratio of full-length Gli (putative activators) and Gli repressors (Liu et al. 2005). However, functional studies to demonstrate how the primary cilium controls Hh signaling are largely lacking. It has not been established that production of Gli activators and repressors occurs on the primary cilium. In addition, whether Smo is activated on the cilium, and how this occurs, is unclear. It is also unknown if Gli protein levels or activity can be regulated by processes independent of the primary cilium.

Studies on Hh signal transduction downstream of Smo in a number of model organisms suggests a modified pathway design (Huangfu and Anderson 2006). In particular, efforts to understand the roles of Fused (Fu), a putative serine-threonine kinase, and Sufu, a novel PEST domain protein in Hh signaling shed light on pathway divergence. *Su(fu)* is dispensable for viability in *Drosophila* and was identified as an extragenic suppressor of *fu* mutations (Préat 1992; Préat et al. 1993). In *Drosophila*, Fu functions in concert with the atypical kinesin Costal-2 (Cos2) (Robbins et al. 1997; Sisson et al. 1997), Ci (ref) and Sufu in transducing the Hh signal. In the absence of extracellular Hh ligand, Cos2 functions as a scaffold in a multimolecular protein complex comprised of Fu, Ci, Cos2, and a small amount of Sufu. Cos2 recruits the kinases PKA, GSK3 and CKI to promote Ci phosphorylation (Zhang et al. 2005), targeting Ci for

98

limited proteolysis via the Slimb/B-TrCP-Cul1 E3 ubiquitin ligase (Di Marcotullio et al.

2007). This cleavage event removes the C-terminal activation domain from Ci and

produces a transcriptional repressor, capable of inhibiting Hh target gene expression (ref).

Hh signal transduction leads to dissociation of the kinases from the Cos2-scaffolded

complex and subsequent inhibition of Ci proteolysis. Instead, Cos2, Fu, and possibly Ci

are recruited to Smo at the plasma membrane through direct associations between Cos-2

and the Smo C-terminus (Stegman et al. 2000; Jia et al. 2003; Lum et al. 2003b; Ogden et

al. 2003; Ruel et al. 2003; Stegman et al. 2004). In this process, Ci is converted into an

activator through unknown mechanisms in order to activate Hh target genes (Ohlmeyer

and Kalderon 1998). Fu and Sufu were proposed to exert opposite effects in controlling

the processing, activity, and shuttling of Ci between the nucleus and the cytoplasm

(Wang and Holmgren 1999; Méthot and Basler 2000; Wang et al. 2000b; Lefers et al.

2001). Sufu is believed to tether Ci in the cytoplasm and repress Hh signaling, a function

that could be antagonized by Fu.

Sufu is a major regulator of mammalian Hh signaling (Cooper et al. 2005; Svärd

et al. 2006), but the molecular mechanisms by which Sufu controls vertebrate Hh

signaling are unknown. *Sufu*-deficient mice die around 9.5 days *post coitus* (*dpc*) with a

ventralized neural tube due to global upregulation of Hh signaling. This is in stark

contrast to the lack of overt phenotypes in *sufu* mutant flies (Préat 1992). By contrast, *Fu*-

deficient mice are viable and display no embryonic phenotypes (Chen et al. 2005;

Merchant et al. 2005). Hh signaling in zebrafish appears to represent a transitional state,

since morpholino-mediated knockdown of *fu* produces phenotypes consistent with loss of

Hh activity, whereas loss of *sufu* results in a mild elevation of Hh signaling (Wolff et al. 2003). These results indicate diverse species employ a modified regulatory circuitry and/or distinct cellular microenvironments for Hh signaling. Given the vital role of Sufu in controlling mammalian Hh signaling, as well as the fact that it is physically present on the cilium, studies of Sufu provide a unique tool to clarify mechanisms of Hh signal transduction and their possible divergence during evolution.

II. Results

Hh pathway components localize to the primary cilium in a dynamic manner

Most mammalian Hh pathway components, including Smo, Ptch1, Sufu, and Gli1, Gli2 and Gli3, localize to the primary cilium (Corbit et al. 2005; Haycraft et al. 2005; Rohatgi et al. 2007) (Figure 3-1, see also Chapter IV). Smo translocates to to primary cilium upon Hh pathway activation, with concomitant loss of Ptch1 from the cilium. While ciliary localization of endogenous Smo, Ptch1 and Sufu has been documented (Corbit et al. 2005; Haycraft et al. 2005; Rohatgi et al. 2007), only overexpressed Gli1, Gli2 and Gli3 proteins have been examined on the cilium (Haycraft et al. 2005). We generated antibodies against Gli2 and Gli3 that are capable of detecting endogenous Gli proteins. Gli2 and Gli3 are present at the primary cilium at low levels in the absence of Hh ligand, and their levels on the cilium dramatically increase with the addition of exogenous ShhN ligand (Figure 3-1, 3-2). This observed dynamic change in endogenous Gli2 and Gli3 levels on the cilium in response to Hh signaling differs from results using overexpressed Gli2 and Gli3 proteins, which can be detected on the cilium regardless of

the state of pathway activation (Haycraft et al. 2005). By contrast, ciliary localization and intensity of Sufu staining are unaffected upon Hh pathway activation (Figure 3-1, 3-2). In some cells, Gli2, Gli3 and Sufu immunofluorescence was detected largely at the tip of the primary cilium, while in other cells it was distributed along the entire cilium, perhaps reflecting trafficking of these proteins on the cilium (Figure 3-1). Gli2 and Gli3 localize to the primary cilium even in the absence of Hh stimulation in *Ptch1 –/–* mouse embryonic fibroblasts (MEFs) (Figure 3-1, 3-2), in which the Hh pathway is maximally activated in a ligand-independent manner. Together, these localization studies suggest that the primary cilium constitutes a critical site for Hh signaling, but further functional studies are required for clarifying how the cilium regulates Hh transduction.

Gli2 and Gli3 protein levels are greatly reduced in the absence of Sufu

To investigate how Sufu regulates Hh signaling, we examined Gli protein levels in *Sufu –/–* embryos and MEFs. We found that endogenous Gli2 and Gli3 proteins (both full-length and repressor) are barely detectable on Western blots in the absence of *Sufu* (Figure 3-3, 3-4). Consistent with this finding, ciliary localization of Gli2 and Gli3 is completely abolished in *Sufu –/–* MEFs (Figure 3-1, Figure 3-2). This is not due to reduced mRNA levels of *Gli2* and *Gli3*, which are comparable between wild-type and *Sufu –/–* MEFs (Figure 3-5). These results reveal a major unappreciated role of mammalian Sufu in controlling full-length Gli protein levels. Consequently, removal of *Sufu* would affect the production of both Gli2/3 activators and repressors.

Sufu functions independently of Fu and the primary cilium in controlling Gli protein levels

Fu-deficient mouse embryos display no Hh phenotype (Chen et al. 2005; Merchant et al. 2005), but exhibit Hh-indepent defects in motile cilia function (see Chapter II). To investigate whether the antagonistic genetic interaction of *Drosophila fu* and *Su(fu)* is conserved in mammals, we asked if loss of *Fu* rescued Hh defects in *Sufu* mutant mice. We observed that *Sufu* phenotypes cannot be rescued by loss of *Fu* in mice, and *Sufu* –/–; *Fu*–/– mutants phenocopy *Sufu* –/– embryos (Figure 3-6). This suggests that the regulatory circuitry involved in cytoplasmic transduction of the mammalian Hh signal has been modified when compared to *Drosophila*. Further, Fu is dispensable for this process.

The observation that Sufu, Gli1, Gli2 and Gli3 localize to the primary cilium, coupled with biochemical data showing that Sufu physically interacts with all three Gli proteins, raised the interesting possibility that Sufu regulates Gli protein function on the primary cilium. To directly test whether Sufu's function is mediated by the cilium, we generated mice deficient in *Sufu* and *Kif3a* (in which primary cilia fail to form) (Marszalek et al. 1999). Unlike *Sufu*-deficient mice, *Kif3a* –/– embryos display reduced Hh signaling in a dorsalized neural tube (Huangfu et al. 2003)(Figure 3-6), and *Kif3a* –/– MEFs are unresponsive to Hh agonists (Figure 3-22). In contrast, loss of *Sufu* results in global upregulation of Hh signaling and ventralization of the neural tube. Specifically, *Shh* expression, which is found in the notochord and floor plate at the ventral midline, is extended dorsally. This is accompanied by a similar dorsal expansion of Hh target genes

such as *Ptch1*, suggesting ventralization of the neural tube. Consistent with this, the expression domains of neural progenitor markers (Class I genes, including *Pax7* and *Pax6*, repressed by Hh signaling, and Class II genes, including *Nkx6.1*, *Nkx2.2* and *Foxa2*, activated by Hh signaling) are shifted. For instance, the dorsal-most marker *Pax7* is not expressed, and *Pax6* expression is restricted to the dorsal neural tube of *Sufu–/–* embryos. Ventral expression of *Nkx6.1*, *Nkx2.2*, and *Foxa2* is expanded dorsally in the absence of *Sufu*. Similarly, the expression domains of markers for differentiated interneurons and motoneurons are altered. For example, expression of *Islet1* and *Oligo2*, which mark motoneurons, is expanded dorsally in the *Sufu–/–* neural tube. If the primary cilium is required for Sufu's function in controlling Gli protein levels, we expected to observe a blockade of elevated Hh signaling in *Sufu* mutants upon genetic elimination of primary cilia. Surprisingly, we found that neural tube defects in *Sufu–/–*; *Kif3a –/–* mutants are identical to those seen in *Sufu –/–* mutants (Figure 3-6). Marker analysis by isotopic *in situ* hybridization revealed increased Hh signaling as shown by the dorsal expansion of Hh target genes (*e.g.* *Ptch1*) and ventral neural tube markers in both *Sufu–/–*; *Kif3a–/–* mutants (Figure 3-6), indicating that Sufu's main function does not require an intact primary cilium.

To confirm that regulation of Gli protein levels by Sufu can still occur in the absence of cilia, we knocked down *Sufu* in wild-type and *Kif3a–/–* MEFs via stable lentiviral delivery of short hairpin RNA (shRNA) (Reynolds et al. 2004). Gli2 and Gli3 protein levels are greatly reduced to the same extent in both cell lines (Figure 3-7). Taken together, these results indicate that Sufu functions independently of the primary cilium in

controlling Gli protein function. This observation highlights the importance of conducting functional studies in determining the mechanisms by which the primary cilium regulates Hh signaling, as opposed to relying solely on protein localization.

Hh signaling is upregulated in Ptch1 and Sufu mutants via distinct mechanisms

To further define cilium-dependent and –independent Hh signaling events we examined molecular defects in *Ptch1*–/– and *Sufu*–/– MEFs. Ptch1 and Sufu are two major regulators of mammalian Hh signaling, and both *Ptch1*- and *Sufu*-deficient mouse embryos display a severely ventralized neural tube due to elevated Hh signaling (Goodrich et al. 1997; Cooper et al. 2005; Svärd et al. 2006) (Figure 3-6). Gli2 and Gli3 protein are barely detectable in *Sufu*–/– MEFs (Fig 3-4). Instead, in *Ptch1*–/– MEFS, which display ligand-independent maximal activation of Hh signaling, Gli2 and Gli3 localize to the primary cilium in the absence of Hh simulation (Figure 3-1, 3-2). Further, full-length Gli2 and Gli3 protein levels are similar to those in wild-type MEFs, with a reduction in Gli3 repressor levels (Figure 3-4).

To assess the requirement of the primary cilium in mediating Ptch1 or Sufu function, we inhibited primary cilium function in either *Ptch1*–/– or *Sufu*–/– MEFs by expressing a dominant negative form of Kif3b (dnKif3b), a subunit of the kinesin-II motor that participates in IFT (Fan and Beck 2004). Inhibition of ciliary function in *Sufu*–/– MEFs had no effect on Gli protein levels or Hh pathway activity (Fig 3-8). Further, overexpressed Gli1, Gli2 and Gli3 localize to the primary cilium in *Sufu*–/–

MEFs, suggesting that Sufu is not essential for ciliary localization of Gli proteins (Fig 3-1).

Moreover, Sufu is able to suppress Gli-mediated Hh activation in *Kif3a*–/– MEFs (Fig 3-7), indicating an essential negative role of Sufu in regulating Gli function independent of the primary cilium. By contrast, the constitutive Hh signaling in *Ptch1*–/– MEFs is greatly reduced compared to *Sufu*–/– MEFs when dnKif3b is expressed (Fig 3-8). Defective ciliary function in *Ptch1*–/– MEFs also changed the ratio of full-length Gli3 to Gli3 repressor, resembling the ratio observed in *Kif3a*–/– mutants or MEFs (Fig 3-8). Thus, despite ciliary localization of Ptch1 and Sufu, and Hh pathway upregulation in *Ptch1*–/– and *Sufu*–/– mutants resulting in similar phenotypes, the molecular mechanisms of Ptch and Sufu are different. Ptch1 function, like Smo, is dependent on the primary cilium, while Sufu functions independently of the cilium.

Drosophila and zebrafish Sufu restore Gli protein levels in Sufu–/– MEFs, while Drosophila and zebrafish Smo fail to rescue Smo-deficient MEFs

We reasoned that if involvement of the primary cilium in mammalian Hh signaling represents a major shift from fly Hh signaling, events mediated by Sufu and thus independent of the cilium would likely be evolutionarily conserved. By contrast, cilium-dependent processes of Hh signal transduction, including ciliary localization of Smo and Ptch and their interactions on the cilium would be divergent amongst different model organisms.

To test this idea, we introduce Smo cDNAs from mouse, zebrafish or *Drosophila* into *Smo*–/– MEFs via transient transfection. We then assayed both ciliary localization of Smo by immunofluorescence, as well as Hh pathway activation by transfecting MEFs with a Hh reporter construct (*8xGliBS-luc*), which has eight Gli-binding sites driving firefly luciferase expression (Sasaki et al. 1999). As expected, expression of mouse Smo in *Smo*–/– MEFs resulted in Smo ciliary localization (Fig 3-9) and conferred Hh responses (Fig 3-9). Interestingly, zebrafish Smo was detected with our antibody directed against mouse Smo, and both localized to the cilium and activated the Hh pathway upon ligand stimulation in *Smo*–/– MEFs (Fig 3-9). Although the role primary cilia play in mediating Hh signaling in zebrafish has not been fully defined, our finding suggests that both cilium-dependent and –independent processes exist. Contrastingly, *Drosophila* Smo failed to reach the shaft or tip of the cilium (Fig 3-9), and no Hh responses were observed (Fig 3-9). These results imply distinct requirements for Smo activation in different species, and underscore the unique role of the primary cilium in vertebrate Hh signaling.

We then assessed the effects of Sufu from different species on Hh pathway activation in *Sufu*–/– MEFs. Sufu from mouse, zebrafish or fly was introduced into *Sufu*–/– MEFs via retroviral infection, and Gli2 and Gli3 protein levels and localization were assessed by immunofluorescence and Western blotting. We first showed that expression of mouse Sufu in *Sufu*–/– MEFs restored both Gli2 and Gli3 protein levels (Fig 3-2, 3-9) and their ciliary localization (Fig 3-2, 3-9). Similarly, zebrafish Sufu was also capable of restoring Gli protein levels (Fig 3-2, 3-9) and their ciliary localization in *Sufu*–/– MEFs (Fig 3-2, 3-9), again consistent with the presence of both cilium-dependent

and –independent processes in this organism. Remarkably, expression of *Drosophila* Sufu in *Sufu*–/– MEFs led to a partial rescue of Gli protein levels (Fig 3-9) and ciliary localization (Fig 3-2). These results are consistent with a conserved biochemical function of Sufu.

Sufu antagonizes Spop in regulating Gli2 and Gli3 protein levels

To further test the idea that Sufu-mediated regulation of Gli protein levels is conserved among different organisms, we asked whether Spop, a homolog of the *Drosophila* MATH and BTB domain-containing protein protein Hib, antagonizes Sufu in regulating Gli protein levels. Hib forms a complex with Ci and Cullin3 (Cul3), and promotes Ci ubiquitinaion by the Cul3-based E3 ubiquitin ligase, resulting in complete degradation of Ci (Zhang et al. 2006a). Sufu appears to protect Ci from Hib-mediated degradation through competitive binding with Hib for Ci (Zhang et al. 2006a).

We first investigated the subcellular distribution of overexpressed Spop and Gli1, Gli2, and Gli3 in MEFs and established cell lines. While Gli proteins are distributed relatively evenly in the cytoplasm and nucleus (Fig 3-11), a prominent feature of Spop protein distribution is the presence of focal densely-stained nuclear speckles (Fig 3-11, 3-12). We also observed foci of Spop staining in the cytoplasm in a subset of cell types examined, indicating that cell-line specific factors may determine the proportion of nuclear and cytosolic Spop. Interestingly, co-expression of Gli2 and Gli3 with Spop recruited Gli2 and Gli3 into Spop-positive foci (Fig 3-11, 3-12). In contrast, the

107

distribution of Gli1 was unchanged in the presence of Spop. These results suggested that

Spop might physically interact with Gli2 and Gli3. To test this, we transfected HEK 293T

cells with constructs encoding Spop-HA and Gli1-FLAG, Gli2-FLAG, or Gli3-FLAG.

Spop physically associates with Gli2 and Gli3, but not Gli1 (Fig 3-13). Further, co-

expression of Spop with Gli proteins in HEK 293T cells led to a significant reduction in

Gli2 and Gli3 protein levels, while Gli1 is unaffected (Fig 3-14). Finally, we reasoned

that if Spop preferentially interacts with Gli2 or Gli3 and reduces the protein levels,

transcriptional activation could be compromised. Co-expression of Spop with Gli1 or

Gli2 resulted in a substantial, dose-dependent reduction in Gli2- but not Gli1-mediated

Hh pathway activation (Fig 3-15). Thus, we conclude that Spop binds Gli2 and Gli3 and

causes a reduction in global Gli2 and Gli3 levels, resulting in a decrease in Gli2-

dependent transcriptional activity. Gli3 cannot be assessed in this assay owing to its weak

transactivation ability (data not shown).

We then asked whether Spop binding to Gli2 and Gli3 promotes their

ubiquitination and subsequent degradation by the 26S proteasome. We carried out an *in*

vivo ubiquitination assay in HEK 293T cells and showed that Spop promotes

ubiquitination of Gli2 and Gli3, but not Gli1 (Figure 3-16). The Spop-dependent

reduction in Gli2 and Gli3 protein levels was rescued with the proteasome inhibitor

MG132 (Fig 3-17), suggesting that Spop directs Gli2 and Gli3 degradation in a

proteasome-dependent manner. This is further supported by the observation that co-

expression of Spop with Gli2/3 and Cul3 recruits Gli2/3 into Spop-positive foci, which

also contain Cul3 (Fig 3-18). In contrast, Cul3 and Gli2/3 do not co-localize in the

absence of Spop, supporting the hypothesis that Spop targets Gli2 and Gli3 for Cul3-mediated proteasomal degradation.

Since Sufu is required for maintaining Gli2 and Gli3 protein levels, we tested whether Sufu antagonizes Spop function and thus preserves Gli2 and Gli3 protein stability. Expression of Sufu was able to block Spop-mediated Gli2 and Gli3 protein reduction (Fig 3-14) and ubiquitination (Fig 3-16), suggesting that Spop and Sufu antagonize each other in the regulation of Gli protein levels. Consistent with this notion, shRNA-mediated knockdown of *Spop* in *Sufu*–/– MEFs partially restored Gli2 and Gli3 protein levels (Fig 3-19). Knockdown of *Spop* in *Sufu*–/– MEFs also increased the basal level of Hh pathway activation (Figure 3-21), consistent with increased levels of Gli2 or Gli3 activator. In addition, recruitment of Gli2 and Gli3 to Spop-positive foci can occur in *Kif3a*–/– MEFs (Fig 3-11), suggesting that the Sufu-Spop Gli circuit is evolutionarily conserved, and is independent of the primary cilium. This is further supported by two observations. First, mouse Spop does not localize to the primary cilium when overexpressed (Fig 3-20). Second, mammalian Gli2 and Gli3 are stabilized when expressed in *Drosophila* deficient in Hib activity (Zhang et al. 2006a). We speculate that Sufu sequesters Gli2/3 protein in the cytoplasm and protects them from Spop-mediated protein degradation, providing a Gli protein pool for the production of Gli2/3 activators and repressors (Fig 3-24). Despite a conserved mechanism of Spop and Sufu function in regulating Gli2/3 protein levels, it is interesting to note that Gli appears to be refractory to Spop regulation, but its transactivation potential is still be inhibited by Sufu. This selective regulation could allow the production of a wide range of Hh responses.

Sufu has an unexpected positive role in controlling mammalian Hh signaling

Elevated Hh signaling in the *Sufu*-deficient neural tube indicates that Sufu is a negative regulator of mammalian Hh signaling (Cooper et al. 2005; Svärd et al. 2006) (Fig 3-6). With the new insight that Sufu regulates full-length Gli protein levels, we surmised that the function of Gli activators (which are derived from full-length Gli proteins) could be compromised in the absence of *Sufu*. Thus, *Sufu*-deficient MEFs or embryos would be predicted to display sub-maximal Hh pathway activation. To test this hypothesis, we investigated the mechanisms by which Sufu controls Hh signaling in MEFs. We first examined Hh responses in wild-type and *Sufu*–/– MEFs. We showed that wild-type MEFs are Hh-responsive by transfecting wild-type MEFs with the *8xGliBS-luc* reporter construct both in the absence and presence of ShhN-conditioned media (Fig 3-22). Hh responsiveness in *Sufu*–/– MEFs was mildly elevated in the absence of Hh stimulation, consistent with the demonstrated negative role of Sufu. Interestingly, exogenous Shh fails to support Hh responses to the same extent in *Sufu*–/– MEFs as in wild-type MEFs (Fig 3-22), consistent with a requirement of Sufu for maximal Hh pathway activation.

To further test this hypothesis, we transfected increasing amounts of Sufu cDNA in *Sufu*–/– MEFs in the absence or presence of exogenous ShhN and assessed its effects on Hh pathway activation, as measured by luciferase activity from the transfected *8xGliBS-luc* reporter. We found that in the absence of exogenous Shh, increasing

amounts of Sufu transfected in *Sufu*–/– MEFs gradually decreased basal reporter levels (Fig 3-23). This is consistent with negative regulation of Hh signaling by Sufu. Interestingly, in the presence of exogenous Shh, increasing the amount of transfected Sufu cDNA in *Sufu*–/– MEFs instead promoted Hh responsiveness. This suggests that Sufu is also required for maximal Hh signaling, and that Sufu is required for generation of a broader dynamic range of Hh responses.

When introduced into *Sufu*–/– MEFs, zebrafish and fly Sufu were also able to promote Hh responsiveness in the presence of exogenous Shh (Fig 3-9), again supporting an evolutionarily conserved role of Sufu. The effect of fly Sufu is less pronounced in this assay than either mouse or zebrafish Sufu. We speculate that this is due to reduced affinity of fly Sufu for Gli proteins (Fig 3-10). Supporting this idea, the mouse Sufu^{D159A} mutant (Merchant et al. 2004), which exhibits reduced binding to Gli proteins in co-immunoprecipitation assays (Fig 3-10), also displayed reduced efficacy in restoring Hh responsiveness in the presence of exogenous Shh (Fig 3-9).

To further validate a dual function of *Sufu* in controlling Hh signaling, we reasoned that if Sufu is required for maximal Hh pathway activation, knockdown of *Sufu* in *Ptch1*–/– MEFs would compromise pathway activation. Indeed, when *Sufu* was efficiently knocked down via shRNA in *Ptch1*–/– MEFs, ciliary localization of Gli2 and Gli3 was largely eliminated (Fig 3-23), and full-length Gli2 and Gli3 protein levels are greatly reduced (Fig 3-23). Consistent with these findings, neural tube defects in *Sufu*–/– embryos (Cooper et al. 2005; Svärd et al. 2006) (Fig 3-X) are slightly less severe than

Ptch1–/– (Goodrich et al. 1997) (data not shown), which can be attributed to a requirement of Sufu in Hh pathway activation. We also assessed how *Sufu* knockdown affects the efficacy of Hh pathway activation and Smo antagonists in *Ptch1*–/– MEFs. Knockdown of *Sufu* in a *Ptch1*–/– background reduced the constitutive level of Gli reporter activation, consistent with a reduction in the levels of Gli2 and Gli3 activator forms caused by elimination of Sufu (Figure 2-23). Hh pathway activation in *Ptch1*–/– MEFs is efficiently inhibited by the Hh antagonists cyclopamine, jervine, and SANT-1 (Chen et al. 2002b), but these Smo inhibitors have no effect on Hh pathway activity in *Sufu*–/– MEFs (Svärd et al. 2006) (Fig 3-23). When *Sufu* is knocked down in *Ptch1*–/– MEFs, these cells become partially insensitive to Smo inhibitors (Fig 3-23), consistent with the observation that activation in *Sufu*–/– MEFs is independent of Smo function. These studies also argue that Sufu functions downstream of Ptch1 and Smo. By stabilizing full-length Gli protein levels, Sufu could shift the contribution of Gli activators and repressors to Hh signaling outputs in various tissues.

III. Discussion

Our studies delineate important aspects of cilium-dependent and –independent Hh signal transduction. Hh binding to Ptch relieves its repression of Smo, and induces a conformational change in Smo that results in dimerization of Smo cytoplasmic tails and is essential for pathway activation (Zhao et al. 2007). Although these events are common across different species, the execution of these steps appears to be accomplished in distinct microenvironments in insects and mammals. The requirement of the primary

112

cilium for Smo function in mammalian Hh pathway activation suggests that important

modifications in Hh pathway design have occurred during evolution (Huangfu and

Anderson 2006). By constrast with non-conserved cilium-dependent processes, Sufu

antagonizes the action of the conserved protein Spop, and thus preserves a pool of full-

length Gli proteins. Consequently, the production of Gli repressors and activators is

dependent on the presence of Sufu, but does not require an intact primary cilium (Figure

3-24).

Despite the ciliary localization of Sufu and Gli proteins, our genetic and cell-

based studies unambiguously demonstrated that Sufu controls Gli2 and Gli3 protein

levels independent of the primary cilium. Further, Sufu is not essential for Gli trafficking

to the cilium. This highlights the importance of functional studies to assess the

physiological relevance of the presence of Hh pathway components, or unrelated non-

structural proteins, on the primary cilium. In contrast to our results, a prior report showed

that knockdown of *Sufu* in *Ift172^{wim}* or *Dync2h1^{ttn}* MEFs (in which primary cilium

function is disrupted) caused no detectable activation of Hh reporters (Ocbina and

Anderson 2008). This was interpreted as Sufu acting within cilia to keep Hh pathway off

in the absence of ligand (Ocbina and Anderson 2008). We suspect that the discrepancy

could be due to incomplete knockdown of *Sufu* using RNAi-based approaches that could

potentially complicate interpretations of genetic epistasis. We cannot rule out the

possibility that Sufu has additional roles in Hh signaling that are regulated or mediated by

the primary cilium. However, our data suggest that these processes most likely either

have minor effects on Hh signaling or are redundant with other events.

A major obstacle in understanding Hh pathway activation by Gli proteins is our inability to understand how a ratio of Gli activators and repressors is mechanistically converted into defined transcriptional events. In vertebrates, this is complicated by the fact that *Gli3* and *Gli1* are negative and positive targets, respectively, of Hh signaling (Marigo et al. 1996; Lee et al. 1997; Bai et al. 2002). This issue is underlined by the observation that the Hh pathway is activated in *Ptch1* and *Sufu* mutants, yet Gli protein levels are affected only in the absence of Sufu. This suggests that different combinations of Gli activators and repressors can lead to similar levels of Hh pathway activation. Our knockdown of *Gli1* in *Sufu* –/– MEFs indicates that Gli1 is likely a major source of transcriptional activation in *Sufu* mutants (Fig 3-8). We hypothesize that reductions in full-length Gli2 and Gli3 proteins, and consequently a reduction in Gli repressor levels, leads to upregulation of *Gli1* and thus ligand-independent activation of the Hh pathway. Supporting this, *Gli1* was shown to be a target of the Gli3 repressor by chromatin immunoprecipitation (Hu et al. 2006; Vokes et al. 2008). Previous studies on Gli-deficient neural tubes have implied that Gli activator function predominates over Gli repressors, and that Gli1 is able to compensate for the loss of Gli2 activator (Bai and Joyner 2001; Bai et al. 2002) (Huangfu and Anderson 2006). Thus, we predict that *Gli1*, whose expression is expanded dorsally in *Sufu* –/– neural tubes (Svärd et al. 2006), is responsible for the upregulated Hh signaling in this tissue. However, since full-length Gli2 and Gli3 protein levels are reduced, maximal Hh signaling fails to occur in *Sufu*-deficient neural tubes. In the developing limb, it is widely believed that the Gli3 repressor is a key player in antagonizing digit formation promoted by the Shh gradient

(Panman and Zeller 2003). Indeed, reduced Gli3 repressor in *Sufu*-deficient limbs led to overall pathway activation and digit duplication. However, the polydactyly in *Sufu* mutants appears to be more severe than in *Gli3* mutants, raising the intriguing possibility that loss of Gli2 repressors could contribute to transcription of Hh target genes in *Sufu–/–* limbs. Maximal Hh target gene induction fails to occur in *Sufu–/–* limbs, indicating a potential loss of Gli activator function, but this does not appear to affect digit patterning. We speculate that reduced Hh signaling in *Sufu*-deficient limbs could affect development at a later stage.

Our studies on Sufu provide important mechanistic insight into how Sufu regulates Hh signaling. Largely based on physical interactions between Sufu and Gli proteins, the traditional model proposed that Sufu tethers Gli proteins in the cytoplasm, preventing nuclear translocation and subsequent activation of target genes (Kogerman et al. 1999). In this study, we showed that Sufu antagonizes Spop, preventing degradation of full-length Gli2 and Gli3. The process of Sufu-Spop antagonism is evolutionarily conserved, since *Drosophila* Sufu protects Ci from Hib-mediated degradation through competitive binding to Ci (Zhang et al. 2006a). As a result, loss of Sufu affects production of Gli2/Gli3 activator and repressor forms, which are both derived from full-length proteins. This is achieved by Hib/Spop forming a complex with Ci/Gli2/Gli3 and Cul3, thus promoting Ci/Gli ubiquitination through the Cul3-based E3 ubiquitin ligase and resulting in complete degradation by the 26S proteasome (Zhang et al. 2006a). *Drosophila* Sufu is able to partially restore the defects in Gli2/Gli3 protein levels, ciliary localization, and Hh pathway activation in *Sufu–/–* MEFs, supporting conservation of this

process. Nevertheless, important differences in the Sufu-Spop-Gli circuit exist between flies and mammals. Gli1, unlike Gli2 and Gli3, does not appear to be subject to Spop regulation. Further, while *sufu* mutant flies are viable, *Sufu*–/– mice die during early embryogenesis (Préat 1992; Cooper et al. 2005; Svärd et al. 2006). Therefore, the gain-of-function phenotype in *Sufu* null mice may result from increased levels of Gli1, triggered by Spop-mediated degradation of full-length Gli2/Gli3. Gli1 may have lost a requisite Spop-interacting domain, allowing it to escape regulation by Spop. Identification of domains in Gli2 and Gli3 that interact with Spop will further clarify this issue. Notably, full-length Ci and Ci repressor levels appear to be proportionately reduced in *sufu* mutant flies, implying that *sufu* affects Ci protein stability (Ohlmeyer and Kalderon 1998). Duplication of the ancestral *Ci/Gli* gene, coupled with subfunctionalization and evolution of negative and positive transcriptional regulatory loops, may account for the vastly different effects of loss of *Sufu* in insects and vertebrates.

Regulation of Gli protein stability is a key step in controlling Hh pathway activity, and multiple, distinct degradation signals have been identified in the three Gli proteins. For instance, two degradation signals are present at the N-termini of Gli1 and Gli2, yet these differentially utilize the b-TrCP adapter protein for proteolysis (Bhatia et al. 2006; Huntzicker et al. 2006; Pan et al. 2006). B-TrCP is also required for limited proteolysis of Gli3 into a truncated repressor form (Wang and Li 2006). A critical unresolved issue is to understand how multiple degradation signals in Gli proteins are utilized to regulate full-length protein stability as well as generation of repressor forms. Further investigation is

116

required to determine if the role of Sufu is specific in antagonizing Spop-mediated degradation, or if it is capable of opposing additional degradative pathways (Di Marcotullio et al. 2006; Di Marcotullio et al. 2007). It is also formally possible that Sufu has a direct effect on Gli repressor stability.

Sufu was postulated to function in both the nucleus and the cytoplasm, as overexpressed Sufu protein in cultured cells could be detected in both compartments (Ding et al. 1999; Kogerman et al. 1999). Further, Sufu can be co-immunoprecipitated with all three Gli proteins, and was shown to cooperate with the SAP18-Sin3 co-repressor complex in repressing transcription from a multimerized Gli-binding site luciferase reporter (Ding et al. 1999; Kogerman et al. 1999; Cheng and Bishop 2002; Paces-Fessy et al. 2004). Thus, it was proposed that Sufu may have a direct role in repressing Gli-mediated transcription in the nucleus. Recent work has challenged Sufu's cytoplasmic function by demonstrating that an overexpressed Gli1-eGFP fusion protein has a similar cytoplasmic distribution in wild-type or *Sufu*-deficient MEFs; in both cell types, Gli1 becomes predominantly nuclear when nuclear export is blocked (Svärd et al. 2006). In agreement with this, we did not observe a significant change in nuclear-cytoplasmic partitioning of endogenous Gli2 or Gli3 when wild-type or *Sufu*–/– lysates were examined (Figure 3-25). Contrary to previous reports (Cheng and Bishop 2002; Paces-Fessy et al. 2004), we failed to observe any discernable effects of SAP18 either singly or in conjunction with other Hh pathway components on Hh pathway activity in MEFs (Figure 3-26). Nevertheless, although our studies highlight a major function of Sufu in regulating cytoplasmic Gli protein levels, we cannot conclusively rule out potential minor

117

roles in the nucleus. We would like to emphasize that previous work that involved manipulating other mammalian Hh pathway components in the absence of Sufu should be considered in light of the fact that Sufu regulates Gli2/Gli3 stability. For instance, protein kinase A (PKA) phosphorylates Gli2 and Gli3, promoting b-TrCP binding and limited proteolysis to generate repressor forms (Pan et al. 2006; Wang and Li 2006). Treatment of multiple *Sufu*–/– MEF clones with either forskolin or IBMX, known PKA agonists, has no convincing effect on elevated Hh pathway levels (Figure 3-27). Since Gli2/Gli3 protein levels are drastically reduced in *Sufu*–/– MEFs, the effects of PKA are expected to be minimized.

Zebrafish or *Drosophila* Sufu can restore Gli protein levels in *Sufu*–/– MEFs, yet Smo from *Drosophila* fails to rescue Hh signaling defects in *Smo*–/– MEFs. This supports our proposal that cilium-independent steps in Hh signaling are evolutionarily conserved. The primary cilium has been shown to be essential for proper Hh pathway activation and the production of a proper ratio of Gli activator and repressor forms. Thus, the primary cilium likely provides an environment in which Hh pathway components interact with each other in response to varying extracellular Hh ligand concentrations. Such obligatory intracellular interactions may have co-evolved to an extent where *Drosophila* Hh pathway components cannot functionally substitute for their mammalian counterparts. Supporting this, prior studies heterologously expressing human SMOH or FU in the developing fly wing disc showed that the mammalian proteins could not completely rescue loss of the cognate fly gene (Daoud and Blanchet-Tournier 2005; De Rivoyre et al. 2006). Further investigation of a possible role of the primary cilium in zebrafish Hh

signaling, which may represent a transitional state between fly and mouse, will provide additional insight into how various vertebrate species have adopted the primary cilium in Hh transduction.

A major unresolved issue in mammalian Hh signaling is understanding the molecular mechanisms of signal transduction from Smo to the Gli proteins. Smo encodes a seven-pass transmembrane protein that resembles a G protein-coupled receptor (GPCR). Gαi has been implicated as a mediator of Smo activity in *Drosophila*, yet manipulation of vertebrate Gαi has little effect on Gli3 processing and chick neural tube patterning (Low et al. 2008; Ogden et al. 2008). These findings not only stress the necessity of additional genetic analysis, particularly loss-of-function studies, and biochemical characterization to settle the role of G proteins in transducing the Hh signal downstream of Smo, but again point to potential divergence in pathway design between species. We consider three unresolved areas of future investigation based on our studies of the relationship between Sufu and Gli proteins.

First, it is unclear if Hh signaling modulates Sufu activity, and if Sufu interacts with other Hh pathway components to control Gli function. This is complicated by the involvement of the primary cilium in mammalian Hh transduction, as well as the current lack of evidence for a Cos2-scaffolded counterpart to the *Drosophila* Hh signaling complex (HSC) (Stegman et al. 2000; Varjosalo et al. 2006). Further, the Fused kinase, which opposes Sufu activity in the fly, is dispensable for mammalian Hh signaling and shows no epistatic relationship with *Sufu* (Chen et al. 2005; Merchant et al. 2005). Sufu

likely functions downstream of Ptch1 and Smo, since expression of a constitutively active form of Smo (SmoM2) in *Sufu*–/– MEFs failed to further activate the Hh pathway (Fig S12), and *Sufu* knockdown in *Ptch1*–/– MEFs led to reduced Gli protein levels (Fig. 6B, 6C). It has been hypothesized that Smo signals to Sufu (Svärd et al. 2006), but no biochemical evidence for this has yet been presented. Definitive *in vivo* loss-of-function studies on the mouse Cos2 orthologs, *Kif7* and *Kif27*, as well as further biochemical characterization of the mammalian Smo-Kif3a-b-arrestin complex (Kovacs et al. 2008), will address whether a conserved cytoplasmic HSC exists in mammals, or if Smo-Kif3a complexes on the primary cilium have replaced the scaffolding function of the HSC. Examination of a potential relationship of Sufu to a mammalian HSC will permit a greater understanding of Hh signal transduction.

Second, the mechanisms of Smo and Gli trafficking to the primary cilium are poorly understood, but the cilium is critical for proper pathway activation and formation of Gli activators and repressors (Corbit et al. 2005; Huangfu and Anderson 2005; Liu et al. 2005). Our data indicate that Sufu is not essential for Gli trafficking to the primary cilium. Thus, identifying signals that confer ciliary localization and trafficking of Hh pathway components and their interacting partners is crucial to understand the role of the cilium in controlling their function. Interestingly, genetic studies of the vesicle transport protein Rab23, a GTPase that is a cell-autonomous negative regulator of vertebrate Hh signaling, showed that Rab23 controls Gli2 and Gli3 activity (Eggenschwiler et al. 2006). This raises the possibility that Rab23 regulates trafficking of Hh pathway components that inhibit Gli activator function. By contrast, the GTPase Arl13b appears to be required

for generation of the Gli2 activator (Caspary et al. 2007). These, and other Rab proteins involved in biogenesis of the primary cilium (Oro 2007; Yoshimura et al. 2007), are likely to be useful targets for investigating the dynamics of Smo and Gli movement on the primary cilium, and their relationships to states of pathway activation. In addition, the steps required for conversion of full-length Gli to Gli activators are poorly understood (Methot and Basler 1999; Smelkinson et al. 2007), and biochemical identification of these events and their relationship to the primary cilium is essential.

Finally, our comprehension of Gli activator and repressor function at endogenous target promoters or enhancers is lacking, but significant progress has recently been made in identifying *bona fide* Gli binding sites via chromatin immunoprecipitation (Vokes et al. 2007; Vokes et al. 2008). Many Gli binding sites were occupied by both Gli1 activator and an artificial Gli3 repressor (Vokes et al. 2007; Vokes et al. 2008), yet the dynamics of activator and repressor binding in the absence or presence of Hh ligand remain to be investigated. Further experiments of this nature, focusing on Gli partner proteins such as Sufu, and potential coactivators and corepressors (such as SAP18, Sin3a, Ski, CBP, and Hoxd12) (Akimaru et al. 1997; Cheng and Bishop 2002; Chen et al. 2004c; Paces-Fessy et al. 2004), will illuminate the mechanism of Gli transcription factor action, and possible Sufu function, at endogenous binding sites.

IV. Figure Legends

Figure 3-1: Endogenous Hh pathway components display dynamic patterns of ciliary localization in response to Hh signaling while overexpressed Gli proteins localize to the primary cilium in the absence of *Sufu*

(**A**) Immunofluorescence of wild-type (wt), *Sufu*$^{-/-}$, and *Ptch1*$^{-/-}$ MEFs using antibodies against acetylated tubulin (AC) (labeling primary cilia, red) and various endogenous Hh pathway components including Smo, Ptch1, Gli2, Gli3 and Sufu (green). Smo translocates to the primary cilium upon Hh pathway activation which is associated with concomitant loss of Ptch1 from the cilium. Low levels of Gli2 and Gli3 can be detected on the primary cilium by immunofluorescence without Hh ligand stimulation (data not shown) and their levels on the cilium significantly increase upon exposure to exogenous Shh ligand. By contrast, ciliary localization and intensity of Sufu are unchanged upon Hh pathway activation (data not shown). Gli2, Gli3 and Sufu immunofluorescence is detected primarily at the end of the primary cilium in some cells, while in others it decorates the entire cilium, perhaps due to dynamic ciliary trafficking of these proteins. Gli2 and Gli3 localize to the primary cilium in the absence of Hh stimulation in *Ptch1*$^{-/-}$ MEFs, in which the Hh pathway is maximally activated. Ciliary localization of Gli2 and Gli3 is completely abolished in *Sufu*$^{-/-}$ MEFs. (**B**) Immunofluorescence of *Sufu*$^{-/-}$ MEFs expressing mouse FLAG-tagged Gli1, 2 or 3 using antibodies against acetylated tubulin (red) and FLAG antibodies against Gli1, 2 or 3 (green). Overexpressed Gli proteins localize to the primary cilium in the absence of *Sufu* and ciliary localization is unaffected by Hh stimulation. We speculate that the amount of overexpressed Gli

proteins exceeds the capacity of Gli-degradation machinery in the absence of *Sufu* (see Fig. 2A).

Figure 3-2: Gli2 and Gli3, but not Sufu, display dynamic localization on the primary cilium

Quantification of the number of cilia showing Gli2, Gli3, and Sufu staining in mouse embryonic fibroblasts (MEFs). For all individual data points, a minimum of two independent experiments was performed, with a minimum of 100 cilia counted in each experiment. (**A**) Gli2 and Gli3 staining on the primary cilium in wild-type MEFs increases after stimulation with ShhN. Gli2 is not observed on the primary cilium in the absence of ShhN, but the number of Gli2+ cilia increase with prolonged exposure to ligand. Gli3 is typically found in approximately 40% of cilia; this number transiently increases to ~90% after brief (1 hr) exposure to ShhN, with a corresponding increase in intensity of staining along the entire length of the cilium. By contrast, mouse Sufu is detected in roughly 90% of cilia irrespective of the state of Hedgehog (Hh) pathway activation. (**B**) Retroviral introduction of FLAG-tagged mouse (m), zebrafish (z), and fly (d) Sufu into *Sufu*–/– MEFs restores Gli2 and Gli3 localization to the primary cilium. Mouse and zebrafish Sufu rescue ciliary localization of Gli2 and Gli3 to a greater extent than fly Sufu, consistent with the ability of the respective Sufu proteins to rescue total cellular Gli2 and Gli3 levels. Expression of mSufuD159A, which has reduced binding affinity for Gli proteins, does not rescue Gli2 or Gli3 ciliary localization. Interestingly, epitope-tagged zSufu and dSufu were not detected on the primary cilium. (**C**)

123

Knockdown of *Sufu* via shRNA in *Ptch1*–/– MEFs eliminates detectable Gli2, Gli3 and Sufu staining from the primary cilium. Error bars are standard deviation (s.d.).

Figure 3-3: Characterization of antibodies against endogenous mouse Gli2 and Gli3

(**A**) Western blots of lysates derived from wild-type (wt), *Gli2*–/–, and *Gli3*–/– mouse embryonic fibroblasts (MEFs) and embryos. Bands corresponding to endogenous Gli2, Gli3 full-length (FL), and Gli3 repressor (R) are not detected in the corresponding null cells and embryos. Note that some non-specific bands are apparent in *Gli3*–/– MEFs, consistent with Gli3 antibodies developed by others that can detect endogenous Gli3 (Wang et al. 2000a). Tubulin was used as the loading control and numbers on the right indicate positions of protein standards.

(**B**) *Gli2*–/– and *Gli3*–/– MEFs were stained with antibodies against either Gli2 or Gli3 and acetylated tubulin (AC) (to mark primary cilia). No Gli2 or Gli3 immunoreactivity was seen in the primary cilium in null cells, in the presence or absence (data not shown) of ShhN.

Figure 3-4: Gli2 and Gli3 protein levels are reduced in *Sufu* null MEFs

Western blots of lysates derived from wild-type (wt), $Gli2^{-/-}$, $Gli3^{-/-}$, $Sufu^{-/-}$; $Ptch1^{-/-}$ and $Kif3a^{-/-}$ mouse embryonic fibroblasts (MEFs) probed with anti-Gli2 and anti–Gli3 antibodies. Endogenous Gli2 and Gli3 protein levels (including full-length Gli3 and Gli3 repressor) are greatly reduced in the absence of *Sufu*. Both full-length Gli3 and Gli3

repressor can be detected in *Ptch1*$^{-/-}$ albeit the Gli3 repressor level is reduced. The ratio of full-length Gli3 to Gli3 repressor is altered in *Kif3a*$^{-/-}$ MEFs as previously reported (Liu et al. 2005). Gli2 processing is known to be extremely inefficient and the Gli2 repressor form cannot be readily detected without additional enrichment steps using specific Gli-binding oligonucleotides (Pan et al. 2006). We also cannot accurately assess the full-length to repressor ratios for Gli2 and Gli3 in *Sufu* mutants. Tubulin was used as the loading control and numbers on the right indicate locations of protein size standards. FL, full-length; R, repressor.

Figure 3-5: *Gli2* and *Gli3* transcript levels are not significantly changed in *Sufu–/–* MEFs or embryos

(**A**) Measurement of *Gli2* transcripts in *Sufu–/–* mouse embryonic fibroblasts (MEFs) or embryos. The ratio of *Gli2* to *b-actin* transcript was calculated and normalized to the wild-type value. Results are the mean of three independent experiments. Error bar indicates standard deviation (s.d.). (**B**) Measurement of *Gli3* transcripts in *Sufu–/–* MEFs or embryos. The ratio of *Gli3* to *b-actin* transcript was calculated and normalized to the wild-type value. Results are the mean of three independent experiments. Error bar indicates standard deviation (s.d.).

Figure 3-6: Sufu functions independently of Fu and the primary cilium

Isotopic *in situ* hybridization using ^{33}P-UTP-labeled ribo-probes (pink) on paraffin sections of wild-type (wt), *Sufu$^{-/-}$*, *Kif3a$^{-/-}$*, *Sufu$^{-/-}$; Kif3a$^{-/-}$*, and *Sufu$^{-/-}$; Fu$^{-/-}$* mouse embryos at 9.5 *dpc*. Loss of *Sufu* resulted in global upregulation of Hh signaling and ventralization of the neural tube. *Shh*, whose expression is restricted to the notochord and floor plate in wt, is extended dorsally in the absence of *Sufu*. Similarly, Hh target genes such as *Patched 1* (*Ptch1*) are expanded dorsally, suggesting ventralization of the neural tube. The expression domains of neuronal progenitor markers (Class I genes, including *Pax7* and *Pax6*, repressed by Hh signaling and Class II genes, including *Nkx6.1*, *Nkx2.2* and *Foxa2*, activated by Hh signaling) are shifted. For instance, *Pax7*, the dorsal–most marker, is not expressed and *Pax6* expression is confined to the dorsal neural tube of *Sufu$^{-/-}$* embryos. Dorsal expansion of *Nkx6.1*, *Nkx2.2* and *Foxa2* was also observed in the absence of *Sufu* (data not shown). Similarly, the expression domains of markers for differentiated interneurons and motoneurons are changed. For instance, *Sufu$^{-/-}$* neural tube displayed dorsal expansion of *Islet1* and *Oligo2* (not shown), which label motoneurons. By comparison, marker analysis revealed a partially dorsalized *Kif3a$^{-/-}$* neural tube. The neural tube defects in *Sufu$^{-/-}$; Kif3a$^{-/-}$* or *Sufu$^{-/-}$; Fu$^{-/-}$* embryos resemble those in *Sufu$^{-/-}$* mutants. n, notochord; fl, floor plate; nt, neural tube.

Figure 3-7: Sufu controls Gli protein levels and activity independent of the primary cilium

(**A**) Western blots of lysates derived from wt, *Sufu$^{-/-}$*, *Kif3a$^{-/-}$* MEFs and *Kif3a$^{-/-}$* MEFs expressing *Sufu* shRNA probed with anti-Gli2 and anti–Gli3 antibodies. Efficient

126

Sufu knockdown in *Kif3a*$^{-/-}$ MEFs was verified by anti-Sufu antibodies. Gli2 and Gli3 protein levels are reduced in *Kif3a*$^{-/-}$ MEFs expressing *Sufu* shRNA to the same extent as in *Sufu*$^{-/-}$ MEFs. (**B**) Hh reporter assays using the *8xGliBS-luc* reporter in wild-type and *Kif3a*$^{-/-}$ MEFs. Expression of Gli1 or Gli2 (but not Gli3) activates the Hh reporter and Hh pathway activation is repressed when Sufu is co-expressed. Gli2 is known to activate Hh reporters less efficiently than Gli1 (Gerber et al. 2007). Loss of the primary cilium in *Kif3a*$^{-/-}$ MEFs does not impair Sufu's ability in repressing Gli-mediated Hh pathway activation. Error bars are standard deviation (s.d.).

Figure 3-8: Loss of the primary cilium impairs ligand-independent Hh pathway activation in *Ptch1*$^{-/-}$ MEFs but has no effect on *Sufu*$^{-/-}$ MEFs

(**A**) Hh reporter assays using the *8xGliBS-luc* reporter in *Sufu*$^{-/-}$ and *Ptch1*$^{-/-}$ MEFs expressing increasing amounts of a dominant negative (dn) Kif3b construct (left panel) or *Kif3a* shRNA, both of which inhibits the function of the primary cilium. While dnKif3b or *Kif3a* shRNA have no effect on Hh pathway activation in *Sufu*$^{-/-}$ MEFs, increasing quantities of dnKif3b or *Kif3a* shRNA reduces Hh pathway activation in *Ptch1*$^{-/-}$ MEFs. (**B**) Western blots of lysates derived from wild-type (wt), *Sufu*$^{-/-}$ and *Ptch1*$^{-/-}$ MEFs and *Sufu*$^{-/-}$ and *Ptch1*$^{-/-}$ MEFs expressing dnKif3b probed with anti-Gli2 and anti–Gli3 antibodies. Inhibition of ciliary function by dnKif3b has no effect on endogenous Gli2 and Gli3 protein levels in *Sufu*$^{-/-}$ MEFs, which are greatly reduced in the absence of *Sufu*. By contrast, defective ciliary function in *Ptch1*$^{-/-}$ MEFs changed the ratio of full-

127

length Gli3 to Gli3 repressor. Tubulin was used as the loading control and numbers on the right indicate locations of protein size standards. FL, full-length; R, repressor. (**C**) Left panel: Hh reporter assays using the *8xGliBS-luc* reporter in *Sufu*$^{-/-}$ MEFs and *Sufu*$^{-/-}$ MEFs expressing *Gli* shRNA in the presence or absence of exogenous Shh. Hh pathway activation is significantly compromised in *Sufu*$^{-/-}$ MEFs in which *Gli1* is efficiently knocked down, consistent with the notion that Gli1 contributes to Hh pathway activation in the absence of *Sufu*. Similar results were obtained using three pairs of *Gli1* shRNA directed against different regions of Gli1. By contrast, *Sufu*$^{-/-}$ MEFs and *Sufu*$^{-/-}$ MEFs expressing *Gli1* shRNA display normal responsiveness to the canonical Wnt ligand Wnt3a assayed by the *SuperTOPflash* reporter (data not shown). Right panel: Semi-quantitative RT-PCR demonstrates that *Gli1* is efficiently knocked down via *Gli1* shRNA; *β-actin* serves as the control.

Figure 3-9: Zebrafish and fly Sufu restore Gli protein levels in mouse *Sufu*$^{-/-}$ MEFs while *Drosophila* Smo fail to rescue Hh defects in mouse *Smo*$^{-/-}$ MEFs

(**A**) Immunofluorescence of *Smo*$^{-/-}$ MEFs expressing Smo from different species including mouse (m), zebrafish (z), and *Drosophila* (d) using antibodies against acetylated tubulin (AC) (labeling the primary cilium, red) and Smo (green). While mSmo and zSmo introduced into *Smo*$^{-/-}$ MEFs via transient transfection led to ciliary localization of Smo, dSmo mainly resides in the cytoplasm and is not found on the cilium. (**B**) Left panel: Hh activity assays using the *8xGliBS-luc* reporter in *Smo*$^{-/-}$

MEFs expressing Smo from different species via transient transfection. Both mouse (m) and zebrafish (z) Smo restored Hh responsiveness in $Smo^{-/-}$ MEFs while expression of *Drosophila* Smo (dSmo) has no effect on Hh activation. Right panel: $Sufu^{-/-}$ MEFs were transfected with mouse Sufu (mSufu), mouse Sufu with the D159A mutation (mSufu^{D159A}), zebrafish Sufu (zSufu), or *Drosophila* Sufu (dSufu). Both mSufu and zSufu repressed basal *8xGliBS-luc* activity in the absence of ShhN, and promoted an increase in ShhN-mediated response. By contrast, the mSufu^{D159A} and dSufu constructs had a less pronounced effect, which may partially be attributed to their weaker Gli-binding capacity (Figure 3-10). The numbers indicate the ratios of Hh responsiveness in the presence and absence of exogenous Shh (*e.g.*, the ratio is 1.23 when no Sufu is added and is 16.99 when mSufu is added). Error bars are s.d. (**C**) Immunofluorescence of $Sufu^{-/-}$ MEFs expressing Sufu from different species via retroviral infection using antibodies against acetylated tubulin (red) and Gli2 or Gli3 (green). Mouse, zebrafish or *Drosophila* Sufu was capable of restoring ciliary localization of endogenous Gli2 and Gli3 to the cilium when expressed in $Sufu^{-/-}$ MEFs, suggesting an evolutionarily conserved function of Sufu. The percentage of cilia that exhibit Gli2 and Gli3 immunoreactivity is lower in $Sufu^{-/-}$ MEFs expressing dSufu compared to mSufu or zSufu, consistent with a partial rescue of Hh defects in $Sufu^{-/-}$ MEFs by dSufu. (**D**) Western blots of lysates derived from wild-type (wt), $Sufu^{-/-}$ MEFs and $Sufu^{-/-}$ MEFs expressing mouse, zebrafish and *Drosophila* Sufu via retroviral infection probed with anti-Gli2 and anti-Gli3 antibodies. Endogenous Gli2 and Gli3 protein levels are restored when Sufu from different species is expressed, suggesting an

evolutionarily conserved biochemical function of Sufu. Tubulin was used as the loading

control and numbers on the right indicate locations of protein size standards. FL, full-

length; R, repressor.

Figure 3-10: Mouse and zebrafish Sufu bind Gli proteins more strongly than

Sufu^{D159A} or fly Sufu

HEK 293T cells were transfected with various Sufu-FLAG constructs and either Gli-

Myc, Gli2, or Gli3 constructs. Immunoprecipitations were performed with anti-FLAG

beads as described in **Materials and Methods**. (**A**) Mouse (mSufu) and zebrafish Sufu

(zSufu) bind strongly to Gli1, Gli2, and Gli3, and zSufu consistently binds more Gli2

than mSufu. Fly Sufu (dSufu) binds weakly to Gli1, Gli2, and Gli3, correlating with its

reduced ability to restore a dynamic range of Hedgehog (Hh) response and the partial

rescue of Gli levels in *Sufu*–/– mouse embryonic fibroblasts (MEFs) (Figure 4B). This

may be due to co-evolution of the relevant interacting surfaces of dSufu and Ci. (**B**)

Wild-type mSufu binds Gli1, Gli2, and Gli3 with greater affinity than mSufuD159A

mutant. As with dSufu, this weakened binding affinity correlates with a reduced rescue

of Hh response in Figure 4B. In, input; IP, immunopreciptate; WB, Western blot.

Figure 3-11: Mouse Spop forces redistribution of Gli2 and Gli3 into Spop+ foci

independent of the primary cilium

Double immunostaining of MEFs transfected singly with FLAG-tagged Gli1, 2 or 3 or

co-transfected with Myc-tagged Spop using FLAG and Myc antibodies against

130

FLAG–tagged Gli1, 2 or 3 (green) and Myc-tagged Spop (red). Both cytoplasmic and nuclear staining of Gli1, 2, and 3 was detected. Punctate Spop immunoreactivity in the nucleus and cytoplasm was evident, consistent with previous reports (Hernandez-Munoz et al. 2005). Immunoreactivity of Gli2 and 3 (and not Gli1) was reduced when co-expressed with Spop and Gli2/3 distribution extensively overlaps with Spop, particularly in the cytoplasm. Loss of the primary cilium in $Kif3a^{-/-}$ MEFs has no effect on the subcellular distributions and interactions of Gli1, Gli2, Gli3 and Spop.

Figure 3-12: Spop and Gli3 localization in CHO, COS7, and MEF cell lines

(**A**) Spop-Myc and Gli3-FLAG were expressed singly or together in CHO and COS7 cells. Notably, both nuclear and cytoplasmic Spop punctae were seen in CHO cells. Spop is primarily nuclear and perinuclear in COS7 cells, similar to published reports in this cell line (Nagai et al. 1997) and HeLa cells (Kwon et al. 2006). Gli3 is concentrated in the nucleus, but is redistributed to Spop-containing foci both in CHO and COS7 cells. (**B**) Spop-Myc was transfected in wild-type mouse embryonic fibroblasts (MEFs), and cells were incubated overnight in the absence or presence of the nuclear export inhibitor leptomycin B (LMB). Spop was largely cytosolic in the absence of LMB, but was retained in the nucleus and formed some foci/punctae after LMB exposure. We speculate that the subcellular distribution of Spop varies from cell line to cell line, and may depend on the relative amounts of both nuclear import/export factors, as well as components of relevant E3 ubiquitin ligase complexes.

131

Figure 3-13: Spop physically interacts with Gli2 and Gli3, but not Gli1

Western blot of immunoprecipitated Gli1, Gli2 and Gli3 (epitope-tagged with one copy of FLAG) to detect physical interaction with Spop (epitope-tagged with one copies of HA) from HEK 293T lysates. Spop physically associates with Gli2 and Gli3 but not Gli1. in, input; IP, immunoprecipitation.

Figure 3-14: Spop expression reduces Gli2 and Gli3 protein levels

Western blots of lysates derived from HEK 293T cells expressing FLAG-tagged Gli3 singly or in combination with FLAG-tagged Spop, Sufu or Ext2 probed with anti-FLAG antibodies. Lack of apparent Gli3 processing in cultured cells has been previously reported (Wang et al. 2000a). Co-expression of Gli2 or Gli3 with Sufu notably enhanced Gli2 and Gli3 protein levels. By contrast, co-expression of Gli2 or Gli3 with Spop (but not the control protein Ext2) significantly reduces Gli2 and Gli3 protein levels, which can then be restored when Sufu is co-expressed. We noticed that reduction in Gli2 protein levels is not as dramatic as Gli3 when Spop is co-expressed. Gli1 or Ext2 protein levels are unaffected when Spop is overexpressed (data not shown). α-tubulin serves as the loading control (not shown).

Figure 3-15: Spop reduces Gli2-mediated transcriptional activation

HEK 293T cells were transfected with either Gli1 (A) or Gli2 (B) and increasing amounts of Spop or EXT2 (control). Spop significantly reduces the ability of Gli2 to transactivate the *8xGliBS-luc* Hh reporter, but has a much less pronounced effect on Gli1. EXT2 expression does not significantly modulate Gli1 or Gli2 transactivation. Data shown are the mean of four independent experiments; error bars are standard error of mean (s.e.m.).

Figure 3-16: Spop promotes ubiquitination of Gli2 and Gli3, but not Gli1

Western blot of immunoprecipitated Gli1, Gli2 and Gli3 (epitope-tagged with one copy of FLAG) to detect poly-ubiquitinated Gli proteins. Spop promotes ubiquitination of Gli2 and Gli3 but not Gli1; Gli2 and Gli3 ubiquitination is abolished when Sufu is co-expressed. WB, Western blot.

Figure 3-17: SPOP reduces Gli2 and Gli3 protein levels in a proteasome-dependent manner

HEK 293T cells were transfected with FLAG-Gli2 or FLAG-Gli3, in the absence or presence of Spop. A reduction in Gli2 (**A**) and Gli3 protein levels (**B**) was seen in the presence of Spop; this was inhibited with the addition of the proteasome inhibitor MG132. Tubulin serves as the loading control.

Figure 3-18: Spop directs Gli2 and Gli3 to Cul3+ foci

Spop has been shown to be an adaptor protein for Cul3 ubiquitin ligases (Kwon et al., 2006). In wild-type mouse embryonic fibroblasts (MEFs), co-expressed Cul3-Myc and Gli2-FLAG or Gli3-FLAG do not extensively overlap (top two rows). By contrast (and in agreement with the above report), co-expressed Spop-HA and Cul3-Myc show overlap in punctae in the nucleus and cytoplasm (middle row). Transfection of Spop with Gli2/Gli3 and Cul3 caused co-localization of Gli2 and Gli3 with Cul3 punctae (bottom two rows). Thus, at the subcellular level, Spop likely directs Gli2 and Gli3 to the Cul3-based E3 ubiquitin ligase complex for polyubiquitination and subsequent degradation.

Figure 3-19: Knockdown of *Spop* in *Sufu*–/– MEFs partially restores Gli2 and Gli3 protein levels

Western blots of lysates derived from wt and *Sufu*$^{-/-}$ MEFs and wt and *Sufu*$^{-/-}$ MEFs expressing *Spop* shRNA probed with anti-Gli2 and anti–Gli3 antibodies. Efficient knockdown of *Spop* was verified by semi-quantitative RT-PCR (data not shown). Gli2 and Gli3 levels are partially restored in *Sufu*$^{-/-}$ MEFs when *Spop* is knocked down, consistent with a model in which Sufu and Spop antagonize each other in regulating Gli2 and 3 (but not Gli1) protein levels. Lack of complete rescue of Gli protein levels could be attributed to the presence of additional mammalian *Spop* homologs (*e.g.*, Spop-like and Tdpoz proteins) (Huang et al. 2004). FL, full-length; R, repressor.

Figure 3-20: Overexpressed Spop does not localize to the primary cilium in MEFs

Myc-tagged Spop was expressed in wild-type (wt) mouse embryonic fibrolblasts (MEFs) and detected using anti-Myc antibodies. Spop (green) does not localize to the primary cilium labeled by anti-acetylated (AC) tubulin antibodies (red).

Figure 3-21: *Spop* knockdown in *Sufu*-deficient MEFs enhances Hh pathway activity

Hedgehog (Hh) reporter assays using the *8xGliBS-luc* reporter in *Sufu*–/– mouse embryonic fibroblasts (MEFs) and *Sufu*–/– MEFs expressing *Spop* shRNA in the presence or absence of exogenous Shh. Hh pathway activation is enhanced in *Sufu*–/– MEFs in which *Spop* is efficiently knocked down, consistent with restored Gli2/3 protein levels (Fig. 5E). Restored Gli proteins mainly reside in the cytoplasm (data not shown). Error bars are standard deviation (s.d.).

Figure 3-22: *Sufu*–/– and *Kif3a*–/– mouse embryonic fibroblasts have altered response to Shh, but not Wnt3a

Mouse embryonic fibroblasts (MEFs) were transfected with Hh reporter (*8xGliBS-luc*) or Wnt reporter (*SuperTOPflash*) and treated with either ShhN- or Wnt3a-conditioned medium. Date are representative of three independent experiments; error bars are standard deviations (s.d.). (**A**) Wild-type MEFs exhibit a robust response to ShhN, whereas *Kif3a*–/– MEFs are unresponsive. (**B**) *Sufu*–/– MEFs show an elevated basal level of *8xGliBS-luc* reporter activity when compared to wild-type MEFs, but do not

exhibit a significantly elevated level of reporter activity when exposed to ShhN. Data are

normalized to basal reporter activity in wild-type MEFs. (**C**) Wild-type, *Sufu–/–*, and

Kif3a–/– MEFs display normal responsiveness to the canonical Wnt ligand Wnt3a

assayed by the *SuperTOPflash* reporter.

Figure 3-23: Mouse Sufu has positive and negative roles in regulating Hh signaling

(**A**) Hh activity assays using the *8xGliBS-luc* reporter in *Sufu$^{-/-}$* MEFs transfected with

varying quantities of Sufu. Addition of increasing amounts of Sufu to *Sufu$^{-/-}$* MEFs

reduces Hh responsiveness in the absence of exogenous Shh, while promoting Hh

activation in the presence of Shh. The numbers indicate the ratios of Hh responsiveness

in the presence and absence of exogenous Shh (*e.g.*, the ratio is 1.27 when no Sufu is

added and is 22.43 when 240 ng of Sufu is added). Similar results were seen in two

additional *Sufu$^{-/-}$* cell lines and with the Smo agonist purmorphamine instead of ShhN

(data not shown). Error bars are s.d. (**B**) Western blots of MEF lysates derived from

wild-type (wt), *Sufu$^{-/-}$*, *Ptch1$^{-/-}$* or *Ptch1$^{-/-}$* expressing *Sufu* shRNA probed with anti-

Gli2 and anti-Gli3 antibodies. Gli2 and Gli3 protein levels are greatly reduced in

Ptch1$^{-/-}$ MEFs when *Sufu* is knocked down. (**C**) Immunofluorescence of *Ptch1$^{-/-}$*

MEFs stably expressing *Sufu* shRNA using antibodies against acetylated tubulin (labeling

the primary cilium) (red) and various Hh pathway components including Smo, Gli2 and

Gli3 (green). Smo, Gli2 and Gli3 localizes to the primary cilium in *Ptch1$^{-/-}$* MEFs in

the absence of exogenous Hh stimulation consistent with maximal Hh pathway

activation. While Smo localization to the primary cilium is unaffected in *Ptch1$^{-/-}$* MEFs

when *Sufu* is knocked down, ciliary localization of Gli2 and Gli3 in *Ptch1*$^{-/-}$ MEFs is

abolished when *Sufu* is eliminated, suggesting compromised Hh pathway activation. (D)

Hh reporter assays using the *8xGliBS-luc* reporter in *Ptch1*$^{-/-}$ MEFs and *Ptch1*$^{-/-}$ MEFs

expressing *Sufu* shRNA. *Sufu* knockdown leads to reduced Hh pathway activity in

Ptch1$^{-/-}$ MEFs. (E) Hh reporter assays using the *8xGliBS-luc* reporter in *Sufu*$^{-/-}$ and

Ptch1$^{-/-}$ MEFs and *Ptch1*$^{-/-}$ MEFs expressing *Sufu* shRNA in the presence of various

Hh antagonists that inhibit Smo function (Chen et al. 2002a; Chen et al. 2002b). Hh

pathway activation in *Ptch1*$^{-/-}$ MEFs is efficiently knocked down in the presence of Hh

antagonists but these Smo inhibitors have no effect on Hh pathway activity in *Sufu*$^{-/-}$

MEFs. When *Sufu* is knocked down in *Ptch1*$^{-/-}$ MEFs, these cells become partially

insensitive to Hh antagonists.

Figure 3-24: A model of Sufu function in mammalian Hh signaling

Sufu plays a pivotal role in controlling Gli protein levels. Sufu protects full-length Gli2

and Gli3 proteins from Spop-mediated ubiquitination and complete degradation by the

proteasome. In this way, Sufu functions as an adaptor to preserve a pool of Gli2 and Gli3

that can be readily converted into Gli activators and repressors. This aspect of Hh

signaling is evolutionarily conserved and independent of the primary cilium. By contrast,

the primary cilium is required for generating Gli repressors via limited proteolysis in the

absence of Hh signaling, and converting full-length Gli proteins into activators through

unknown mechanisms upon Hh pathway activation. These events occurs downstream of

Smo which translocates to the primary cilium when Hh ligand binds to Ptch1 and

removes it from the cilium. How other Hh pathway components or ciliary proteins particulate in cilium-dependent and –independent activity needs to be further investigated.

Figure 3-25: Gli2 and Gli3 protein levels are greatly reduced in both the nuclear and cytoplasmic fractions in the absence of *Sufu*

Western blots of nuclear (N) and cytoplasmic (C) fractions derived from wild-type (wt) and *Sufu*–/– mouse embryonic fibroblasts (MEFs) through differential salt extraction. Gli2 is present in the cytoplasmic fraction and is barely detectable in the nuclear fraction of wt MEFs. Gli2 distribution is unaffected by Shh treatment. Gli3 repressor (R) is present in the nuclear fraction of untreated MEFs and disappears upon addition of Shh ligand. Full-length (FL) Gli3 mainly resides in the cytoplasm and its level is enhanced by Shh stimulation. Lack of full-length nuclear Gli2 and Gli3 could be due to rapid nuclear export or nuclear degradation, similar to Ci. Gli2 and Gli3 are barely detectable in either the nucleus or cytoplasm of *Sufu*-deficient MEFs. BRG1 and tubulin were used to assess successful isolation of the nuclear and cytoplasmic fractions respectively; numbers on the right indicate positions of protein standards.

Figure 3-26: SAP18 localization is unaffected by Sufu, and SAP18 does not significantly affect Gli1 or Gli2 activity

(**A**) Human SAP18-FLAG and mouse Sufu-Myc were co-expressed in wild-type (top

row), *Sufu–/–* (middle row), and *Ptch1–/–* (bottom row) mouse embryonic fibroblasts

(MEFs). In all cases, SAP18 was found primarily in the nucleus, and Sufu in both the

cytoplasm and nucleus. SAP18 was also found in the nucleus in the absence of Sufu in

all three MEF lines (data not shown). (**B**) SAP18 was transfected alone, with Gli1, Gli2,

or with Sufu and Gli1 or Gli2 in wild-type, *Sufu–/–*, or *Ptch1–/–* MEFs. Gli3R (truncated

after amino acid residue 722) was used as a positive control. Notably, SAP18 alone or in

combination with Gli1 or Gli2 did not affect basal or stimulated levels of the *8xGliBS-luc*

reporter. A small amount of overexpressed Sufu had a modest effect on Gli activation,

similar to what was previously reported (Cheng and Bishop 2002). No synergistic

repression of Gli1 or Gli2 activity with Sufu and SAP18 was observed in any of the cell

lines. By contrast, Gli3R consistently inhibited basal and Gli1/Gli2-stimulated reporter

activity. Data are the mean of three independent experiments.

**Figure 3-27: The Hh pathway is largely unaffected by pharmacologic modulation of
protein kinase A (PKA) activity in *Sufu–/–* MEFs**

Three independent clones of *Sufu–/–* mouse embryonic fibroblasts (MEFs) were

transfected with *8xGliBS-luc* Hh reporter and either *pRL-TK* or *hsp68-LacZ* for

normalization. Treatment with ShhN-conditioned medium had no effect. Stimulation of

the PKA pathway with forskolin (FSK, which activates adenylyl cyclase) or 3-isobutyl-1-

methylxanthine (IBMX, which inhibits cAMP and cGMP phosphodiesterases) had no

stimulatory or inhibitory effect in clones #16 and 17. We observed an increase in *pRL-*

TK reporter activity upon FSK or IBMX treatment in clone #1, and thus normalized to

hsp68-LacZ, which showed no increase in b-galactosidase activity after PKA stimulation.

Taken together, activation of PKA through two different mechanisms in three different

cell lines resulted in either no change, or a modest increase in Hh reporter activity in the

absence of *Sufu*. Error bars are standard deviation (s.d.).

Figure 3-1: Endogenous Hh pathway components display dynamic patterns of ciliary localization in response to Hh signaling while overexpressed Gli proteins localize to the primary cilium in the absence of Sufu
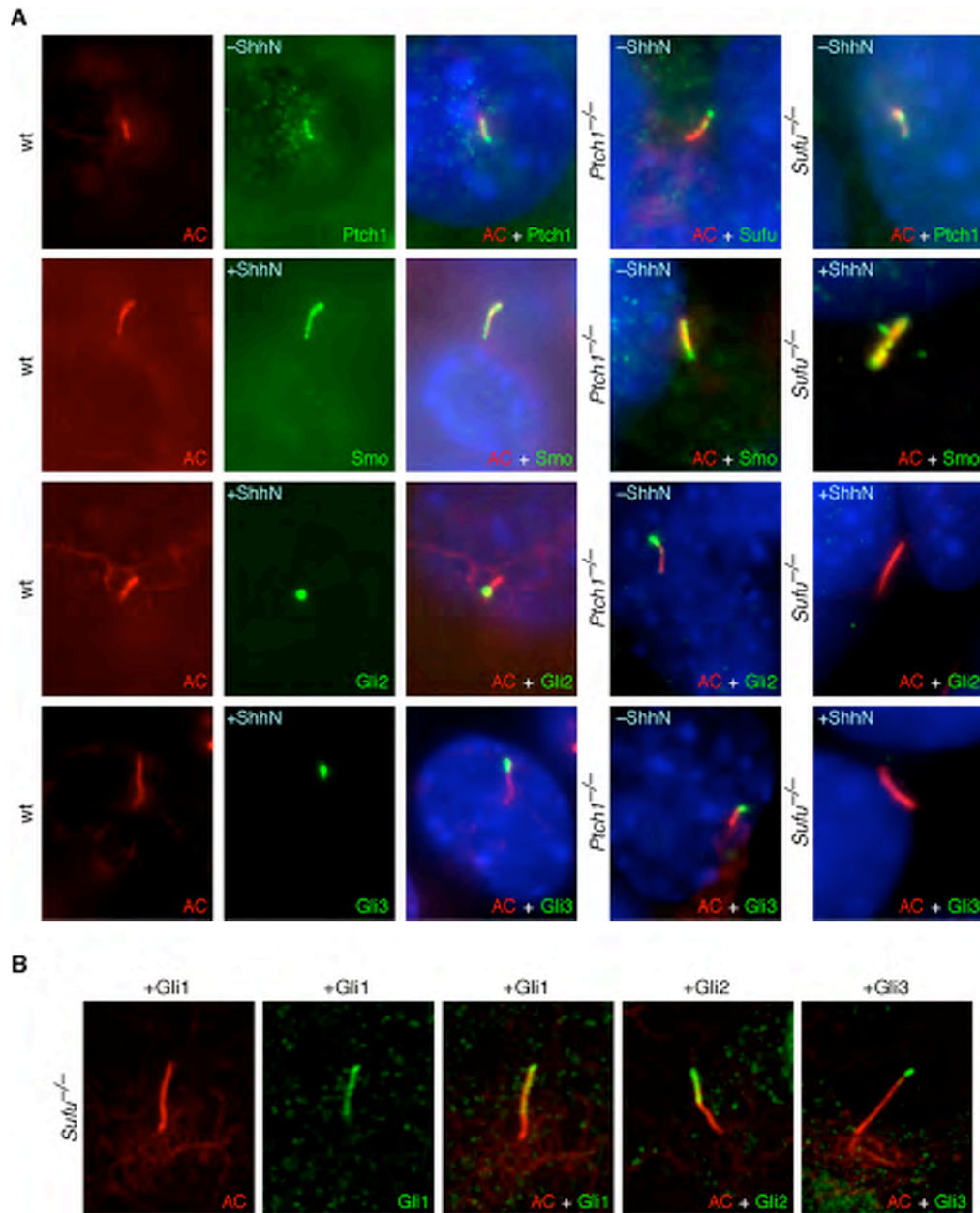
Figure 3-2: Gli2 and Gli3, but not Sufu, display dynamic localization on the primary cilium
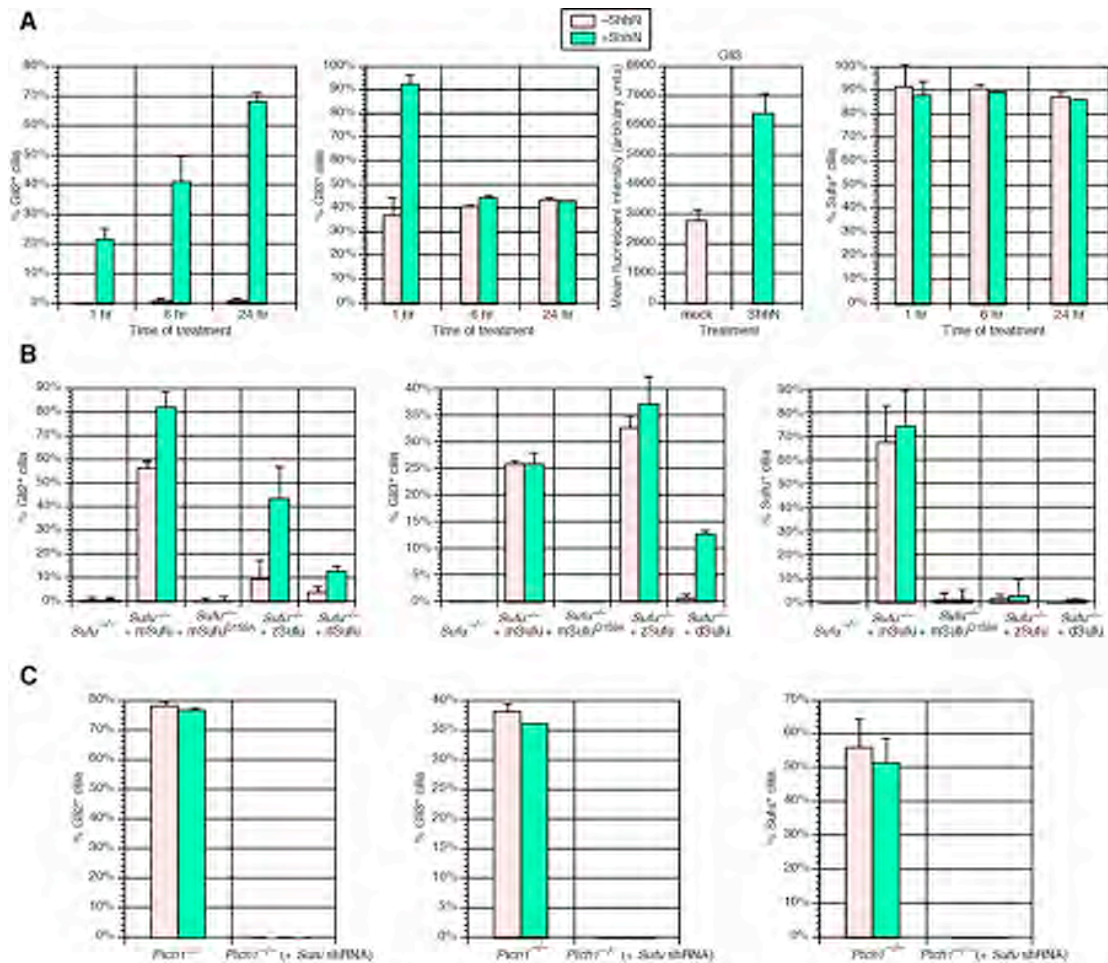
Figure 3-3: Characterization of antibodies against endogenous mouse Gli2 and Gli3
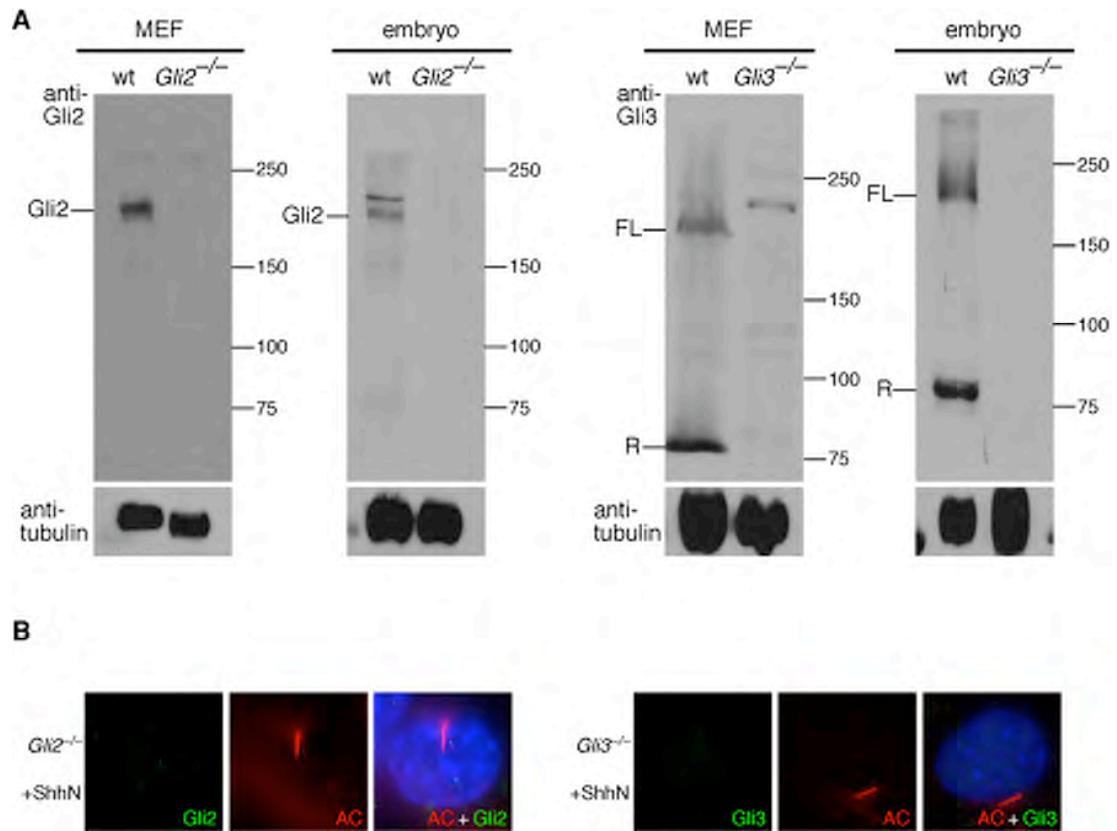
Figure 3-4: Gli2 and Gli3 protein levels are reduced in *Sufu* null MEFs
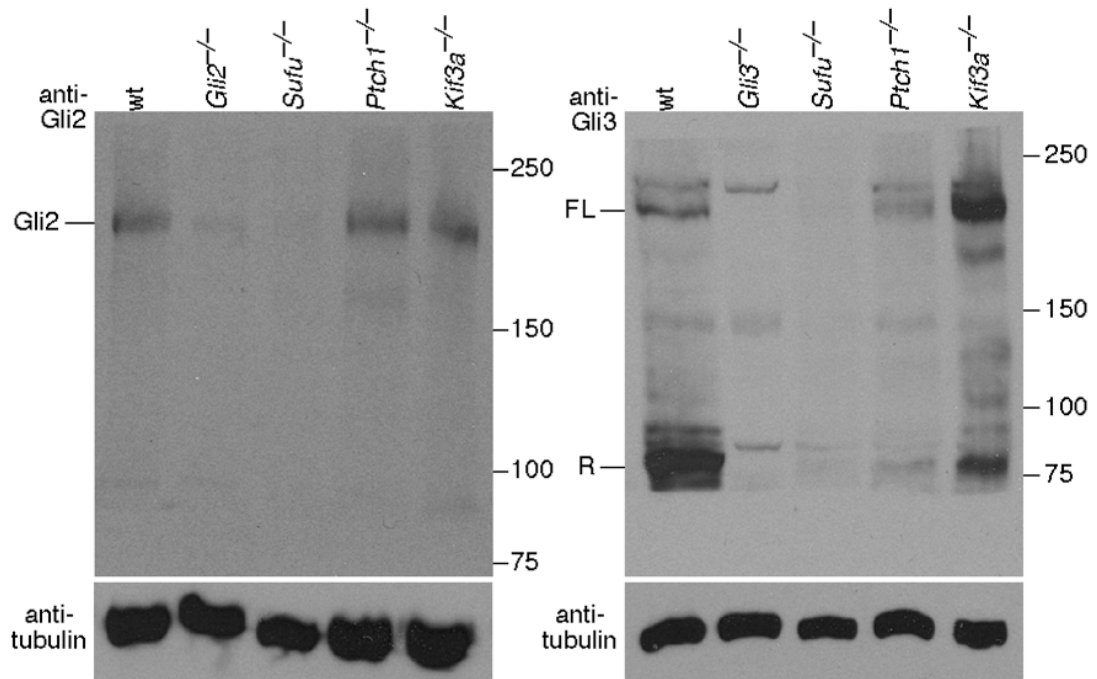
Figure 3-5: *Gli2* and *Gli3* transcript levels are not significantly changed in Sufu−/− MEFs or embryos
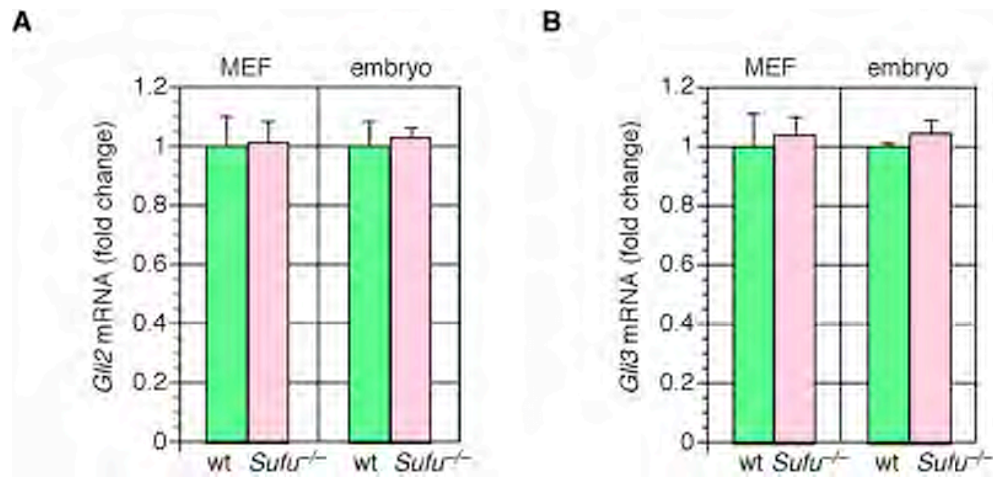
Figure 3-6: Sufu functions independently of Fu and the primary cilium
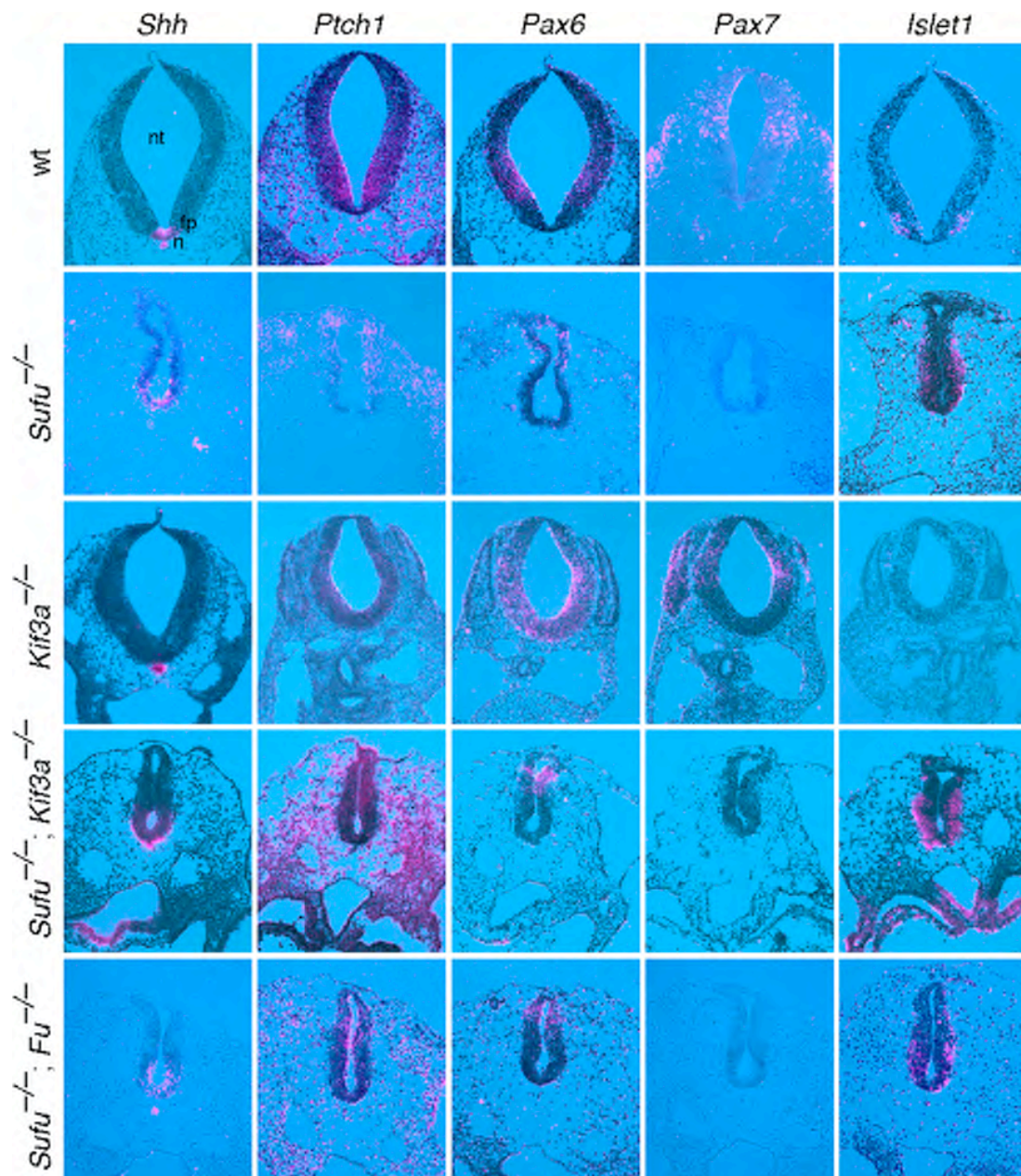
Figure 3-7: Sufu controls Gli protein levels and activity independent of the primary cilium
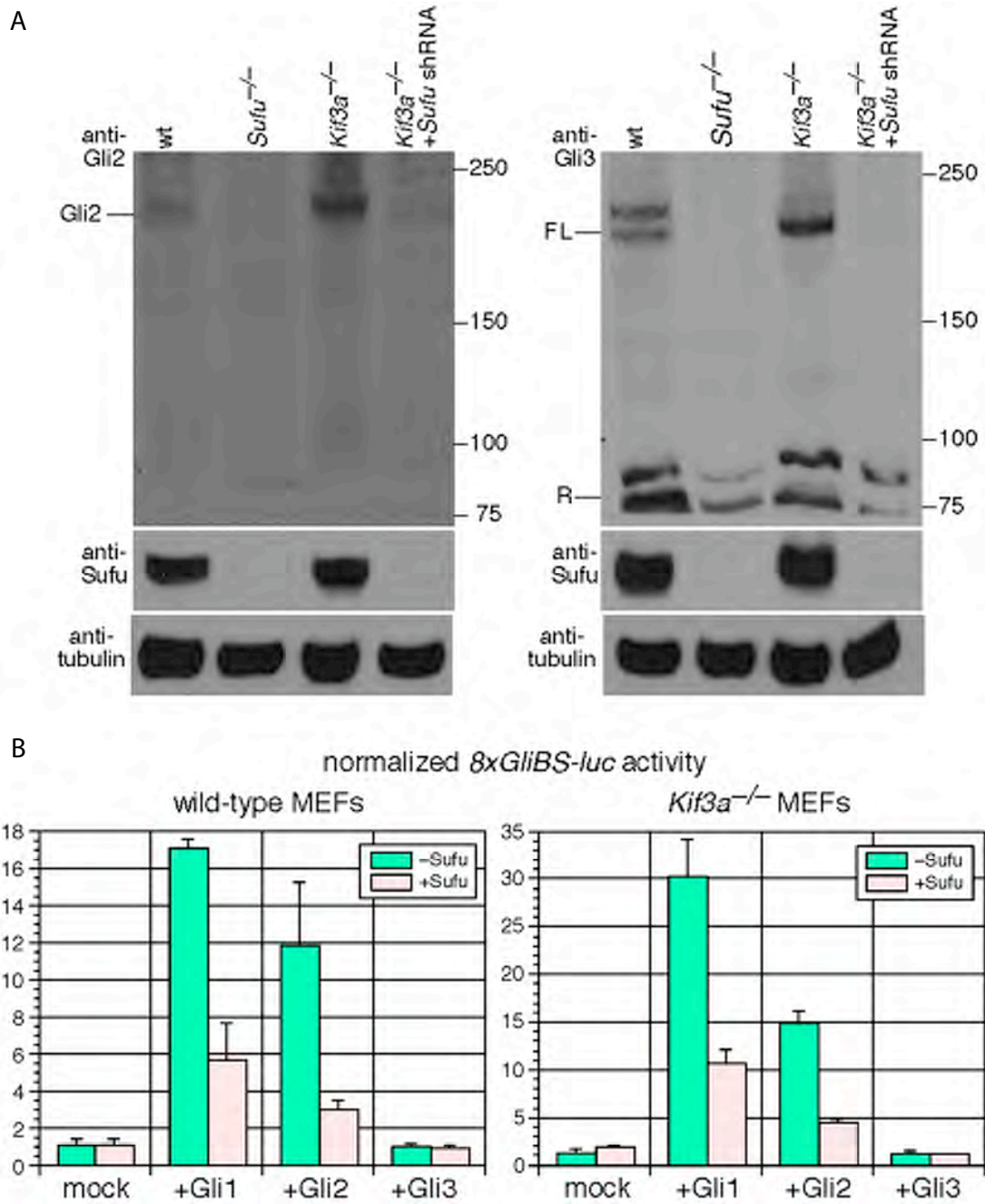
Figure 3-8: Loss of the primary cilium impairs ligand-independent Hh pathway activation in *Ptch1−/−* MEFs but has no effect on *Sufu−/−* MEFs
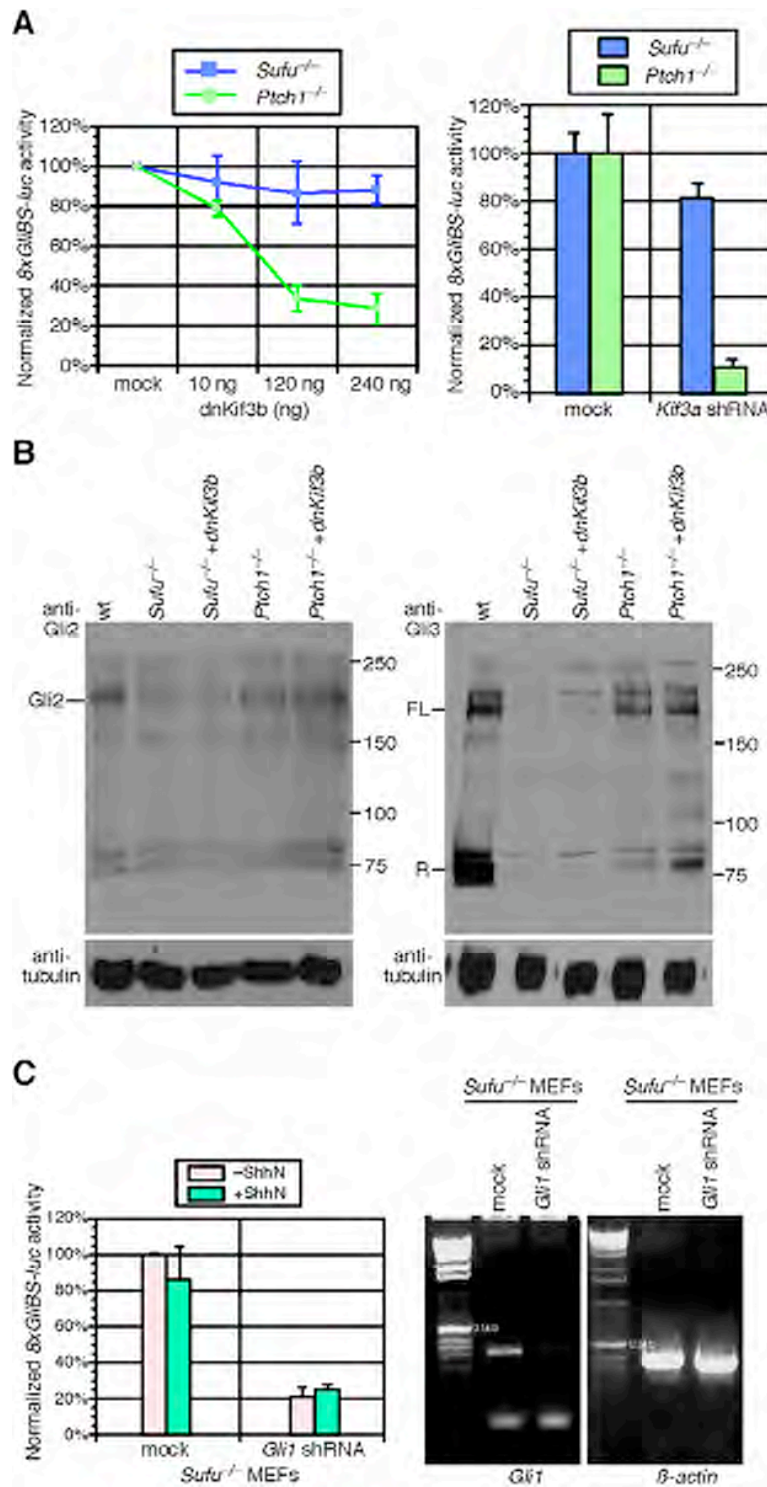
Figure 3-9: Zebrafish and fly Sufu restore Gli protein levels in mouse *Sufu–/–* MEFs while Drosophila Smo fails to rescue Hh defects in mouse *Smo–/–* MEFs
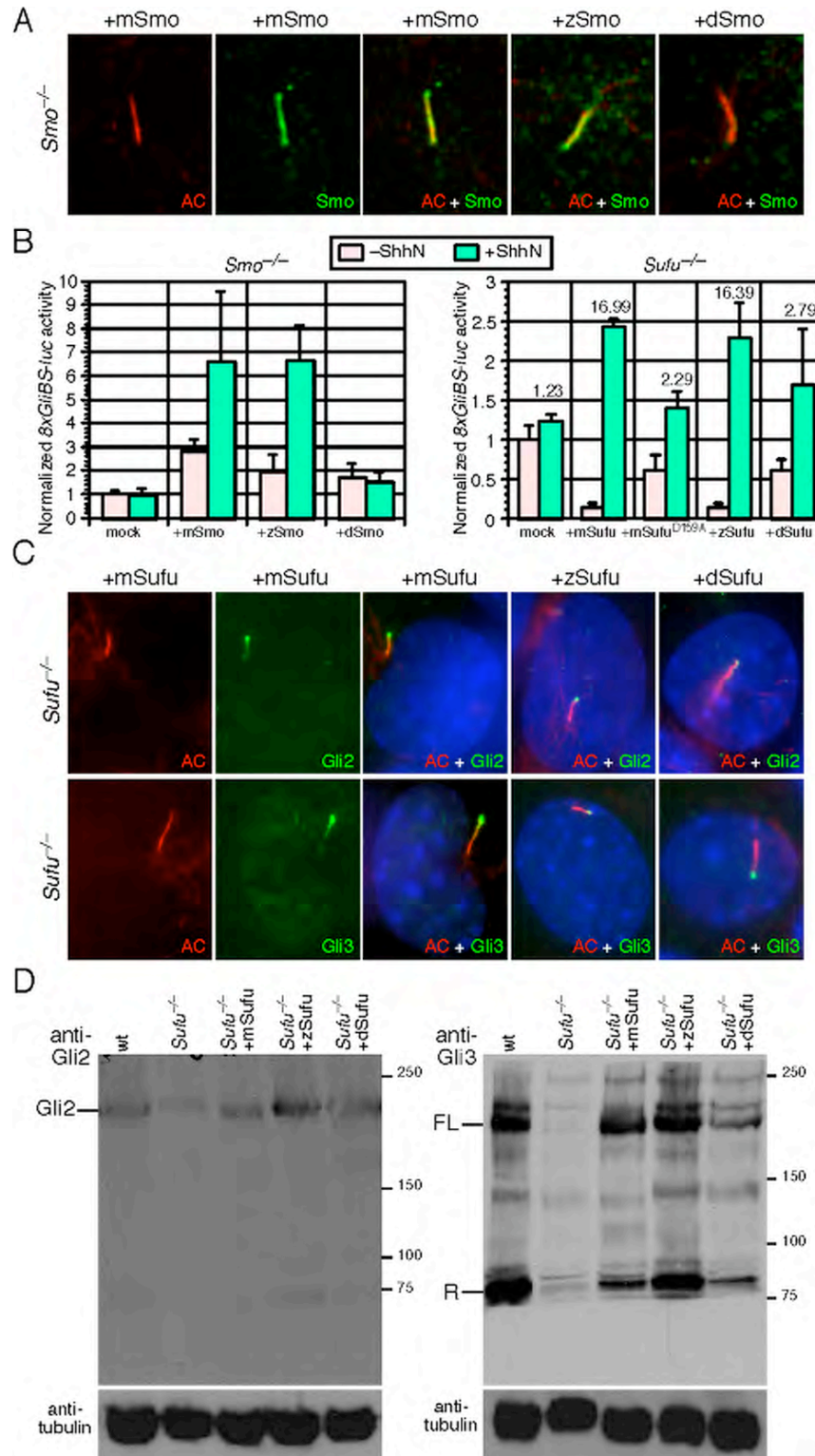
Figure 3-10: Mouse and zebrafish Sufu bind Gli proteins more strongly than SufuD159A or fly Sufu

150
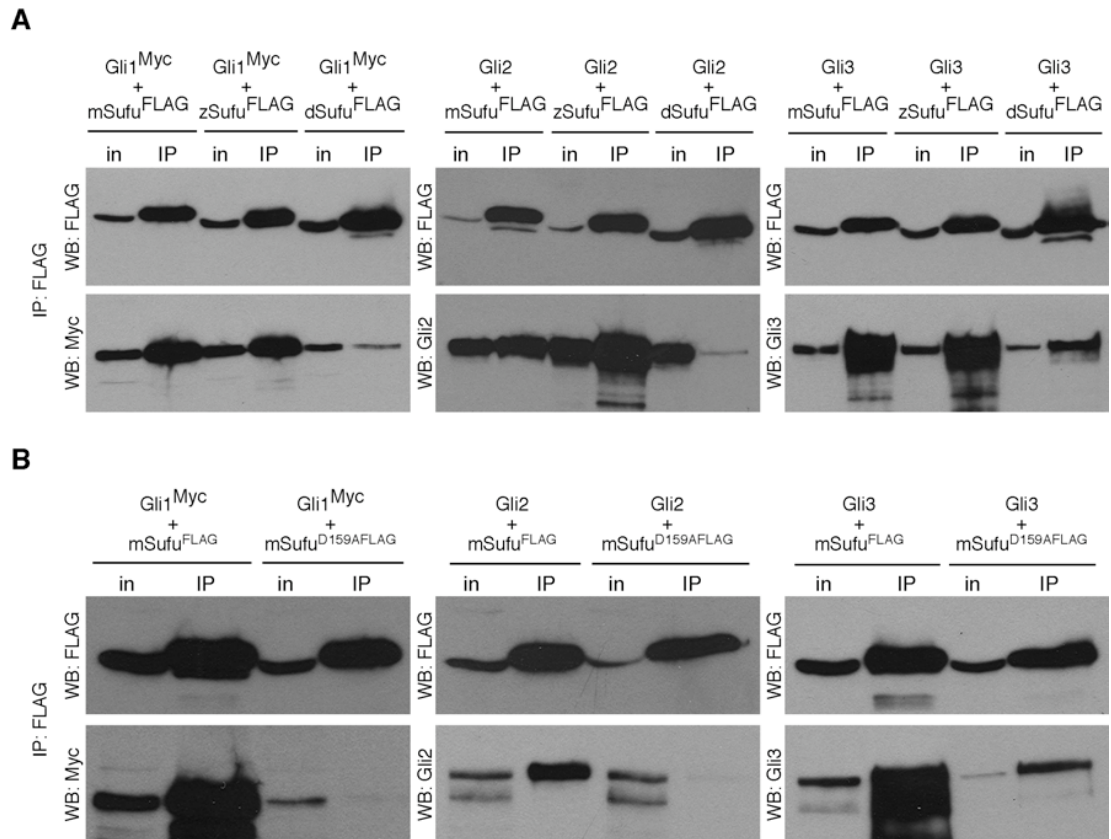
Figure 3-11: Mouse Spop forces redistribution of Gli2 and Gli3 into Spop+ foci independent of the primary cilium
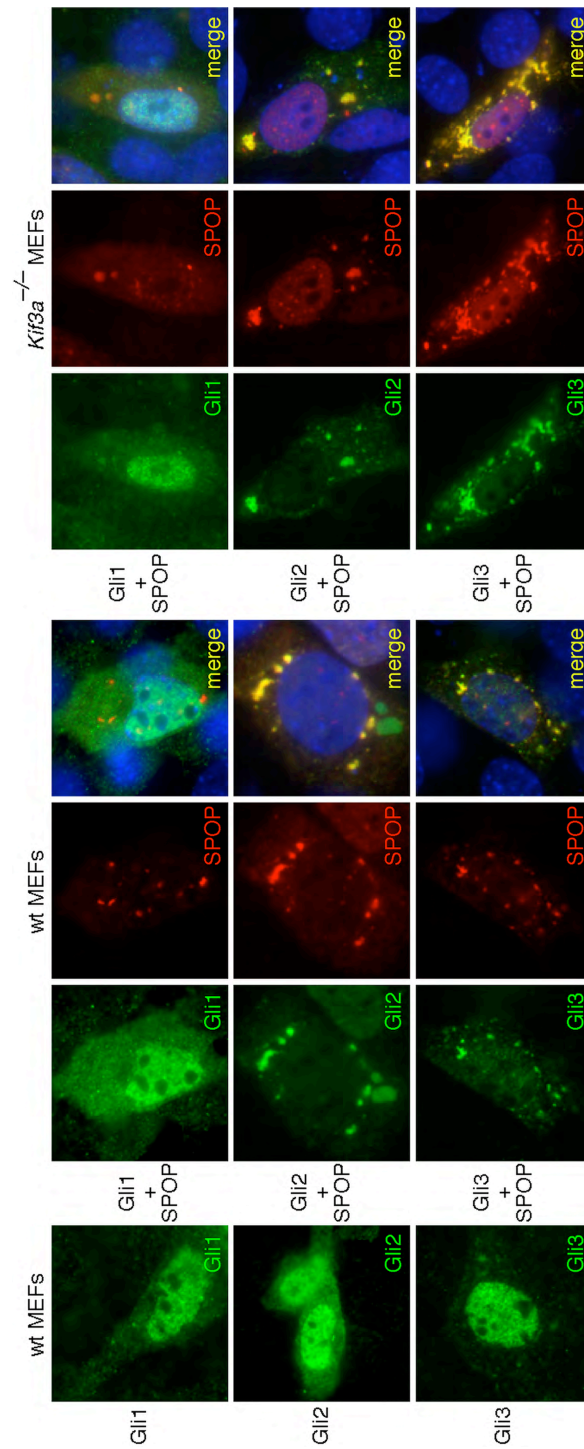
Figure 3-12: Spop and Gli3 localization in CHO, COS7, and MEF cell lines
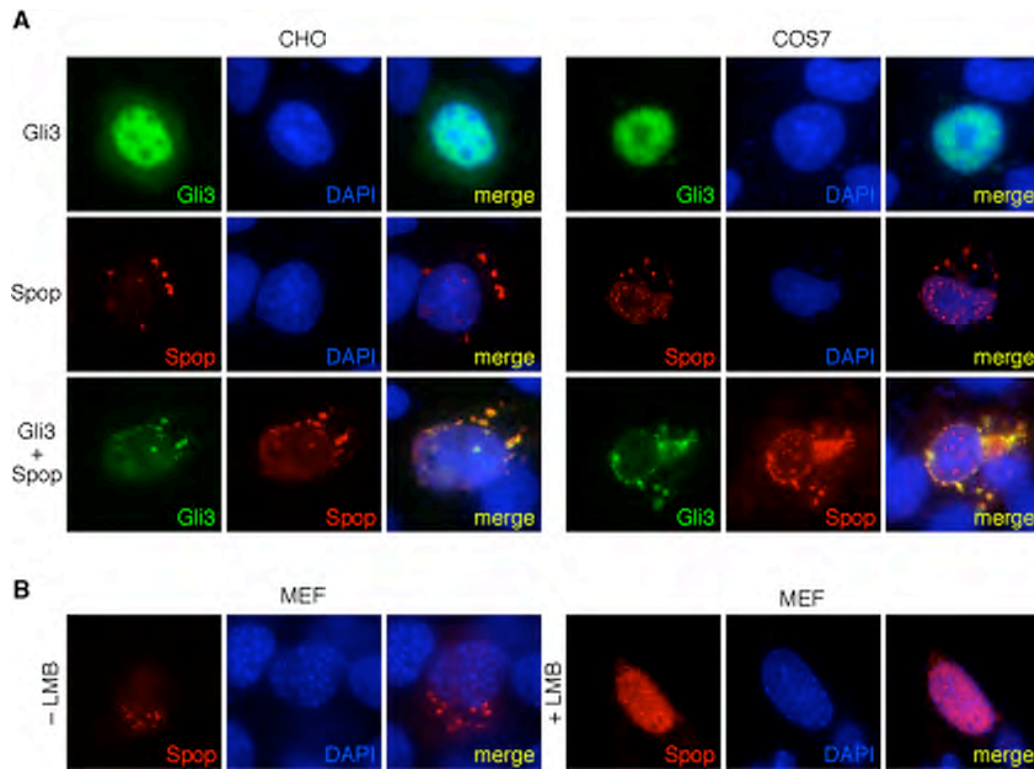
Figure 3-13: Spop physically interacts with Gli2 and Gli3, but not Gli1
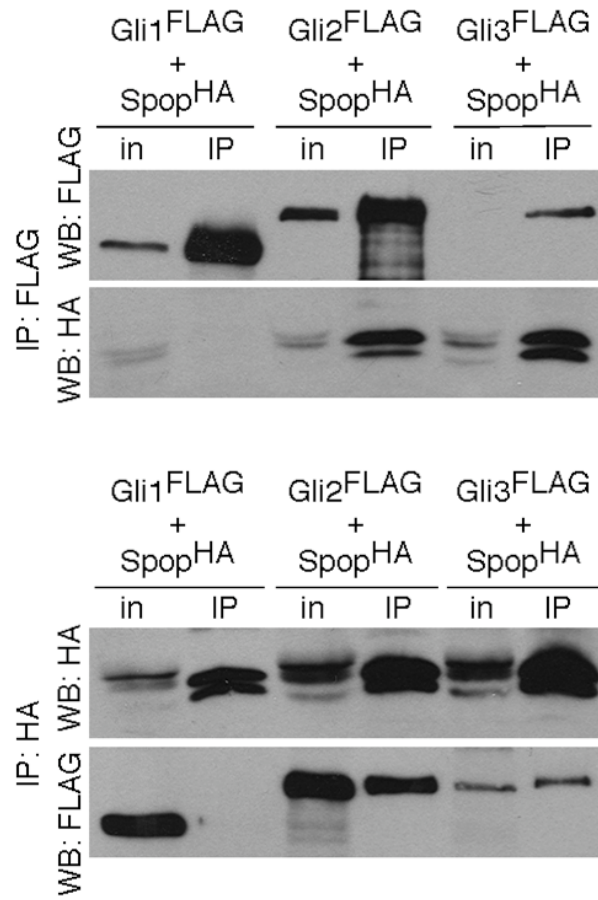
Figure 3-14: Spop expression reduces Gli2 and Gli3 protein levels
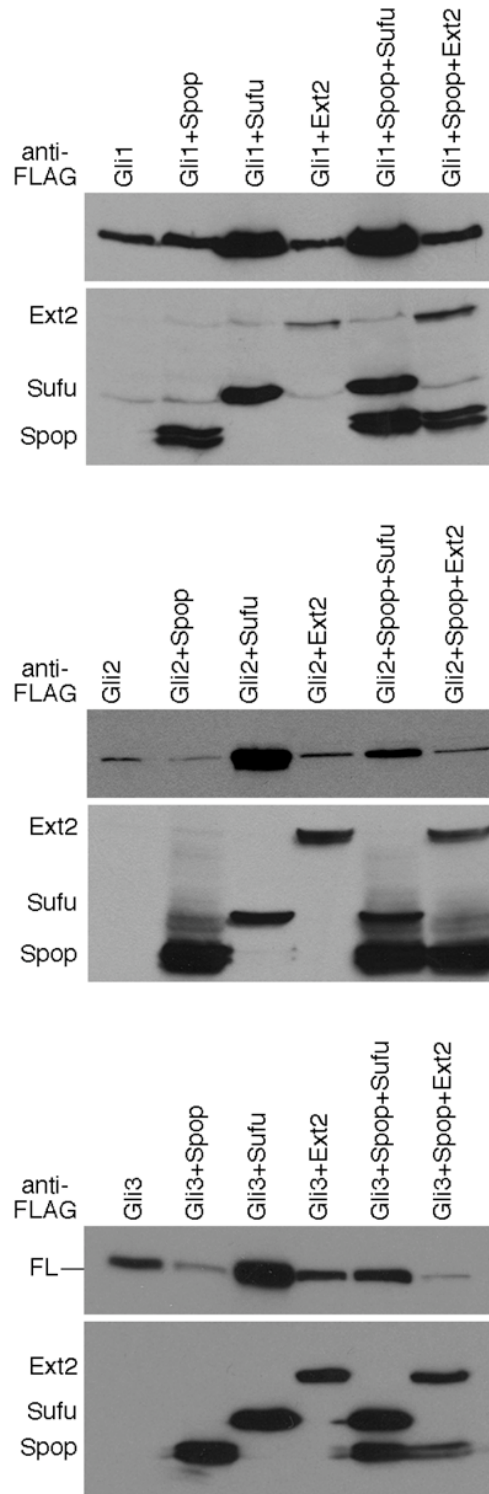
Figure 3-15: Spop reduces Gli2-mediated transcriptional activation
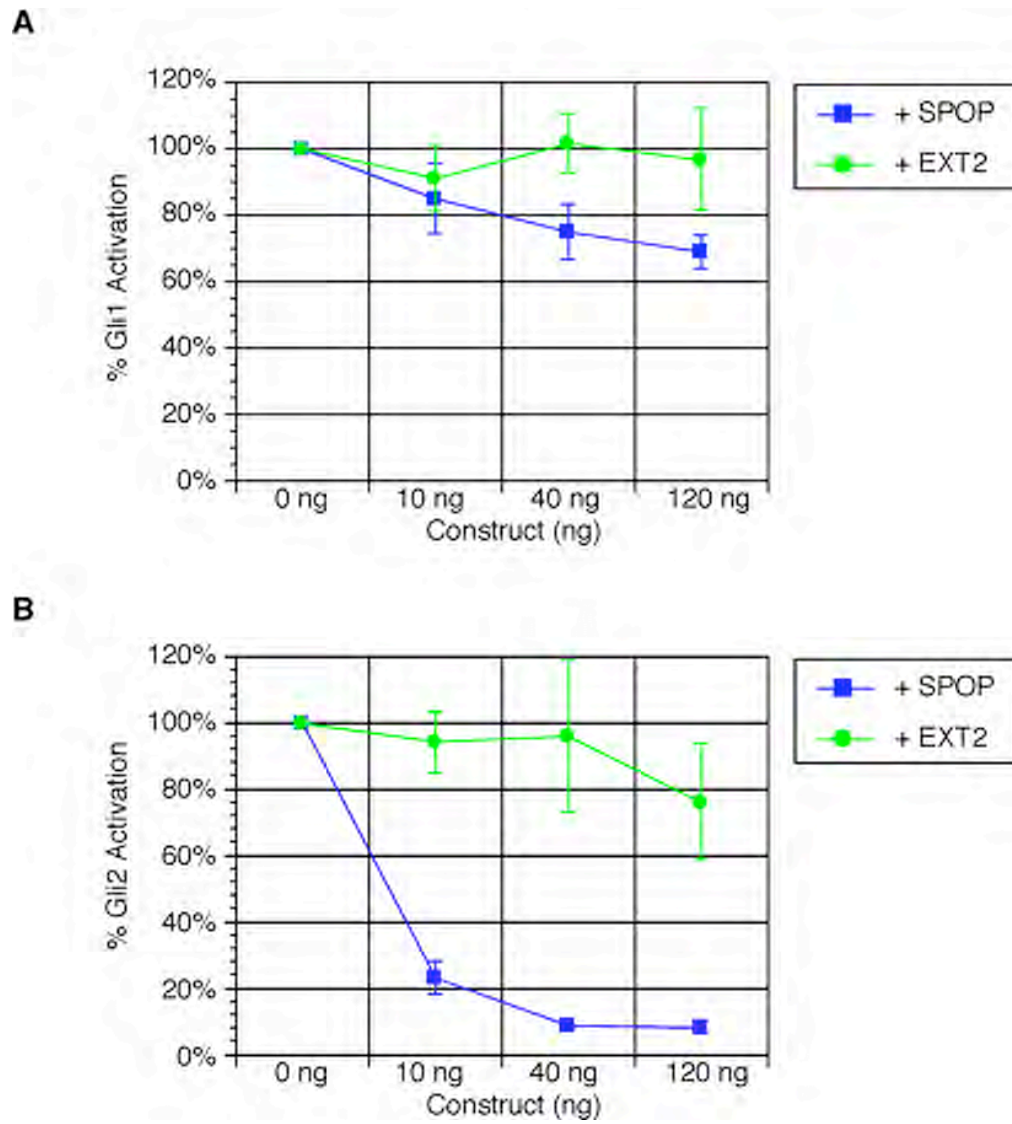
Figure 3-16: Spop promotes ubiquitination of Gli2 and Gli3, but not Gli1
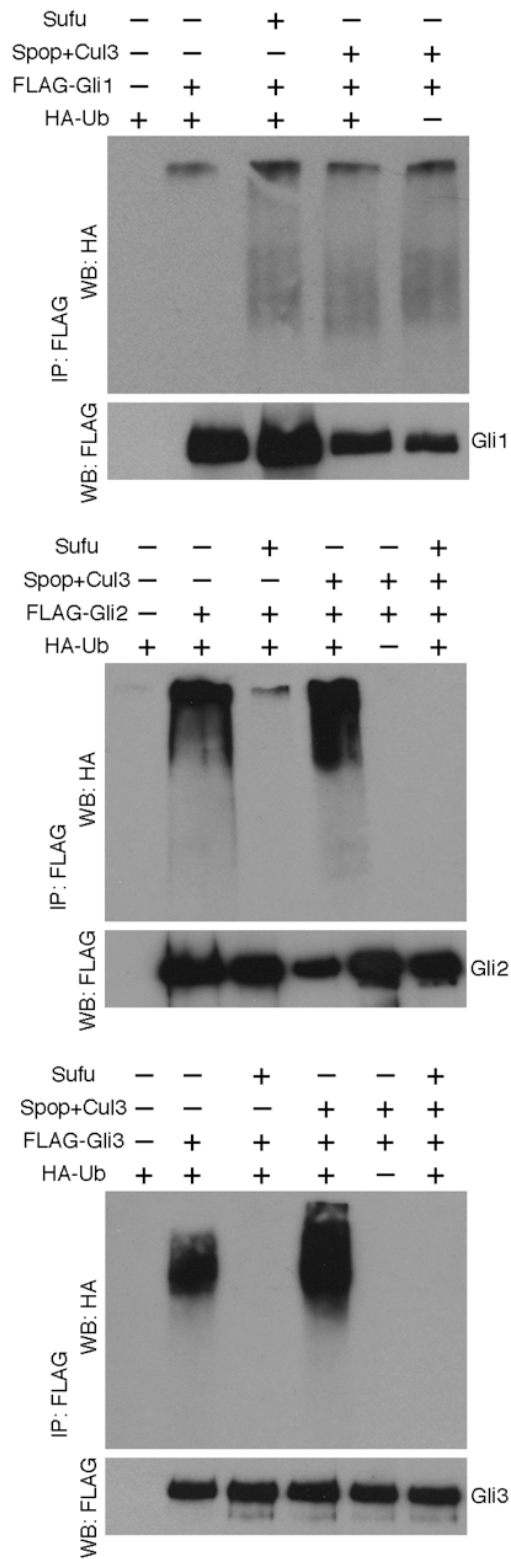
Figure 3-17: SPOP reduces Gli2 and Gli3 protein levels in a proteasome-dependent manner
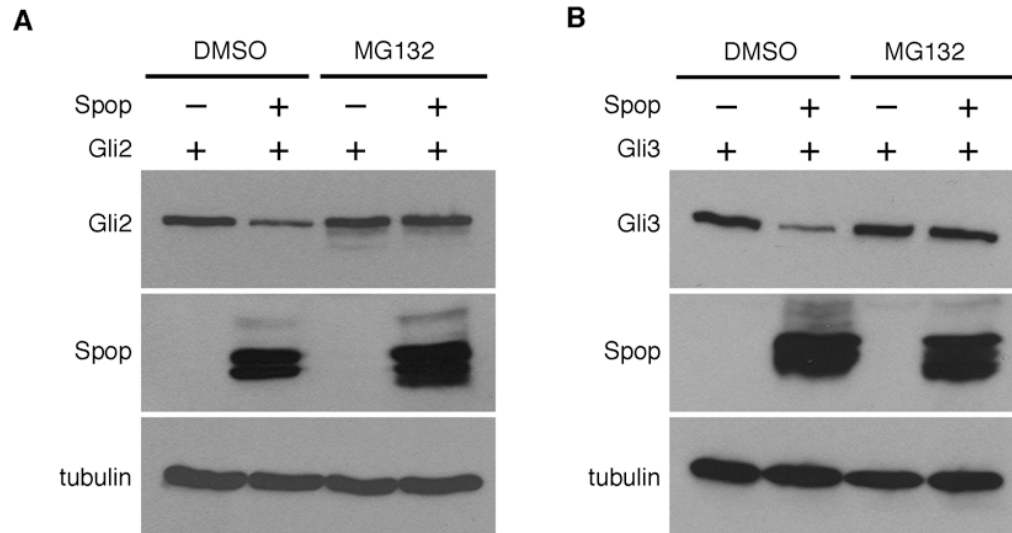
Figure 3-18: Spop directs Gli2 and Gli3 to Cul3+ foci
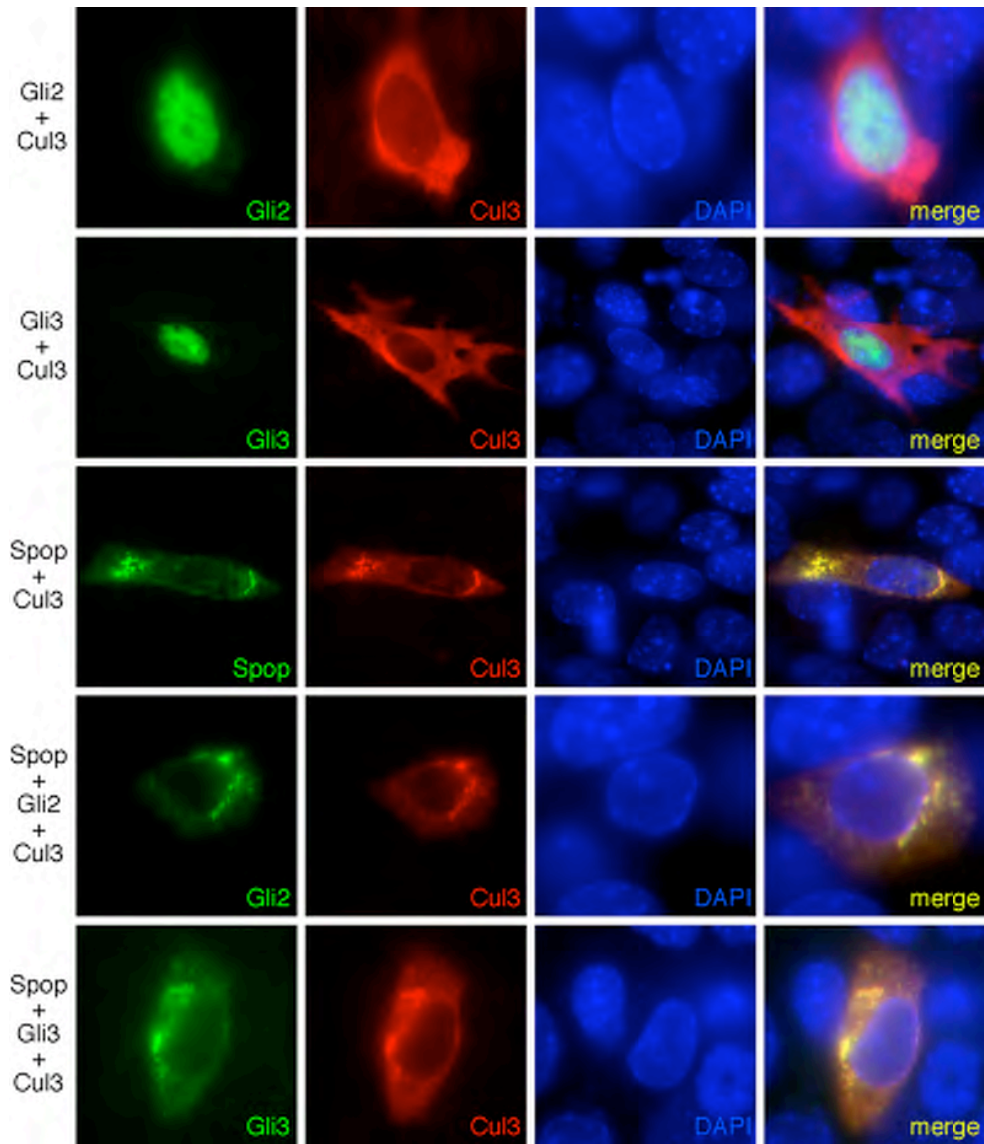
Figure 3-19: Knockdown of Spop in Sufu–/– MEFs partially restores Gli2 and Gli3 protein levels
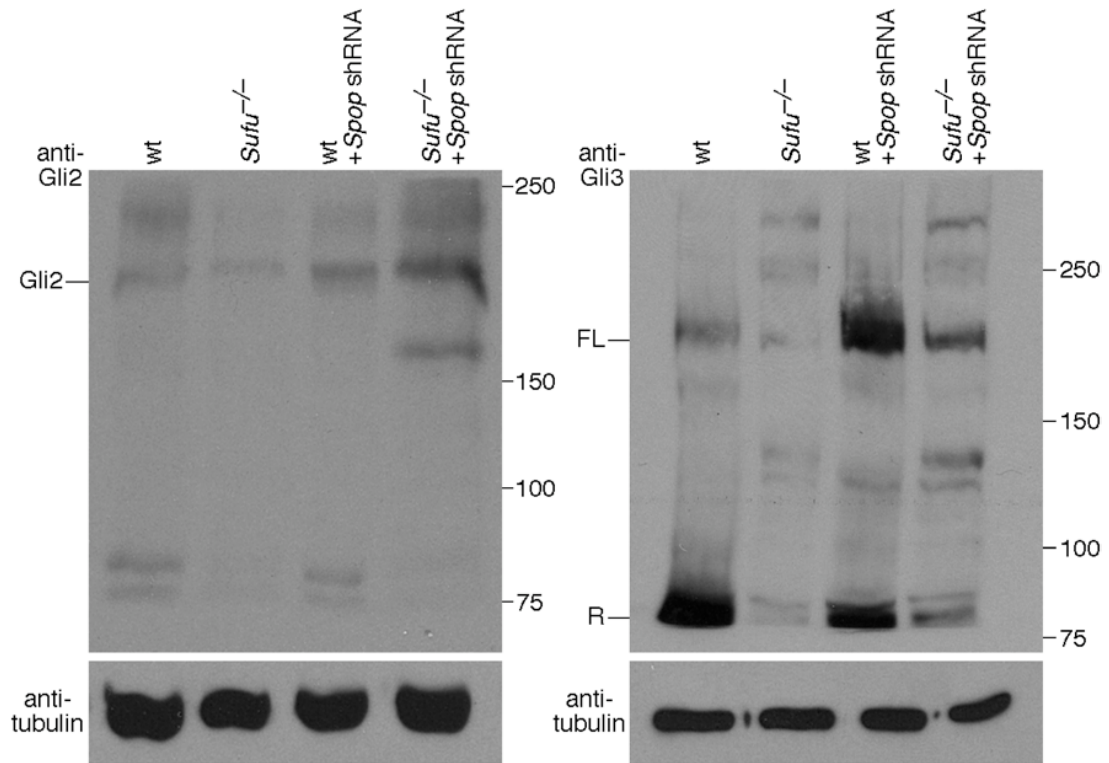
Figure 3-20: Overexpressed Spop does not localize to the primary cilium in MEFs
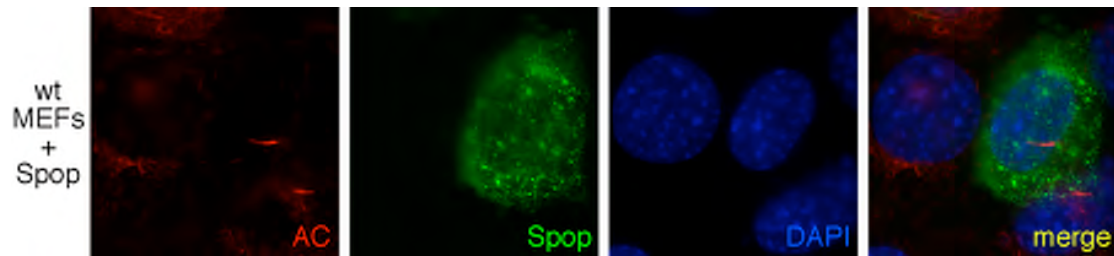
Figure 3-21: Spop knockdown in Sufu-deficient MEFs enhances Hh pathway activity
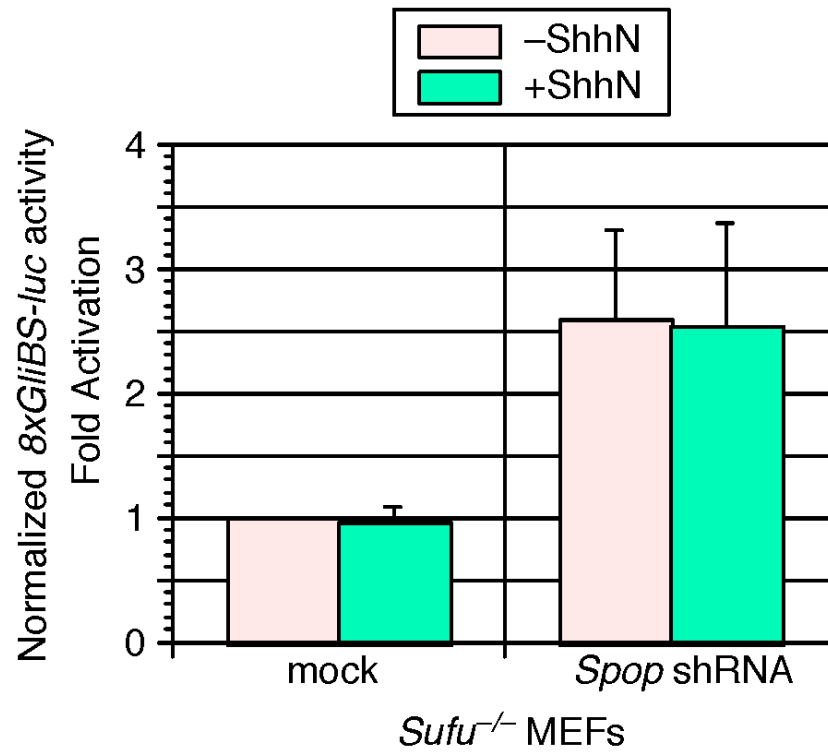
Figure 3-22: *Sufu*–/– and *Kif3a*–/– mouse embryonic fibroblasts have altered response to Shh, but not Wnt3a
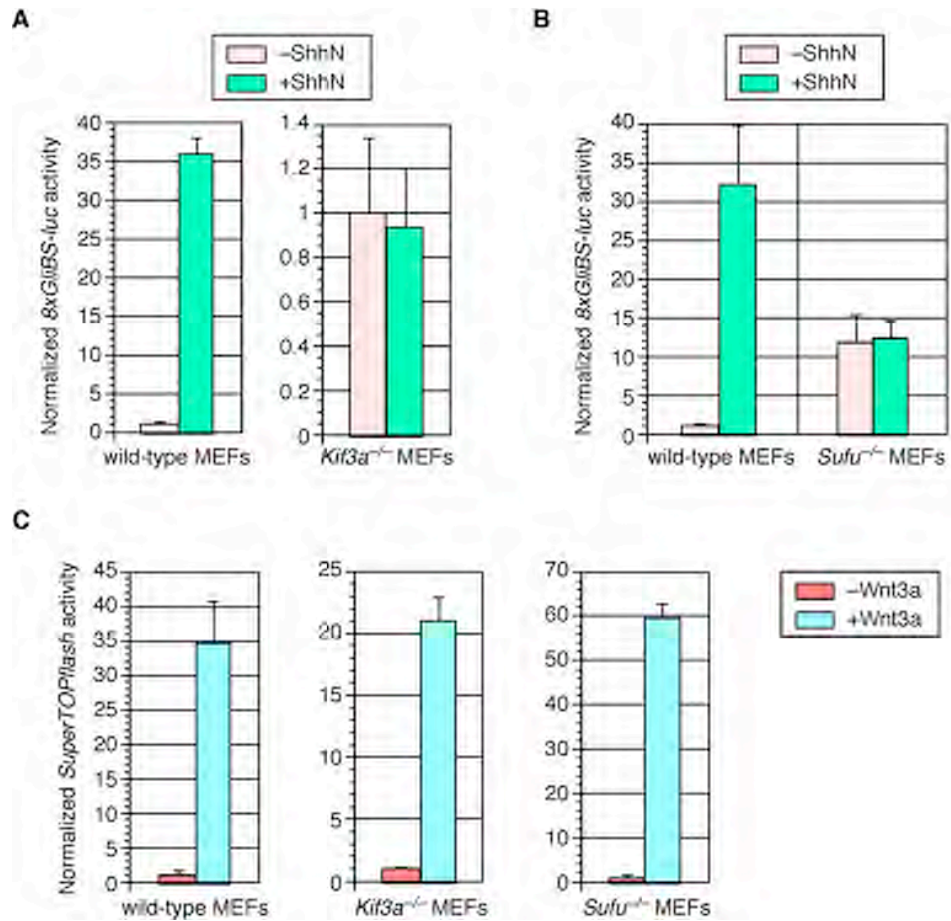
Figure 3-23: Mouse Sufu has positive and negative roles in regulating Hh signaling
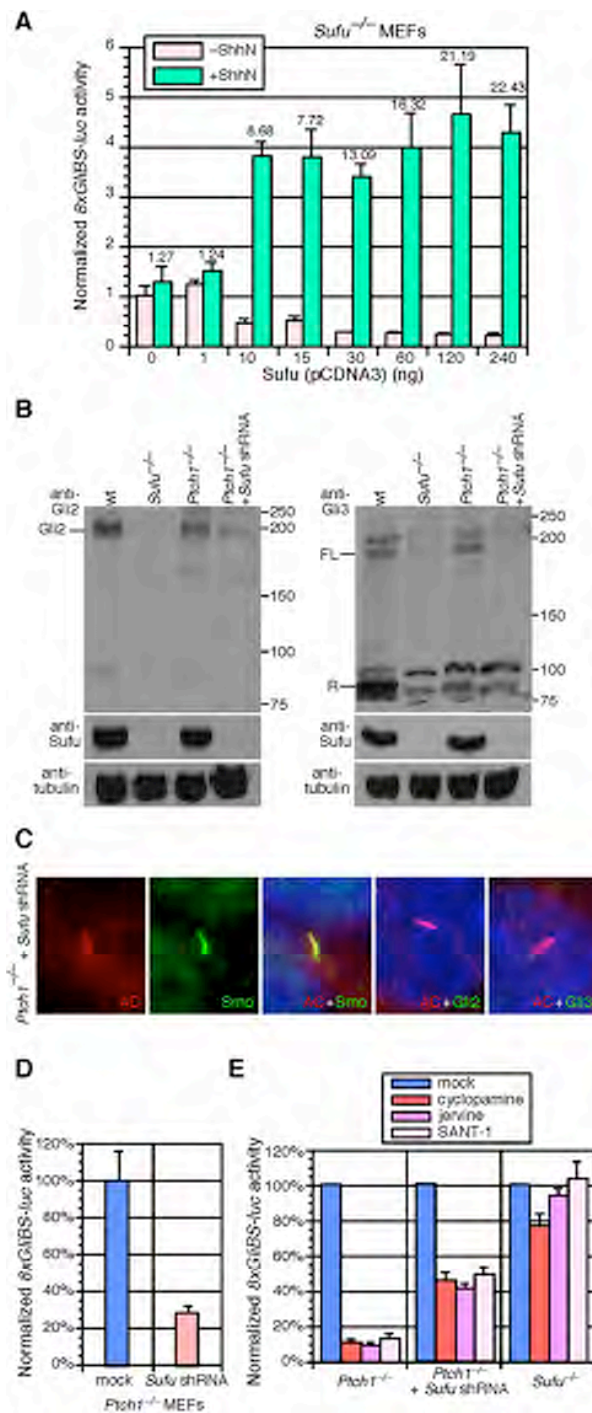
Figure 3-24: A model of Sufu function in mammalian Hh signaling
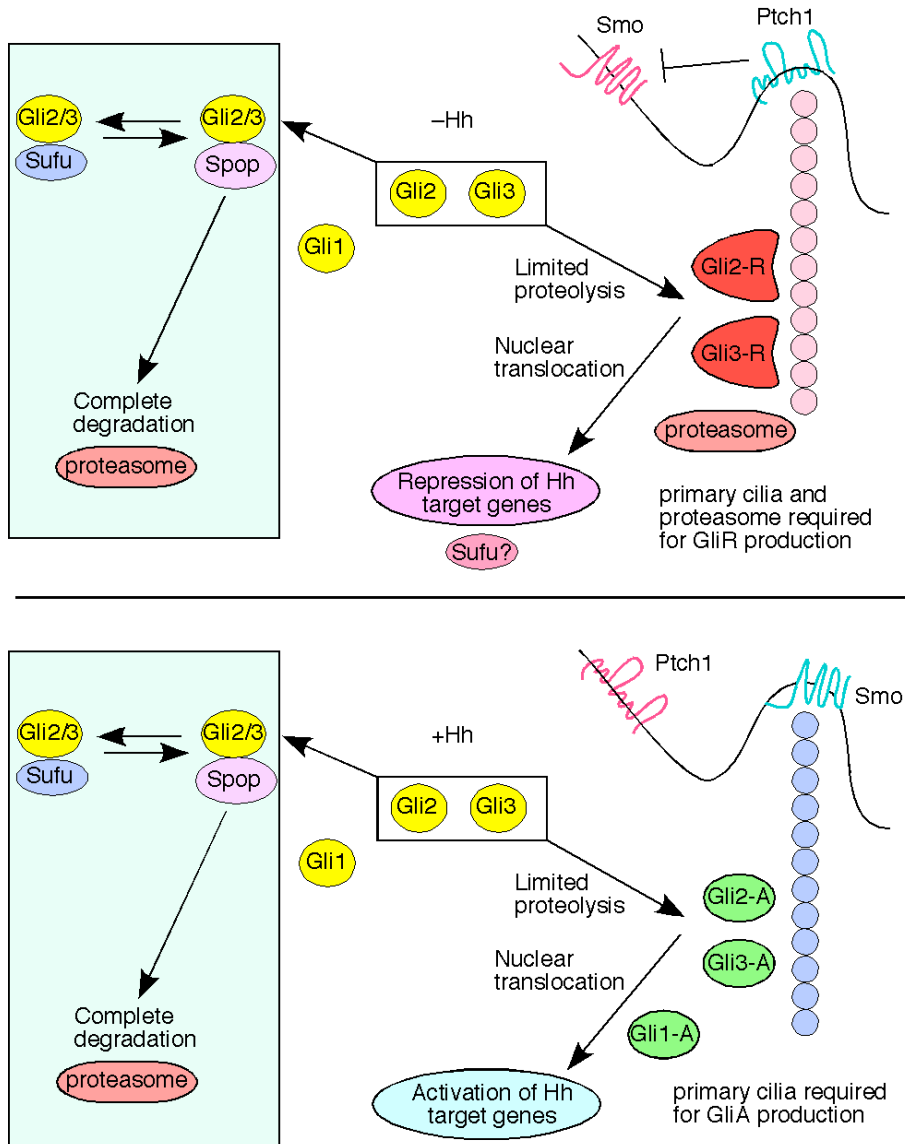
Figure 3-25: Gli2 and Gli3 protein levels are greatly reduced in both the nuclear and cytoplasmic fractions in the absence of *Sufu*
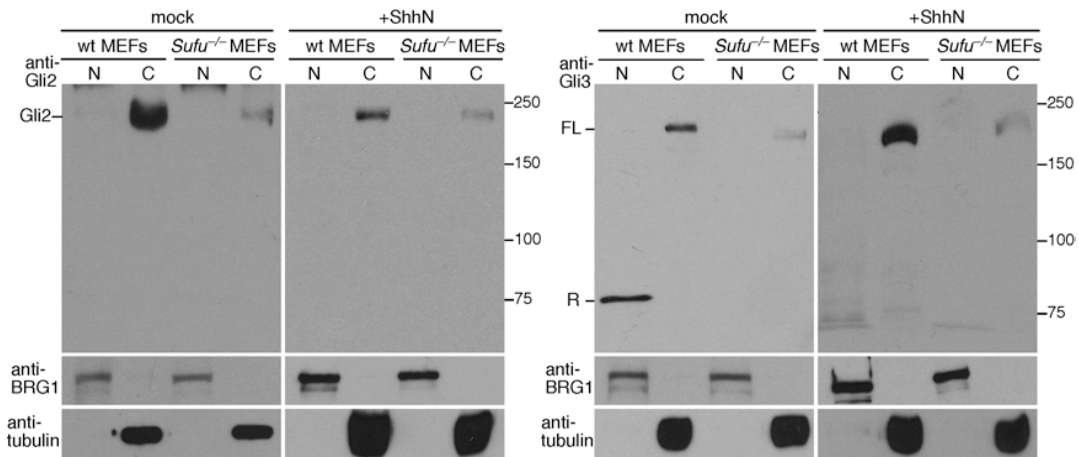
Figure 3-26: SAP18 localization is unaffected by Sufu, and SAP18 does not significantly affect Gli1 or Gli2 activity
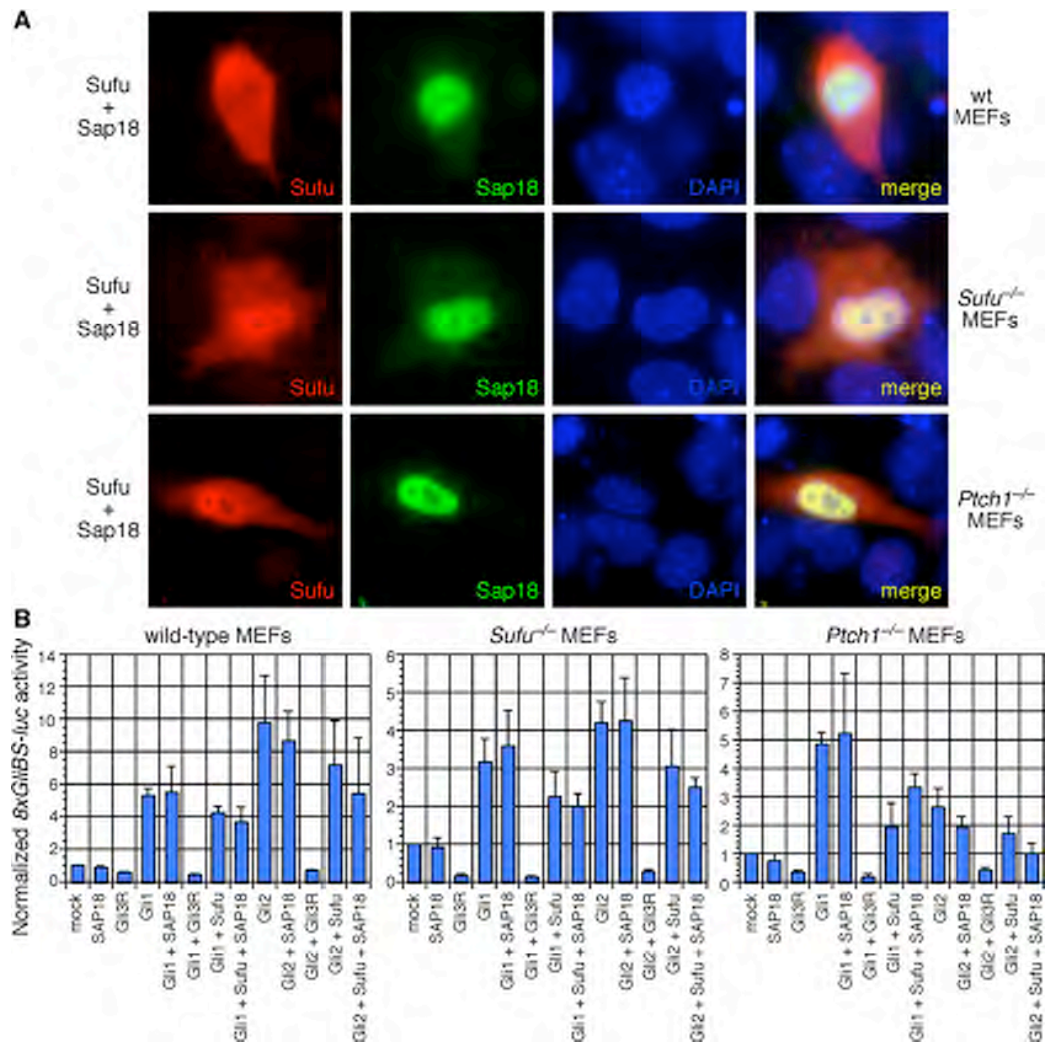
Figure 3-27: The Hh pathway is largely unaffected by pharmacologic modulation of protein kinase A (PKA) activity in *Sufu−/−* MEFs
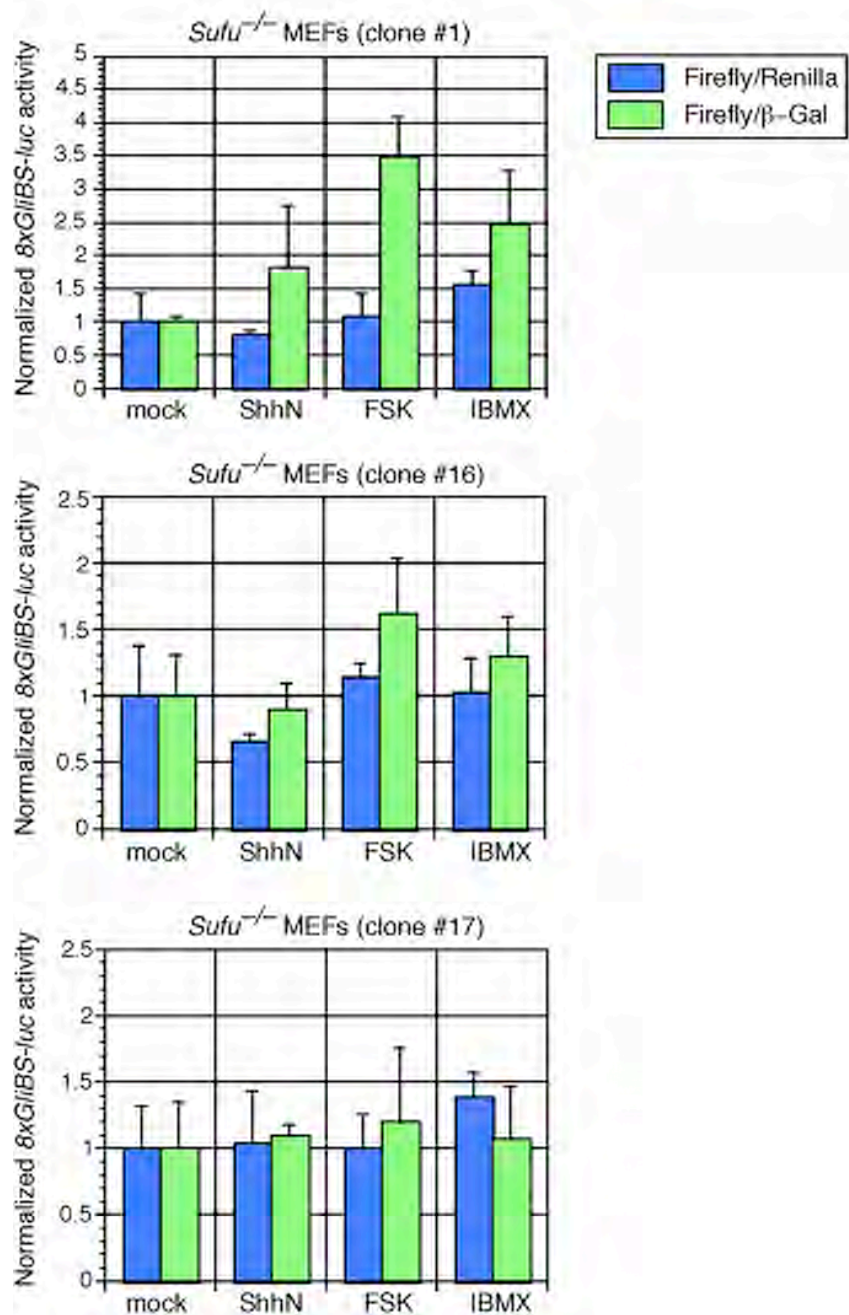
CHAPTER IV

Smoothened adopts multiple active and inactive conformations capable of

trafficking to the primary cilium

I. Introduction

The Hedgehog (Hh) signal transduction cascade is critical for many aspects of embryonic development, and aberrant regulation of the pathway results in a wide variety of congenital defects and cancers (McMahon et al. 2003). Activation of the pathway is initiated by binding of Hh ligand to the core receptor Patched (Ptch1 in mammals), a twelve-pass membrane protein with distant similarity to the resistance-nodulation division (RND) of bacterial transporters (Taipale et al. 2002). The interaction of Hh with Ptch1 relieves inhibition of Smoothened (Smo), a seven-pass transmembrane protein with structural similarity to G-protein coupled receptors (GPCRs), via unknown mechanisms. Once released from Ptch1-mediated inhibition, Smo communicates the status of pathway activation to the Ci/Gli transcription factors, which commence transcription of Hh target genes. This is achieved through the production of Gli activators, derived from full-length Gli proteins, and a concomitant reduction in levels of Gli repressors resulting from limited proteolysis of full-length Gli proteins (Jiang and Hui 2008). The mechanistic details of Smo activation are unclear and may differ between invertebrates and vertebrates (Huangfu and Anderson 2006; Varjosalo et al. 2006). In addition, the means by which Smo relays the status of pathway activation to the Gli proteins do not appear to be evolutionarily conserved (Huangfu and Anderson 2006), particularly the cellular microenvironment in which Smo is activated and the downstream components it interacts with. Nevertheless, two general features of Smo activation that are shared between species are a change in its subcellular distribution after relief of Ptch1 inhibition (Zhu et al. 2003; Corbit et al. 2005), and conformational changes in the extracellular and

169

cytosolic domains (Zhao et al. 2007). A conserved series of arginine (Arg) residues in the C-tail of both fly and mammalian Smo plays a critical role in modulation of conformation. How these events lead to Smo activation remains a central unresolved issue in understanding the molecular mechanisms of Hh signaling.

In mammals, the primary cilium is essential for proper interpretation of the Hh signal. Cilia contain a long microtubular axoneme, extending from the basal body and surrounded by an external membrane that is continuous with the plasma membrane. Assembly and maintenance of the primary cilium are mediated by the process called intraflagellar transport (IFT), which involves bidirectional movement of IFT particles powered by anterograde kinesin (Kif3a, b and c) and retrograde dynein motors (Rosenbaum and Witman 2002; Eggenschwiler and Anderson 2007). Mutations that abolish the biogenesis or function of the primary cilium lead to defective Hh signaling (Huangfu et al. 2003). Further, the production of both Gli activators and repressors is affected in the absence of the cilium, leading to a loss of Gli repressive activity without a corresponding gain of transcriptional activation (Huangfu and Anderson 2005; Liu et al. 2005; Eggenschwiler and Anderson 2007). Smo localization to the primary cilium is associated with Hh pathway activation, and other components of the pathway, including Gli proteins and Ptch1, are also found in this organelle (Haycraft et al. 2005; Rohatgi et al. 2007). Mutations in Smo that confer constitutive Hh pathway activation (SmoA1) promote ciliary localization of Smo in the absence of Hh stimulation; conversely mutations that abolish ciliary localization (CLDSmo) appear to render the protein incapable of activating the pathway in the presence of the primary cilium (Corbit et al.

2005). Ptch1 localizes to the cilium in the absence of Hh ligand, and traffics off the cilium after Hh binding, allowing movement of Smo to the axoneme (Rohatgi et al. 2007). It has been proposed that the cilium acts as a scaffold or provides a specialized microenvironment for relaying the Hh signal (Davenport and Yoder 2005; Eggenschwiler and Anderson 2007). This led to a model in which Smo adopts an active conformation upon localizing to the primary cilium, which is capable of coupling to yet-to-be identified downstream components, thus resulting in stimulation of Gli activators, reduction in Gli repressors, and induction of target gene expression. Here, we show that a distinct class of Smo antagonists which suppress Smo-mediated pathway activation also unexpectedly stimulate translocation of Smo to the primary cilium. In addition, modulation of protein kinase A (PKA) activity by chemical means causes a partial accumulation of Smo on a proximal segment of the primary cilium. We propose that multiple conformational changes of Smo are required for ciliary translocation and subsequent pathway activation.

II. Results and Discussion

Smo localizes to the cilium upon both activation and repression of the Hh pathway

We generated antibodies against the C-terminal domain of mouse Smo (Gerber et al. 2007) to examine the ciliary localization of endogenous Smo in response to known Hh pathway agonists and antagonists. When exposed to conditioned media (CM) collected from cells expressing the N-terminal signaling fragment of Sonic hedgehog (ShhN), wild-type mouse embryonic fibroblasts (MEFs) accumulated Smo in primary cilia, and nearly

171

100% of cilia were positive for Smo (Smo[+]) after 6 hours of treatment (Fig. 4-1, 4-2A).

In agreement with previously published results (Corbit et al. 2005), a reduced number of

cilia were Smo[+] after brief (1 hour) treatment with cyclopamine, a teratogen derived from

the *Veratrum* genus of plants and a well-defined Smo antagonist known to bind to the

heptahelical bundle of Smo (Figure 4-1, 4-2A) (Chen et al. 2002a). Surprisingly,

prolonged treatment of MEFs with cyclopamine resulted in a significant number of Smo[+]

cilia, with roughly 70% displaying strong Smo signal along the entire length of the cilium

after 24 hours of exposure to cyclopamine (Figure 4-1, 4-2A). We speculate that the

increased time of cyclopamine treatment required to generate a high number of Smo[+]

cilia underlies the difference between our observation and prior reports. This finding also

provided a unique opportunity to examine the relationship between ciliary localization of

Smo and Hh pathway activation.

This unexpected result prompted us to screen a number of previously reported

modulators of Smo activity for their ability to induce or prevent Smo translocation to the

primary cilium. The Smo agonists 20-α-hydroxysterol (Corcoran and Scott 2006) and

purmorphamine (Sinha and Chen 2006) caused a significant translocation of Smo to the

cilium, comparable to that seen after treatment with ShhN-CM (Figure 4-1A, 4-2B)

(Rohatgi et al. 2007). As previously described, the related oxysterol, 7β-hydroxysterol,

neither induced Smo translocation nor activated the pathway (Figure 4.2B, Figure 4-3B)

(Rohatgi et al. 2007). 7-dehydrocholesterol and its metabolite, pro-vitamin D3, had no

effect on the subcellular distribution of Smo (Figure 4-2B) although pro-vitamin D3 was

proposed to be transported by Ptch1 to inhibit Gli activity (Bijlsma et al. 2006; Koide et

al. 2006). Notably, jervine, a close chemical relative of cyclopamine, was also able to induce trafficking of Smo to the primary cilium (Figure 4-1, 4-2B). By contrast, SANT-1, a structurally unrelated Smo antagonist (Chen et al. 2002b), did not induce Smo trafficking to the cilium (Figure 4-1A, 4-2B). We next correlated induction of Smo ciliary translocation with activation of endogenous Gli transcription factors. Measurement of activation of a firefly luciferase reporter driven by eight multimerized Gli-binding sites (8xGliBS-luc) (Sasaki et al. 1997) in wild-type MEFs showed that only treatment with ShhN-CM, 20-α-hydroxysterol, or purmorphamine (but not cyclopamine, jervine, SANT1 or pro-vitamin D3) activated a Gli transcriptional response (Figure 4-3B). Taken together, the data indicate that while ciliary translocation of Smo can be associated with Gli transcriptional activation, trafficking to the axoneme is not sufficient for Hh pathway activation. Moreover, as cyclopamine is not known to affect the subcellular distribution of Ptch1, our results suggest that Ptch1 may co-exist with inactive Smo conformations on the ciliary axoneme. Recent studies of Ptch1 and Smo trafficking have revealed that Smo bound to a Hh agonist, SAG, is found on the cilium with Ptch1 (Rohatgi et al. 2007). We hypothesize that both inactive and active states of Smo may be decoupled from Ptch1-mediated inhibition of ciliary trafficking and Smo activation on the cilium thus requires additional steps.

SANT-1 inhibits cyclopamine- and jervine-induced Smo ciliary translocation

SANT-1 incompletely inhibits cyclopamine binding to cells expressing Smo, and this led to the hypothesis that SANT-1 may change the ability of Smo to interact with

173

cyclopamine (Chen et al. 2002b). We speculated that this competition between different classes of Smo antagonists could be utilized to control Smo ciliary localization and gain insight into why inactive Smo might traffic to the cilium. In wild-type MEFs, SANT-1 efficiently inhibited cyclopamine- and jervine- induced translocation of Smo to the primary cilium (Figure 4-3A). To further investigate competition between SANT-1 and cyclopamine, we utilized *Ptch1*$^{-/-}$ MEFs, which display constitutive ciliary localization of Smo and Hh pathway activation (Figure 4-4) (Rohatgi et al. 2007). Treatment with cyclopamine and jervine inhibited Gli reporter activity in *Ptch1*$^{-/-}$ MEFs, but did not eliminate Smo staining from the cilium (Figure 4-3C, 4-3D). SANT-1 inhibited the Hh pathway to a similar extent, but drastically reduced the number of Smo$^+$ cilia (Figure 4-3C, 4-3D, 4-4). Thus, our results suggest that *Veratrum* alkaloids and SANT-1 comprise two distinct classes of Smo inhibitors whose binding to Smo induces conformations that are differentially competent for cilium targeting. Cyclopamine treatment induces an inactive conformation of Smo that is capable of translocating to the primary cilium. Subsequent treatment with SANT-1 could convert inactive Smo into another state that could no longer associate with the cilium. Since SANT-1 can effectively block cyclopamine-induced translocation of Smo to the primary cilium, this suggests that the inactive state of Smo induced by SANT-1 represents the dominant form when both cyclopamine and SANT-1 are present.

The precise mechanism for cyclopamine-induced Smo translocation remains to be elucidated. Cyclopamine-bound Smo may adopt a conformation that allows increased coupling to the anterograde IFT motor subunit Kif3a via β-arrestins (Kovacs et al. 2008).

β-arrestins have been shown to mediate the interaction between Smo and Kif3a, thus promoting ciliary localization of Smo and Smo-dependent activation of Gli. The Smo conformation induced by cyclopamine binding may either be incapable of coupling to downstream effectors, or might not interact with retrograde IFT components. Consistent with this latter hypothesis, *Dync2h1* mutant MEFs, which are deficient in retrograde IFT, accumulate Smo on the cilium but do not properly transduce the Hh signal (Ocbina and Anderson 2008).

Gαs-mediated activation of protein kinase A stimulates translocation of Smo to a proximal region of the primary cilium

Smo structurally resembles a GPCR, but it is currently unclear whether physical coupling of Smo to a Gα subunit is essential for proper Hh signal transduction (Riobo et al. 2006; Low et al. 2008). Studies in cultured insect and mammalian cells showed that Smo specifically stimulates GTP binding to Gαi family members, and inhibition of Gαi reduces activation of Gli reporters (Riobo et al. 2006). However, no effect on Hh patterning of the chick neural tube or formation of Gli3 repressor was observed with activation or inhibition of Gαi *in vivo* (Low et al. 2008). Recent data indicates that Gαi impacts Hh transduction in *Drosophila melanogaster* through its effects on PKA activity, although a direct biochemical interaction between Smo and Gαi remains unreported (Ogden et al. 2008). It is unknown whether GPCR signaling affects Smo localization, either through direct binding to Smo, or through crosstalk via other signaling pathways.

175

To investigate whether modulation of Gα subunit activity might impact Smo ciliary trafficking, we treated wild-type MEFs with cholera toxin (CTX), which activates Gαs (Gill and Meren 1978), and pertussis toxin (PTX), which inhibits Gαi (Codina et al. 1983). CTX, but not PTX, caused an accumulation of Smo on the primary cilium, which increased with prolonged exposure to the toxin (Figure 4-5A, 4-5B). The CTX-induced Smo distribution was not uniform along the length of the cilium, when compared to ShhN-CM induced Smo translocation (compare Figure 4-1 to 4-5A). We fixed MEFs with methanol to better visualize basal bodies, which comprise the base of the primary cilium, and observed that CTX-induced Smo cilium staining was concentrated in a region proximal to the basal body (Figure 4-5C). Interestingly, this region appeared similar to a recently defined inversin compartment on the proximal primary cilium (Shiba et al. 2008). As CTX treatment is expected to activate adenylyl cyclase and thus stimulate PKA, we next asked if direct stimulation of adenylyl cyclase in MEFs with forskolin (FSK) recapitulated CTX-stimulated Smo translocation (Seamon and Daly 1981). FSK treatment resulted in a comparable localization of Smo to the proximal region of the cilium (Figure 4-5B, 4-5C). CTX, PTX, and FSK alone did not activate the Hh pathway significantly as assayed by Gli reporters (Figure 4-5D).

We examined the relationship of PKA-mediated Smo translocation to the proximal cilium with ShhN-mediated pathway activation and SANT-1 inhibition. Exposure of MEFs to both ShhN and CTX or FSK resulted in restoration of Smo staining along the entire length of the primary cilium (Figure 4-6, 4-7A). In contrast, SANT-1 inhibited PKA stimulation of Smo trafficking to the proximal cilium (Figure 4-6, 4-7B).

Two conclusions may be drawn from these results. First, the Smo conformation adopted when bound to SANT-1 is refractory to both cyclopamine- and PKA-stimulated cilium trafficking, suggesting that SANT-1 may act upstream to sequester Smo from or inhibit its interaction with β-arrestins or IFT particles (Kovacs et al. 2008). Second, addition of ShhN overrides accumulation of Smo in the proximal region of the primary cilium. Restricted Smo localization to this region could be a prerequisite for pathway activation, or a means to inhibit Smo trafficking or coupling to downstream components. Consistent with previous reports (Fan et al. 1995; Epstein et al. 1996; Hammerschmidt et al. 1996; Pan et al. 2009), we observed that activation of the Hh reporter was blocked by CTX- and FSK-mediated PKA stimulation, but PTX treatment produced only a modest reduction (Fig 4-7C). We speculate that if PKA positively regulates Smo while promoting Gli repressor production, any potential positive effect on Hh signaling due to partial Smo translocation induced by CTX or FSK may be offset by negative regulation of Gli factors by PKA (Wang et al. 2000a). Additional studies using endogenous levels of PKA-refractory forms of the Gli proteins will be necessary to rigorously resolve this issue.

D. melanogaster Smo utilizes a series of PKA sites in its C-terminal tail to neutralize the inhibitory effects of several clusters of Arg residues (Zhao et al. 2007). These Arg clusters, but not the PKA sites, are conserved in vertebrates and are critical for maintenance of Smo in an inhibited state that is incapable of trafficking to the cell surface. Further investigation is required to clarify if repression of the autoinhibitory Arg clusters results in Smo ciliary translocation, and if PKA acts directly or indirectly on Smo for targeting to a proximal region of the cilium. Nonetheless, our data raise the

possibility that signaling through Gαs-coupled receptors and activation of PKA could influence Smo trafficking both to and on the primary cilium. This could provide a means for crosstalk between signaling pathways.

In this study, we show that Hh pathway agonists, a specific class of antagonists, and PKA activity induce accumulation of Smo in different regions of the primary cilium. Smo localization to the cilium is therefore necessary, but not sufficient, for activation of the Hh pathway. Taken together, the data suggest that Smo can adopt multiple conformations that allow ciliary trafficking, but only a subset of these are competent to activate the Hh cascade. In addition, the precise location of Smo on the primary cilium may be important for activation of the pathway. Further analysis of Smo conformations and identification of factors that communicate these conformations to Gli proteins are necessary for a comprehensive understanding of the role of the primary cilium in Smo function.

III. **Figure Legends**

Figure 4-1: Hh pathway agonists and antagonists stimulate Smo translocation to the primary cilium

Wild-type mouse embryonic fibroblasts (MEFs) stained with antibodies against endogenous Smo (green), acetylated (AC) tubulin (red), and DAPI (blue). MEFs treated with ShhN-conditioned media (ShhN-CM), purmorphamine, cyclopamine, and jervine

display Smo staining along the entire length of the cilium. Note that fixation with paraformaldehyde produces artifactual nuclear staining with the Smo antibody; this nuclear staining is not visible after fixation in methanol (See Figure 4-5C).

Figure 4-2: Quantification of Smo translocation to the primary cilium

(**A**) Quantification of the percentage of Smo-positive (Smo[+]) cilia in MEFs after treatment with ShhN CM and cyclopamine for the indicated times. Cyclopamine induces Smo translocation to a significant number of cilia after 6 hr of treatment, although this is less than that induced by ShhN CM. All quantification of cilia staining in this and subsequent figures represents at least two separate experiments with a minimum of 100 cilia scored per time point and condition. Error bars indicate +/- standard deviation (SD). (**B**) Quantification of Smo[+] cilia in MEFs after treatment with indicated compounds for 24 hr. 20-α-hydroxysterol (20α-OHC), purmorphamine, cyclopamine, and jervine induce Smo translocation to the cilium. Error bars indicate +/- SD.

Figure 4-3: SANT-1 inhibits cyclopamine-and jervine- induced Smo translocation to the primary cilium

(**A**) Quantification of Smo[+] cilia in wild-type MEFs after treatment with indicated compounds for 24 hr. SANT-1 inhibits cyclopamine- and jervine-induced ciliary translocation of Smo. Error bars indicate +/- SD. (**B**) Fold activation of *8xGliBS-luciferase* Hh reporter in wild-type MEFs after agonist and antagonist treatment for 48 hr.

Treatment with ShhN-CM, 20-α-hydroxysterol (20α-OHC), or purmorphamine [but not 7β-hydroxysterol (7β-OHC), pro-vitamin D3, 7-dehydrocholesterol (7-DHC), cyclopamine, jervine or SANT-1] activated a Gli transcriptional response. Results are representative of three experiments in two wild-type MEF lines, and were normalized to a constitutively active *Renilla* luciferase reporter. Error bars indicate +/- SD. (**C**) Quantification of Smo$^+$ cilia in *Ptch1$^{-/-}$* MEFs after treatment for 24 hr. Cyclopamine and jervine do not disrupt constitutive Smo localization. SANT-1 removes Smo from the cilium of *Ptch1$^{-/-}$* MEFs in the presence or absence of cyclopamine and jervine. Error bars indicate +/- SD. (**D**) Percentage activity of *8xGliBS-luciferase* reporter in *Ptch1$^{-/-}$* MEFs after treatment for 48 hr. Cyclopamine, jervine or SANT-1 efficiently block Hh responses. Note that 7-DHC and pro-vitamin D3 do not significantly inhibit the activity of the reporter. Results are the mean of three independent experiments, and were normalized to a constitutively active *Renilla* luciferase reporter. Error bars indicate +/- SD.

Figure 4-4: SANT-1 dominantly inhibits Smo ciliary translocation in *Ptch1$^{-/-}$* MEFs

Ptch1$^{-/-}$ MEFs stained with antibodies against acetylated (AC) tubulin (red), Smo (green) and DAPI (blue). SANT-1 removes Smo from the cilium of *Ptch1$^{-/-}$* MEFs in the presence or absence of cyclopamine.

Figure 4-5: Modulation of Gαs and protein kinase A (PKA) causes Smo accumulation in a proximal region of the primary cilium

(**A**) Treatment of wild-type MEFs with cholera toxin (CTX) for 24 hr induces Smo (green) translocation to the cilium (red). (**B**) Quantification of CTX- and FSK-induced Smo ciliary translocation after treatment for the indicated times. Treatment of wild-type MEFs with pertussis toxin (PTX) does not stimulate ciliary translocation of Smo. Error bars indicate +/- SD. (**C**) Wild-type MEFs were fixed in methanol and stained with antibodies against γ-tubulin (red; label the basal body) and Smo (green). In contrast to the relatively uniform Smo staining on the cilium induced by ShhN, CTX treatment causes Smo accumulation proximal to the basal body. (**D**) *8xGliBS-luciferase* Hh reporter activity in wild-type MEFs with the indicated treatment. CTX and FSK do not activate the Hh pathway despite inducing ciliary localization of Smo. Data are representative of three independent experiments. Hh reporter activity was normalized to *β-galactosidase* activity produced from a constitutive *hsp68*-lacZ reporter, as alteration of PKA affected *Renilla* luciferase activity (data not shown). Error bars indicate +/- SD.

Figure 4-6: ShhN ligand and SANT-1 act dominantly to PKA-induced Smo translocation

Wild-type MEFs treated with indicated compounds for 24 hr stained with antibodies against acetylated (AC) tubulin (red), Smo (green) and DAPI (blue). ShhN causes Smo distribution along the length of the cilium when PKA is activated, whereas SANT-1 inhibits any type of Smo trafficking on the cilium.

Figure 4-7: Quantification and activity of Gαs/PKA-mediated Smo ciliary translocation

(**A**) Quantification of Smo+ cilia in wild-type MEFs after treatment for 24 hr. Nearly all cilia are Smo+ when treated with ShhN and CTX or FSK. Error bars indicate +/- SD. (**B**) Quantification of Smo+ cilia in wild-type MEFs after 24 hr. SANT-1 inhibits CTX- and FSK-mediated stimulation of Smo translocation to the proximal region of the primary cilium. Error bars indicate +/- SD. (**C**) *8xGliBS-luciferase* reporter activity in wild-type MEFs with indicated treatments for 48 hr. CTX and FSK, but not PTX inhibit ShhN stimulation of the reporter. Normalization was performed as in Figure 4-5. Error bars indicate +/- SD.

Figure 4-1: Hh pathway agonists and antagonists stimulate Smo translocation to the primary cilium
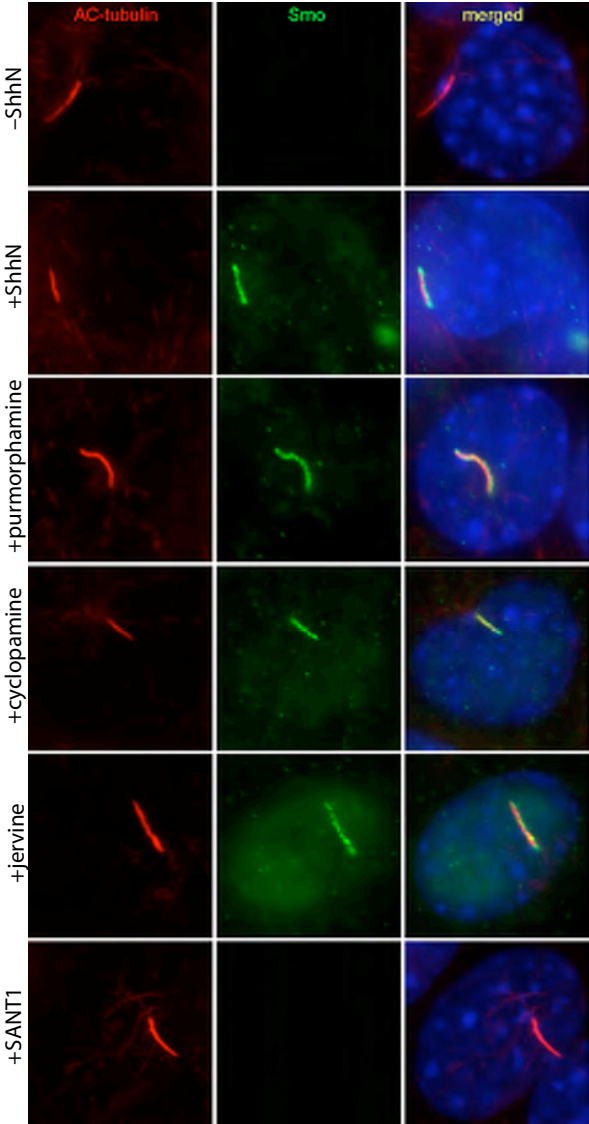
Figure 4-2: Quantification of Smo translocation to the primary cilium
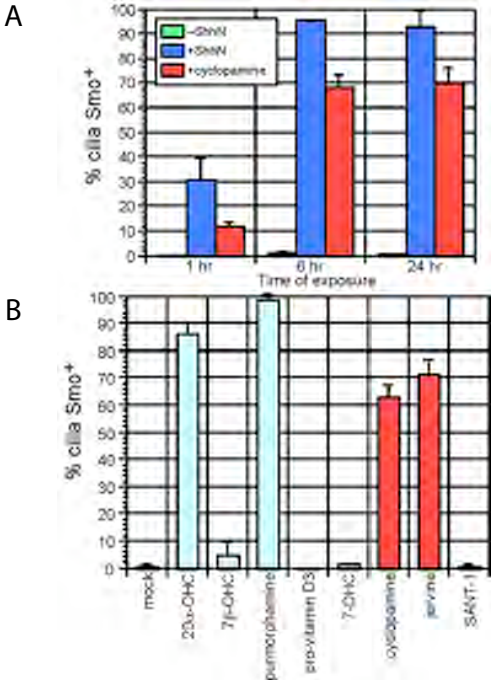
Figure 4-3: SANT-1 inhibits cyclopamine- and jervine-induced Smo translocation to the primary cilium
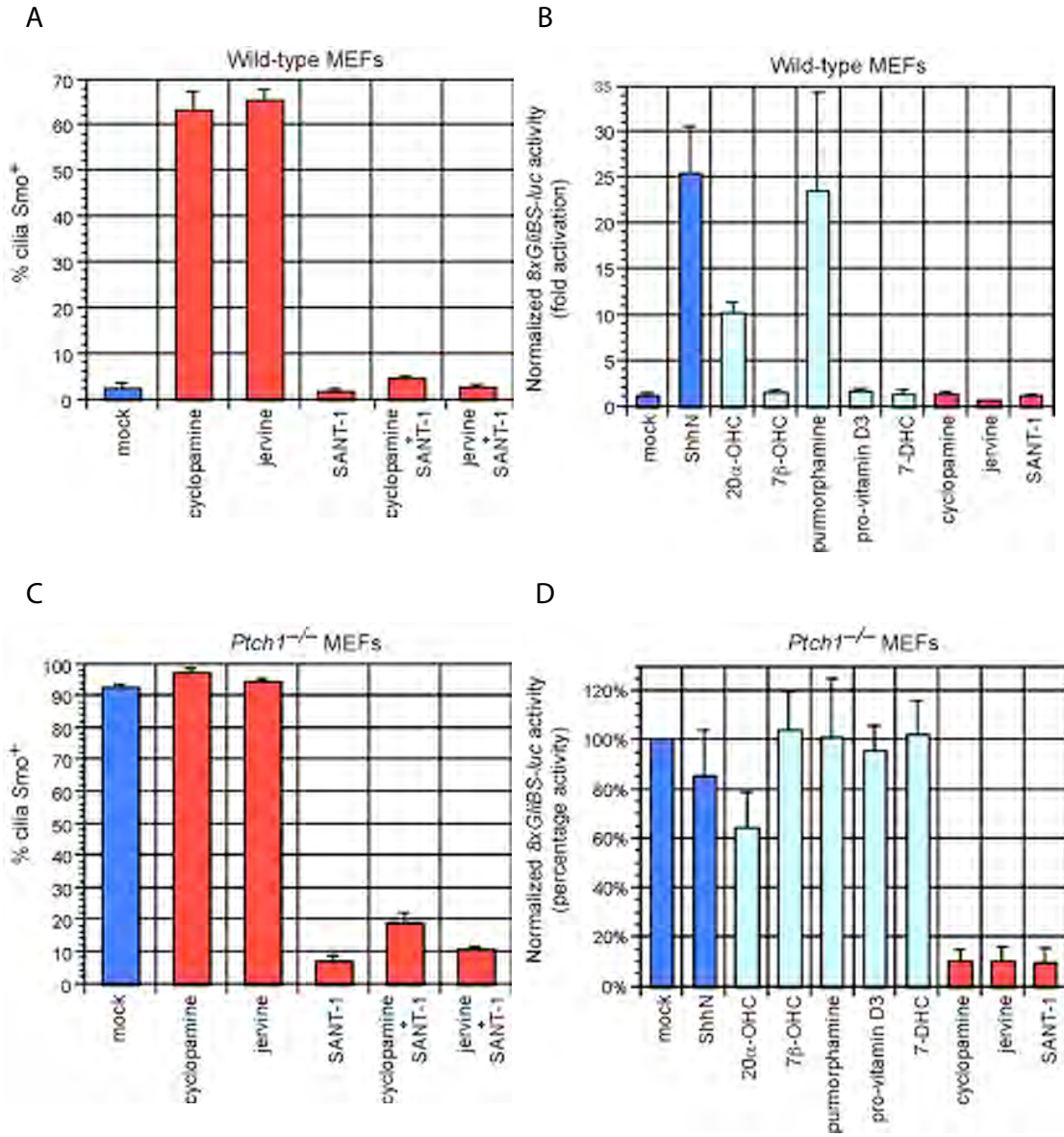
Figure 4-4: SANT-1 dominantly inhibits Smo ciliary translocation in *Ptch1−/−* MEFs
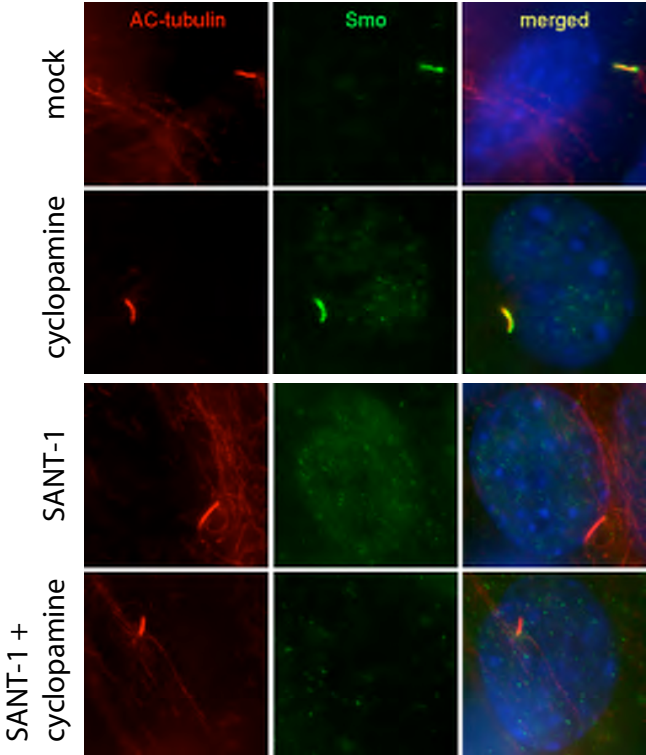
Figure 4-5: Modulation of Gαs and protein kinase A (PKA) causes Smo accumulation in a proximal region of the primary cilium
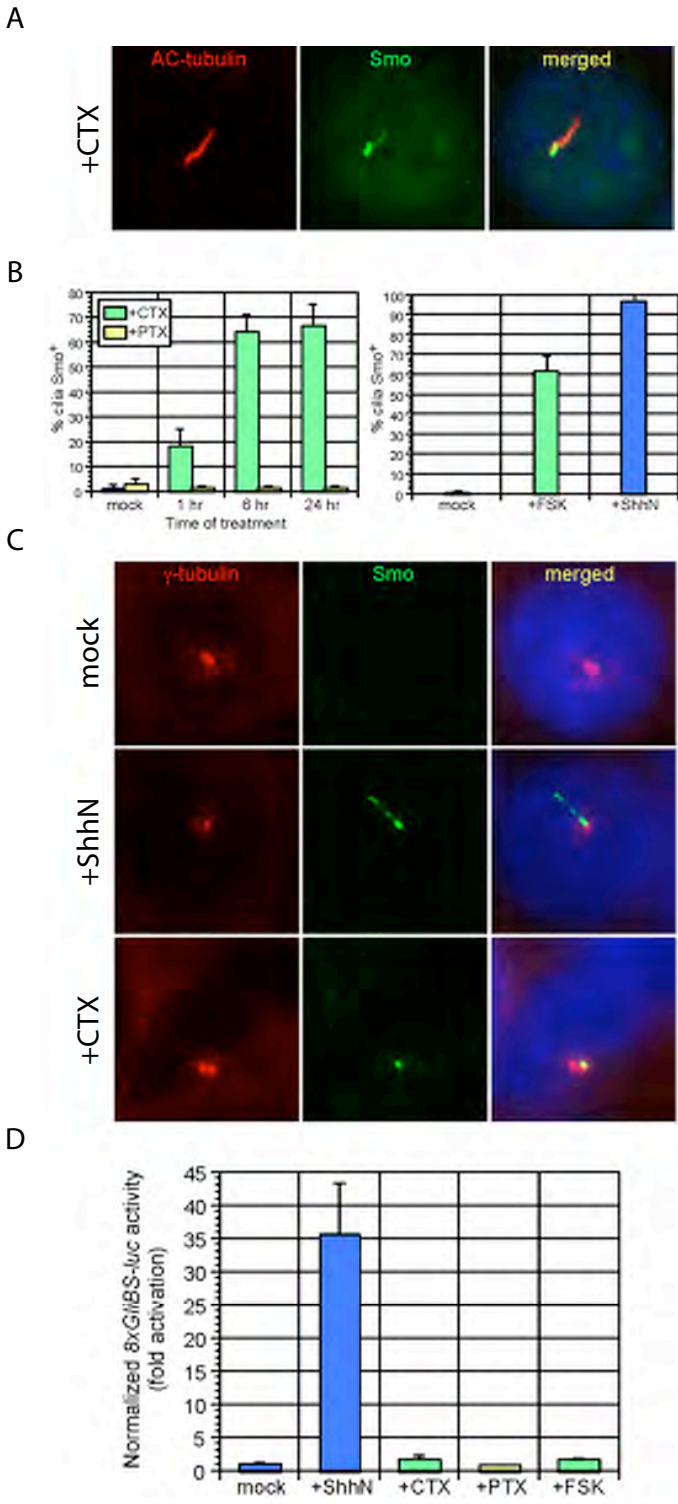
Figure 4-6: ShhN ligand and SANT-1 act dominantly to PKA-induced Smo translocation
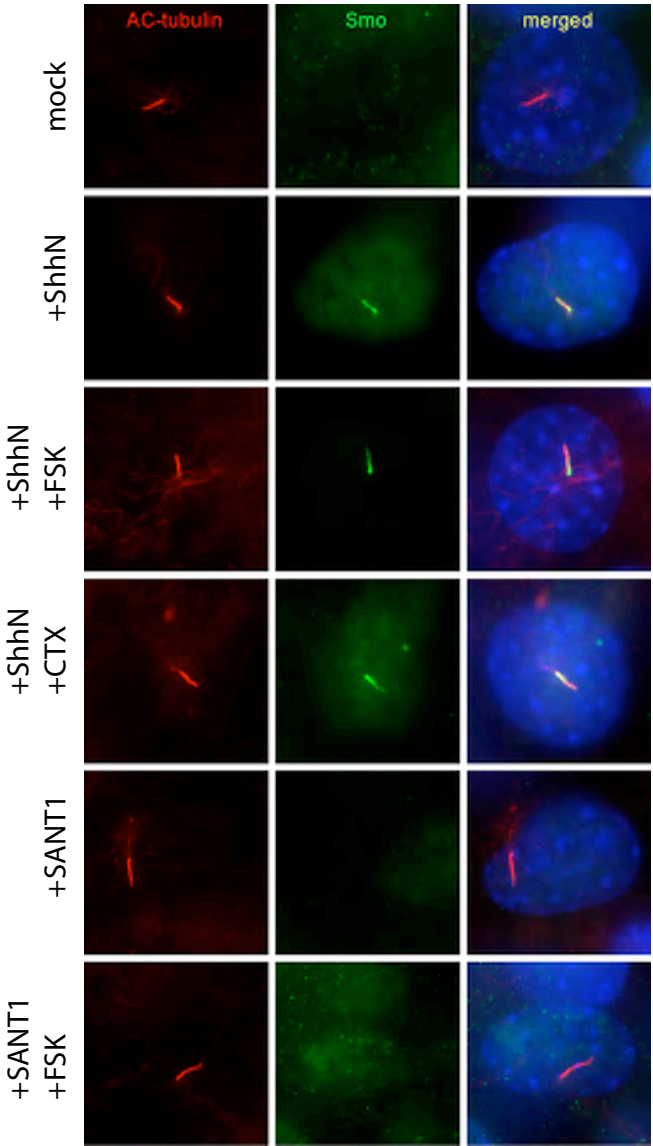
Figure 4-7: Quantification and activity of Gαs/PKA-mediated Smo ciliary translocation
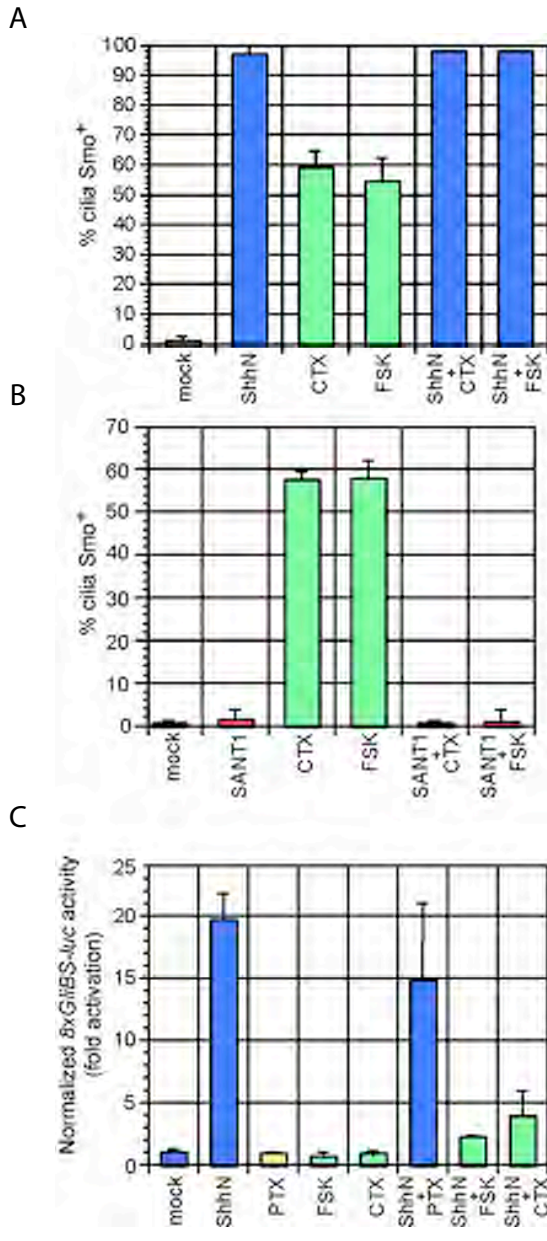
CHAPTER V

Conclusions

Summary

The work presented in Chapters II through IV describes significant progress in our understanding of the mechanisms of Hh signal transduction in mammals, and also sheds light on the poorly understood process of motile cilium construction. In Chapter II, the post-embryonic role for the single mouse ortholog of the *Drosophila* Fu kinase was described. Notably, *Fu/Stk36* plays an essential role in motile ciliogenesis in mice, yet is critical for both Hh signaling and proper formation of 9+2 cilia in Kupffer's vesicle in zebrafish. This finding, along with other recent studies, may force a re-evaluation of the precise biological role of the Fu kinase, and suggests that a common mechanism underlies these two distinct processes. In Chapter III, an evolutionarily conserved role of Sufu was described. In both *Drosophila* and mice, Sufu promotes the stability of Ci in fly, and Gli2 and Gli3 in mice, and thus affects the availability of activator and repressor forms of the Ci/Gli proteins. In both model systems, Sufu antagonizes the activity of HIB/Spop, an adaptor protein for E3 ubiquitin ligases. A potential explanation for the embryonic lethality observed in mouse *Sufu* mutants, but not in fly, is the fact that Gli1 appears to be independent of Spop-promoted degradation. In Chapter IV, data concerning the mechanism of Smo translocation to the primary cilium is described, and indicates that this event requires multiple steps to induce pathway activity. Smo translocation to the primary cilium is therefore necessary, but not sufficient, for activation of Hh signaling. In the following sections, I briefly discuss the broader implications of these findings, with attention to how they may fit in the broader context of evolutionary theory.

191

Gene duplication is proposed to be a mechanism of evolving or partitioning new functions and regulatory modules

Over 40 years ago, Susumu Ohno proposed that whole-genome duplication was a major means for the evolution of novel functions (Ohno et al. 1968; Ohno 1970). After duplication, selective constraints on mutation within the coding or regulatory regions of the two duplicate genes are relaxed, as the presence of two gene copies allows for buffering of potentially deleterious mutations (Ohta 1987). Building on this hypothesis, subsequent groups have hypothesized that three possible events may occur after duplication of a gene. First, one copy of the gene may become silenced through accumulation of degenerative mutations in regulatory or coding regions; this is termed nonfunctionalization (Force et al. 1999; Lynch and Conery 2000). Second, one gene copy may acquire a novel function that is either neutral or beneficial to the organism; this is described as neofunctionalization (Force et al. 1999; Lynch and Conery 2000). Third, neutral or degenerative mutations may develop in each gene copy, so that the total capability of the two derived genes is equivalent to that of the ancestral gene copy; this is termed subfunctionalization (Force et al. 1999; Lynch and Conery 2000). Originally, these models focused on these three events occurring in regulatory regions of genes, but in principle, the concepts could also be applied to mutational events in coding regions (Force et al. 1999; Lynch and Conery 2000). With these complementary sets of mutations, it can also be inferred that gene copies will lose, or potentially gain new protein interacting partners. Thus gene duplication, in combination with a number of

192

possible outcomes following the duplication event, provides one mechanism to create or modify existing protein interaction modules and networks.

A Fused–Kinesin-IV module in Hh signaling and motile ciliogenesis

The fact that most eukaryotes have a single ortholog of the *Drosophila* Fu kinase, with the kinase domain being well-conserved at the amino acid identity level, leads to several interesting hypotheses. Further, the physical interaction between Fu and Cos2 and its vertebrate orthologs is also evolutionarily conserved. This suggests that an ancestral Fu–kinesin-IV protein interaction module may have been present in early eukaryotes, which has subsequently been co-opted into various cellular, and thus developmental processes. With the availability of genome and predicted coding regions for organisms such as *Dictysotelium discoideum*, *Chlamydomonas reinhardtii*, and *Trypanosoma brucei*, and loss-of function studies through mutagenesis or RNAi, it will be interesting to investigate the role of a Fu–kinesin IV complex and its relationship to microtubule-based functions in these single-celled eukaryotes. As these organisms lack an intact Hh signaling network, and many of the associated genes, these may be attractive model systems to study the ancestral function of these proteins. As every reported role of a Fu kinase affects cell polarity or some aspect of a microtubule-derived structure (Oh et al. 2005; Tang et al. 2008), it is tempting to speculate that the ancestral Fu-kinesin-IV complex participated in the assembly or maintenance of a microtubule-based structure such as the microtubule organizing center (MTOC) or centriole/basal body. Notably, fungi, which lack a centriole proper, and utilize spindle pole bodies for cell division, also

lack a recognizable Fu kinase (data not shown). Studies of Fu and ancient kinesin IV proteins in other model metazoans, such as *Strongylocentrus purpuratus*, *Ciona intestinalis*, and *Branchiostoma floridae*, which do possess most of the core components of the Hh signaling pathway as well as flagella or motile cilia, will provide additional insight into the pathways these genes participate in.

A striking aspect of the studies on zebrafish Kif7 described in Chapter II is that it appears to be essential for both Hh transduction and central pair formation. This suggests that the Fu-Kif7 complex in zebrafish has perhaps retained ancestral roles in microtubule regulation, as well as in cytosolic Hh signal transduction. In constrast, *Drosophila* likely utilizes Fu and Cos2 solely for Hh signaling. Few cells in developing or adult *Drosophila* are ciliated, and construction of sperm flagella was reported to be independent of IFT (Han et al. 2003). It is possible that *Drosophila* Fu/Cos2 lost the ability to participate in central pair apparatus formation, but this requires further analysis of these genes and their protein product function in other insects and Ecdysoa.

In mammals, two Cos2 orthologs, Kif7 and Kif27, have been identified. A recent study of *Kif7* knockout mice indicates that *Kif7* functions in Hh transduction, possibly in a manner similar to Cos2 (Cheung et al. 2009; Endoh-Yamagami et al. 2009). *Kif27* and *Fu* are not essential for Hh signaling, but mutants in both genes share a common defect in assembly of central pair microtubules (see Chapter II). Thus, it seems probable that duplication of the ancestral *Cos2/Kif7* gene, followed by subfunctionalization of Hh-dependent and microtubule/central pair-dependent functions, has led to the current

194

situation in mammals, and other tetrapods. This is supported by the ability of Kif27, but not Kif7, to physically associate with Fu protein. Further analysis of *Fu*, *Kif7*, and *Kif27* in other organisms, such as *Xenopus* and chick, is needed to confirm this hypothesis.

Duplication and subfunctionalization of *Gli* genes, combined with evolution of transcriptional feedback loops, contributes to the mouse *Sufu* phenotype

Strikingly, elimination of *Sufu* in mice results in perturbation of Hh signaling and embryonic lethality in mid-gestation (see Chapter III). In contrast, *sufu* mutant fruit flies exhibit no phenotype (Préat 1992). In contrast to Fu, however, the role of Sufu appears to be broadly conserved between insects and mammals. Sufu promotes the stability of Ci, Gli2, and Gli3, through binding to Ci/Gli proteins. This binding event prevents association of the Cul3 E3 ligase adaptor protein Spop with Ci/Gli, an event that results in complete degradation of Ci/Gli.

There are two major differences between Hh transduction in insects and mammals which most likely contribute to the observed mouse phenotype. First, duplication of the ancestral Ci gene in the vertebrate lineage led to the retention of three *Gli* genes in mice. Further subfunctionalization of ancestral Ci function has partitioned activator and repressor functions amongst the three Gli proteins, with Gli3 serving as the major repressor form, and Gli1 and Gli2 providing the bulk of transcriptional activation. The data suggest that Gli1 has also lost the ability to physically interact with Spop (see Chapter III). Thus, the conserved Sufu-Spop interaction circuit is functional only with

195

respect to Gli2 and Gli3, in contrast to action on Ci in *Drosophila*. Future work should include studies of Spop action on Gli proteins in other organisms, such as zebrafish or *Xenopus*, where the mode of Gli action or regulation is likely to have subtle differences (Ruiz i Altaba 1999; Karlstrom et al. 2003).

An additional complexity of mouse *Gli* regulation is the fact that *Gli1*, although not essential for normal mouse embryonic development, is a target of Hh signaling (Bai et al. 2002). This has recently been confirmed through *in vivo* chromatin immunoprecipitation analysis (Vokes et al. 2007; Vokes et al. 2008). Interestingly, Gli3 may repress transcription from the *Gli1* locus. The most likely scenario for the ectopic, ligand-independent Hh pathwy activation in *Sufu* mutant mice is therefore as follows. Loss of Sufu disrupts equilibrium between stabilization of full-length Gli2 and Gli3 (from which both activator and repressor Gli forms are derived) and Spop-mediated degradation. This leads to a drastic reduction of Gli2 and Gli3 activators and repressors. Loss of the Gli3 repressor contributes to constitutive derepression or activation at the *Gli1* locus, resulting in Gli1-dependent transcriptional activation of Hh target genes. This is supported by the data demonstrating that knockdown of *Gli1* in *Sufu* null MEFs drastically reduces Hh reporter activation (see Chapter III). Further genetic confirmation of this hypothesis is needed, and will be provided by analysis of *Sufu*; *Gli1*, *Sufu*; *Gli2*, and *Sufu*; *Gli3* double mutant mice. It is also formally possible that a small amount of Gli2 or Gli3 activator protein is still present, at least for a short period of time prior to degradation, and this is sufficient to induce transcription of *Gli1*.

The *Drosophila* ortholog of Spop, Hib, was demonstrated to be a target of Hh signaling in the developing eye, and it has been hypothesized that Hib functions as part of a negative feedback loop to downregulate the pathway after activation. We have not observed any changes in *Spop* regulation or Spop function in response to Hh ligand (data not shown). However, with the plethora of Hib homologs in the mouse genome, this may also be an area where subfunctionalization of ancestral Hib function contributes to the complexity of Gli regulation, possibly through changes in gene regulatory elements (Huang et al. 2004). Further analysis of the spatiotemporal expression of *Spop* and related genes in the developing mouse embryo is required to answer this question.

Mouse Smoothened activation requires multiple steps involving subcellular trafficking and conformational changes

Mouse, and likely zebrafish Smo, require the primary cilium for full activation of the Hh pathway (Corbit et al. 2005; Aanstad et al. 2009). Interestingly, translocation of Smo to the primary cilium is not sufficient for pathway activation, since inhibition of the pathway with the *Veratrum* alkaloids cyclopamine or jervine counterintuitively causes Smo movement to the cilium (see Chapter IV). This data indicates that Smo may adopt more than one conformation that allows it to move to the cilium, but only a subset of these conformations are competent to communicate Smo activation to the Gli transcription factors. In *Drosophila*, Cos2 is a key scaffold protein that functions as a molecular switch to convert Hh pathway status from "off" to "on". Mouse Kif7 may play this role, but as yet, has not been shown to couple directly to Smo (Varjosalo et al. 2006;

197

Cheung et al. 2009; Endoh-Yamagami et al. 2009). The means of communication between Smo and the mammalian Gli proteins is still mysterious, and is one of the major unsolved questions in mammalian Hh transduction. Identification of proteins that interact with the cytosolic domain of Smo is paramount to understanding this question, as is a subsequent characterization of the protein complexes they form, and the dynamics of trafficking on the cilium. Presumably only activated conformations of Smo are capable to couple to these downstream components. Comparative biochemical and cell biological studies of 'locked' active (such as SmoM2) or inactive (potentially Smo Arg mutants) are necessary to address these questions, and will form the basis of future work aimed at understanding the mechanism of cytosolic transduction of the Hh signal.

MATERIALS AND METHODS

Molecular biology

Standard molecular biology techniques, including molecular cloning, genomic DNA preparation, RNA isolation, PCR, RT-PCR, and Southern analysis were performed as described (Sambrook and Russell 2001; Nagy 2003). Fu-FLAG, Fu-4xFLAG, Fu-mCherry, Kif7-3xmyc, Kif27-3xmyc, Kif27-GFP, SPAG16L-3xHA, and SPAG6-3xHA were cloned into pCAGGS (for immunoprecipitation and immunofluorescence), pCS2+ (for expression in zebrafish), pcDNA3 (for immunoprecipitation and immunofluorescence), or FuPw (for lentiviral expression) vectors. FLAG-mGli1, FLAG-mGli2, and FLAG-hGli3 were previously described (Gerber et al. 2007). Mouse Sufu cDNA was N-terminally tagged with FLAG or Myc. The fly Sufu and Smo cDNAs were gifts from Dr. Jin Jiang. cDNAs encoding zebrafish Sufu and mouse Spop and Ext2 were obtained from Open BioSystems and N- or C-terminally tagged with FLAG or Myc. Gli, Sufu and Spop cDNAs were cloned into pcDNA3 (Invitrogen) for transient overexpression or pBABE-puro for retroviral overexpression. Detailed cloning strategies and maps are available upon request. A dominant negative eGFP-Kif3b construct was a gift from Dr. Andy Peterson and Cul3-Myc construct was from Dr. P. Renee Yew. MyoD-FLAG, FoxC2-FLAG, and *hsp68*-LacZ were gifts from Dr. Brian Black. The zebrafish Smo cDNA was provided by Dr. Monte Westerfield.

Animal husbandry

$Fu^{+/-}$ mice were maintained as described (Chen et al. 2005). Wild-type AB fish were used and raised as described (Westerfield 1995). The *slow muscle omitted/smoothened* allele (Chen et al. 2001) used in this study is *smo*^{hi1640Tg}. A conditional allele of *Sufu* was generated by flanking exons 4-8 with loxP sites using gene targeting (Joyner 2000). A null allele of *Sufu* was subsequently produced by Cre-mediated excision of sequences between the two loxP sites. *Kif3a* mice were obtained from MMRRC (Mutant Mouse Regional Resource Centers); *Ptch1* mice were provided by Dr. Matt Scott (Stanford University); and *Smo* mice were provided by Dr. Andy McMahon (Harvard University). Gli2^{zfd} and Gli3^{xt} mice have been previously described (Hui and Joyner 1993; Mo et al. 1997).

Transmission electron microscopy (TEM)

Mouse tissue was fixed in 3% glutaraldehyde /1% paraformaldehyde /0.1 M sodium cacodylate, pH 7.4 at 4˚C overnight. Fish embryos were fixed in 2% paraformaldehyde /2% glutaradehyde (EM grade) at RT for 2 hr. Standard processing, embedding and sectioning procedures were followed. Samples were examined on a JEOL 100CX or JEM-1230 transmission electron microscope.

Basal foot polarity

The orientation and circular standard deviation (CSD) of basal feet in EM micrographs was calculated as described (Mitchell et al. 2007). Circular statistics were calculated using Oriana 2.0 (Kovachs Computing Services).

Tracheal flow assays

Tracheae from postnatal (p) day 14 wild-type and $Fu^{-/-}$ mice were excised, cleaned of muscle and vasculature, opened longitudinally, and placed in a drop of PBS on a glass slide. 5 ml of a 0.01% solution of Fluospheres (Invitrogen) were added on top of a single trachea to visualize the direction of ciliary flow. Images were acquired using a SPOT 2.3 camera connected to a Nikon E1000 epifluorescence microscope. Images were captured at a rate of 26 frames per second (fps) over a 50 mm by 50 mm area and were saved as .tiff stacks. Movies were examined in NIH Image J using the enhancing feature of the SpotTracker plugin (Daniel Sage and Susan Gasser) to optimize sphere intensity, and the MtrackJ plugin (Erik Meijering, Biomedical Imaging Group, University Medical Center, Rotterdam) to trace the direction and path length of the sphere. Average velocity was taken to be the straight-line distance a particle traveled from its originating point divided by time, and was calculated in Microsoft Excel.

Morpholino (MO) Injections

Wild-type zebrafish embryos were injected with 1.6–4 ng *fu* or 8–12 ng *kif7* or 0.2 ng *ptc1* MO at the one- to two- cell stage. Fluorescein-tagged *fu* MO (4 ng) was injected

into the yolk of 128-cell stage embryos to target dorsal forerunner cells (DFCs). A *p53* morpholino was co-injected with *fu* or *kif7* morpholino at the same concentration to block non-specific cell death (Eisen and Smith 2008). In rescue experiments, 400 pg of mouse *Fu* mRNA was co-injected with *fu* MO. In testing genetic epistasis, 0.2 ng of *ptc1* and 2ng of *fu* MO were co-injected. The *fu* (5' TGGTACTGATCCATCTCCAGCGACG 3'), *kif7* (5' GCCGACTCCTTTTGGAGACATAGCT 3') and *ptc1* MO (5' CATAGTCCAAACGGGAGGCAGAAGA 3') were described previously (Wolff et al. 2003).

Histology and *in situ* hybridization

Histological analysis and section *in situ* hybridization using ^{33}P-labeled riboprobes were performed as described (Chen et al. 2005). Probes for chick, zebrafish and *X. tropicalis Fu* were amplified by PCR using partial or full-length cDNAs (Open Biosystems) as templates. Zebrafish embryos were raised in medium treated with 0.2 mM 1-phenyl-1-2-thiourea to maintain optical transparency. Whole mount *in situ* hybridization was performed as described(Chen and Fishman 1996); probes used were *cmlc2* (*myl7*), *fkd2* (*foxa3*), *fkd4* (*foxa*), *fused*, *shh*, *ptc1*, *spaw*, and *pitx2*.

For the Sufu studies, embryos collected at various developmental stages were fixed in 4% paraformaldehyde at 4°C overnight and processed and embedded in paraffin (Nagy 2003). All the embryos collected were sectioned at 6 μ thickness for histological analysis and *in situ* hybridization (Nagy 2003). Whole mount *in situ* hybridization using

digoxigenin-labeled probes and section *in situ* hybridization using ^{33}P-labeled riboprobes were performed as described (Chen et al. 2004a).

Ciliary beat frequency (CBF) and waveform measurements

Tracheae were dissected out from p10-p14 wild-type and $Fu^{-/-}$ animals, and were cut into rings or strips. Tracheae were washed briefly in PBS and placed in DMEM supplemented with 10% FBS, penicillin-streptomycin and L-glutamate. Tissue was placed in a few drops of medium in a 35 mm glass bottom microwell dish (MatTek). Cilia beating was observed using differential interference contrast (DIC) microscopy on a Nikon TE2000E inverted microscope equipped with Perfect Focus, a 60x water immersion objective, 1.5x zoom adapter and an In Vivo Scientific incubator set at 37˚C and 5% CO_2. A Photometrics Coolsnap HQ2 camera and NIS Elements 2.3 software were used to acquire videos of beating cilia at frame rates of 60-70 fps, depending on the size of the defined region of interest (ROI). CBF was measured by defining an ROI in the upper third of the ciliary shaft, and plotting the changes in pixel intensity over time in the obtained image series. This data was subsequently Fourier transformed in order to obtain the frequency using MatLab. Waveform was analyzed by tracing of cilia from individual movie frames in Adobe Illustrator, or by manual tracking using the MtrackJ plugin (Erik Meijering, Biomedical Imaging Group, University Medical Center, Rotterdam) in NIH ImageJ.

Immunohistochemistry staining

Immunohistochemistry staining using anti-Engrailed (4D9, Developmental Studies Hybridoma Bank) at 1:100 dilution and anti-acetylated tubulin (Sigma, MO) at 1:200 dilution was conducted as described (Wolff et al. 2003). Confocal images were acquired with an LSM510 confocal microscope (Zeiss, Germany).

Fluorescent bead injection

Fluorescent beads diluted 1:100 in 1x PBS were injected into Kupffer's vesicle (KV) at the 8- to 10-somite stage (Shu et al. 2007). Embryos were imaged on a Zeiss Axioplan 2 microscope using a 63x water immersion lens (Zeiss, Germany).

Cell culture, transfections, and immunoprecipitation

For Fu, Kif27 and Spag6/16 immunoprecipitation, HEK 293T cells were maintained in DMEM supplemented with 10% FBS, penicillin-streptomycin, and L-glutamate. Cells were transfected with Lipofectamine 2000 (Invitrogen) according to manufacturer's instructions. 48 hr post-transfection, cells were harvested and lysed in lysis buffer (1% Triton X-100, 150 mM NaCl, 50 mM Tris-Cl pH 7.5, 1 mM EDTA, 0.5 mM PMSF, 2 mg/mL pepstatin A, 10 mg/mL leupeptin, 5 mg/mL aprotinin). Lysates were sheared with a 20-gauge needle and remained on ice for 30 min. Lysates were then

clarified by centrifugation at 20817 x g for 20 min at 4˚C. The supernatant was removed

and bound to 50 ml of anti-FLAG M2 agarose beads (Sigma) for 4 hr at 4˚C with

constant nutation. Beads were washed five times with lysis buffer prior to addition of

sample buffer. Immunoprecipitated proteins were analyzed by 7.5% SDS-PAGE and

transferred to PVDF for immunoblotting. Antibodies used were rabbit anti-FLAG

(Sigma, 1:2000), rabbit anti-myc (Sigma, 1:2000), and rabbit anti-HA (Sigma, 1:1000).

For the Sufu studies, HEK 293T cells and transformed MEF lines were

maintained in DMEM supplemented with 10% fetal bovine serum (Invitrogen),

penicillin/streptomycin (Invitrogen) and L-glutamate (Invitrogen). For protein

expression, cells were transfected with Lipofectamine 2000 (Invitrogen) according to

manufacturer's instructions. 48 hr later, cells were harvested and lysed in RIPA buffer

(50 mM Tris-Cl pH 7.5, 150 mM NaCl, 5 mM EDTA, 1% Triton X-100, 0.1% SDS, 1%

Na deoxycholate, and protease inhibitors). Lysates were sheared with a $26_G x^1/_2$" needle

and 6x Laemmli loading buffer was added. For detecting Gli2 and Gli3 proteins, samples

were resolved on 5% SDS-PAGE gels and transferred to PVDF membranes following

standard procedures (Harlow and Lane 1999). After transfer, membranes were blocked

for 1 hr in TBST (Tris-buffered saline with 0.1% Tween-20) /5% non-fat dry milk at

room temperature and incubated with rabbit anti-Gli2 (1:3000) or rabbit anti-Gli3

(1:1000) antibodies in TBST/3% bovine serum albumin (BSA) overnight at 4ºC. The

membranes were then washed extensively with TBST and incubated with donkey anti-

rabbit HRP (1:3000) for 1 hr at room temperature. For detecting mouse Sufu, FLAG-

Spop, Myc-Spop, FLAG-Ext2, and tubulin, the following primary and secondary

antibodies were used: rabbit anti-Gli3 (1:200), rabbit anti-Myc (Sigma, 1:1000), rabbit anti-FLAG (Sigma, 1:1000), mouse anti-FLAG (Sigma, 1:1000), mouse anti-a tubulin (Sigma, 1:2000), rabbit anti-Sufu (Santa Cruz, 1:500); donkey anti-rabbit HRP (Jackson Laboratories, 1:2000), donkey anti-mouse HRP (Jackson Laboratories, 1:2000). Chemiluminescent detection was performed using ECL Plus detection reagents (Amersham).

For immunoprecipitation, cells were harvested 48 hr post-transfection and lysed in lysis buffer (1% Triton X-100, 150 mM NaCl, 50 mM Tris-Cl pH 7.5, 1 mM EDTA, 0.5 mM PMSF, 2 mg/mL pepstatin A, 10 mg/mL leupeptin, 5 mg/mL aprotinin). Lysates were sheared with a 20-gauge needle and remained on ice for 30 min. Lysates were then clarified by centrifugation at 20817 x g for 20 min at 4˚C. The supernatant was removed and bound to 50 ml of anti-FLAG M2 or anti-HA agarose beads (Sigma) for 4 hr at 4˚C with constant nutation. Beads were washed three times with lysis buffer prior to addition of sample buffer. Immunoprecipitated proteins were analyzed by 7.5% SDS-PAGE and transferred to PVDF for immunoblotting. Antibodies used were rabbit anti-FLAG (Sigma, 1:2000) and rabbit anti-HA (Sigma, 1:1000).

Primary MTEC culture and viral transduction

Primary mouse tracheal epithelial cells (MTECs) were derived from postnatal day 10 to 21 mice and cultured as described (You et al. 2002). Lentivirus was produced by co-transfecting cDNAs cloned into the FuPw vector with pCMVΔ8,9 and pVSV-G into HEK 293T cells as described above. Supernatant was harvested 72-96 hr post-

transfection, filtered through a 0.45m PES membrane syringe filter unit (Nalgene), and
concentrated ten-fold using a Centriprep Ultracel YM-10 device (Millipore). Infection of
MTECs was performed as described (Vladar and Stearns 2007).

Immunofluorescence and microscopy

Cells were fixed in 4% paraformaldehyde for most applications, or in ice-cold
methanol for visualization of basal bodies. Standard procedures were used for
immunostaining. Primary antibodies used were mouse anti-acetylated-a-tubulin (Sigma,
1:2000) and mouse anti-γ tubulin (Sigma, 1:2000). Secondary antibodies and conjugates
used were donkey anti-mouse AlexaFluor 594 (Molecular Probes, 1:2000), donkey anti-
mouse FITC (Molecular Probes, 1:2000), and rhodamine-conjugated phalloidin (Sigma,
1:200). Fluorescent confocal images were acquired using a Nikon TE2000U inverted
microscope with a Yogokawa CSU22 spinning disk confocal (Solamere Technology
Group), a Photometrics Cascade II Camera, and MicroManager software (Vale lab,
University of California-San Francisco). Images were acquired with a 100x oil-
immersion lens and a 1.5x zoom adapter (Nikon) using two laser lines (488 nm and 568
nm). Confocal stacks were collected using a 0.25 mm step size along the *z*-axis. Stacks
were analyzed and *xy*, *xz*, and *yz* projections generated using ImageJ and the
VolumeViewer plugin (Kai Uwe Barthel, Internationale Medieninformatik, Berlin,
Germany). Deconvolution was performed with the Iterative Deconvolve 3D plugin
(Robert Dougherty, OptiNav, Inc.).

For Sufu and Smo studies, confluent MEFs were grown on gelatin-coated glass coverslips (Fisher) and treated with conditioned media or compounds in DMEM supplemented with 0.5% newborn calf serum and penicillin/streptomycin for the indicated times. Cells were washed with PBS, fixed in 4% paraformaldehyde in PBS (Sigma) for 15 min at room temperature, and permeabilized in 0.2% Triton X-100/PBS for 10 min. Alternatively, to better visualize basal bodies, MEFs were fixed in ice-cold methanol for 10 min at $-20°C$. Blocking was performed in 10% sheep serum/0.02%Triton X-100/PBS for 1 hr at room temperature. Cells were stained with the following primary antibodies in 2% sheep serum/0.02% Triton X-100/PBS at 4°C, overnight: rabbit anti-Smo (1:500, (Gerber et al. 2007)), mouse anti-acetylated tubulin (1:2000, Sigma), and mouse anti-γ-tubulin (1:1000, Sigma). Cells were washed three times in 0.02% Triton X-100/PBS and probed with the following secondary antibodies: mouse Alexa 594 (1:2000) and rabbit Alexa 488 (1:2000, Invitrogen). Cells were washed as before, stained with DAPI (1:10,000, Sigma), and mounted in VectaShield (Vector Laboratories, Burlingame, CA).

Ubiquitination assays

HEK 293T cells were transfected with HA-tagged Ub, FLAG-tagged Glis (Gli1, Gli2, or Gli3), Sufu, Spop and Cullin3 using Lipofectamine 2000 (Invitrogen). 40 hr post-transfection, cells were treated with 50 μM MG132 (Sigma). Six hours later, cells were harvested and lysed in 1% SDS lysis buffer (50 mM Tris-HCl pH 7.5, 0.5 mM EDTA, 1% SDS), and boiled for 10 min. Lysates were cleared by centrifugation at 14,000 x g

for 10 min. The supernatant was diluted 10 times with NETN buffer (150 mM NaCl, 5

mM EDTA, 50 mM Tris-HCl pH 7.5, 0.1 % NP 40), and then immunoprecipitated with

mouse anti-FLAG agarose beads (Sigma) at 4°C overnight. The beads were washed with

ice-cold NETN buffer three times and then subjected to immunoblot analysis with mouse

anti-HA antibody.

Standard molecular biology techniques, including molecular cloning, genomic

DNA preparation, RNA isolation, PCR, RT-PCR, and Southern analysis were performed

as described (Ausubel 2001; Sambrook and Russell 2001; Nagy 2003).

Derivation of mouse embryonic fibroblasts (MEFs)

Mouse embryonic fibroblasts (MEFs) were derived from wild-type (wt), $Sufu^{-/-}$,

$Kif3a^{-/-}$, $Ptch1^{-/-}$, $Smo^{-/-}$, $Gli2^{-/-}$, $Gli3^{-/-}$ embryos at 9.5 dpc and cultured in DMEM,

supplemented with 15% fetal bovine serum (FBS), L-glutamine (Invitrogen), non-

essential amino acids (Invitrogen), 1mM sodium pyruvate (Invitrogen), and penicillin G-

streptomycin (Invitrogen). These cells were subsequently immortalized with

recombinant retroviruses encoding the simian virus (SV) 40 large T antigen (Brown et al.

1986).To immortalize MEFs, 2 ml of viral conditioned-medium mixed with polybrene (8

μg/ml) was added to MEFs at ~50% confluence on a 6-cm plate. After 1 hr incubation,

viral conditioned-medium was removed and replaced with fresh medium. Viral infection

210

was repeated several times in 48 hr to achieve maximum infection efficiency. MEFs were subsequently selected by adding G418 (500 μg/ ml) to the medium 24 hr after viral infection was completed. G418-resistant clones which appeared after two weeks of G418 selection were picked and expanded. Immortalized MEFs were maintained in culture medium supplemented with 100-200 μg/ml G418.

Antibody production

Partial mouse cDNAs encoding Smoothened (Smo, a.a. 550–793), Patched 1 (Ptch1, a.a. 1235–1414), Gli2 (a.a. 327-442) and Gli3 (a.a. 395–500) were cloned into pRSET (Invitrogen), pVCH6 or pGEX (Amersham) expression vectors. 6xHis or GST fusion proteins were expressed in BL21 (DE3) pLys bacteria and purified on Ni-NTA (Qiagen) or glutathione sepharose resin (Amersham) according to the manufacturer's instructions. Purified antigen was injected into rabbits (Animal Pharm) for generation of polyclonal antibodies. Antibodies were affinity purified from crude serum using Affigel-10 beads (Biorad) conjugated with Ni-NTA purified 6xHis-antigen fusion proteins. Sufu antibodies (sc-28847) were purchased from Santa Cruz Biotechnology.

Generation and treatment of cell lines

Mouse embryonic fibroblasts (MEFs) were derived from wild-type embryos at embryonic days (E) 9.5 or E10.5, and from $Ptch1^{-/-}$ embryos at E9.5. These cells were subsequently immortalized with recombinant retroviruses encoding the simian virus (SV)

211

40 large T antigen (Brown et al. 1986). MEFs were maintained in DMEM (Cellgro)

supplemented with 10% fetal bovine serum (Cellgro), L-glutamine (Gibco),

penicillin/streptomycin (Gibco), and 200 mg/ml G418 (Gibco). ShhN-conditioned media

(CM) was produced as previously described (Chen et al. 2004a). Briefly, HEK293T cells

were transfected with 10 ug of pcDNA3::ShhN using Lipofectamine 2000 (Invitrogen).

Conditioned media was harvested 48 and 96 hours post-transfection, pooled, filtered

through a 0.22 um PES syringe filter (Millipore), and buffered with 5 mM HEPES, pH

7.5. Compounds used for treatment of MEFs and their concentrations were as follows:

20-a-hydroxysterol (10 mM, Sigma), 7-b-hydroxysterol (10 mM, Sigma), 7-

dehydrocholesterol (10 mM, Sigma), cholecalciferol (pro-vitamin D3, 10 mM, Sigma),

cyclopamine (10 mM, Toronto Research Chemicals), jervine (10 mM, Toronto Research

Chemicals), SANT-1 (10 mM, Calbiochem), cholera toxin (CTX, 100 ng/ml, Sigma),

pertussis toxin (PTX, 100 ng/ml, Calbiochem), forskolin (FSK, 10 mM, Sigma).

Retroviral generation and transduction of stable cell lines

HEK 293T cells were transfected with pCL-ECO (Naviaux et al. 1996) and

pBABE-puro containing Smo or Sufu cDNAs derived from mouse, zebrafish or fly.

Supernatant was collected 72 hr post-transfection, filtered through a 0.45μ syringe filter

(Nalgene) and added to 50% confluent MEFs with 8 μg/mL polybrene (Sigma). Two

days after the addition of retroviral supernatant, MEFs were split 1:10 and selected with

puromycin (2.5 μg/mL). Presence of stable expression was verified by Western blotting

and/or immunofluorescence.

shRNA design, lentiviral design, production, and infection

Short hairpin RNAs (shRNAs) were designed using the pSicOligomaker application (Reynolds et al. 2004). To select shRNA sequences with minimal homology to other mouse transcripts, sequences were compared against the mouse non-Refseq RNA database using BLAST. Oligonucleotides encoding shRNAs were annealed and inserted into the pLentiLox3.7 vector. To create lentiviral supernatants, HEK 293T cells were transfected with the appropriate pLentiLox3.7 vector and the packaging vectors pLP1, pLP2, and pLP/VSV-G using Lipofectamine (Invitrogen). 72 hr post-transfection, supernatants were harvested and filtered through a 0.45μ cellulose acetate filter (Nalgene). Lentivirus was concentrated either 10-fold using a Centriprep Ultracel YM-10 device (Millipore), or 100-fold by ultracentrifugation. MEFs at 50% confluence were infected with concentrated lentivirus supplemented with 8 μg/mL polybrene. Knockdown was verified by Western blotting if appropriate antibodies were available or in other cases knockdown was assessed by extracting RNA using an RNA Midi kit (Qiagen) followed by RT-PCR following standard procedures. The following 19-mer sequences were used for shRNA-mediated knockdown. Mouse Sufu (NM_015752): GAGTTGACGTTTCGTCTGA (nt 540-558); GTAGTGACTTTCTTCCAGA (nt 765-783); GGCGGGGACTGGAGATTAA (nt 1126-1144); GGAGGACTTAGAAGATCTA (nt 1520-1538). Mouse Spop (NM_025287): GACTCAGTTTAACCTTCAA (nt 163-181); GAAAGGGCTAGATGAAGAA (nt 407-425); GTACAAGACTCTGTCAATA (nt 670-696); GAAGCGGTAGGATTTATTT (nt 2615-2633). Mouse Kif3a (NM_008443): GAACTATCACCGTCCATAA (nt 278-296), GGAGAGAGACCCATTTGAA (nt 2070-

2088), GACCGTAATTGATTCTTTA (nt 2226-2244). Mouse Gli1 (NM_010296):

TCGGAGTTCAGTCAAATTA (nt 383-391), ACATGCTCCGTGCCAGATA (nt 1927-

1945), AAGCTCAGCTGGTGTGTAA (nt 2848-66).

Activity assays

MEFs were seeded in 24-well plates at a concentration of 5 x 10^4 cells/ml the day

prior to transfection. Fugene 6 (Roche) was used for transfection of reporter constructs

according to manufacturer's instructions. We transfected a mix of pcDNA3 (Invitrogen)

: 8xGliBS-firefly luciferase [24] : pRL-TK (Promega) or *hsp68*-lacZ with a ratio of 4:5:1.

48 hr post-transfection, media was changed to low serum, and ShhN-CM or compounds

were added for 36-48 hr. Cells were harvested and reporter activity measured using a

Dual Luciferase kit (Promega) and a Luminescent b-galactosidase detection kit II

(Clontech), on an LmaxII 384 luminometer (Molecular Devices).

Immunofluorescence

Cells were fixed in 4% paraformaldehyde for 15 min at room temperature.

Standard procedures for immunostaining were subsequently followed. Primary

antibodies used were: mouse anti-acetylated tubulin (Sigma, 1:2000), mouse anti-FLAG

(Sigma, 1:1000), mouse anti-Myc (Santa Cruz, 1:1000), rabbit anti-Myc (Sigma, 1:1000),

rabbit anti-Smo (1:500); rabbit anti-Gli2 (1:500), rabbit anti-Gli3 (1:500), and rabbit anti-

Sufu (Santa Cruz, 1:100). Secondary antibodies and conjugates used were donkey anti-

214

mouse AlexaFluor 594 (Molecular Probes, 1:2000), donkey anti-rabbit AlexaFluor 488 (Molecular Probes, 1:2000), and DAPI (Sigma, 1:10,000). Fluorescent images were acquired using a SPOT 2.3 camera connected to a Nikon E1000 epifluorescence microscope. Adjustment of RGB histograms and channel merges were performed using Advanced SPOT and NIH Image J. Fluorescent confocal images were acquired using a Nikon TE2000U inverted microscope with a Yogokawa CSU22 spinning disk confocal (Solamere Technology Group), a Photometrics Cascade II Camera, and MicroManager software (Vale lab, University of California-San Francisco). Images were acquired with a 100x oil-immersion lens and a 1.5x zoom adapter (Nikon) using two laser lines (488 nm and 568 nm). Confocal stacks were collected using a 0.25 mm step size along the *z*-axis. Stacks were analyzed and *xy* projections generated using NIH ImageJ. Deconvolution was performed with the Iterative Deconvolve 3D plugin (Robert Dougherty, OptiNav, Inc.).

For Smo studies, images were taken with a Nikon Eclipse E1000 epifluorescence microscope using a Plan Apochromat 100x/1.40 oil objective (Nikon) and a SPOT 2.3 RT Slider cooled CCD camera. Images were acquired using SPOT Advanced software (Diagnostic Instruments), converted to 24 bit (RGB) images, and the RGB histograms were adjusted to reduce background fluorescence.

REFERENCES

Aanstad, P., Santos, N., Corbit, K.C., Scherz, P.J., Trinh le, A., Salvenmoser, W., Huisken, J., Reiter, J.F., and Stainier, D.Y. 2009. The extracellular domain of Smoothened regulates ciliary localization and is required for high-level Hh signaling. *Curr Biol* **19**(12): 1034-1039.

Afzelius, B.A. 2004. Cilia-related diseases. *J Pathol* **204**(4): 470-477.

Akimaru, H., Chen, Y., Dai, P., Hou, D.X., Nonaka, M., Smolik, S.M., Armstrong, S., Goodman, R.H., and Ishii, S. 1997. Drosophila CBP is a co-activator of cubitus interruptus in hedgehog signalling. *Nature* **386**(6626): 735-738.

Allen, J.J., Li, M., Brinkworth, C.S., Paulson, J.L., Wang, D., Hübner, A., Chou, W.H., Davis, R.J., Burlingame, A.L., Messing, R.O., Katayama, C.D., Hedrick, S.M., and Shokat, K.M. 2007. A semisynthetic epitope for kinase substrates. *Nat Methods* **4**(6): 511-516.

Amanai, K. and Jiang, J. 2001. Distinct roles of Central missing and Dispatched in sending the Hedgehog signal. *Development* **128**(24): 5119-5127.

Ascano, M. and Robbins, D.J. 2004. An intramolecular association between two domains of the protein kinase Fused is necessary for Hedgehog signaling. *Mol Cell Biol* **24**(23): 10397-10405.

Ausubel, F.M. 2001. *Current protocols in molecular biology*. J. Wiley, New York.

Aza-Blanc, P., Ramírez-Weber, F.A., Laget, M.P., Schwartz, C., and Kornberg, T.B. 1997. Proteolysis that is inhibited by hedgehog targets Cubitus interruptus protein to the nucleus and converts it to a repressor. *Cell* **89**(7): 1043-1053.

Bai, C.B., Auerbach, W., Lee, J.S., Stephen, D., and Joyner, A.L. 2002. Gli2, but not Gli1, is required for initial Shh signaling and ectopic activation of the Shh pathway. *Development* **129**(20): 4753-4761.

Bai, C.B. and Joyner, A.L. 2001. Gli1 can rescue the in vivo function of Gli2. *Development* **128**(24): 5161-5172.

Bhatia, N., Thiyagarajan, S., Elcheva, I., Saleem, M., Dlugosz, A., Mukhtar, H., and Spiegelman, V.S. 2006. Gli2 is targeted for ubiquitination and degradation by beta-TrCP ubiquitin ligase. *J Biol Chem* **281**(28): 19320-19326.

Bijlsma, M.F., Spek, C.A., Zivkovic, D., van de Water, S., Rezaee, F., and Peppelenbosch, M.P. 2006. Repression of smoothened by patched-dependent (pro-)vitamin D3 secretion. *PLoS Biol* **4**(8): e232.

Brown, M., McCormack, M., Zinn, K.G., Farrell, M.P., Bikel, I., and Livingston, D.M. 1986. A recombinant murine retrovirus for simian virus 40 large T cDNA transforms mouse fibroblasts to anchorage-independent growth. *J Virol* **60**(1): 290-293.

Bumcrot, D.A., Takada, R., and McMahon, A.P. 1995. Proteolytic processing yields two secreted forms of sonic hedgehog. *Mol Cell Biol* **15**(4): 2294-2303.

Burke, R., Nellen, D., Bellotto, M., Hafen, E., Senti, K.A., Dickson, B.J., and Basler, K. 1999. Dispatched, a novel sterol-sensing domain protein dedicated to the release of cholesterol-modified hedgehog from signaling cells. *Cell* **99**(7): 803-815.

Caspary, T., García-García, M.J., Huangfu, D., Eggenschwiler, J.T., Wyler, M.R., Rakeman, A.S., Alcorn, H.L., and Anderson, K.V. 2002. Mouse Dispatched homolog1 is required for long-range, but not juxtacrine, Hh signaling. *Curr Biol* **12**(18): 1628-1632.

Caspary, T., Larkins, C.E., and Anderson, K.V. 2007. The graded response to Sonic Hedgehog depends on cilia architecture. *Dev Cell* **12**(5): 767-778.

Chamoun, Z., Mann, R.K., Nellen, D., von Kessler, D.P., Bellotto, M., Beachy, P.A., and Basler, K. 2001. Skinny hedgehog, an acyltransferase required for palmitoylation and activity of the hedgehog signal. *Science* **293**(5537): 2080-2084.

Chen, J.K., Taipale, J., Cooper, M.K., and Beachy, P.A. 2002a. Inhibition of Hedgehog signaling by direct binding of cyclopamine to Smoothened. *Genes Dev* **16**(21): 2743-2748.

Chen, J.K., Taipale, J., Young, K.E., Maiti, T., and Beachy, P.A. 2002b. Small molecule modulation of Smoothened activity. *Proc Natl Acad Sci USA* **99**(22): 14071-14076.

Chen, J.N. and Fishman, M.C. 1996. Zebrafish tinman homolog demarcates the heart field and initiates myocardial differentiation. *Development* **122**(12): 3809-3816.

Chen, M.H., Gao, N., Kawakami, T., and Chuang, P.T. 2005. Mice deficient in the fused homolog do not exhibit phenotypes indicative of perturbed hedgehog signaling during embryonic development. *Mol Cell Biol* **25**(16): 7042-7053.

Chen, M.H., Li, Y.J., Kawakami, T., Xu, S.M., and Chuang, P.T. 2004a. Palmitoylation is required for the production of a soluble multimeric Hedgehog protein complex and long-range signaling in vertebrates. *Genes Dev* **18**(6): 641-659.

Chen, W., Burgess, S., and Hopkins, N. 2001. Analysis of the zebrafish smoothened mutant reveals conserved and divergent functions of hedgehog activity. *Development* **128**(12): 2385-2396.

Chen, W., Ren, X.R., Nelson, C.D., Barak, L.S., Chen, J.K., Beachy, P.A., de Sauvage, F., and Lefkowitz, R.J. 2004b. Activity-dependent internalization of smoothened mediated by beta-arrestin 2 and GRK2. *Science* **306**(5705): 2257-2260.

Chen, Y., Knezevic, V., Ervin, V., Hutson, R., Ward, Y., and Mackem, S. 2004c. Direct interaction with Hoxd proteins reverses Gli3-repressor function to promote digit formation downstream of Shh. *Development* **131**(10): 2339-2347.

Cheng, S.Y. and Bishop, J.M. 2002. Suppressor of Fused represses Gli-mediated transcription by recruiting the SAP18-mSin3 corepressor complex. *Proc Natl Acad Sci USA* **99**(8): 5442-5447.

Cheung, H.O., Zhang, X., Ribeiro, A., Mo, R., Makino, S., Puviindran, V., Law, K.K., Briscoe, J., and Hui, C.C. 2009. The kinesin protein Kif7 is a critical regulator of Gli transcription factors in mammalian hedgehog signaling. *Sci Signal* **2**(76): ra29.

Chilvers, M.A., Rutman, A., and O'Callaghan, C. 2003a. Ciliary beat pattern is associated with specific ultrastructural defects in primary ciliary dyskinesia. *J Allergy Clin Immunol* **112**(3): 518-524.

-. 2003b. Functional analysis of cilia and ciliated epithelial ultrastructure in healthy children and young adults. *Thorax* **58**(4): 333-338.

Claret, S., Sanial, M., and Plessis, A. 2007. Evidence for a novel feedback loop in the Hedgehog pathway involving Smoothened and Fused. *Curr Biol* **17**(15): 1326-1333.

Codina, J., Hildebrandt, J., Iyengar, R., Birnbaumer, L., Sekura, R.D., and Manclark, C.R. 1983. Pertussis toxin substrate, the putative Ni component of adenylyl cyclases, is an alpha beta heterodimer regulated by guanine nucleotide and magnesium. *Proceedings of the National Academy of Sciences of the United States of America* **80**(14): 4276-4280.

Cooper, A.F., Yu, K.P., Brueckner, M., Brailey, L.L., Johnson, L., McGrath, J.M., and Bale, A.E. 2005. Cardiac and CNS defects in a mouse with targeted disruption of suppressor of fused. *Development* **132**(19): 4407-4417.

Corbit, K.C., Aanstad, P., Singla, V., Norman, A.R., Stainier, D.Y., and Reiter, J.F. 2005. Vertebrate Smoothened functions at the primary cilium. *Nature* **437**(7061): 1018-1021.

Corbit, K.C., Shyer, A.E., Dowdle, W.E., Gaulden, J., Singla, V., Chen, M.H., Chuang, P.T., and Reiter, J.F. 2008. Kif3a constrains beta-catenin-dependent Wnt signalling through dual ciliary and non-ciliary mechanisms. *Nat Cell Biol* **10**(1): 70-76.

Corcoran, R.B. and Scott, M.P. 2006. Oxysterols stimulate Sonic hedgehog signal transduction and proliferation of medulloblastoma cells. *Proc Natl Acad Sci USA* **103**(22): 8408-8413.

Dai, P., Akimaru, H., and Ishii, S. 2003. A hedgehog-responsive region in the Drosophila wing disc is defined by debra-mediated ubiquitination and lysosomal degradation of Ci. *Dev Cell* **4**(6): 917-928.

Dai, P., Akimaru, H., Tanaka, Y., Maekawa, T., Nakafuku, M., and Ishii, S. 1999. Sonic Hedgehog-induced activation of the Gli1 promoter is mediated by GLI3. *J Biol Chem* **274**(12): 8143-8152.

Dai, P., Shinagawa, T., Nomura, T., Harada, J., Kaul, S.C., Wadhwa, R., Khan, M.M., Akimaru, H., Sasaki, H., Colmenares, C., and Ishii, S. 2002. Ski is involved in transcriptional regulation by the repressor and full-length forms of Gli3. *Genes Dev* **16**(22): 2843-2848.

Daoud, F. and Blanchet-Tournier, M.F. 2005. Expression of the human FUSED protein in Drosophila. *Dev Genes Evol* **215**(5): 230-237.

Davenport, J.R. and Yoder, B.K. 2005. An incredible decade for the primary cilium: a look at a once-forgotten organelle. *American journal of physiology* **289**(6): F1159-1169.

Dawe, H.R., Farr, H., and Gull, K. 2007. Centriole/basal body morphogenesis and migration during ciliogenesis in animal cells. *J Cell Sci* **120**(Pt 1): 7-15.

De Rivoyre, M., Ruel, L., Varjosalo, M., Loubat, A., Bidet, M., Therond, P., and Mus-Veteau, I. 2006. Human receptors patched and smoothened partially transduce hedgehog signal when expressed in Drosophila cells. *J Biol Chem* **281**(39): 28584-28595.

DeCamp, D.L., Thompson, T.M., de Sauvage, F.J., and Lerner, M.R. 2000. Smoothened activates Galphai-mediated signaling in frog melanophores. *J Biol Chem* **275**(34): 26322-26327.

Denef, N., Neubüser, D., Perez, L., and Cohen, S.M. 2000. Hedgehog induces opposite changes in turnover and subcellular localization of patched and smoothened. *Cell* **102**(4): 521-531.

Di Marcotullio, L., Ferretti, E., Greco, A., De Smaele, E., Po, A., Sico, M.A., Alimandi, M., Giannini, G., Maroder, M., Screpanti, I., and Gulino, A. 2006. Numb is a suppressor of Hedgehog signalling and targets Gli1 for Itch-dependent ubiquitination. *Nat Cell Biol* **8**(12): 1415-1423.

Di Marcotullio, L., Ferretti, E., Greco, A., De Smaele, E., Screpanti, I., and Gulino, A. 2007. Multiple ubiquitin-dependent processing pathways regulate hedgehog/gli signaling: implications for cell development and tumorigenesis. *Cell cycle (Georgetown, Tex* **6**(4): 390-393.

Ding, Q., Fukami, S., Meng, X., Nishizaki, Y., Zhang, X., Sasaki, H., Dlugosz, A., Nakafuku, M., and Hui, C. 1999. Mouse suppressor of fused is a negative regulator of

222

sonic hedgehog signaling and alters the subcellular distribution of Gli1. *Curr Biol* **9**(19): 1119-1122.

Dutcher, S.K., Huang, B., and Luck, D.J. 1984. Genetic dissection of the central pair microtubules of the flagella of Chlamydomonas reinhardtii. *J Cell Biol* **98**(1): 229-236.

Eggenschwiler, J.T. and Anderson, K.V. 2007. Cilia and developmental signaling. *Annu Rev Cell Dev Biol* **23**: 345-373.

Eggenschwiler, J.T., Bulgakov, O.V., Qin, J., Li, T., and Anderson, K.V. 2006. Mouse Rab23 regulates hedgehog signaling from smoothened to Gli proteins. *Dev Biol* **290**(1): 1-12.

Eisen, J.S. and Smith, J.C. 2008. Controlling morpholino experiments: don't stop making antisense. *Development* **135**(10): 1735-1743.

Elzi, D.J., Bjornsen, A.J., MacKenzie, T., Wyman, T.H., and Silliman, C.C. 2001. Ionomycin causes activation of p38 and p42/44 mitogen-activated protein kinases in human neutrophils. *Am J Physiol, Cell Physiol* **281**(1): C350-360.

Endoh-Yamagami, S., Evangelista, M., Wilson, D., Wen, X., Theunissen, J.W., Phamluong, K., Davis, M., Scales, S.J., Solloway, M.J., de Sauvage, F.J., and Peterson, A.S. 2009. The Mammalian Cos2 Homolog Kif7 Plays an Essential Role in Modulating Hh Signal Transduction during Development. *Curr Biol*.

Epstein, D.J., Marti, E., Scott, M.P., and McMahon, A.P. 1996. Antagonizing cAMP-dependent protein kinase A in the dorsal CNS activates a conserved Sonic hedgehog signaling pathway. *Development* **122**(9): 2885-2894.

Evangelista, M., Lim, T.Y., Lee, J., Parker, L., Ashique, A., Peterson, A.S., Ye, W., Davis, D.P., and de Sauvage, F.J. 2008. Kinome siRNA screen identifies regulators of ciliogenesis and hedgehog signal transduction. *Science signaling* **1**(39): ra7.

Fan, C.M., Porter, J.A., Chiang, C., Chang, D.T., Beachy, P.A., and Tessier-Lavigne, M. 1995. Long-range sclerotome induction by sonic hedgehog: direct role of the amino-terminal cleavage product and modulation by the cyclic AMP signaling pathway. *Cell* **81**(3): 457-465.

Fan, J. and Beck, K.A. 2004. A role for the spectrin superfamily member Syne-1 and kinesin II in cytokinesis. *J Cell Sci* **117**(Pt 4): 619-629.

Farzan, S.F., Ascano, M., Ogden, S.K., Sanial, M., Brigui, A., Plessis, A., and Robbins, D.J. 2008. Costal2 Functions as a Kinesin-like Protein in the Hedgehog Signal Transduction Pathway. *Curr Biol* **18**(16): 1215-1220.

Force, A., Lynch, M., Pickett, F.B., Amores, A., Yan, Y.L., and Postlethwait, J. 1999. Preservation of duplicate genes by complementary, degenerative mutations. *Genetics* **151**(4): 1531-1545.

Frisch, D. and Farbman, A.I. 1968. Development of order during ciliogenesis. *The Anatomical record* **162**(2): 221-232.

Gerber, A.N., Wilson, C.W., Li, Y.J., and Chuang, P.T. 2007. The hedgehog regulated oncogenes Gli1 and Gli2 block myoblast differentiation by inhibiting MyoD-mediated transcriptional activation. *Oncogene* **26**(8): 1122-1136.

Gerdes, J.M., Liu, Y., Zaghloul, N.A., Leitch, C.C., Lawson, S.S., Kato, M., Beachy, P.A., Beales, P.L., DeMartino, G.N., Fisher, S., Badano, J.L., and Katsanis, N. 2007.

224

Disruption of the basal body compromises proteasomal function and perturbs intracellular Wnt response. *Nat Genet* **39**(11): 1350-1360.

Gill, D.M. and Meren, R. 1978. ADP-ribosylation of membrane proteins catalyzed by cholera toxin: basis of the activation of adenylate cyclase. *Proc Natl Acad Sci USA* **75**(7): 3050-3054.

Goodrich, L.V., Milenkovic, L., Higgins, K.M., and Scott, M.P. 1997. Altered neural cell fates and medulloblastoma in mouse patched mutants. *Science* **277**(5329): 1109-1113.

Hammerschmidt, M., Bitgood, M.J., and McMahon, A.P. 1996. Protein kinase A is a common negative regulator of Hedgehog signaling in the vertebrate embryo. *Genes Dev* **10**(6): 647-658.

Han, Y.G., Kwok, B.H., and Kernan, M.J. 2003. Intraflagellar transport is required in Drosophila to differentiate sensory cilia but not sperm. *Curr Biol* **13**(19): 1679-1686.

Harlow, E. and Lane, D. 1999. *Using antibodies : a laboratory manual*. Cold Spring Harbor Laboratory Press, Cold Spring Harbor, N.Y.

Haycraft, C.J., Banizs, B., Aydin-Son, Y., Zhang, Q., Michaud, E.J., and Yoder, B.K. 2005. Gli2 and Gli3 localize to cilia and require the intraflagellar transport protein polaris for processing and function. *PLoS Genet* **1**(4): e53.

Hernandez-Munoz, I., Lund, A.H., van der Stoop, P., Boutsma, E., Muijrers, I., Verhoeven, E., Nusinow, D.A., Panning, B., Marahrens, Y., and van Lohuizen, M. 2005. Stable X chromosome inactivation involves the PRC1 Polycomb complex and requires histone MACROH2A1 and the CULLIN3/SPOP ubiquitin E3 ligase. *Proc Natl Acad Sci U S A* **102**(21): 7635-7640.

Hino, K., Satou, Y., Yagi, K., and Satoh, N. 2003. A genomewide survey of developmentally relevant genes in Ciona intestinalis. VI. Genes for Wnt, TGFbeta, Hedgehog and JAK/STAT signaling pathways. *Dev Genes Evol* **213**(5-6): 264-272.

Hooper, J.E. and Scott, M.P. 2005. Communicating with Hedgehogs. *Nat Rev Mol Cell Biol* **6**(4): 306-317.

Hu, M.C., Mo, R., Bhella, S., Wilson, C.W., Chuang, P.T., Hui, C.C., and Rosenblum, N.D. 2006. GLI3-dependent transcriptional repression of Gli1, Gli2 and kidney patterning genes disrupts renal morphogenesis. *Development* **133**(3): 569-578.

Huang, C.J., Chen, C.Y., Chen, H.H., Tsai, S.F., and Choo, K.B. 2004. TDPOZ, a family of bipartite animal and plant proteins that contain the TRAF (TD) and POZ/BTB domains. *Gene* **324**: 117-127.

Huangfu, D. and Anderson, K.V. 2005. Cilia and Hedgehog responsiveness in the mouse. *Proceedings of the National Academy of Sciences of the United States of America* **102**(32): 11325-11330.

-. 2006. Signaling from Smo to Ci/Gli: conservation and divergence of Hedgehog pathways from Drosophila to vertebrates. *Development* **133**(1): 3-14.

Huangfu, D., Liu, A., Rakeman, A.S., Murcia, N.S., Niswander, L., and Anderson, K.V. 2003. Hedgehog signalling in the mouse requires intraflagellar transport proteins. *Nature* **426**(6962): 83-87.

Hui, C.C. and Joyner, A.L. 1993. A mouse model of greig cephalopolysyndactyly syndrome: the extra-toesJ mutation contains an intragenic deletion of the Gli3 gene. *Nat Genet* **3**(3): 241-246.

Hui, C.C., Slusarski, D., Platt, K.A., Holmgren, R., and Joyner, A.L. 1994. Expression of three mouse homologs of the Drosophila segment polarity gene cubitus interruptus, Gli, Gli-2, and Gli-3, in ectoderm- and mesoderm-derived tissues suggests multiple roles during postimplantation development. *Dev Biol* **162**(2): 402-413.

Huntzicker, E.G., Estay, I.S., Zhen, H., Lokteva, L.A., Jackson, P.K., and Oro, A.E. 2006. Dual degradation signals control Gli protein stability and tumor formation. *Genes Dev* **20**(3): 276-281.

Jia, J. and Jiang, J. 2006. Decoding the Hedgehog signal in animal development. *Cell Mol Life Sci* **63**(11): 1249-1265.

Jia, J., Kolterud, A., Zeng, H., Hoover, A., Teglund, S., Toftgard, R., and Liu, A. 2009. Suppressor of Fused inhibits mammalian Hedgehog signaling in the absence of cilia. *Dev Biol* **330**(2): 452-460.

Jia, J., Tong, C., and Jiang, J. 2003. Smoothened transduces Hedgehog signal by physically interacting with Costal2/Fused complex through its C-terminal tail. *Genes Dev* **17**(21): 2709-2720.

Jiang, J. and Hui, C.C. 2008. Hedgehog signaling in development and cancer. *Dev Cell* **15**(6): 801-812.

Joyner, A.L. 2000. *Gene targeting : a practical approach*. Oxford University Press, Oxford ; New York.

Kaesler, S., Luscher, B., and Ruther, U. 2000. Transcriptional activity of GLI1 is negatively regulated by protein kinase A. *Biological chemistry* **381**(7): 545-551.

Kalderon, D. 2002. Similarities between the Hedgehog and Wnt signaling pathways. *Trends Cell Biol* **12**(11): 523-531.

Karlstrom, R.O., Talbot, W.S., and Schier, A.F. 1999. Comparative synteny cloning of zebrafish you-too: mutations in the Hedgehog target gli2 affect ventral forebrain patterning. *Genes Dev* **13**(4): 388-393.

Karlstrom, R.O., Tyurina, O.V., Kawakami, A., Nishioka, N., Talbot, W.S., Sasaki, H., and Schier, A.F. 2003. Genetic analysis of zebrafish gli1 and gli2 reveals divergent requirements for gli genes in vertebrate development. *Development* **130**(8): 1549-1564.

Katoh, Y. and Katoh, M. 2004a. Characterization of KIF7 gene in silico. *International journal of oncology* **25**(6): 1881-1886.

-. 2004b. KIF27 is one of orthologs for Drosophila Costal-2. *International journal of oncology* **25**(6): 1875-1880.

Kawakami, T., Kawcak, T., Li, Y.J., Zhang, W., Hu, Y., and Chuang, P.T. 2002. Mouse dispatched mutants fail to distribute hedgehog proteins and are defective in hedgehog signaling. *Development* **129**(24): 5753-5765.

Ke, Z., Emelyanov, A., Lim, S.E., Korzh, V., and Gong, Z. 2005. Expression of a novel zebrafish zinc finger gene, gli2b, is affected in Hedgehog and Notch signaling related mutants during embryonic development. *Dev Dyn* **232**(2): 479-486.

Ke, Z., Kondrichin, I., Gong, Z., and Korzh, V. 2008. Combined activity of the two Gli2 genes of zebrafish play a major role in Hedgehog signaling during zebrafish neurodevelopment. *Molecular and cellular neurosciences* **37**(2): 388-401.

Kent, D., Bush, E.W., and Hooper, J.E. 2006. Roadkill attenuates Hedgehog responses through degradation of Cubitus interruptus. *Development* **133**(10): 2001-2010.

King, N., Westbrook, M.J., Young, S.L., Kuo, A., Abedin, M., Chapman, J., Fairclough, S., Hellsten, U., Isogai, Y., Letunic, I., Marr, M., Pincus, D., Putnam, N., Rokas, A.,

Wright, K.J., Zuzow, R., Dirks, W., Good, M., Goodstein, D., Lemons, D., Li, W., Lyons, J.B., Morris, A., Nichols, S., Richter, D.J., Salamov, A., Sequencing, J.G., Bork, P., Lim, W.A., Manning, G., Miller, W.T., McGinnis, W., Shapiro, H., Tjian, R., Grigoriev, I.V., and Rokhsar, D. 2008. The genome of the choanoflagellate Monosiga brevicollis and the origin of metazoans. *Nature* **451**(7180): 783-788.

Kodadek, T., Sikder, D., and Nalley, K. 2006. Keeping transcriptional activators under control. *Cell* **127**(2): 261-264.

Kogerman, P., Grimm, T., Kogerman, L., Krause, D., Undén, A.B., Sandstedt, B., Toftgård, R., and Zaphiropoulos, P.G. 1999. Mammalian suppressor-of-fused modulates nuclear-cytoplasmic shuttling of Gli-1. *Nat Cell Biol* **1**(5): 312-319.

Koide, T., Hayata, T., and Cho, K.W. 2006. Negative regulation of Hedgehog signaling by the cholesterogenic enzyme 7-dehydrocholesterol reductase. *Development* **133**(12): 2395-2405.

Kovacs, J.J., Whalen, E.J., Liu, R., Xiao, K., Kim, J., Chen, M., Wang, J., Chen, W., and Lefkowitz, R.J. 2008. Beta-arrestin-mediated localization of smoothened to the primary cilium. *Science* **320**(5884): 1777-1781.

Kramer-Zucker, A.G., Olale, F., Haycraft, C.J., Yoder, B.K., Schier, A.F., and Drummond, I.A. 2005. Cilia-driven fluid flow in the zebrafish pronephros, brain and Kupffer's vesicle is required for normal organogenesis. *Development* **132**(8): 1907-1921.

Kwon, J.E., La, M., Oh, K.H., Oh, Y.M., Kim, G.R., Seol, J.H., Baek, S.H., Chiba, T., Tanaka, K., Bang, O.S., Joe, C.O., and Chung, C.H. 2006. BTB domain-containing speckle-type POZ protein (SPOP) serves as an adaptor of Daxx for ubiquitination by Cul3-based ubiquitin ligase. *J Biol Chem* **281**(18): 12664-12672.

229

Lee, J., Platt, K.A., Censullo, P., and Ruiz i Altaba, A. 1997. Gli1 is a target of Sonic hedgehog that induces ventral neural tube development. *Development* **124**(13): 2537-2552.

Lee, J.J., Ekker, S.C., von Kessler, D.P., Porter, J.A., Sun, B.I., and Beachy, P.A. 1994. Autoproteolysis in hedgehog protein biogenesis. *Science* **266**(5190): 1528-1537.

Lefers, M.A., Wang, Q.T., and Holmgren, R.A. 2001. Genetic dissection of the Drosophila Cubitus interruptus signaling complex. *Dev Biol* **236**(2): 411-420.

Liu, A., Wang, B., and Niswander, L.A. 2005. Mouse intraflagellar transport proteins regulate both the activator and repressor functions of Gli transcription factors. *Development* **132**(13): 3103-3111.

Long, S., Ahmad, N., and Rebagliati, M. 2003. The zebrafish nodal-related gene southpaw is required for visceral and diencephalic left-right asymmetry. *Development* **130**(11): 2303-2316.

Low, W.C., Wang, C., Pan, Y., Huang, X.Y., Chen, J.K., and Wang, B. 2008. The decoupling of Smoothened from Galphai proteins has little effect on Gli3 protein processing and Hedgehog-regulated chick neural tube patterning. *Dev Biol* **321**(1): 188-196.

Lu, X., Liu, S., and Kornberg, T.B. 2006. The C-terminal tail of the Hedgehog receptor Patched regulates both localization and turnover. *Genes Dev* **20**(18): 2539-2551.

Lum, L., Yao, S., Mozer, B., Rovescalli, A., Von Kessler, D., Nirenberg, M., and Beachy, P.A. 2003a. Identification of Hedgehog pathway components by RNAi in Drosophila cultured cells. *Science* **299**(5615): 2039-2045.

Lum, L., Zhang, C., Oh, S., Mann, R.K., von Kessler, D.P., Taipale, J., Weis-Garcia, F., Gong, R., Wang, B., and Beachy, P.A. 2003b. Hedgehog signal transduction via Smoothened association with a cytoplasmic complex scaffolded by the atypical kinesin, Costal-2. *Mol Cell* **12**(5): 1261-1274.

Lunt, S.C., Haynes, T., and Perkins, B.D. 2009. Zebrafish ift57, ift88, and ift172 intraflagellar transport mutants disrupt cilia but do not affect hedgehog signaling. *Dev Dyn* **238**(7): 1744-1759.

Lynch, M. and Conery, J.S. 2000. The evolutionary fate and consequences of duplicate genes. *Science* **290**(5494): 1151-1155.

Ma, Y., Erkner, A., Gong, R., Yao, S., Taipale, J., Basler, K., and Beachy, P.A. 2002. Hedgehog-mediated patterning of the mammalian embryo requires transporter-like function of dispatched. *Cell* **111**(1): 63-75.

Malpel, S., Claret, S., Sanial, M., Brigui, A., Piolot, T., Daviet, L., Martin-Lannerée, S., and Plessis, A. 2007. The last 59 amino acids of Smoothened cytoplasmic tail directly bind the protein kinase Fused and negatively regulate the Hedgehog pathway. *Dev Biol* **303**(1): 121-133.

Mao, J., Wang, J., Liu, B., Pan, W., Farr, G.H., 3rd, Flynn, C., Yuan, H., Takada, S., Kimelman, D., Li, L., and Wu, D. 2001. Low-density lipoprotein receptor-related protein-5 binds to Axin and regulates the canonical Wnt signaling pathway. *Mol Cell* **7**(4): 801-809.

Marigo, V., Johnson, R.L., Vortkamp, A., and Tabin, C.J. 1996. Sonic hedgehog differentially regulates expression of GLI and GLI3 during limb development. *Dev Biol* **180**(1): 273-283.

Marshall, W.F. 2008. The cell biological basis of ciliary disease. *J Cell Biol* **180**(1): 17-21.

Marshall, W.F. and Kintner, C. 2008. Cilia orientation and the fluid mechanics of development. *Curr Opin Cell Biol* **20**(1): 48-52.

Marshall, W.F. and Nonaka, S. 2006. Cilia: tuning in to the cell's antenna. *Curr Biol* **16**(15): R604-614.

Marszalek, J.R., Ruiz-Lozano, P., Roberts, E., Chien, K.R., and Goldstein, L.S. 1999. Situs inversus and embryonic ciliary morphogenesis defects in mouse mutants lacking the KIF3A subunit of kinesin-II. *Proceedings of the National Academy of Sciences of the United States of America* **96**(9): 5043-5048.

Matise, M.P., Epstein, D.J., Park, H.L., Platt, K.A., and Joyner, A.L. 1998. Gli2 is required for induction of floor plate and adjacent cells, but not most ventral neurons in the mouse central nervous system. *Development* **125**(15): 2759-2770.

May, S.R., Ashique, A.M., Karlen, M., Wang, B., Shen, Y., Zarbalis, K., Reiter, J., Ericson, J., and Peterson, A.S. 2005. Loss of the retrograde motor for IFT disrupts localization of Smo to cilia and prevents the expression of both activator and repressor functions of Gli. *Dev Biol* **287**(2): 378-389.

McKean, P.G., Baines, A., Vaughan, S., and Gull, K. 2003. Gamma-tubulin functions in the nucleation of a discrete subset of microtubules in the eukaryotic flagellum. *Curr Biol* **13**(7): 598-602.

McMahon, A.P., Ingham, P.W., and Tabin, C.J. 2003. Developmental roles and clinical significance of hedgehog signaling. *Current topics in developmental biology* **53**: 1-114.

Meloni, A.R., Fralish, G.B., Kelly, P., Salahpour, A., Chen, J.K., Wechsler-Reya, R.J., Lefkowitz, R.J., and Caron, M.G. 2006. Smoothened signal transduction is promoted by G protein-coupled receptor kinase 2. *Mol Cell Biol* **26**(20): 7550-7560.

Merchant, M., Evangelista, M., Luoh, S.M., Frantz, G.D., Chalasani, S., Carano, R.A., van Hoy, M., Ramirez, J., Ogasawara, A.K., McFarland, L.M., Filvaroff, E.H., French, D.M., and de Sauvage, F.J. 2005. Loss of the serine/threonine kinase fused results in postnatal growth defects and lethality due to progressive hydrocephalus. *Mol Cell Biol* **25**(16): 7054-7068.

Merchant, M., Vajdos, F.F., Ultsch, M., Maun, H.R., Wendt, U., Cannon, J., Desmarais, W., Lazarus, R.A., de Vos, A.M., and de Sauvage, F.J. 2004. Suppressor of fused regulates Gli activity through a dual binding mechanism. *Mol Cell Biol* **24**(19): 8627-8641.

Methot, N. and Basler, K. 1999. Hedgehog controls limb development by regulating the activities of distinct transcriptional activator and repressor forms of Cubitus interruptus. *Cell* **96**(6): 819-831.

-. 2001. An absolute requirement for Cubitus interruptus in Hedgehog signaling. *Development* **128**(5): 733-742.

Méthot, N. and Basler, K. 2000. Suppressor of fused opposes hedgehog signal transduction by impeding nuclear accumulation of the activator form of Cubitus interruptus. *Development* **127**(18): 4001-4010.

Miki, H., Okada, Y., and Hirokawa, N. 2005. Analysis of the kinesin superfamily: insights into structure and function. *Trends Cell Biol* **15**(9): 467-476.

Mitchell, B., Jacobs, R., Li, J., Chien, S., and Kintner, C. 2007. A positive feedback mechanism governs the polarity and motion of motile cilia. *Nature* **447**(7140): 97-101.

Mo, R., Freer, A.M., Zinyk, D.L., Crackower, M.A., Michaud, J., Heng, H.H., Chik, K.W., Shi, X.M., Tsui, L.C., Cheng, S.H., Joyner, A.L., and Hui, C. 1997. Specific and redundant functions of Gli2 and Gli3 zinc finger genes in skeletal patterning and development. *Development* **124**(1): 113-123.

Monnier, V., Dussillol, F., Alves, G., Lamour-Isnard, C., and Plessis, A. 1998. Suppressor of fused links fused and Cubitus interruptus on the hedgehog signalling pathway. *Curr Biol* **8**(10): 583-586.

Motoyama, J., Liu, J., Mo, R., Ding, Q., Post, M., and Hui, C.C. 1998. Essential function of Gli2 and Gli3 in the formation of lung, trachea and oesophagus. *Nat Genet* **20**(1): 54-57.

Motoyama, J., Milenkovic, L., Iwama, M., Shikata, Y., Scott, M.P., and Hui, C.C. 2003. Differential requirement for Gli2 and Gli3 in ventral neural cell fate specification. *Dev Biol* **259**(1): 150-161.

Muratani, M. and Tansey, W.P. 2003. How the ubiquitin-proteasome system controls transcription. *Nat Rev Mol Cell Biol* **4**(3): 192-201.

Murone, M., Luoh, S.M., Stone, D., Li, W., Gurney, A., Armanini, M., Grey, C., Rosenthal, A., and de Sauvage, F.J. 2000. Gli regulation by the opposing activities of fused and suppressor of fused. *Nat Cell Biol* **2**(5): 310-312.

Nagai, Y., Kojima, T., Muro, Y., Hachiya, T., Nishizawa, Y., Wakabayashi, T., and Hagiwara, M. 1997. Identification of a novel nuclear speckle-type protein, SPOP. *FEBS Lett* **418**(1-2): 23-26.

Nagy, A. 2003. *Manipulating the mouse embryo : a laboratory manual*. Cold Spring Harbor Laboratory Press, Cold Spring Harbor, N.Y.

Naviaux, R.K., Costanzi, E., Haas, M., and Verma, I.M. 1996. The pCL vector system: rapid production of helper-free, high-titer, recombinant retroviruses. *J Virol* **70**(8): 5701-5705.

Nusse, R. 2003. Wnts and Hedgehogs: lipid-modified proteins and similarities in signaling mechanisms at the cell surface. *Development* **130**(22): 5297-5305.

Nusslein-Volhard, C. and Wieschaus, E. 1980. Mutations affecting segment number and polarity in Drosophila. *Nature* **287**(5785): 795-801.

Ocbina, P.J. and Anderson, K.V. 2008. Intraflagellar transport, cilia, and mammalian Hedgehog signaling: analysis in mouse embryonic fibroblasts. *Dev Dyn* **237**(8): 2030-2038.

Odenthal, J. and Nüsslein-Volhard, C. 1998. fork head domain genes in zebrafish. *Dev Genes Evol* **208**(5): 245-258.

Odenthal, J., van Eeden, F.J., Haffter, P., Ingham, P.W., and Nüsslein-Volhard, C. 2000. Two distinct cell populations in the floor plate of the zebrafish are induced by different pathways. *Dev Biol* **219**(2): 350-363.

Ogden, S.K., Ascano, M., Stegman, M.A., Suber, L.M., Hooper, J.E., and Robbins, D.J. 2003. Identification of a functional interaction between the transmembrane protein Smoothened and the kinesin-related protein Costal2. *Curr Biol* **13**(22): 1998-2003.

Ogden, S.K., Fei, D.L., Schilling, N.S., Ahmed, Y.F., Hwa, J., and Robbins, D.J. 2008. G protein Galpha(i) functions immediately downstream of Smoothened in Hedgehog signalling. *Nature*.

Oh, S.A., Johnson, A., Smertenko, A., Rahman, D., Park, S.K., Hussey, P.J., and Twell, D. 2005. A divergent cellular role for the FUSED kinase family in the plant-specific cytokinetic phragmoplast. *Curr Biol* **15**(23): 2107-2111.

Ohlmeyer, J.T. and Kalderon, D. 1998. Hedgehog stimulates maturation of Cubitus interruptus into a labile transcriptional activator. *Nature* **396**(6713): 749-753.

Ohno, S. 1970. *Evolution by gene duplication*. Springer-Verlag, Berlin, New York,.

Ohno, S., Wolf, U., and Atkin, N.B. 1968. Evolution from fish to mammals by gene duplication. *Hereditas* **59**(1): 169-187.

Ohta, T. 1987. Simulating evolution by gene duplication. *Genetics* **115**(1): 207-213.

Okabe, N., Xu, B., and Burdine, R.D. 2008. Fluid dynamics in zebrafish Kupffer's vesicle. *Dev Dyn* **237**(12): 3602-3612.

Oro, A.E. 2007. The primary cilia, a 'Rab-id' transit system for hedgehog signaling. *Curr Opin Cell Biol* **19**(6): 691-696.

Paces-Fessy, M., Boucher, D., Petit, E., Paute-Briand, S., and Blanchet-Tournier, M.F. 2004. The negative regulator of Gli, Suppressor of fused (Sufu), interacts with SAP18, Galectin3 and other nuclear proteins. *Biochem J* **378**(Pt 2): 353-362.

Pan, Y., Bai, C.B., Joyner, A.L., and Wang, B. 2006. Sonic hedgehog signaling regulates Gli2 transcriptional activity by suppressing its processing and degradation. *Mol Cell Biol* **26**(9): 3365-3377.

Pan, Y. and Wang, B. 2007. A novel protein-processing domain in Gli2 and Gli3 differentially blocks complete protein degradation by the proteasome. *J Biol Chem* **282**(15): 10846-10852.

Pan, Y., Wang, C., and Wang, B. 2009. Phosphorylation of Gli2 by protein kinase A is required for Gli2 processing and degradation and the Sonic Hedgehog-regulated mouse development. *Dev Biol* **326**(1): 177-189.

Panakova, D., Sprong, H., Marois, E., Thiele, C., and Eaton, S. 2005. Lipoprotein particles are required for Hedgehog and Wingless signalling. *Nature* **435**(7038): 58-65.

Panman, L. and Zeller, R. 2003. Patterning the limb before and after SHH signalling. *Journal of anatomy* **202**(1): 3-12.

Park, H.L., Bai, C., Platt, K.A., Matise, M.P., Beeghly, A., Hui, C.C., Nakashima, M., and Joyner, A.L. 2000. Mouse Gli1 mutants are viable but have defects in SHH signaling in combination with a Gli2 mutation. *Development* **127**(8): 1593-1605.

Park, T.J., Mitchell, B.J., Abitua, P.B., Kintner, C., and Wallingford, J.B. 2008. Dishevelled controls apical docking and planar polarization of basal bodies in ciliated epithelial cells. *Nat Genet* **40**(7): 871-879.

Pennarun, G., Bridoux, A.M., Escudier, E., Dastot-Le Moal, F., Cacheux, V., Amselem, S., and Duriez, B. 2002. Isolation and expression of the human hPF20 gene orthologous to Chlamydomonas PF20: evaluation as a candidate for axonemal defects of respiratory cilia and sperm flagella. *Am J Respir Cell Mol Biol* **26**(3): 362-370.

Pham, A., Therond, P., Alves, G., Tournier, F.B., Busson, D., Lamour-Isnard, C., Bouchon, B.L., Préat, T., and Tricoire, H. 1995. The Suppressor of fused gene encodes a novel PEST protein involved in Drosophila segment polarity establishment. *Genetics* **140**(2): 587-598.

Philipp, M. and Caron, M.G. 2009. Hedgehog signaling: is Smo a G protein-coupled receptor? *Curr Biol* **19**(3): R125-127.

Philipp, M., Fralish, G.B., Meloni, A.R., Chen, W., MacInnes, A.W., Barak, L.S., and Caron, M.G. 2008. Smoothened signaling in vertebrates is facilitated by a G protein-coupled receptor kinase. *Mol Biol Cell* **19**(12): 5478-5489.

Pires-daSilva, A. and Sommer, R.J. 2003. The evolution of signalling pathways in animal development. *Nat Rev Genet* **4**(1): 39-49.

Porter, J.A., Ekker, S.C., Park, W.J., von Kessler, D.P., Young, K.E., Chen, C.H., Ma, Y., Woods, A.S., Cotter, R.J., Koonin, E.V., and Beachy, P.A. 1996. Hedgehog patterning activity: role of a lipophilic modification mediated by the carboxy-terminal autoprocessing domain. *Cell* **86**(1): 21-34.

Porter, J.A., von Kessler, D.P., Ekker, S.C., Young, K.E., Lee, J.J., Moses, K., and Beachy, P.A. 1995. The product of hedgehog autoproteolytic cleavage active in local and long-range signalling. *Nature* **374**(6520): 363-366.

Préat, T. 1992. Characterization of Suppressor of fused, a complete suppressor of the fused segment polarity gene of Drosophila melanogaster. *Genetics* **132**(3): 725-736.

Préat, T., Thérond, P., Lamour-Isnard, C., Limbourg-Bouchon, B., Tricoire, H., Erk, I., Mariol, M.C., and Busson, D. 1990. A putative serine/threonine protein kinase encoded by the segment-polarity fused gene of Drosophila. *Nature* **347**(6288): 87-89.

Préat, T., Thérond, P., Limbourg-Bouchon, B., Pham, A., Tricoire, H., Busson, D., and Lamour-Isnard, C. 1993. Segmental polarity in Drosophila melanogaster: genetic dissection of fused in a Suppressor of fused background reveals interaction with costal-2. *Genetics* **135**(4): 1047-1062.

Price, M.A. and Kalderon, D. 1999. Proteolysis of cubitus interruptus in Drosophila requires phosphorylation by protein kinase A. *Development* **126**(19): 4331-4339.

-. 2002. Proteolysis of the Hedgehog signaling effector Cubitus interruptus requires phosphorylation by Glycogen Synthase Kinase 3 and Casein Kinase 1. *Cell* **108**(6): 823-835.

Ramaswamy, N.T., Ronai, Z., and Pelling, J.C. 1998. Rapid activation of JNK1 in UV-B irradiated epidermal keratinocytes. *Oncogene* **16**(11): 1501-1505.

Reiter, J.F. and Skarnes, W.C. 2006. Tectonic, a novel regulator of the Hedgehog pathway required for both activation and inhibition. *Genes Dev* **20**(1): 22-27.

Reynolds, A., Leake, D., Boese, Q., Scaringe, S., Marshall, W.S., and Khvorova, A. 2004. Rational siRNA design for RNA interference. *Nat Biotechnol* **22**(3): 326-330.

Riobo, N.A., Saucy, B., Dilizio, C., and Manning, D.R. 2006. Activation of heterotrimeric G proteins by Smoothened. *Proc Natl Acad Sci USA* **103**(33): 12607-12612.

Robbins, D.J., Nybakken, K.E., Kobayashi, R., Sisson, J.C., Bishop, J.M., and Thérond, P.P. 1997. Hedgehog elicits signal transduction by means of a large complex containing the kinesin-related protein costal2. *Cell* **90**(2): 225-234.

Rohatgi, R., Milenkovic, L., Corcoran, R.B., and Scott, M.P. 2009. Hedgehog signal transduction by Smoothened: Pharmacologic evidence for a 2-step activation process. *Proc Natl Acad Sci USA*.

Rohatgi, R., Milenkovic, L., and Scott, M.P. 2007. Patched1 regulates hedgehog signaling at the primary cilium. *Science* **317**(5836): 372-376.

Rosenbaum, J.L. and Witman, G.B. 2002. Intraflagellar transport. *Nat Rev Mol Cell Biol* **3**(11): 813-825.

Ross, A.J., May-Simera, H., Eichers, E.R., Kai, M., Hill, J., Jagger, D.J., Leitch, C.C.,

Chapple, J.P., Munro, P.M., Fisher, S., Tan, P.L., Phillips, H.M., Leroux, M.R.,

Henderson, D.J., Murdoch, J.N., Copp, A.J., Eliot, M.M., Lupski, J.R., Kemp, D.T.,

Dollfus, H., Tada, M., Katsanis, N., Forge, A., and Beales, P.L. 2005. Disruption of

Bardet-Biedl syndrome ciliary proteins perturbs planar cell polarity in vertebrates. *Nat*

Genet **37**(10): 1135-1140.

Ruel, L., Gallet, A., Raisin, S., Truchi, A., Staccini-Lavenant, L., Cervantes, A., and

Thérond, P.P. 2007. Phosphorylation of the atypical kinesin Costal2 by the kinase Fused

induces the partial disassembly of the Smoothened-Fused-Costal2-Cubitus interruptus

complex in Hedgehog signalling. *Development* **134**(20): 3677-3689.

Ruel, L., Rodriguez, R., Gallet, A., Lavenant-Staccini, L., and Thérond, P.P. 2003.

Stability and association of Smoothened, Costal2 and Fused with Cubitus interruptus are

regulated by Hedgehog. *Nat Cell Biol* **5**(10): 907-913.

Ruiz i Altaba, A. 1999. Gli proteins encode context-dependent positive and negative

functions: implications for development and disease. *Development* **126**(14): 3205-3216.

Sambrook, J. and Russell, D.W. 2001. *Molecular cloning : a laboratory manual*. Cold

Spring Harbor Laboratory Press, Cold Spring Harbor, N.Y.

Sapiro, R., Kostetskii, I., Olds-Clarke, P., Gerton, G.L., Radice, G.L., and Strauss III, J.F.

2002. Male infertility, impaired sperm motility, and hydrocephalus in mice deficient in

sperm-associated antigen 6. *Mol Cell Biol* **22**(17): 6298-6305.

Sapiro, R., Tarantino, L.M., Velazquez, F., Kiriakidou, M., Hecht, N.B., Bucan, M., and

Strauss, J.F. 2000. Sperm antigen 6 is the murine homologue of the Chlamydomonas

reinhardtii central apparatus protein encoded by the PF16 locus. *Biol Reprod* **62**(3): 511-518.

Sasaki, H., Hui, C., Nakafuku, M., and Kondoh, H. 1997. A binding site for Gli proteins is essential for HNF-3beta floor plate enhancer activity in transgenics and can respond to Shh in vitro. *Development* **124**(7): 1313-1322.

Sasaki, H., Nishizaki, Y., Hui, C., Nakafuku, M., and Kondoh, H. 1999. Regulation of Gli2 and Gli3 activities by an amino-terminal repression domain: implication of Gli2 and Gli3 as primary mediators of Shh signaling. *Development* **126**(17): 3915-3924.

Schauerte, H.E., van Eeden, F.J., Fricke, C., Odenthal, J., Strahle, U., and Haffter, P. 1998. Sonic hedgehog is not required for the induction of medial floor plate cells in the zebrafish. *Development* **125**(15): 2983-2993.

Seamon, K.B. and Daly, J.W. 1981. Forskolin: a unique diterpene activator of cyclic AMP-generating systems. *Journal of cyclic nucleotide research* **7**(4): 201-224.

Sekimizu, K., Nishioka, N., Sasaki, H., Takeda, H., Karlstrom, R.O., and Kawakami, A. 2004. The zebrafish iguana locus encodes Dzip1, a novel zinc-finger protein required for proper regulation of Hedgehog signaling. *Development* **131**(11): 2521-2532.

Sheng, T., Chi, S., Zhang, X., and Xie, J. 2006. Regulation of Gli1 localization by the cAMP/protein kinase A signaling axis through a site near the nuclear localization signal. *J Biol Chem* **281**(1): 9-12.

Shiba, D., Yamaoka, Y., Hagiwara, H., Takamatsu, T., Hamada, H., and Yokoyama, T. 2008. Localization of Inv in a distinctive intraciliary compartment requires the C-terminal ninein-homolog-containing region. *J Cell Sci*.

Shimeld, S.M. 1999. The evolution of the hedgehog gene family in chordates: insights from amphioxus hedgehog. *Dev Genes Evol* **209**(1): 40-47.

Shimeld, S.M., van den Heuvel, M., Dawber, R., and Briscoe, J. 2007. An amphioxus Gli gene reveals conservation of midline patterning and the evolution of hedgehog signalling diversity in chordates. *PLoS ONE* **2**(9): e864.

Shu, X., Huang, J., Dong, Y., Choi, J., Langenbacher, A., and Chen, J.N. 2007. Na,K-ATPase alpha2 and Ncx4a regulate zebrafish left-right patterning. *Development* **134**(10): 1921-1930.

Simons, M., Gloy, J., Ganner, A., Bullerkotte, A., Bashkurov, M., Kronig, C., Schermer, B., Benzing, T., Cabello, O.A., Jenny, A., Mlodzik, M., Polok, B., Driever, W., Obara, T., and Walz, G. 2005. Inversin, the gene product mutated in nephronophthisis type II, functions as a molecular switch between Wnt signaling pathways. *Nat Genet* **37**(5): 537-543.

Sinha, S. and Chen, J.K. 2006. Purmorphamine activates the Hedgehog pathway by targeting Smoothened. *Nat Chem Biol* **2**(1): 29-30.

Sisson, J.C., Ho, K.S., Suyama, K., and Scott, M.P. 1997. Costal2, a novel kinesin-related protein in the Hedgehog signaling pathway. *Cell* **90**(2): 235-245.

Smelkinson, M.G., Zhou, Q., and Kalderon, D. 2007. Regulation of Ci-SCFSlimb binding, Ci proteolysis, and hedgehog pathway activity by Ci phosphorylation. *Dev Cell* **13**(4): 481-495.

Smith, E.F. 2002. Regulation of flagellar dynein by the axonemal central apparatus. *Cell Motil Cytoskeleton* **52**(1): 33-42.

Smith, E.F. and Lefebvre, P.A. 1996. PF16 encodes a protein with armadillo repeats and localizes to a single microtubule of the central apparatus in Chlamydomonas flagella. *J Cell Biol* **132**(3): 359-370.

-. 1997. The role of central apparatus components in flagellar motility and microtubule assembly. *Cell Motil Cytoskeleton* **38**(1): 1-8.

Stegman, M.A., Goetz, J.A., Ascano, M., Ogden, S.K., Nybakken, K.E., and Robbins, D.J. 2004. The Kinesin-related protein Costal2 associates with membranes in a Hedgehog-sensitive, Smoothened-independent manner. *J Biol Chem* **279**(8): 7064-7071.

Stegman, M.A., Vallance, J.E., Elangovan, G., Sosinski, J., Cheng, Y., and Robbins, D.J. 2000. Identification of a tetrameric hedgehog signaling complex. *J Biol Chem* **275**(29): 21809-21812.

Stone, D.M., Hynes, M., Armanini, M., Swanson, T.A., Gu, Q., Johnson, R.L., Scott, M.P., Pennica, D., Goddard, A., Phillips, H., Noll, M., Hooper, J.E., de Sauvage, F., and Rosenthal, A. 1996. The tumour-suppressor gene patched encodes a candidate receptor for Sonic hedgehog. *Nature* **384**(6605): 129-134.

Svärd, J., Heby-Henricson, K., Henricson, K.H., Persson-Lek, M., Rozell, B., Lauth, M., Bergström, A., Ericson, J., Toftgård, R., and Teglund, S. 2006. Genetic elimination of Suppressor of fused reveals an essential repressor function in the mammalian Hedgehog signaling pathway. *Dev Cell* **10**(2): 187-197.

Taipale, J., Cooper, M.K., Maiti, T., and Beachy, P.A. 2002. Patched acts catalytically to suppress the activity of Smoothened. *Nature* **418**(6900): 892-897.

Takatori, N., Satou, Y., and Satoh, N. 2002. Expression of hedgehog genes in Ciona intestinalis embryos. *Mech Dev* **116**(1-2): 235-238.

Tang, L., Franca-Koh, J., Xiong, Y., Chen, M.Y., Long, Y., Bickford, R.M., Knecht, D.A., Iglesias, P.A., and Devreotes, P.N. 2008. tsunami, the Dictyostelium homolog of the Fused kinase, is required for polarization and chemotaxis. *Genes Dev* **22**(16): 2278-2290.

Tay, S.Y., Ingham, P.W., and Roy, S. 2005. A homologue of the Drosophila kinesin-like protein Costal2 regulates Hedgehog signal transduction in the vertebrate embryo. *Development* **132**(4): 625-634.

Thérond, P.P., Knight, J.D., Kornberg, T.B., and Bishop, J.M. 1996. Phosphorylation of the fused protein kinase in response to signaling from hedgehog. *Proc Natl Acad Sci USA* **93**(9): 4224-4228.

Tian, L., Holmgren, R.A., and Matouschek, A. 2005. A conserved processing mechanism regulates the activity of transcription factors Cubitus interruptus and NF-kappaB. *Nat Struct Mol Biol* **12**(12): 1045-1053.

Tolwinski, N.S., Wehrli, M., Rives, A., Erdeniz, N., DiNardo, S., and Wieschaus, E. 2003. Wg/Wnt signal can be transmitted through arrow/LRP5,6 and Axin independently of Zw3/Gsk3beta activity. *Dev Cell* **4**(3): 407-418.

Tyurina, O.V., Guner, B., Popova, E., Feng, J., Schier, A.F., Kohtz, J.D., and Karlstrom, R.O. 2005. Zebrafish Gli3 functions as both an activator and a repressor in Hedgehog signaling. *Dev Biol* **277**(2): 537-556.

van Eeden, F.J., Granato, M., Schach, U., Brand, M., Furutani-Seiki, M., Haffter, P., Hammerschmidt, M., Heisenberg, C.P., Jiang, Y.J., Kane, D.A., Kelsh, R.N., Mullins, M.C., Odenthal, J., Warga, R.M., Allende, M.L., Weinberg, E.S., and Nusslein-Volhard,

C. 1996. Mutations affecting somite formation and patterning in the zebrafish, Danio rerio. *Development* **123**: 153-164.

Varga, Z.M., Amores, A., Lewis, K.E., Yan, Y.L., Postlethwait, J.H., Eisen, J.S., and Westerfield, M. 2001. Zebrafish smoothened functions in ventral neural tube specification and axon tract formation. *Development* **128**(18): 3497-3509.

Varjosalo, M., Li, S.P., and Taipale, J. 2006. Divergence of hedgehog signal transduction mechanism between Drosophila and mammals. *Dev Cell* **10**(2): 177-186.

Vladar, E.K. and Stearns, T. 2007. Molecular characterization of centriole assembly in ciliated epithelial cells. *J Cell Biol* **178**(1): 31-42.

Vokes, S.A., Ji, H., McCuine, S., Tenzen, T., Giles, S., Zhong, S., Longabaugh, W.J., Davidson, E.H., Wong, W.H., and McMahon, A.P. 2007. Genomic characterization of Gli-activator targets in sonic hedgehog-mediated neural patterning. *Development* **134**(10): 1977-1989.

Vokes, S.A., Ji, H., Wong, W.H., and McMahon, A.P. 2008. A genome-scale analysis of the cis-regulatory circuitry underlying sonic hedgehog-mediated patterning of the mammalian limb. *Genes Dev* **22**(19): 2651-2663.

Wagner, G.P., Pavlicev, M., and Cheverud, J.M. 2007. The road to modularity. *Nat Rev Genet* **8**(12): 921-931.

Wang, B., Fallon, J.F., and Beachy, P.A. 2000a. Hedgehog-regulated processing of Gli3 produces an anterior/posterior repressor gradient in the developing vertebrate limb. *Cell* **100**(4): 423-434.

Wang, B. and Li, Y. 2006. Evidence for the direct involvement of {beta}TrCP in Gli3 protein processing. *Proc Natl Acad Sci USA* **103**(1): 33-38.

Wang, G., Amanai, K., Wang, B., and Jiang, J. 2000b. Interactions with Costal2 and suppressor of fused regulate nuclear translocation and activity of cubitus interruptus. *Genes Dev* **14**(22): 2893-2905.

Wang, Q.T. and Holmgren, R.A. 1999. The subcellular localization and activity of Drosophila cubitus interruptus are regulated at multiple levels. *Development* **126**(22): 5097-5106.

-. 2000. Nuclear import of cubitus interruptus is regulated by hedgehog via a mechanism distinct from Ci stabilization and Ci activation. *Development* **127**(14): 3131-3139.

Wang, Y., Zhou, Z., Walsh, C.T., and McMahon, A.P. 2009. Selective translocation of intracellular Smoothened to the primary cilium in response to Hedgehog pathway modulation. *Proc Natl Acad Sci USA*.

Westerfield, M. 1995. *The zebrafish book : a guide for the laboratory use of zebrafish (Danio rerio)*. M. Westerfield, Eugene, OR.

Whittle, J.R. 1976. Clonal analysis of a genetically caused duplication of the anterior wing in Drosophila melanogaster. *Dev Biol* **51**(2): 257-268.

Wilson, C.W., Chen, M.H., and Chuang, P.T. 2009a. Smoothened adopts multiple active and inactive conformations capable of trafficking to the primary cilium. *PLoS ONE* **4**(4): e5182.

Wilson, C.W., Nguyen, C.T., Chen, M.H., Yang, J.H., Gacayan, R., Huang, J., Chen, J.K., and Chuang, P.T. 2009b. Fused has evolved divergent roles in vertebrate Hedgehog signalling and motile ciliogenesis. *Nature*.

Wolff, C., Roy, S., and Ingham, P.W. 2003. Multiple muscle cell identities induced by distinct levels and timing of hedgehog activity in the zebrafish embryo. *Curr Biol* **13**(14): 1169-1181.

Wolff, C., Roy, S., Lewis, K.E., Schauerte, H., Joerg-Rauch, G., Kirn, A., Weiler, C., Geisler, R., Haffter, P., and Ingham, P.W. 2004. iguana encodes a novel zinc-finger protein with coiled-coil domains essential for Hedgehog signal transduction in the zebrafish embryo. *Genes Dev* **18**(13): 1565-1576.

Yamada, L., Kobayashi, K., Degnan, B., Satoh, N., and Satou, Y. 2003. A genomewide survey of developmentally relevant genes in Ciona intestinalis. IV. Genes for HMG transcriptional regulators, bZip and GATA/Gli/Zic/Snail. *Dev Genes Evol* **213**(5-6): 245-253.

Yan, D. and Lin, X. 2008. Opposing roles for glypicans in Hedgehog signalling. *Nat Cell Biol* **10**(7): 761-763.

Yang, J., Liu, X., Yue, G., Adamian, M., Bulgakov, O., and Li, T. 2002. Rootletin, a novel coiled-coil protein, is a structural component of the ciliary rootlet. *J Cell Biol* **159**(3): 431-440.

Yang, X., Dillon, R.H., and Fauci, L.J. 2008. An integrative computational model of multiciliary beating. *Bull Math Biol* **70**(4): 1192-1215.

Yin, Y., Bangs, F., Paton, I.R., Prescott, A., James, J., Davey, M.G., Whitley, P., Genikhovich, G., Technau, U., Burt, D.W., and Tickle, C. 2009. The Talpid3 gene (KIAA0586) encodes a centrosomal protein that is essential for primary cilia formation. *Development* **136**(4): 655-664.

Yoshimura, S., Egerer, J., Fuchs, E., Haas, A.K., and Barr, F.A. 2007. Functional dissection of Rab GTPases involved in primary cilium formation. *J Cell Biol* **178**(3): 363-369.

You, Y., Richer, E.J., Huang, T., and Brody, S.L. 2002. Growth and differentiation of mouse tracheal epithelial cells: selection of a proliferative population. *Am J Physiol Lung Cell Mol Physiol* **283**(6): L1315-1321.

Zariwala, M.A., Knowles, M.R., and Omran, H. 2007. Genetic defects in ciliary structure and function. *Annual review of physiology* **69**: 423-450.

Zeng, X., Goetz, J.A., Suber, L.M., Scott, W.J., Jr., Schreiner, C.M., and Robbins, D.J. 2001. A freely diffusible form of Sonic hedgehog mediates long-range signalling. *Nature* **411**(6838): 716-720.

Zhang, C., Williams, E.H., Guo, Y., Lum, L., and Beachy, P.A. 2004. Extensive phosphorylation of Smoothened in Hedgehog pathway activation. *Proc Natl Acad Sci USA* **101**(52): 17900-17907.

Zhang, Q., Zhang, L., Wang, B., Ou, C.Y., Chien, C.T., and Jiang, J. 2006a. A hedgehog-induced BTB protein modulates hedgehog signaling by degrading Ci/Gli transcription factor. *Dev Cell* **10**(6): 719-729.

Zhang, W., Zhao, Y., Tong, C., Wang, G., Wang, B., Jia, J., and Jiang, J. 2005. Hedgehog-regulated Costal2-kinase complexes control phosphorylation and proteolytic processing of Cubitus interruptus. *Dev Cell* **8**(2): 267-278.

Zhang, Z., Kostetskii, I., Tang, W., Haig-Ladewig, L., Sapiro, R., Wei, Z., Patel, A.M., Bennett, J., Gerton, G.L., Moss, S.B., Radice, G.L., and Strauss, J.F. 2006b. Deficiency

of SPAG16L causes male infertility associated with impaired sperm motility. *Biol Reprod* **74**(4): 751-759.

Zhang, Z., Sapiro, R., Kapfhamer, D., Bucan, M., Bray, J., Chennathukuzhi, V., McNamara, P., Curtis, A., Zhang, M., Blanchette-Mackie, E.J., and Strauss, J.F. 2002. A sperm-associated WD repeat protein orthologous to Chlamydomonas PF20 associates with Spag6, the mammalian orthologue of Chlamydomonas PF16. *Mol Cell Biol* **22**(22): 7993-8004.

Zhang, Z., Tang, W., Zhou, R., Shen, X., Wei, Z., Patel, A.M., Povlishock, J.T., Bennett, J., and Strauss, J.F. 2007. Accelerated mortality from hydrocephalus and pneumonia in mice with a combined deficiency of SPAG6 and SPAG16L reveals a functional interrelationship between the two central apparatus proteins. *Cell Motil Cytoskeleton* **64**(5): 360-376.

Zhao, Y., Tong, C., and Jiang, J. 2007. Hedgehog regulates smoothened activity by inducing a conformational switch. *Nature* **450**(7167): 252-258.

Zhou, H., Kim, S., Ishii, S., and Boyer, T.G. 2006. Mediator modulates Gli3-dependent Sonic hedgehog signaling. *Mol Cell Biol* **26**(23): 8667-8682.

Zhu, A.J., Zheng, L., Suyama, K., and Scott, M.P. 2003. Altered localization of Drosophila Smoothened protein activates Hedgehog signal transduction. *Genes Dev* **17**(10): 1240-1252.